REPORT OF RESEARCH AND TECHNOLOGIC WORK ON EXPLOSIVES, EXPLOSIONS, AND FLAMES FISCAL YEARS 1953 AND 1954

BY RUTH F. BRINKLEY AND ROBERT W. VAN DOLAH

* * * * * * * * * * Information Circular 7804

UNITED STATES DEPARTMENT OF THE INTERIOR
Fred A. Seaton, Secretary
BUREAU OF MINES
Marling J. Ankeny, Director

Work on manuscript completed August 1957. The Bureau of Mines will welcome reprinting of this paper, provided the following footnote acknowledgment is made: "Reprinted from Bureau of Mines Information Circular 7804."

November 1957

Generated on 2024-09-21 14:35 GMT / https://hdl.handle.net/2027/osu.32435030643506
Public Domain, Google-digitized / http://www.hathitrust.org/access_use#pd-google
Digitized by Google
Original from THE OHIO STATE UNIVERSITY

REPORT OF RESEARCH AND TECHNOLOGIC WORK ON EXPLOSIVES, EXPLOSIONS, AND FLAMES FISCAL YEARS 1953 AND 1954

by

Ruth F. Brinkley[1/] and Robert W. Van Dolah[2/]

CONTENTS

	Page
Summary and introduction	1
Explosives research and testing	2
Image-converter camera for study of explosives phenomena	2
Oscillographic measurement of detonation velocities	7
Structure of plane detonation waves	8
Explosibility of ammonium nitrate	11
Ignition of firedamp by explosives	27
Tests of explosives	50
Factors influencing permissibility of explosives	50
Current trends in usage of explosives and coal-breakage devices	56
Short-delay blasting in Experimental Coal Mine	59
Revised schedule for testing blasting devices	61
Flammability of gases and vapors	62
Investigation of surge-ignition sparks	62
Limits of flammability of complex hydrocarbon fuels at high altitudes	63
Flammability of carbon disulfide in mixtures of air and water vapor	76
Dust-explosion investigations	76
Incombustible requirements on floors and overhead surfaces in coal mines	76
Intensive sampling of coal-mine dusts	83
Laboratory studies of dust explosibility	86
Explosibility of American coals	86

1/ Technical assistant, Office of the Chief, Division of Explosives Technology, Bureau of Mines, Region V, Pittsburgh, Pa.

2/ Physical science administrator, Chief, Division of Explosives Technology, Bureau of Mines, Region V, Pittsburgh, Pa.

Information Circular 7804

Generated on 2024-09-21 14:44 GMT / https://hdl.handle.net/2027/osu.32435030643506
Public Domain, Google-digitized / http://www.hathitrust.org/access_use#pd-google

Digitized by Google

Original from THE OHIO STATE UNIVERSITY

CONTENTS (Con.)

	Page
Combustion research	98
Problems of ignition	98
Burning velocities on slot burners	98
Burning-velocity measurements in a spherical vessel	102
Flame stabilization on burners with short or noncircular ports	104
Gas-burner flashback on turndown	109
Calibration of glass-wool flowmeters	112
Research on turbulent flames	112
Relation between sampling-tube measurements and concentration fluctuations in a turbulent gas jet	113
Combustion of carbon in high-temperature, high-velocity air streams	113
Mathematical model of a combustion wave	119
Mathematical representation of flame propagation	120
Thermodynamics of combustion gases	120
Miscellaneous investigations	121
Surface reaction of oxygen with carbon on a tungsten crystal	121
Capillary jump and capillary vortex in liquid flow along flat plates	126

ILLUSTRATIONS

Fig.		
1.	Block diagram of apparatus, showing explosive charge, camera equipment, and auxiliary apparatus for external lighting	3
2.	Image-converter camera	5
3.	Typical photographs taken with image-converter camera	6
4.	Block diagram of velocity of detonation apparatus	8
5.	Typical oscillogram of a multichannel velocity record, showing step structure and calibration	9
6.	Velocity of detonation vs. density relationship for PETN; comparison of data accumulated by oscillographic method with those by optical methods	10
7.	Velocity of detonation decay for TNT of 500- and 1,000-micron particle size at 3 loading densities for each size	10
8.	Bombs used for testing ammonium nitrate	13
9.	Diagram of apparatus and equipment used to determine explosibility of ammonium nitrate	14
10.	Bomb test-temperature data: Test 27, C.P. ammonium nitrate (M-8188)	15
11.	Bomb test-temperature data: Test 45, ammonium nitrate fertilizer (M-8137) (with internal heater)	16
12.	Bomb test-temperature data: Test 55, ammonium nitrate fertilizer (M-8138) + 1.5 percent of bag paper (with internal heater)	17
13.	Bomb fragments, test 55	19

Generated on 2024-09-21 14:38 GMT / https://hdl.handle.net/2027/osu.32435030643506
Public Domain, Google-digitized / http://www.hathitrust.org/access_use#pd-google
Digitized by Google
Original from THE OHIO STATE UNIVERSITY

ILLUSTRATIONS (Con.)

Fig.		Page
14.	Location of thermocouples in holds 3 and 4, SS. Henry T. Scott, May-June 1947	25
15.	Time-temperature plot	26
16.	Schematic diagrams showing flow of streamlines and entrapment of natural gas-air in pockets within hot gaseous products	28
17.	Cross-sectional diagram of loaded small cannon with half-full borehole	29
18.	Small experimental gallery, taken from position of Fastax camera	30
19.	Results of experiments with 5-inch small cannons fired into 8-percent natural gas-air mixture in large gallery	31
20.	Effect of oxygen content of gallery atmosphere on ignition probability	31
21.	Shot 1197; half-full borehole side-view small-cannon shot in oxygen-deficient air (6 percent O_2), taken at 7,500 frames per second	33
22.	Shot 1202; half-full borehole side-view small-cannon shot in oxygen-enriched air (32 percent O_2), taken at 7,500 frames per second	34
23.	Brilliant primary flame, as obtained with photograph of shot 1195	35
24.	Cutaway sections of boreholes after firing	35
25.	Types of suspended tetryl charges, unsheathed and sheathed	37
26.	Types of sheathed tetryl charges	38
27.	Plot of ignition probabilities vs. oxygen percentage for 1/4-inch sheaths	39
28.	High-speed photographs of 4 types of sheathed cartridges having 1/8-inch-thick sodium bicarbonate sheaths and showing comparative flame patterns	40
29.	High-speed photographs of unsheathed tetryl charge and 7 types of sheathed cartridges having 1/4-inch-thick sodium bicarbonate sheaths and showing comparative flame patterns (sheet 1)	41
30.	Same (sheet 2)	42
31.	Development of cloud of detonation products and shock wave	43
32.	Development of shock wave and gaseous products of detonation when an unstemmed charge of high explosive is fired from a steel borehole into a flammable atmosphere of firedamp and air	45
33.	A, Cross-sectional sketches of boreholes of small cannon, showing dimensions with variable weights of fireclay stemming; B, effect of stemming on incendivity to firedamp	46
34.	Shock-wave photographs of stemmed shots	47
35.	Gallery explosion to test explosives for permissibility	52

Generated on 2024-09-21 14:30 GMT / https://hdl.handle.net/2027/osu.32435030643506
Public Domain, Google-digitized / http://www.hathitrust.org/access_use#pd-google
Digitized by Google
Original from THE OHIO STATE UNIVERSITY

ILLUSTRATIONS (Con.)

Fig.		Page
36.	Abbreviated sigmoid curves for two hypothetical explosives illustrating graphical plot of relative incendivity according to oxygen values	53
37.	Block diagram of apparatus for measuring spark ignition energy	64
38.	A, Oscillogram of spark voltage vs. time; B, Oscillogram of spark current vs. time	65
39.	Analysis of oscillograms in figure 38	66
40.	Schematic diagram of F-24 limit-of-flammability apparatus	68
41.	Absolute limits of flammability for Avgas 100/130 vapor-air mixtures at 78±1° F.	70
42.	Absolute limits of flammability for A, Avgas 100/130 vapor-air-carbon dioxide mixtures at 16 inches Hg absolute pressure and 80±1° F.; B, Avgas 100/130 vapor-air-nitrogen mixtures at 16 inches Hg absolute pressure and 80±2° F.	71
43.	Saturated limits of flammability of 0- to 5-percent fraction of Avgas 100/130 vapor-air mixtures over temperature range - 100° to 0° F.	72
44.	General flammable volume of a combustible vapor-air mixture	74
45.	General form of absolute limit-of-flammability curve and its traces for a combustible vapor-air-inert mixture at constant pressure and temperature	75
46.	Distribution of coal dust-limestone mixture in test zone of main entry	78
47.	Sources of ignition used in Experimental Coal-Mine explosion tests	80
48.	Incombustible content of floor and rib-roof dusts in explosion-limiting mixtures	81
49.	Relation of incombustible contents in total dust to floor dust in explosion-limiting mixtures	82
50.	Explosibility of mine-size coal dusts based on tests in Experimental Coal Mine and in laboratory	89
51.	Minimum explosive concentration, minimum igniting energy, and ignition temperature of through-200-mesh coal dusts in air and in oxygen	90
52.	Maximum pressures and rates of pressure rise developed by explosions of through-200-mesh coal dusts in air and in oxygen (dust concentration = 0.50 oz./cu.ft.)	91
53.	Effect of concentration on maximum pressure and rates of pressure rise developed by explosions of through-200-mesh bituminous-coal dust in air and in oxygen	92
54.	Effect of particle size on minimum explosive concentration, minimum igniting energy, and pressures developed by explosions of dust clouds of bituminous Pittsburgh coal in air and in oxygen	93
55.	Relation of particle size to ignition temperature, relative flammability, and volatile ratio of bituminous Pittsburgh coal	94

Generated on 2024-09-21 14:37 GMT / https://hdl.handle.net/2027/osu.32435030643506
Public Domain, Google-digitized / http://www.hathitrust.org/access_use#pd-google
Digitized by Google
Original from THE OHIO STATE UNIVERSITY

ILLUSTRATIONS (Con.)

Fig.		Page
56.	Effect of various proportions of through-200-mesh particles in through-20-mesh dust on minimum explosive concentration, minimum igniting energy, and relative flammability of bituminous Pittsburgh-coal dust clouds in air	95
57.	Effect of moisture on minimum explosive concentration and minimum electrical spark energy required to ignite dust clouds of through-200-mesh bituminous Pittsburgh coal in air	96
58.	Venting coal-dust explosions from 1-cu.-ft. gallery to atmosphere and to cubical chambers of various sizes, (dust concentration = 0.60 oz./cu.ft.)	97
59.	Burning velocities of methane-air mixtures	101
60.	Flame-stability diagram for 100-percent methane	106
61.	Flame-stability diagram for 100-percent methane; comparison of points for square, rectangular, and triangular channels and curves for long, cylindrical tubes	108
62.	Burner flames during turndown of two-position gas valve	110
63.	Air entrainment and flow of fuel in burner during turndown of two-position gas valve	111
64.	Combustion apparatus	115
65.	Variation of radius of carbon cylinder with time (900°C.)	117
66.	Effect of sample size on reaction rate	118
67.	Field-emission microscope assembly for oxygen-carbon reaction on tungsten	123
68.	Surface reaction of carbon with oxygen on tungsten	124
69.	Surface reaction of carbon with oxygen on tungsten (con.)	125
70.	Vertical cross section of flow pattern	127

TABLES

1.	Physical and chemical properties of ammonium nitrate fertilizer, Texas City, Tex.	12
2.	Bomb tests with pure ammonium nitrate	20
3.	Bomb tests with ammonium nitrate fertilizer (bomb, 3 by 20 inches)	21
4.	Bomb tests with ammonium nitrate fertilizer plus 1.5 percent of paper-bag container (bomb, 3 by 20 inches)	22
5.	Results of pressure measurements	23
6.	Incendivity of various explosives to firedamp-air mixtures	49
7.	Effect of oxygen balance on incendivity	54
8.	Effect of sodium nitrate, sodium chloride, and potassium chloride in gallery tests, in percent	54
9.	Chemical analyses of samples tested for incendivity to methane-air mixtures, in percent	55
10.	Results of incendivity tests in methane-air mixture showing effect of nitrocellulose, sodium chloride, and pregelling of explosive oil in the experimental gallery and gallery 1	56
11.	Comparison of chemical analysis and physical properties of 2 permissible explosives with 40-percent dynamite	58
12.	Classification and analysis of coal samples	87
13.	Observed specific reaction rates of spectroscopic carbon cylinders	116

Generated on 2024-09-21 14:32 GMT / https://hdl.handle.net/2027/osu.32435030643506
Public Domain, Google-digitized / http://www.hathitrust.org/access_use#pd-google
Digitized by Google
Original from THE OHIO STATE UNIVERSITY

SUMMARY AND INTRODUCTION

This report is the 16th of a series of reports originally issued annually and more recently biennially to acquaint the reader with the work of the Explosives and Physical Sciences Division, Region VIII.[3/]

In the majority of instances the results of the investigations are made available to the public through Government publications and journal articles. In certain instances (specifically as regards security-classified research, investigations of a confidential nature, and short-range programs of very limited scope) results are reported only to those immediately concerned.

The text summarizes the fundamental research and technological studies published during fiscal years 1953 and 1954. In addition, summaries of tests of explosives, hazardous chemicals, dusts, etc., are included.

As is common in continuing research programs, some of the data presented and conclusions drawn in the papers reviewed have been modified by virtue of subsequent research. In general, no attempt has been made to effect such modifications in these summaries, in the feeling that this publication should retain as much as possible the character of the original papers, which are referred to throughout the report.

In addition to published and unpublished research, the Division continued to participate actively in national and international scientific meetings. During the fiscal years 1953 and 1954, the Division was represented at meetings of leading American scientific societies; the Seventh International Conference of Directors of Safety in Mines Research at Buxton, England; NATO Colloquia on Aeronautical Research and Development at Rome, Italy, and London, England; the Fourth Symposium on Combustion, Cambridge, Mass.; and a number of security-classified symposia.

As in previous years, the twofold program of disaster prevention through on-the-spot investigation of explosion disasters and public demonstrations of hazardous practices and conditions was pursued. During the fiscal years 1953 and 1954 approximately 15 major gas and dust explosions were investigated, as well as a number of potentially hazardous situations. Recommendations were made to prevent the future occurrence of similar disasters. More than 3,000 doctors, nurses, and other hospital personnel witnessed demonstrations of static electricity hazards as related to explosions of anesthetic gas in surgical operations. The consequences of safe and unsafe blasting practices in coal mining were presented in three large-scale demonstrations at the Experimental Coal Mine, Bruceton, Pa., witnessed by some 1,500 people.

3/ In January 1955 the name of this Division was changed to the Division of Explosives Technology, and the Region became Region V.

Generated on 2024-09-21 14:33 GMT / https://hdl.handle.net/2027/osu.32435030643506
Public Domain, Google-digitized / http://www.hathitrust.org/access_use#pd-google
Digitized by Google
Original from THE OHIO STATE UNIVERSITY

EXPLOSIVES RESEARCH AND TESTING

Image-Converter Camera for Study of Explosives Phenomena

Major problems in studying detonation phenomena are direct observation and recording. Too violent and rapid to be accessible to visual observation or by ordinary photographic methods, the performance of detonating high explosives is best evaluated by special, high-speed, electronic equipment. For this purpose the Division has developed a single-frame camera that uses a pulsed image-converter tube to attain exposure time of 0.1 microsecond (μ sec.) or less.[4/] This means that a detonation wave moving at a speed of 8,000 m. per sec. travels 0.8 mm. during an exposure interval, and the wave motion is virtually arrested. The image-converter tube converts an optical image into an electron image and reconverts it to a luminous optical image. The exposure time is regulated by "gating" the stream of electrons through this tube for the desired interval.

Principle and Apparatus

The use of image-converter tubes as photographic shutters is not new,[5/] but much of the earlier work was done with tubes designed for other purposes. The image-converter tube used in the image-converter camera developed in these laboratories consists of an evacuated glass cylinder with flat ends. A photoemissive layer is deposited on the inner surface at one end to form the cathode, and metalized phosphor applied at the other end forms the anode. When an image is focused optically on the photocathode, electrons are released in the form of an electron image and accelerated toward the anode by application of a positive potential. An axial magnetic field focuses the electron image on the phosphor, where it is converted to an optical image that can be photographed by conventional means. The shutter action is obtained by application of anode potential for the desired exposure time.

Figure 1 is a block diagram of the apparatus, showing the basic elements necessary for application of the camera to photography of detonation in an explosive charge. These include: (1) A camera field lens for focusing the object image on the photoemissive surface of the image-converter tube; (2) the image-converter tube proper; (3) a magnetic lens or coil for focusing the electron image formed at the photocathode on the fluorescent screen of the image-converter tube; (4) a copy camera for recording on film the image produced on the fluorescent screen of the image-converter tube; (5) a pulse circuit for applying the accelerating potential to the image-converter tube; (6) a synchronizer for timing the camera exposure to the event being photographed; (7) the object or explosive charge primed and wired with pickup stations. A trigger and a pulser are used to explode a wire that produces a light flash intense enough to illuminate the scene being photographed. Photographic exposures in the fractional microsecond range require very intense external illumination; when used with explosives the illuminating source should be expendable. The exploding wire satisfies both these requirements.

4/ Gibson, F. C., Bowser, M. L., Ramaley, C. W., and Scott, F. H., Image-Converter Camera for Studies of Explosives Phenomena: Rev. Sci. Instr., vol. 25, No. 2, 1954, pp. 173-176.

5/ Courtney-Pratt, J. S., Some New Methods of Fast Photography and Their Application to Combustion Processes: Research, vol. 2, 1949, p. 287; and Fourth Symposium (International) on Combustion, Williams & Wilkins Co., Baltimore, Md., 1953, pp. 508-526.
Hogan, A. W., Use of Image Converter Tube for High Speed Shutter Action: Proc. Inst. Radio Eng., vol. 39, No. 3, 1951, pp. 268-270.
Weil, Herbert, Radio and Television News (Radio-Electronic Engineering ed.) vol. 47, No. 4, 1952, pp. 12, 13.

Generated on 2024-09-21 14:37 GMT / https://hdl.handle.net/2027/osu.32435030643506
Public Domain, Google-digitized / http://www.hathitrust.org/access_use#pd-google
Digitized by Google
Original from THE OHIO STATE UNIVERSITY

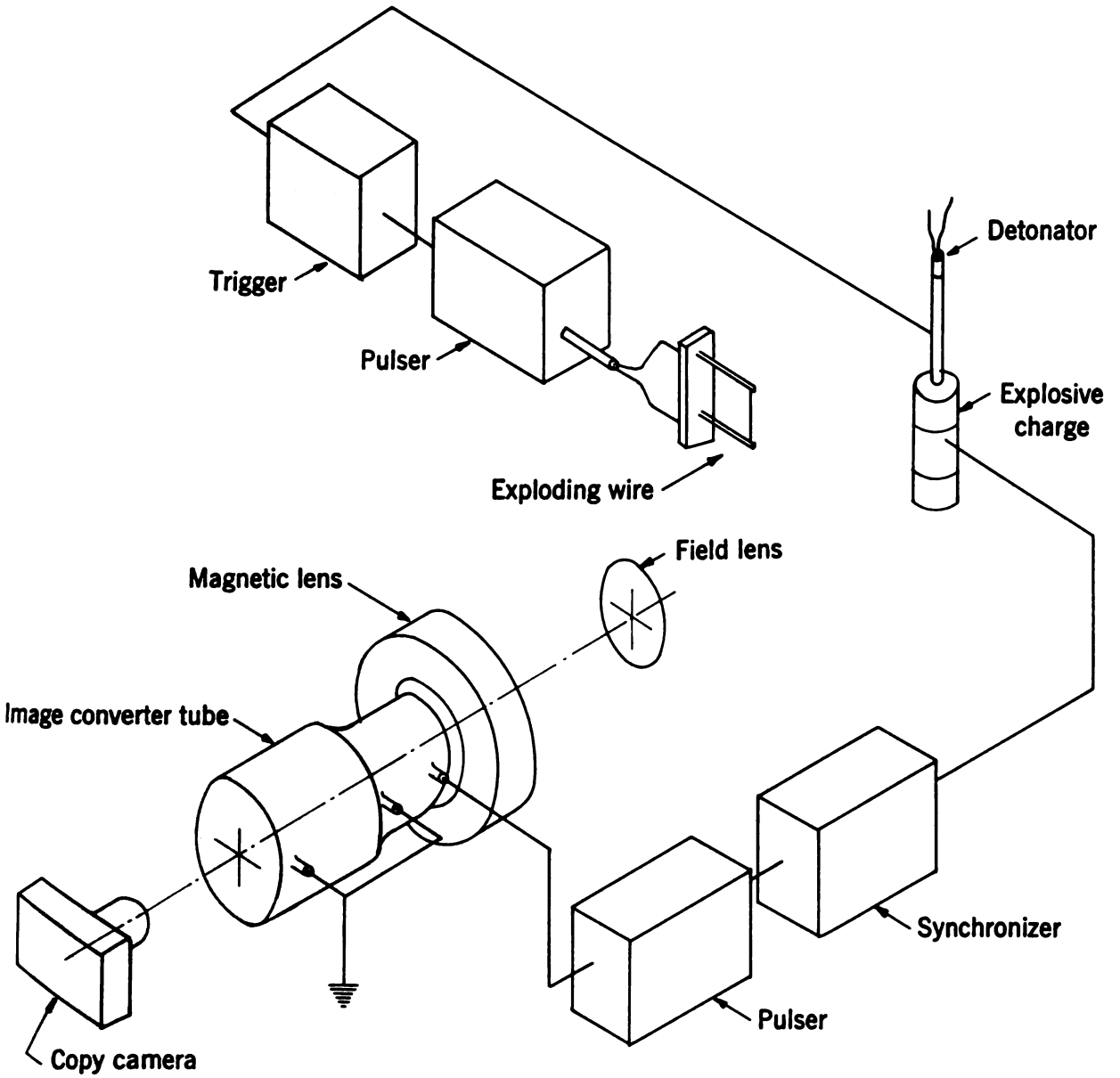

Figure 1. - Block diagram of apparatus, showing explosive charge, camera equipment, and auxiliary apparatus for external lighting.

Generated on 2024-09-21 14:38 GMT / https://hdl.handle.net/2027/osu.32435030643506
Public Domain, Google-digitized / http://www.hathitrust.org/access_use#pd-google
Digitized by Google
Original from THE OHIO STATE UNIVERSITY

The camera tube and a pulser unit are shown in figure 2. The f/5.4, 16-inch focal-length field lens is supported in the concrete wall common to the control room and explosives test area. A 1-inch-thick multiplate window on the far side of the wall protects the lens from flying fragments. The camera is focused by moving the entire unit on the floor track. The tube is carried in a Plexiglas saddle and retained by an elastic band drawn around the large-diameter end of the tube. The photocathode is inserted into the focus coil supported on the fixed baffle plate. An adjustable camera front is used to support shorter-focus field lenses and auxiliary equipment. An adjustable bracket at the rear supports the copy camera. The cabinet contains the high-voltage, line-type pulser; a hinged door panel has been removed to show the pulse-forming line entering the pulser unit on the left. A tap placed on the shield braid passes to the cradle. The variable transformer mounted on the camera base is used for adjusting the focus current, which is controlled by a foot-actuated switch.

Typical Application

Typical photographs with the image-converter camera are shown in figure 3. Figure 3, A, is a time exposure of the explosive charge before detonation. This charge consists of 3 cylindrical pellets 3/4 inch in diameter and about 1 inch in length cemented together. The boundaries between the pellets are clearly visible; the camera-synchronizing leads can be seen entering the right side of the charge at a pellet boundary; the trigger leads for the exploding wire are out of the field of view at the top. To the left of the charge is a troughlike paper reflector used behind the exploding wire.

Figure 3, B, is a 0.1-μsec. photograph of this charge during detonation. The detonation front has reached the middle of the center pellet. The cloud of detonation products is visible above the undetonated charge. The luminosity of this cloud is the result of the shock wave on air, and the dark band across it is due to the boundary between the upper and center pellets. The synchronizing leads are still discernible at the right. The bright streak to the left was caused by direct light from the exploding wire.

Figure 3, C, is a 0.1-μsec. photograph of a charge similar to that described above, except that it was detonated in an atmosphere of propane. The bright streak down the right side of the photograph is due to a reflection of the exploding wire on the outer surface of the cellulose acetate container used to retain the gas. It will be noted that the shock wave propagating through the propane is nonluminous.

These photographs are part of a series taken in an investigation into the luminosities that accompany detonation. Among other uses, the equipment is being employed to assess the value of a new method for distinguishing luminosities due to the shock wave in air from luminosities due to the detonation temperature.

The image-converter technique has been applied to preliminary studies in streak or time-displacement photography, for which the equipment is especially suited. An electron image of a phenomenon moving along a slit is deflected parallel to the slit by means of a varying transverse magnetic field. If the field varies uniformly with time, a linear time-displacement record of motion along the slit is obtained. The principal advantages of this system are high sweep speeds and the absence of mechanical vibration. In basic experiments with a simple sweep generator, sweep speeds of more than 15 mm. per μsec. were readily obtained.

Generated on 2024-09-21 14:32 GMT / https://hdl.handle.net/2027/osu.32435030643506
Public Domain, Google-digitized / http://www.hathitrust.org/access_use#pd-google
Digitized by Google
Original from THE OHIO STATE UNIVERSITY

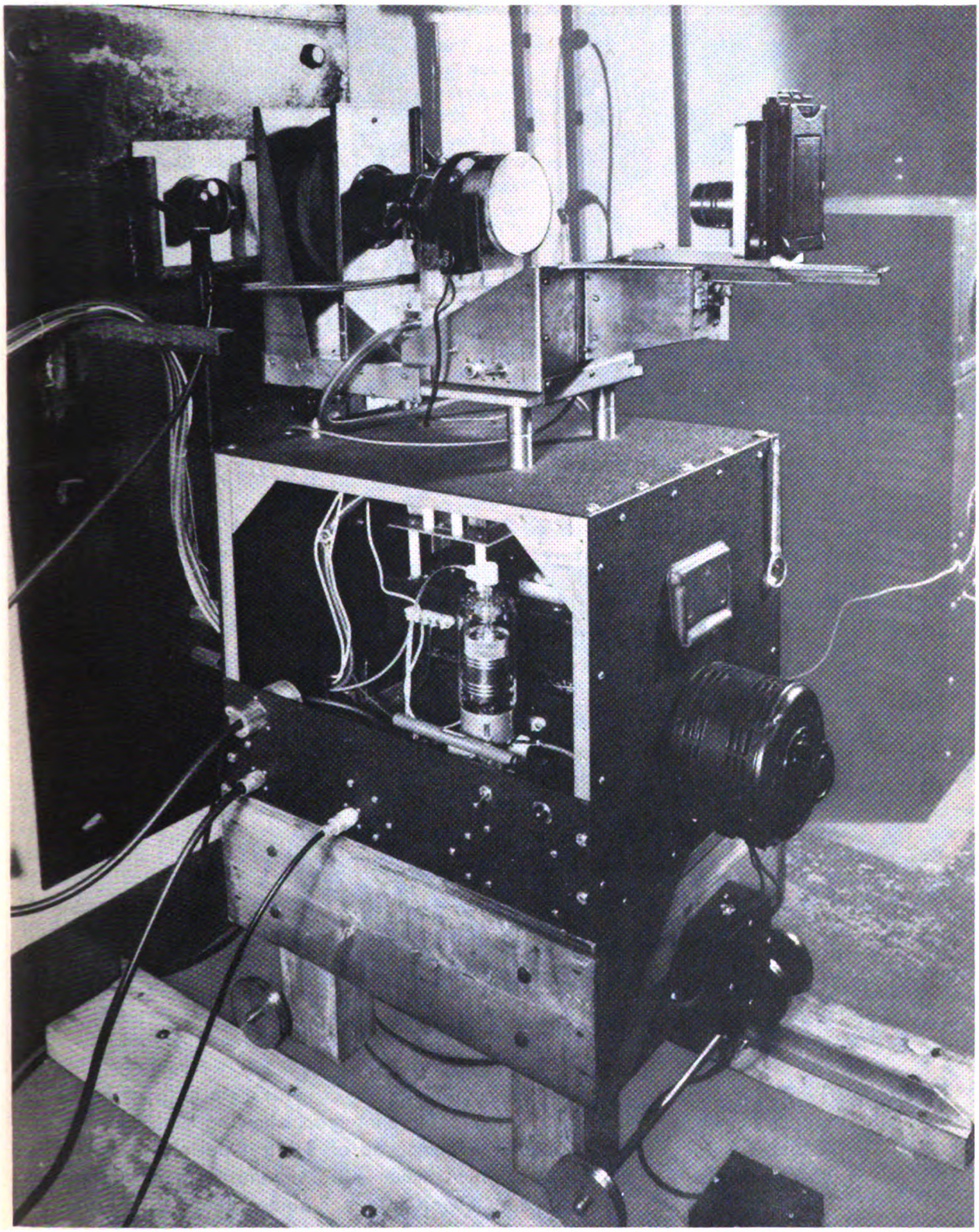

Figure 2. - Image-converter camera. Image-converter tube is shown top center; camera base houses pulse generator.

Generated on 2024-09-21 14:41 GMT / https://hdl.handle.net/2027/osu.32435030643506
Public Domain, Google-digitized / http://www.hathitrust.org/access_use#pd-google
Digitized by Google
Original from THE OHIO STATE UNIVERSITY

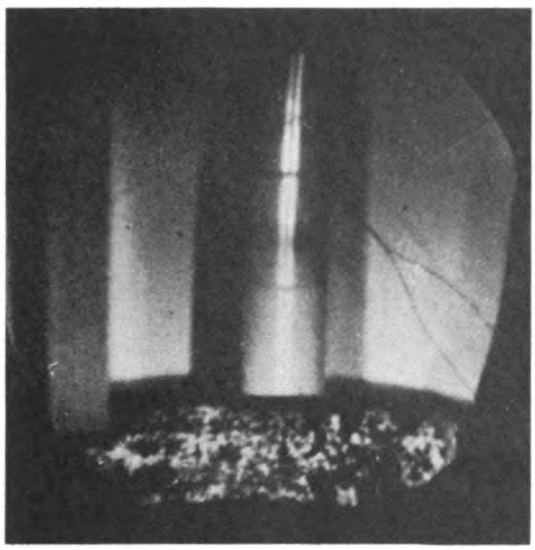

A

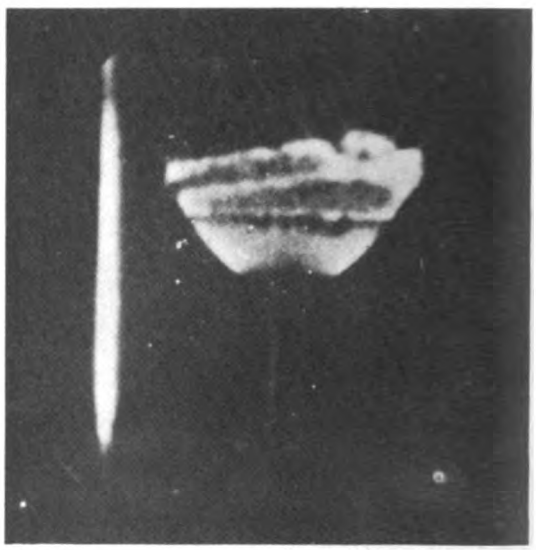

B

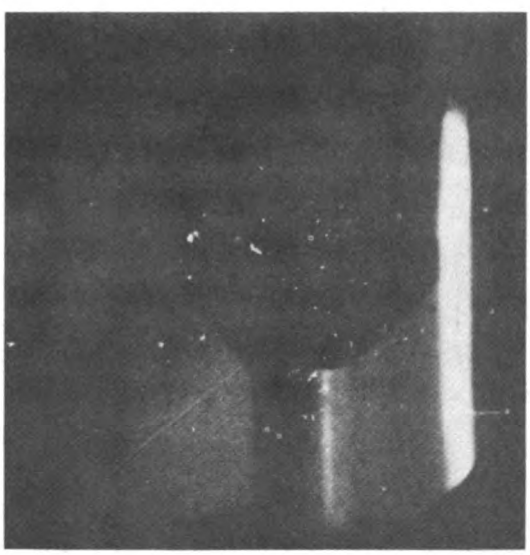

C

Figure 3. - Typical photographs taken with image-converter camera; a white paper background has been provided: A, Preexplosion photograph showing a high-density, ¾-inch-diameter, cylindrical charge composed of 3 tetryl pellets; B, 0.1-μ second exposure of charge shown in A (movement of detonation front has been "stopped" below pellet boundary owing to synchronizer delays); C, same type of charge fired in an atmosphere of propane (shock wave is now nonluminous).

Generated on 2024-09-21 14:31 GMT / https://hdl.handle.net/2027/osu.32435030643506
Public Domain, Google-digitized / http://www.hathitrust.org/access_use#pd-google

Digitized by Google

Original from
THE OHIO STATE UNIVERSITY

Oscillographic Measurement of Detonation Velocities

There are at present five standard methods for determining the speed with which a detonation wave travels along an explosive. The simplest of these - the D'Autriche method[6] - depends on the use of one explosive to evaluate another and is not very precise for short lengths of explosives. Rotating-drum chronographs, such as the Mettegang recorder,[7] are only accurate for intervals of 10 μsec. or more. The photographic methods, involving rotating-drum and mirror systems, give continuous displacement-time records but depend on exterior luminosities from the explosive and are not entirely applicable to cased charges. The development of electronic measuring devices has introduced a radically new approach to the determination of detonation velocities, but commercially available chronographs and chronoscopes offer various drawbacks such as inadequate time resolution, instability, etc.[8]

To eliminate these difficulties and retain the advantages of electronic procedures, the Division has developed a new method based on the use of a multichannel oscillograph designed and constructed in its physics laboratories.[9] In this method the time interval required for a detonation wave to travel between two predetermined points on an explosive charge is measured by the distance of the travel of a spot on a cathode-ray-tube screen. It offers the following advantages:

(1) A quartz crystal is used for calibration.

(2) Detonation velocities can be determined over 1 to 5 adjacent segments of an explosive charge, the time intervals being determined to the nearest 0.1 μsec.

(3) Measurements can be made between points within the charge and independent of external luminosities.

(4) The equipment requires a minimum of operator adjustment.

(5) A permanent record is obtained.

A block diagram of the apparatus (fig. 4) shows the explosive charge, end-initiated and wired with seven pickup stations; each station provides an electrical impulse to the apparatus as the flame or detonation wave passes it. The first station triggers the driven sweep of the oscilloscope, causing a spot to move across the face of the cathode-ray tube. As the detonation wave passes each successive station, the spot is given an abrupt vertical deflection. The result after calibration is a steplike trace with a superimposed radio-frequency sine wave that serves as a time base (fig. 5).

The test and calibration traces are recorded with a copy camera. The developed negative film is analyzed under a standard 10X laboratory microscope or comparator. The station spacing in the charge is measured accurately before the explosion, and the velocity of detonation is calculated readily from the time intervals determined by measurements on the photographic negative.

6/ Munroe, C. E., and Tiffany, J. E., Physical Testing of Explosives: Bureau of Mines Bull. 346, 1931, p. 64.

7/ Work cited in footnote 6, pp. 60-63.

8/ An exception is the currently available 10-mc. counter chronographs which have 0.1 m. per sec. revolution but compose only a single channel, so that for each segment velocity an additional counter is required.

9/ Gibson, F. C., An Oscillographic Method for Determining Velocities of Detonation in Explosives: Rev. Sci. Instr., vol. 25, No. 3, 1954, pp. 226-231.

Generated on 2024-09-21 14:31 GMT / https://hdl.handle.net/2027/osu.32435030643506
Public Domain, Google-digitized / http://www.hathitrust.org/access_use#pd-google
Digitized by Google
Original from THE OHIO STATE UNIVERSITY

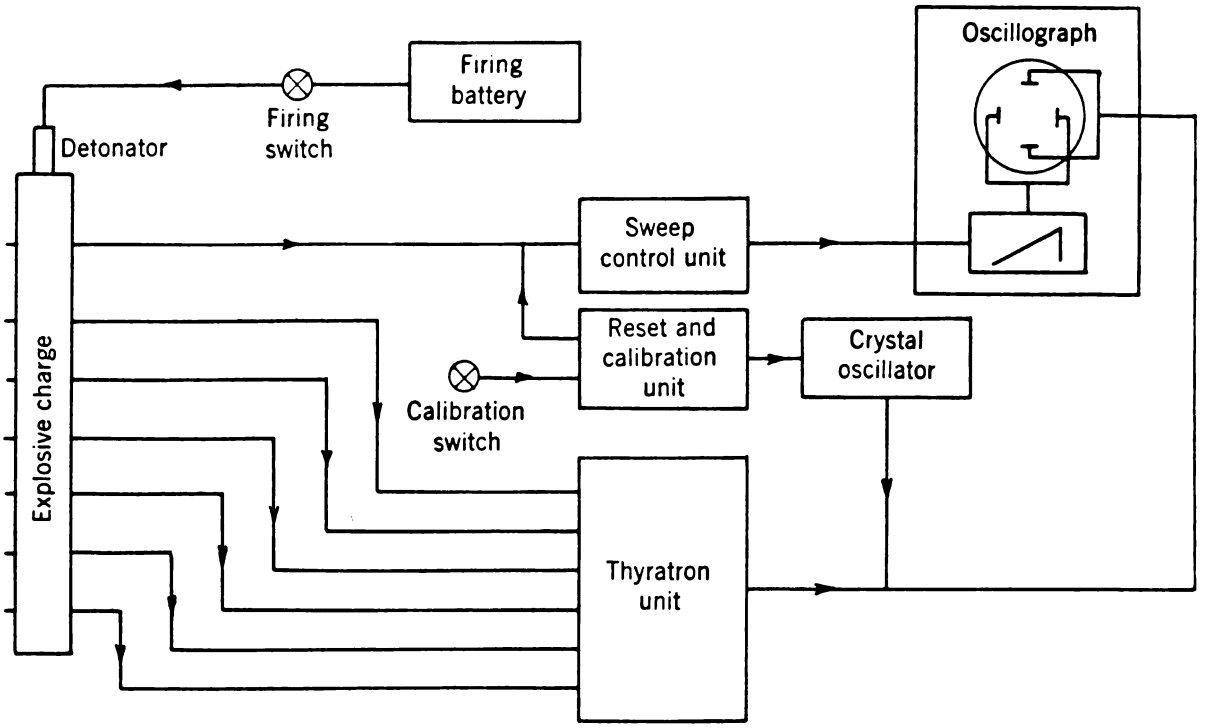

Figure 4. - Block diagram of velocity-of-detonation apparatus.

The reliability of the method is illustrated in figure 6, where detonation velocities of PETN at five loading densities are compared with data obtained by optical methods. The variation is of the order of 1 percent.

To illustrate the applicability of the oscillographic method to nonsteady detonation propagation, charges of TNT were tested at 2 particle sizes (500 and 1,000 microns) and 3 loading densities (fig. 7).

As it is not direct-reading but requires use of a photographic process, the multichannel oscillograph is not designed primarily for routine measurements. As a research tool, it permits study of variations in propagation between adjacent charge segments of unequal density, unequal charge diameter, and different materials, as well as determination of average velocities over short segments of homogeneous charges. This latter is of particular advantage, as it permits precise determination of detonation velocities, using only small amounts of explosive, which are difficult or tedious to prepare.

Structure of Plane Detonation Waves

Classical treatments of the detonation wave are based on the simplifying assumption that the detonation reaction is instantaneous and hence occurs in a mathematical plane. During World War II the theory of detonation waves was extended to include consideration of a finite reaction zone, most notably by J. von Neumann.[10/] More recently, the von Neumann model of the detonation wave has been refined and extended

10/ von Neumann, J., O.S.R.D., Rept. 549, 1942.

Generated on 2024-09-21 14:35 GMT / https://hdl.handle.net/2027/osu.32435030643506
Public Domain, Google-digitized / http://www.hathitrust.org/access_use#pd-google
Digitized by Google
Original from THE OHIO STATE UNIVERSITY

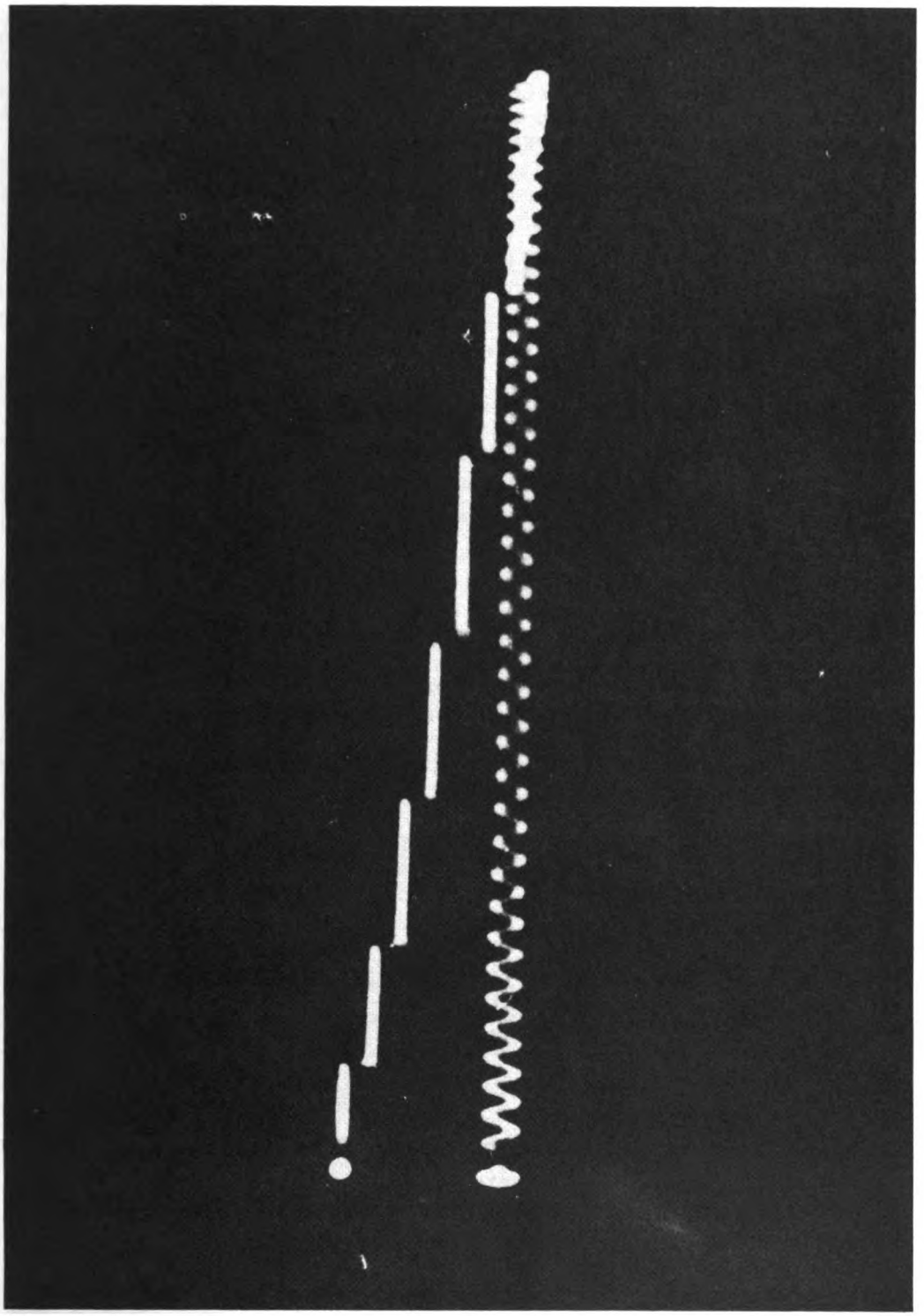

Figure 5. - Typical oscillogram of a multichannel velocity record, showing step structure and calibration. Since three densities were employed in the test charge, the steps become progressively longer. A 1-mc. calibration wave is superimposed.

Generated on 2024-09-21 14:37 GMT / https://hdl.handle.net/2027/osu.32435030643506
Public Domain, Google-digitized / http://www.hathitrust.org/access_use#pd-google
Digitized by Google
Original from THE OHIO STATE UNIVERSITY

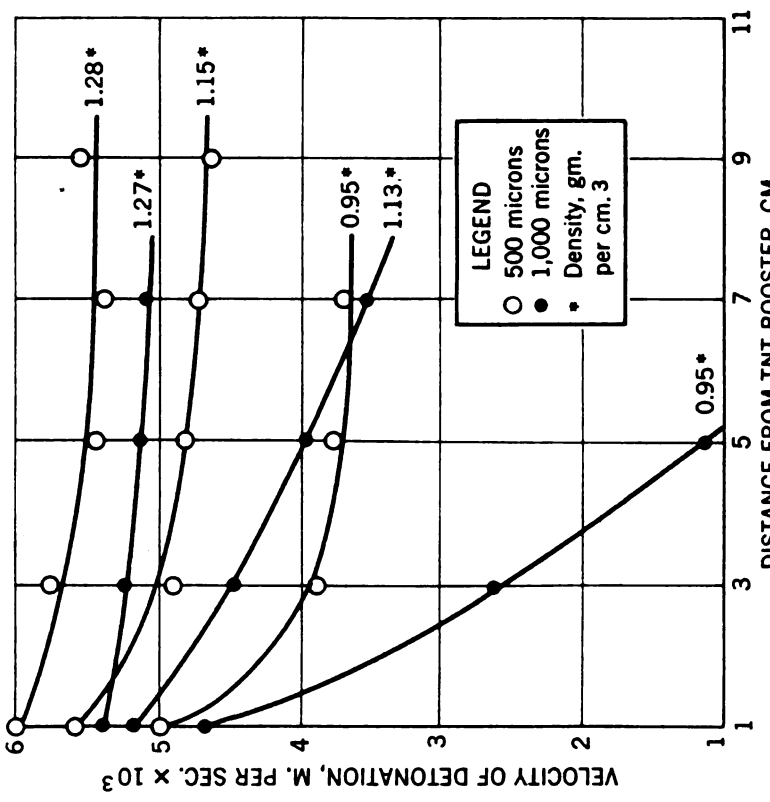

Figure 7. - Velocity of detonation decay for TNT of 500- and 1,000-micron particle size at 3 loading densities for each size.

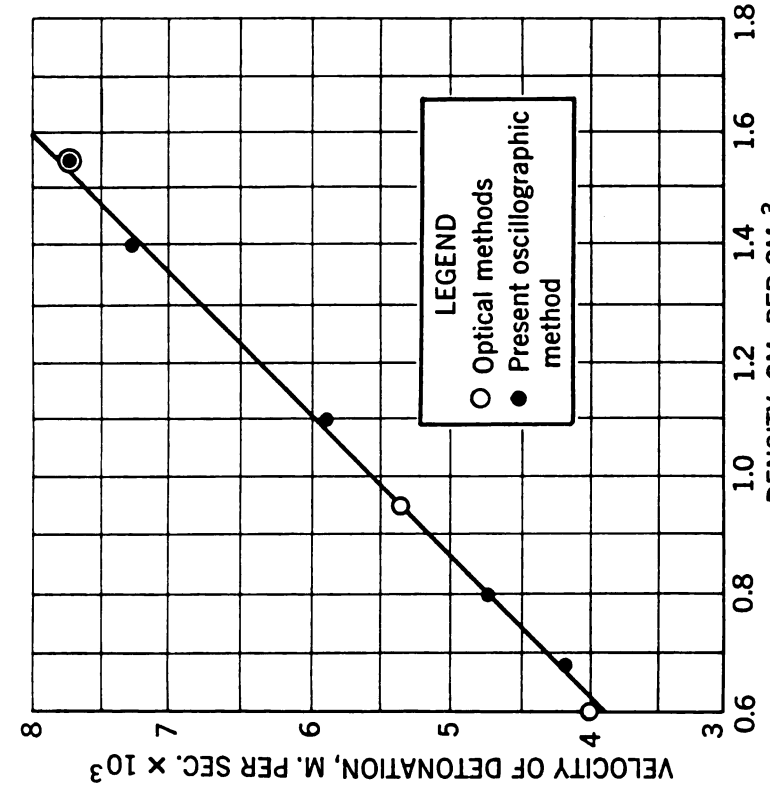

Figure 6. - Velocity of detonation vs. density relationship for PETN; comparison of data accumulated by oscillographic method with those by optical methods.

Generated on 2024-09-21 14:30 GMT / https://hdl.handle.net/2027/osu.32435030643506
Public Domain, Google-digitized / http://www.hathitrust.org/access_use#pd-google
Digitized by Google
Original from THE OHIO STATE UNIVERSITY

to waves with finite reaction rate.[11] The classical hypothesis of Chapman and Jouguet that the detonation velocity is the minimum velocity compatible with the conservation laws has been confirmed for waves of this type. The stability has been demonstrated of a class of "sub-ideal Chapman-Jouguet detonations" resulting from the incomplete release to the detonation front of the chemical energy of the explosive. Although limited to the plane detonation wave, this study permits a qualitative discussion of two-dimensional effects, such as the charge-diameter effect and the limit of detonability. It offers a conceptual framework in which more detailed investigations can be carried out.

Explosibility of Ammonium Nitrate

The existence of an explosive hazard associated with the manufacture, storage, and transportation of ammonium nitrate has been clearly indicated by the disasters at Oppau, Germany, in 1921; at Tessenderloo, Belgium, in 1942; and in this country at Texas City, Tex., in 1947. The importance and extent of this hazard in the United States may be judged from the large amount of ammonium nitrate produced and transported annually. It is estimated that, from July 1947 to June 1948, the United States produced 461,528 tons of ammonium nitrate for agricultural purposes alone. In addition, Army Ordnance plants manufactured and shipped 779,730 tons of ammonium nitrate fertilizer to Germany, Japan, and Korea. These considerations, and especially the 1947 disaster at Texas City, led the Bureau of Mines to investigate the explosibility of ammonium nitrate.[12]

Evidence collected following the Texas City disaster[13] pointed to heat as one of the causes of the explosion; however, as it is known that ammonium nitrate can burn without detonating, the work of the Bureau was directed toward determining conditions under which ammonium nitrate explodes when heated. A survey of the literature[14] having indicated that confinement might be an important factor, tests were made to study the simultaneous effects of confinement and heat on ammonium nitrate. In addition, possible spontaneous heating of ammonium nitrate was investigated by placing thermocouples in the holds of a Liberty-type ship during the loading of an ammonium nitrate fertilizer shipment and recording the temperature during the passage from Louisiana to the Panama Canal Zone in hot weather.

Bomb Tests

Source and Composition of Samples.- Thirteen bomb tests were run on chemically pure ammonium nitrate, 16 tests on fertilizer-grade ammonium nitrate (FGAN), and 29 tests on fertilizer-grade ammonium nitrate, plus 1.5 percent by weight of bag paper. Nineteen tests were made to determine the effect of inert diluents, such as chalk, limestone, dolomite, etc.

11/ Brinkley, S. R., Jr., and Richardson, J. M., On the Structure of Plane Detonation Waves With Finite Reaction Velocity: 4th Symposium (International) on Combustion, Williams & Wilkins Co., Baltimore, Md., 1953, pp. 450-457.

12/ Burns, J. J., Scott, G. S., Jones, G. W., and Lewis, B., Investigations on the Explosibility of Ammonium Nitrate: Bureau of Mines Rept. of Investigations 4994, 1953, 19 pp.

13/ Kintz, G. M., Jones, G. W., and Carpenter, C. B., Explosions of Ammonium Nitrate Fertilizer on Board the SS. Grandcamp and SS. High Flyer at Texas City, Tex., April 16 and 17, 1947: Bureau of Mines Rept. of Investigations 4245, 1948, 57 pp.

14/ Scott, G. S., and Grant, R. L., Ammonium Nitrate: Its Properties and Fire and Explosion Hazards: Bureau of Mines Inf. Circ. 7463, 1948, 32 pp.

Generated on 2024-09-21 14:36 GMT / https://hdl.handle.net/2027/osu.32435030643506
Public Domain, Google-digitized / http://www.hathitrust.org/access_use#pd-google
Digitized by Google
Original from THE OHIO STATE UNIVERSITY

The materials used in this investigation included three 100-pound samples of fertilizer-grade ammonium nitrate (M-8136, M-8137, M-8138) obtained in the Texas City area and manufactured by the 3 ordnance plants that had supplied the material on the ships where the explosions occurred. An additional 100-pound sample (M-8120) from pier "O" at Texas City was collected by the Coast Guard after the explosions. Table 1 gives analytical data for the physical, chemical, and explosive properties of these samples.

TABLE 1. - Physical and chemical properties of ammonium nitrate fertilizer, Texas City, Tex.

Sample No.	M-8120	M-8136	M-8137	M-8138
Source	Unknown	Iowa Ordnance Plant	Cornhusker Ordnance Plant	Nebraska Ordnance Plant
Sample obtained from	Pier O, Texas City, Tex.	Car LC-15181, Galveston, Tex.	Pier 38, Galveston, Tex.	Car PM-89262 Texas City, Tex.
	Chemical analysis of whole sample			
	Percent	Percent	Percent	Percent
Moisture[1/]	0.18	0.05	0.09	0.02
Ammonium nitrate	94.85	96.08	95.73	95.92
Coating	.81	.74	.73	2/.88
Kaolin	4.16	3.13	3.45	3.18
	Ultimate analysis of coating material			
Carbon	84.80	84.16	83.70	78.40
Hydrogen	14.06	13.90	13.88	10.42
	Screen analysis - U. S. Standard screens			
Retained on No. 8 screen	0.00	0.00	0.00	0.00
Passed through 8 on 35	91.55	86.75	97.00	84.50
Passed through 35 on 100	8.05	12.50	2.50	14.75
Passed through 100 on 200	.05	.35	.25	.25
Passed through 200	.35	.40	.25	.50
Ammonium nitrite	.00124	.00184	.00194	.00112

1/ Includes ammonium nitrite.
2/ Coating contains rosin.

Apparatus and Procedure.- In the bomb tests, 5-pound charges of nitrate were packed into seamless steel tubes that were closed at one end and had vents measuring up to 3/4 inch in diameter at the other (fig. 8). These bombs were wired for electric heating using electrical-energy inputs up to about 1,700 watts. Thermocouples, peened into the bomb shell and inserted in wells inside the charge, were connected to a recorder. The charged bombs were placed in a bombproof shelter (building X-73) and the tests were carried out by remote control (building X-77, fig. 9). The heat input to the bomb was controlled by two variable transformers. Time-temperature records were made throughout each run. Examples are given for chemically pure ammonium nitrate (fig. 10); fertilizer-grade ammonium nitrate (fig. 11); and fertilizer-grade ammonium nitrate plus 1.5 percent bag paper (fig. 12).

The degree of confinement was varied by inserting plugs containing various size openings (0 to 3/4 inch in diameter) into the hole through which the bomb was loaded.

Generated on 2024-09-21 14:31 GMT / https://hdl.handle.net/2027/osu.32435030643506
Public Domain, Google-digitized / http://www.hathitrust.org/access_use#pd-google
Digitized by Google
Original from THE OHIO STATE UNIVERSITY

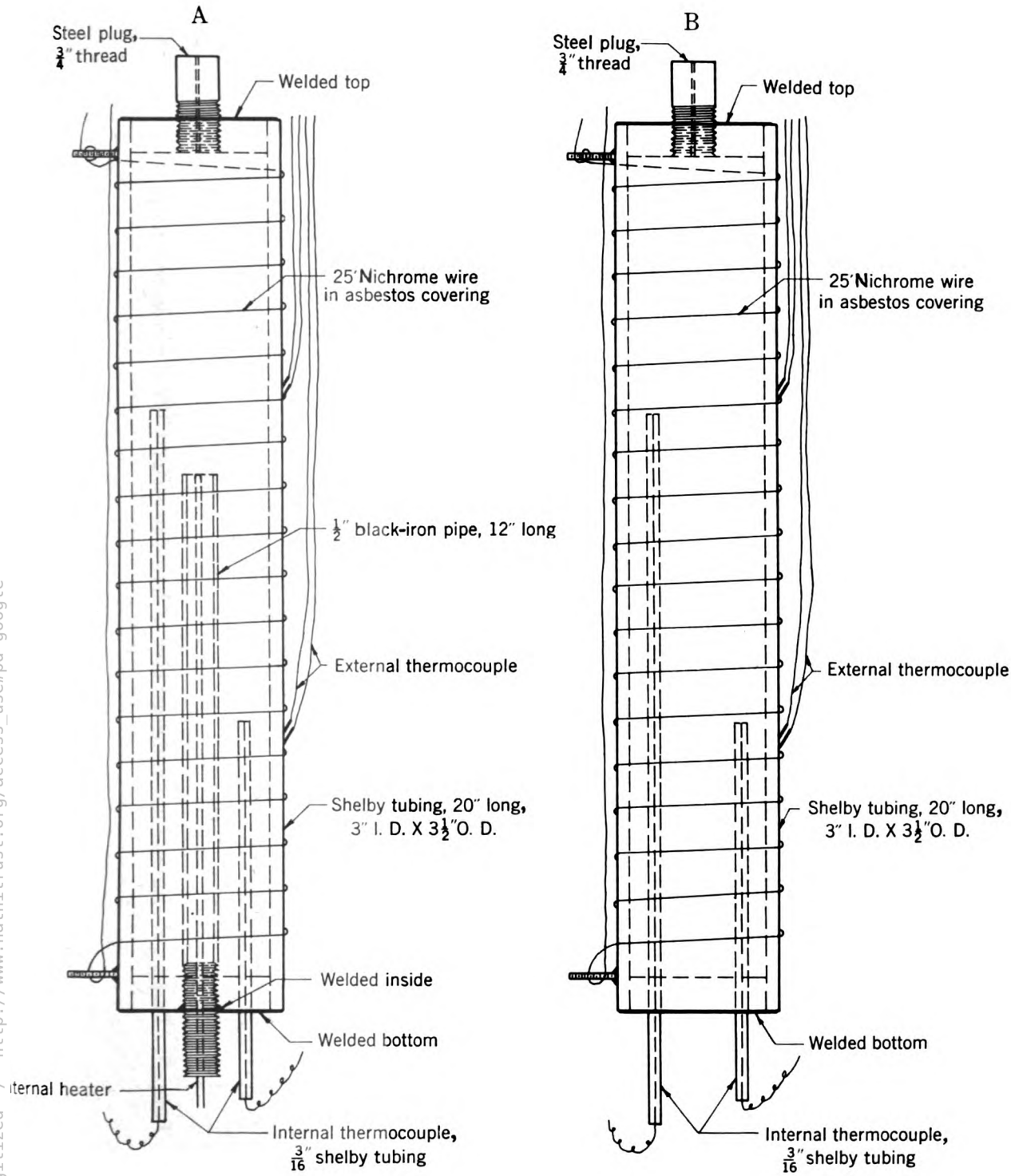

Figure 8. - Bombs used for testing ammonium nitrate.

Generated on 2024-09-21 14:40 GMT / https://hdl.handle.net/2027/osu.32435030643506
Public Domain, Google-digitized / http://www.hathitrust.org/access_use#pd-google
Digitized by Google
Original from THE OHIO STATE UNIVERSITY

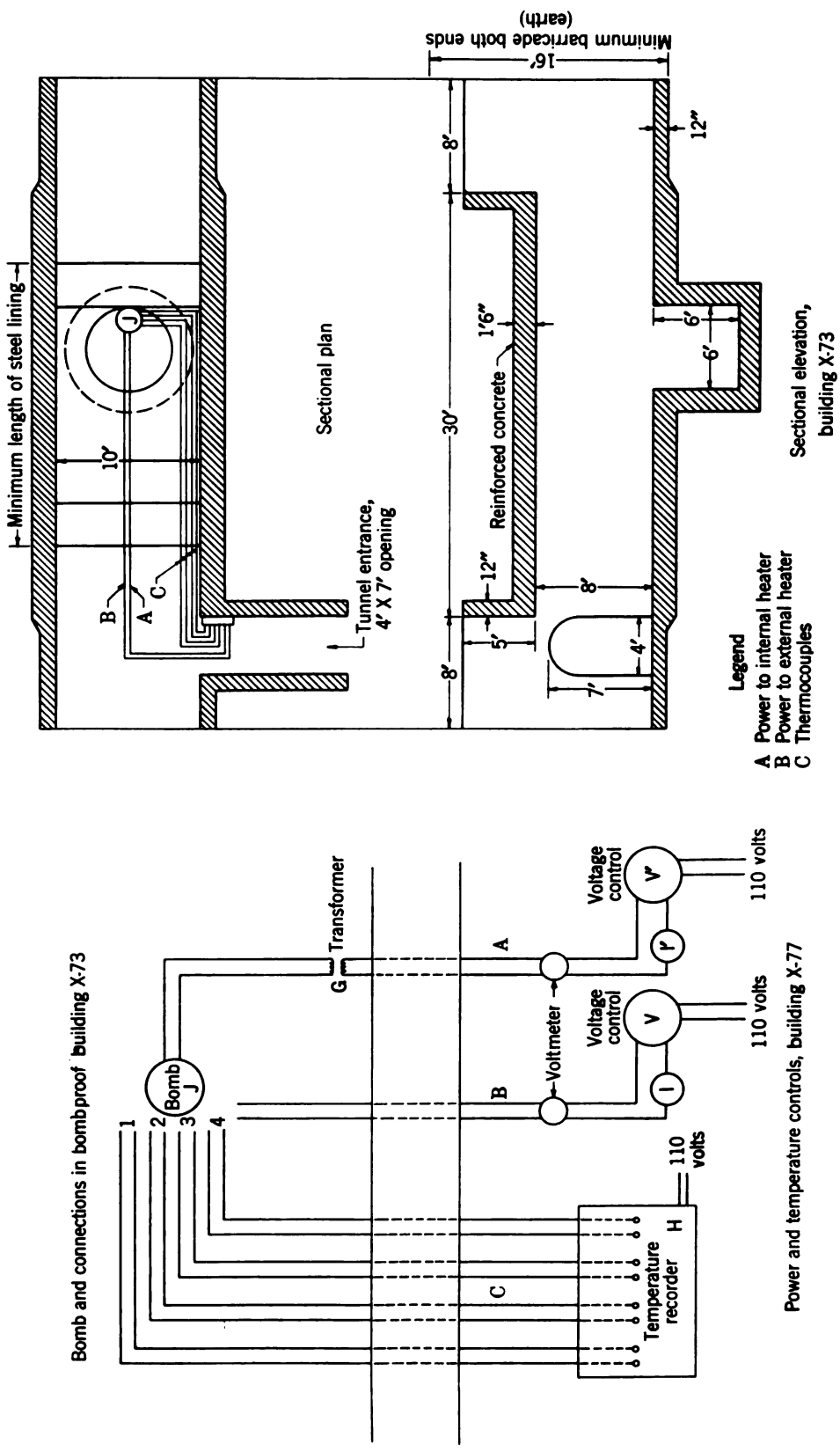

Figure 9. - Diagram of apparatus and equipment used to determine explosibility of ammonium nitrate.

Generated on 2024-09-21 14:37 GMT / https://hdl.handle.net/2027/osu.32435030643506
Public Domain, Google-digitized / http://www.hathitrust.org/access_use#pd-google
Digitized by Google
Original from THE OHIO STATE UNIVERSITY

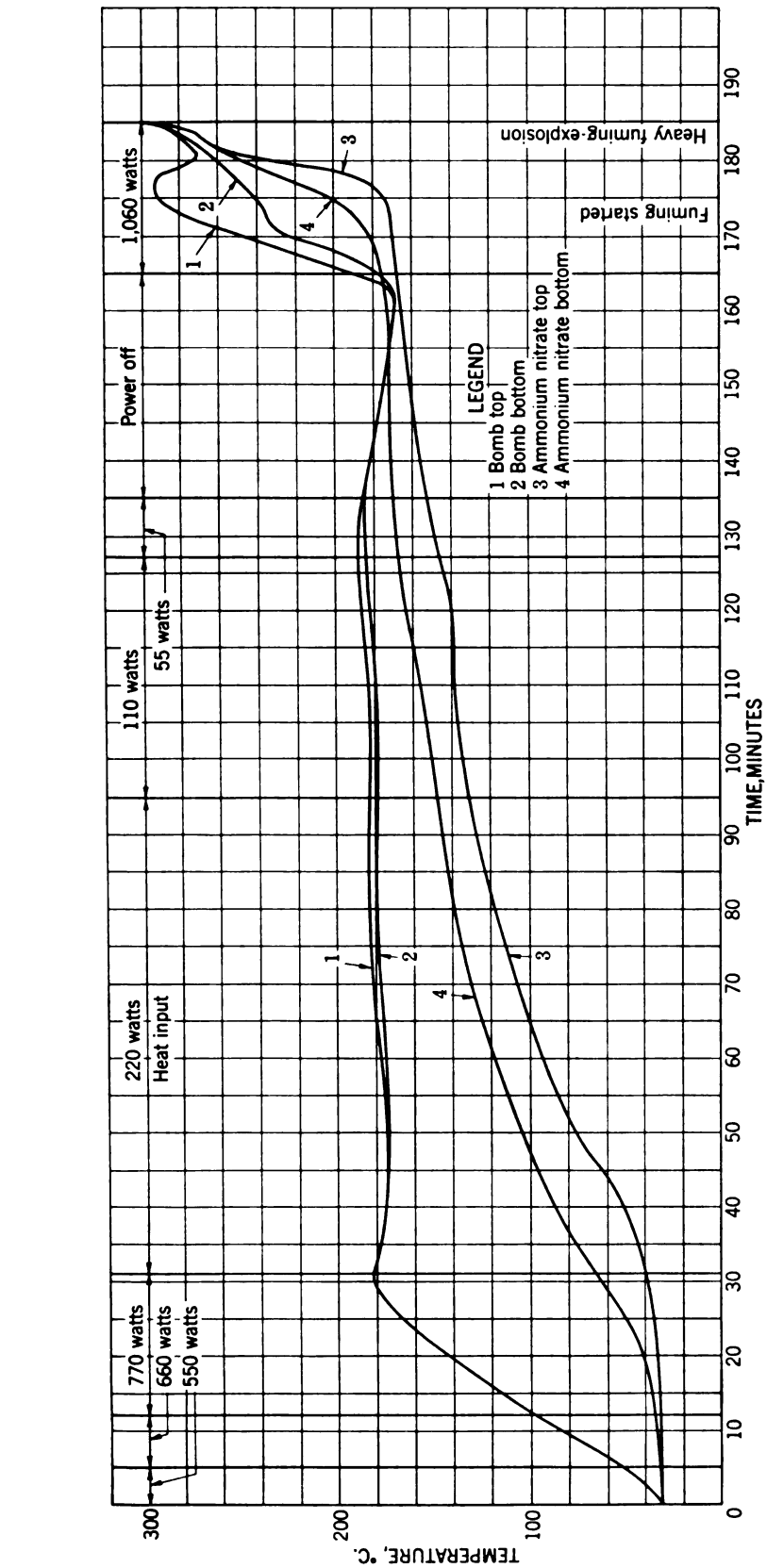

Figure 10. - Bomb test—temperature data: Test 27, C. P. ammonium nitrate (M-8188).

Generated on 2024-09-21 14:34 GMT / https://hdl.handle.net/2027/osu.32435030643506
Public Domain, Google-digitized / http://www.hathitrust.org/access_use#pd-google
Digitized by Google
Original from THE OHIO STATE UNIVERSITY

Generated on 2024-09-21 14:39 GMT / https://hdl.handle.net/2027/osu.32435030643506
Public Domain, Google-digitized / http://www.hathitrust.org/access_use#pd-google

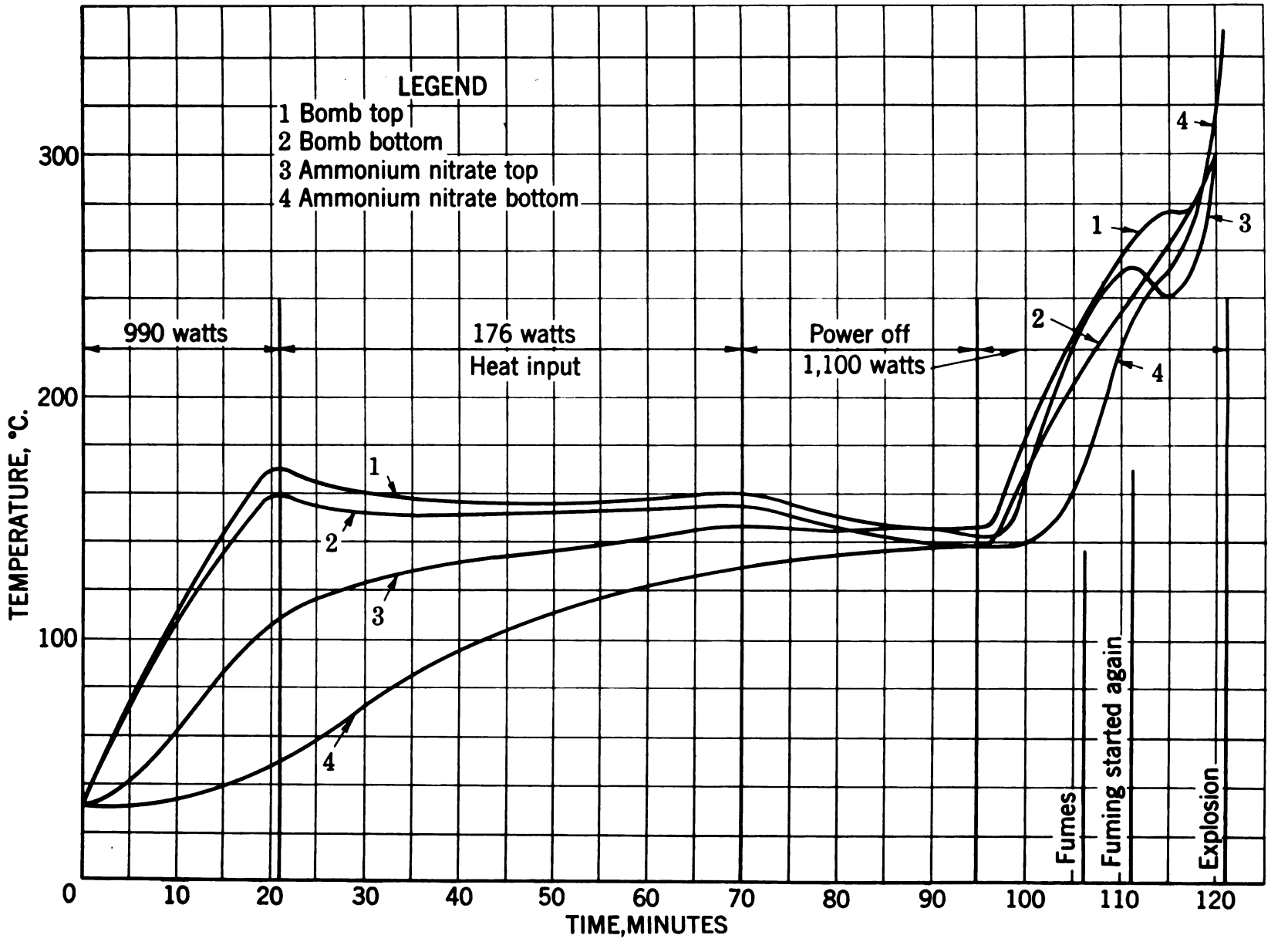

...data: Test 45, ammonium nitrate fertilizer (M-8137) (with internal heater).

Digitized by Google
Original from THE OHIO STATE UNIVERSITY

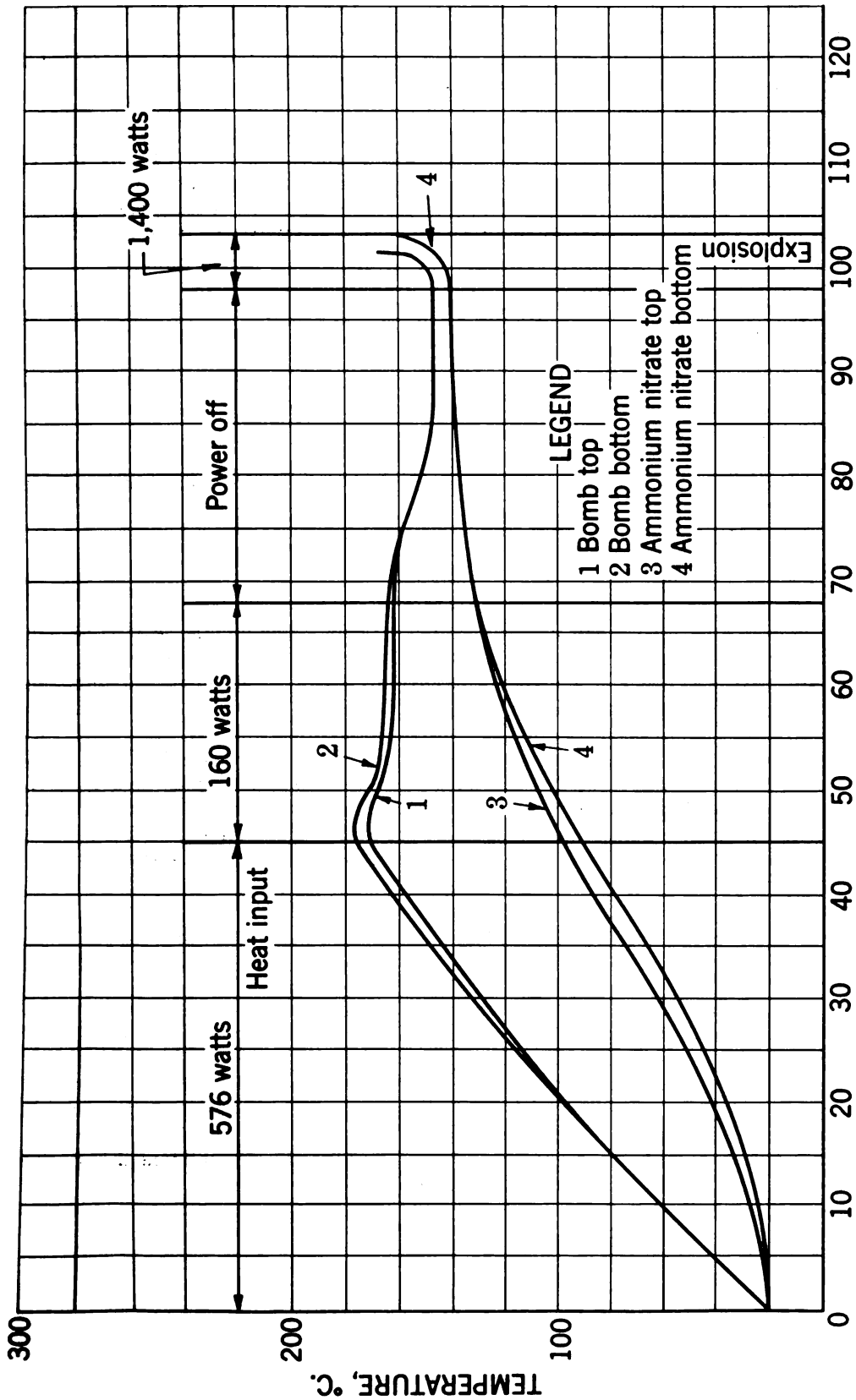

Figure 12. - Bomb test–temperature data: Test 55, ammonium nitrate fertilizer (M-8138) + 1.5 percent of bag paper (with internal heater).

Generated on 2024-09-21 14:36 GMT / https://hdl.handle.net/2027/osu.32435030643506
Public Domain, Google-digitized / http://www.hathitrust.org/access_use#pd-google
Digitized by Google
Original from THE OHIO STATE UNIVERSITY

As it was observed that when the vents were larger than 1/8 inch the confinement was not generally enough to cause explosion at the heating rate employed, 15 tests were made to determine the order of magnitude of the pressures developed up to the point of explosion of the nitrate. In some tests the gas-release vent plugs were replaced by conventional pressure-relief valves, calibrated rupture disk, etc.

In tests where no explosion occurred, it was noted that most or all of the ammonium nitrate fumed off. To obtain some idea of the actual amount of ammonium nitrate taking part in the explosions, a few tests were made in which the bombs were quenched at or near the explosion point and weighed to determine the amount of nitrate lost during heating.

Results of Bomb Tests.-In analyzing the results of the bomb tests various factors were considered:

(1) The degree of fragmentation of the bomb produced by the explosion: High fragmentation (13 or more fragments); low fragmentation (12 or less fragments); ruptures (end blown off or plug expelled); bomb intact.

(2) The degree of confinement of the charge, based on the diameter of the vent.

(3) The temperature immediately preceding the explosion.

(4) Fuming and fuming loss.

Tests for chemically pure ammonium nitrate, fertilizer-grade ammonium nitrate, and fertilizer-grade ammonium nitrate plus bag are summarized in tables 2, 3, and 4, respectively. Figure 13 shows a typical example of high fragmentation obtained for degrees of confinement corresponding to a vent diameter of 1/8 inch or less.

Tests with inert diluents showed that, in general, addition of about 25 percent of chalk, dolomite, magnesite, or diatomite-limestone mixture to ammonium nitrate makes it nonexplosive. However, in 2 tests enough pressure was developed with mixtures containing over 40 percent inert to blow out the end of the bomb, indicating that thorough mixing of the ingredients is essential and that fineness of the diluent probably is important.

Results of tests to determine the pressures at which explosions of ammonium nitrate occurred are summarized in table 5.

Conclusions. - Explosions were observed with chemically pure ammonium nitrate at temperatures between 277° and 344° C. and pressures between 2,600 and 3,000 p.s.i.; with ammonium nitrate fertilizer at temperatures between 114° and 350° C. and pressures between 2,000 and 2,600 p.s.i.; and with ammonium nitrate fertilizer plus carbonaceous material (1.5 percent bag paper) at temperatures between 134° and 153° C. and pressures between 250 and 300 p.s.i. It was concluded that the explosion hazard of ammonium nitrate can be decreased materially by adding 25 percent, by weight, of an inert diluent, such as limestone.

Generated on 2024-09-21 14:32 GMT / https://hdl.handle.net/2027/osu.32435030643506
Public Domain, Google-digitized / http://www.hathitrust.org/access_use#pd-google
Digitized by Google
Original from THE OHIO STATE UNIVERSITY

Figure 13. - Bomb fragments, test 55.

Generated on 2024-09-21 14:34 GMT / https://hdl.handle.net/2027/osu.32435030643506
Public Domain, Google-digitized / http://www.hathitrust.org/access_use#pd-google
Digitized by Google
Original from
THE OHIO STATE UNIVERSITY

Generated on 2024-09-21 14:34 GMT / https://hdl.handle.net/2027/osu.32435030643506
Public Domain, Google-digitized / http://www.hathitrust.org/access_use#pd-google

TABLE 2. - Bomb tests with pure ammonium nitrate

Test No.	Vent diam., inch	Size of bomb, inches	Bomb heated	Temperature of charge, ° C.		Time of heating, min.		Interval from fuming to explosion, min.	Remarks
				When fuming began	When explosion occurred	When fuming began	When explosion occurred		
35	1/8	3 by 20	Externally	270-300	304-306	138	140	2	Bomb exploded. 24 fragments.
58	1/8	3 by 20	do.	228-236	277-283	146	151	5	Bomb exploded. 11 fragments.
29	1/8	3 by 20	do.	226-260	306	164	170	6	Bomb exploded. 20 fragments.
27	1/8	3 by 20	do.	202-230	300	179	188	9	Bomb exploded. 37 fragments.
49	1/8	4-1/2 by 20	do.	260-262	294-300	258	266	8	Bomb exploded. 22 fragments.
57	1/8	3 by 20	Externally and internally	143-151	284-334	109	122	13	Bomb exploded. 7 fragments.
48	1/4	4-1/2 by 20	Externally	254-257	-	284	-	-	Bomb intact.
28	1/4	3 by 20	do.	226-239	-	168	-	-	Do.
30	3/16	3 by 20	do.	252-258	-	173	-	-	Do.
31	3/16	3 by 20	do.	260-280	-	173	-	-	Do.
47	1/2	4-1/2 by 20	do.	257-259	-	218	-	-	Do.
6	1/2	3 by 20	do.	260	-	110	-	-	Do.
46	3/4	4-1/2 by 20	do.	143-146	-	271	-	-	Do.

Digitized by Google
Original from THE OHIO STATE UNIVERSITY

Generated on 2024-09-21 14:39 GMT / https://hdl.handle.net/2027/osu.32435030643506
Public Domain, Google-digitized / http://www.hathitrust.org/access_use#pd-google

TABLE 3. - Bomb tests with ammonium nitrate fertilizer (bomb, 3 by 20 inches)

Test No.	Vent diam., inch	Bomb heated	Temperature of charge, ° C.		Time of heating, min.		Interval from fuming to explosion, min.	Remarks
			When fuming began	When explosion occurred	When fuming began	When explosion occurred		
1	Closed	Externally	No fumes	114-235	81	81	0	Bomb exploded. 36 fragments.
45	1/8	Externally and internally	159-217	304-350	107	121	14	Bomb exploded. 34 fragments.
13	1/8	Externally	195-200	200	105	106	1	Bomb exploded. 2 fragments.
34	1/8	do.	183-209	200-210	154	155	1	Bomb exploded. 3 fragments.
39	1/8	do.	No fumes	115-150	50	50	0	Bomb exploded. 4 fragments.
53	1/8	Externally and internally	do.	255-259	141	141	0	Bomb exploded. 8 fragments.
56	1/8	do.	150-162	182-203	116	118	2	Bomb exploded. 5 fragments.
26	1/4	Externally	177-202	177-202	193	194	1	Bomb exploded. 4 fragments.
51	1/8	Externally and internally	182-201	190-205	120	122	2	Bomb exploded. 4 fragments.
8	1/16	Externally	120-140	145-195	98	104	6	Bomb ruptured. End blown off.
11	1/8	do.	182-185	303-306	44	58	14	Do.
38	1/8	do.	171-197	175-197	90	91	1	Do.
42	1/8	do.	146-230	296-302	158	169	11	Do.
43	1/8	Externally	169-178	173-189	151	153	2	Do.
44	1/8	Externally and internally	220	-	36	-	-	Bomb intact.
9	1/8	Externally	144-154	-	100	-	-	Do.
33	3/16	do.	189-225	-	169	-	-	Do.
7	1/4	do.	109-143	-	95	-	-	Do.
23	1/4	do.	198	-	147	-	-	Do.
24	1/4	do.	162-182	-	207	-	-	Do.
25	1/4	do.	170-172	-	304	-	-	Do.
32	1/4	do.	160-194	-	160	-	-	Do.
21	3/8	do.	175-180	-	187	-	-	Do.
2	1/2	do.	138-180	-	103	-	-	Do.
3	1/2	do.	110-235	-	100	-	-	Do.
4	1/2	do.	95-195	-	95	-	-	Do.
5	1/2	do.	110-230	-	102	-	-	Do.
22	3/4	do.	189-210	-	199	-	-	Do.
18	1	do.	142-147	-	167	-	-	Do.

Digitized by Google
Original from THE OHIO STATE UNIVERSITY

Generated on 2024-09-21 14:35 GMT / https://hdl.handle.net/2027/osu.32435030643506
Public Domain, Google-digitized / http://www.hathitrust.org/access_use#pd-google

TABLE 4. - Bomb tests with ammonium nitrate fertilizer plus 1.5 percent of paper-bag container (bomb, 3 by 20 inches)

Test No.	Vent diam., inch	Bomb heated	Temperature of charge, ° C.		Time of heating, min.		Interval from fuming to explosion, min.	Remarks
			When fuming began	When explosion occurred	When fuming began	When explosion occurred		
61	Closed	Externally and internally	No fumes	134-136	120	120	0	Bomb exploded. 33 fragments.
50	1/8	do.	do.	142-143	104	104	0	Bomb exploded. 30 fragments.
54	1/8	do.	do.	144-146	95	95	0	Bomb exploded. 41 fragments.
55	1/8	do.	do.	140-153	103	103	0	Bomb exploded. 43 fragments.
60	1/4	do.	136-142	181-191	94	98	4	Bomb exploded. 27 fragments.
16	1/8	Externally	139-152	152	158	159	1	Bomb exploded. 6 fragments.
17	1/8	do.	No fumes	140-142	151	151	0	Bomb exploded. 11 fragments.
36	1/8	do.	do.	145-177	136	136	0	Bomb exploded. 4 fragments.
40	1/8	do.	do.	148	167	167	0	Bomb exploded. 5 fragments.
37	3/16	do.	do.	161-189	118	118	0	Bomb exploded. 4 fragments.
19	1/4	do.	144-147	145-148	168	171	3	Bomb exploded. 2 fragments.
10	1/8	do.	141-143	141-143	90	90	0	Bomb ruptured. End blown off.
41	5/32	do.	135-151	136-209	162	165	3	Do.
12	1/8	do.	No fumes	150-200	117	117	0	Vent plug blown out.
20	3/8	do.	162-169	-	215	-	-	Bomb intact. NH_4NO_3 boiled out.
59	1/2	Externally and internally	144-151	-	135	-	-	Do.

Digitized by Google
Original from THE OHIO STATE UNIVERSITY

Generated on 2024-09-21 14:30 GMT / https://hdl.handle.net/2027/osu.32435030643506
Public Domain, Google-digitized / http://www.hathitrust.org/access_use#pd-google

TABLE 5. - Results of pressure measurements

Test No.	Pressure measurement: Apparatus	Pressure measurement: Pressure, p.s.i.	Temperature of charge, ° C.: When fuming began	Temperature of charge, ° C.: When explosion occurred	Time of heating, min.: When fuming began	Time of heating, min.: When explosion occurred	Interval from fuming to explosion, min.	Remarks
			Pure ammonium nitrate					
80	Strain gage	?	147-148	306-315	115	134	19	Pressure built up to 4,000 p.s.i.; dropped to 400 p.s.i.; was 250 p.s.i. when bomb exploded. 15 fragments recovered. 1/
81	do.	?	167-237	302-311	110	118	8	Pressure increased gradually to 800 p.s.i. at time of explosion. 40 fragments recovered. 1/
98	Rupture disk	2,582	256-258	-	90	-	-	Disk burst. Charge boiled out. Bomb intact.
97	do.	3,022	224-229	301-330	132	139	7	Bomb exploded. 8 fragments.
			Fertilizer-grade ammonium nitrate					
14	Relief valve	50	120-170	-	87	-	-	Charge boiled out. Bomb intact.
72	Rupture disk	630	147-173	-	97	-	-	Disk burst. Charge boiled out. Bomb intact.
68	Relief valve	700	144-162	-	94	-	-	Charge boiled out. Bomb intact.
73	Rupture disk	1,210	153-190	-	91	-	-	Disk burst. Charge boiled out. Bomb intact.
95	do.	2,000	-	-	-	-	-	Do.
96	do.	2,582	-	145-218	-	99	-	Bomb exploded. 16 fragments recovered.
94	do.	3,022	-	148-184	-	80	-	Do.
			Fertilizer-grade ammonium nitrate + 1.5 percent bag paper					
15	Relief valve	100	150	-	-	72	-	Charge boiled out. Bomb intact.
65	do.	250	132-133	-	84	-	-	Do.
93	do.	300	-	132-140	-	71	-	Bomb exploded.
66	do.	400	-	134-138	-	81	-	Bomb exploded. 54 fragments recovered.

1/ These pressure results are doubtful, as operation of strain-gage equipment appeared to be abnormal.

Digitized by Google
Original from THE OHIO STATE UNIVERSITY

Spontaneous Evolution of Heat During Stowage and Transportation on Shipboard

Spontaneous reaction of ammonium nitrate with its environment (coating material used to prevent caking, containers, dunnage, etc.) would generage heat, constituting an explosion hazard. Accordingly, the possibility of such a reaction was investigated.

For this purpose, temperature-measuring apparatus was installed throughout the cargo in two holds of the Liberty-type ship SS. Henry T. Scott carrying a shipment of ammonium nitrate to Korea, and temperature measurements were made between the point of origin, Braithwaite, La., and the Panama Canal Zone.[15/] The nitrate was packed in six-ply waterproofed paper bags of the type used for packaging the nitrate that exploded at Texas City. When fully loaded, the ship had a draft of 27.3 feet, with the nitrate distributed as follows (fig. 14):

Hold	Volume of hold, cubic feet	Dimensions of hatch	Long tons, including bags
1	76,077	33 ft. 9 in. by 20 ft.	1,532.0
2	134,638	35 ft. by 20 ft.	2,070.5
3	83,697	20 ft. by 20 ft.	1,967.0
4	82,263	35 ft. by 20 ft.	1,620.5
5	82,435	35 ft. by 20 ft.	1,362.0
Total..	459,110		8,552.0

Before loading, the holds were well-cleaned, and the bottom was covered with two layers of rough boards. Waterproofed paper was placed against the sides and bulkheads, around the propeller-shaft tunnel, and against other metal parts. Bags were piled 64 deep in the bottom holds. When the lower hold was filled, the hatch was closed on the 'tween deck, and the 'tween-deck hold was loaded in the same manner.

Ten thermocouples were installed in hold 3 and 9 in hold 4. Figure 14 gives the location of the various thermocouple "hot junctions" and the "cold junctions" (marked C. J.). The highest temperature observed in either hold was 107° F. Maximum temperatures at the firewall on the machinery side were 151° F. (port), 136° (center), and 140° (starboard). Barometer readings varied between 29.89 and 30.08 inches of mercury. The relative humidity varied between 74 and 93 percent during loading and between 90 and 97 percent during the trip to Cristobal.

Figure 15 shows the average temperature of the 19 thermocouples in the 2 holds, the sea temperature, and the air temperature, plotted against time. The average temperature in the two holds is between the sea and air temperatures, with no tendency to rise above them, indicating that no heat was generated in the holds. The average hold temperatures tend to follow the air temperatures, indicating effective ventilation.

Conclusions. - Although research by the United States Department of Agriculture[16] has shown that certain ammonium nitrate-organic matter mixtures can heat spontaneously, the tests on the SS. Henry T. Scott gave no evidence of spontaneous heating in the bagged fertilizer-grade ammonium nitrate.

15/ Through courtesy of Lykes Bros. Steamship Co.

16/ Hardesty, J. O., and Davis, R. O. E., Spontaneous Development of Heat in Mixed Fertilizers: Ind. Eng. Chem., vol. 38, No. 12, 1946, pp. 1298-1303.

Generated on 2024-09-21 14:32 GMT / https://hdl.handle.net/2027/osu.32435030643506
Public Domain, Google-digitized / http://www.hathitrust.org/access_use#pd-google
Digitized by Google
Original from THE OHIO STATE UNIVERSITY

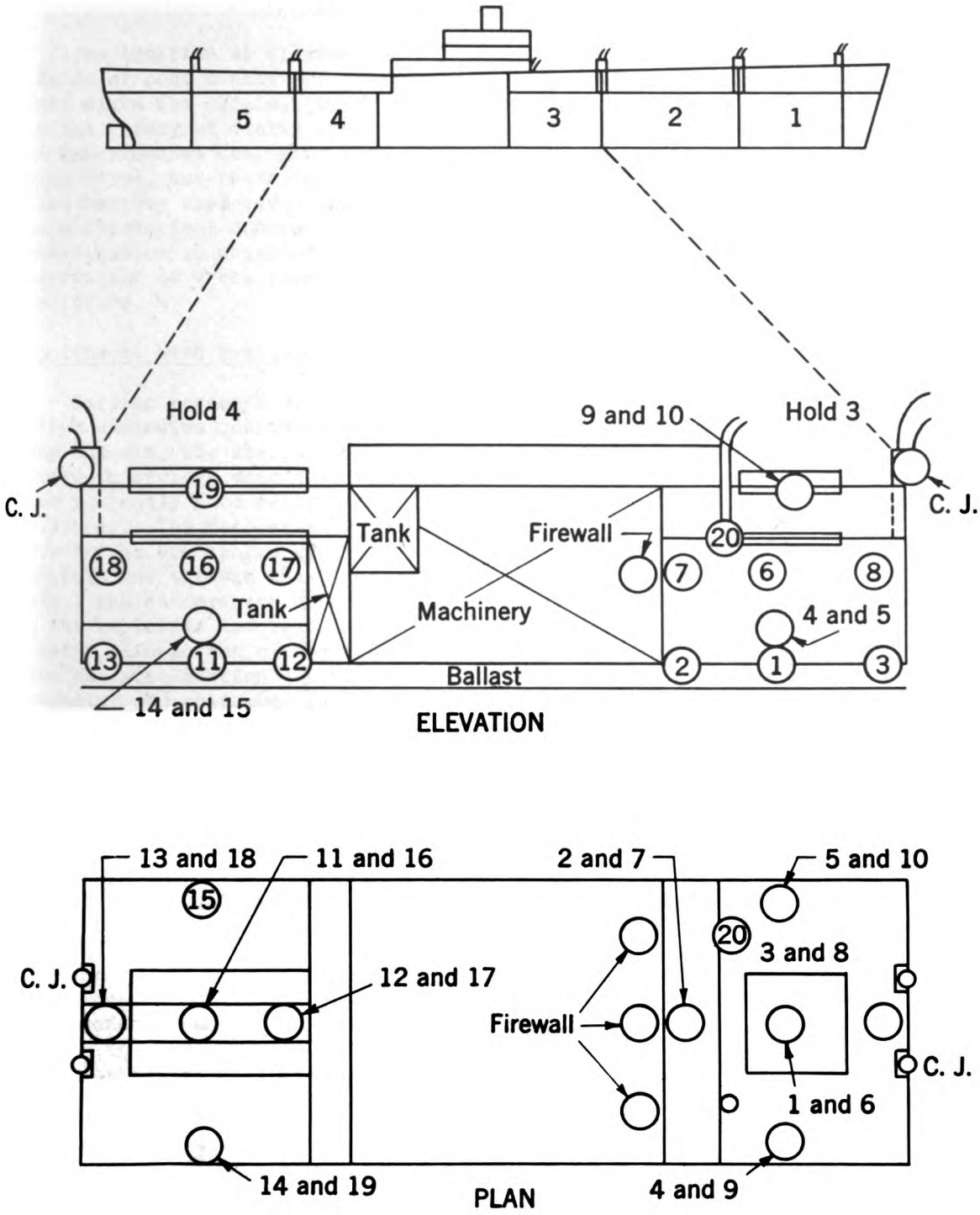

Figure 14. - Location of thermocouples in holds 3 and 4, SS. Henry T. Scott, May-June 1947.

Generated on 2024-09-21 14:39 GMT / https://hdl.handle.net/2027/osu.32435030643506
Public Domain, Google-digitized / http://www.hathitrust.org/access_use#pd-google
Digitized by Google
Original from
THE OHIO STATE UNIVERSITY

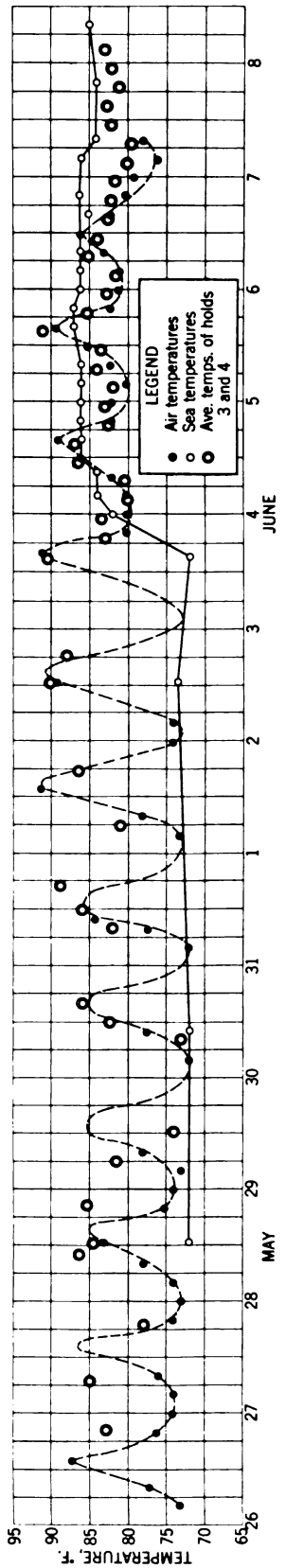

Figure 15. - Time-temperature plot.

Generated on 2024-09-21 14:34 GMT / https://hdl.handle.net/2027/osu.32435030643506
Public Domain, Google-digitized / http://www.hathitrust.org/access_use#pd-google
Digitized by Google
Original from
THE OHIO STATE UNIVERSITY

Ignition of Firedamp by Explosives

The ignition of firedamp during blasting of coal constitutes one of the major hazards of coal mining and as such is a problem that has confronted the Bureau of Mines since its origin. Over the years, development of standard tests for evaluating the safety of mining explosives and extensive research on blasting procedures in the Experimental Coal Mine have done much to improve the safe use of explosives in gassy mines, but there remained the need for information on the fundamental mechanism whereby explosives ignite firedamp. To study this problem and obtain evidence for a theoretical concept of firedamp ignition, the division undertook a systematic investigation in which modern methods of high-speed photography were applied to the observation of shots fired into firedamp atmospheres under carefully controlled conditions.

Experiments With Small-Bore Cannon

Earlier research by the Bureau of Mines and others[17/] had indicated that when a high explosive confined in a borehole is fired into a flammable mixture of firedamp and air, the sequence of events may be visualized as follows: First, the explosive cartridge detonates within the borehole, converting the solid explosive almost instantly into substantially gaseous material at very high pressures and temperatures. The detonation wave that travels along the cartridge sets up a shock wave in the atmosphere at the end of the charge. The shock wave moves out of the borehole and through the firedamp-air atmosphere, followed by the detonation products. The temperature of these products is determined by the chemical composition of the explosive and by the energy expended in work done within the borehole - plastic deformation of the steel in case of a shot from a steel cannon; fragmentation and acceleration of rock; shock waves generated in the medium surrounding the borehole. In unstemmed shots the first products to emerge from the borehole are always luminous and are followed by gases that usually are nonluminous. This luminous discharge - the primary flame - frequently disappears, and a secondary flame subsequently forms outside the borehole by reaction of the combustible constituents of the detonation products with the oxygen of the atmosphere. In some instances the secondary flame is a continuation of the primary flame. It does not develop at all in the absence of oxygen.

If the detonation does not convert all of the solid material into gases, solid particles are ejected from the borehole behind the shock wave and primary flame. Traveling at almost constant velocity, these particles soon overtake the decelerating shock wave, some of them piercing it to produce open, cored, and blistered prominences. Subsequent processes are more complex, involving reflected shock waves and secondary combustion phenomena.

Consideration of the role of compression, heat conduction, and diffusion in the ignition process led to the concept of folds or pockets in the boundary layer between the burning gases and the surrounding firedamp-air atmosphere, acting as focal ignition points (fig. 16). High-speed photographs have been obtained showing the existence of such annular pockets.

17/ Grant, R. L., Mason, C. M., von Elbe, G., and Lewis, B., Progress in Research on the Mechanism of Ignition of Firedamp by Explosives: Pres. at 6th Internat. Conf. of Directors of Mine-Safety Research, Verneuil, France, July 24-29, 1950; pub. in Rev. ind. min., vol. 32, 1951, pp. 486-490.

Generated on 2024-09-21 14:35 GMT / https://hdl.handle.net/2027/osu.32435030643506
Public Domain, Google-digitized / http://www.hathitrust.org/access_use#pd-google
Digitized by Google
Original from THE OHIO STATE UNIVERSITY

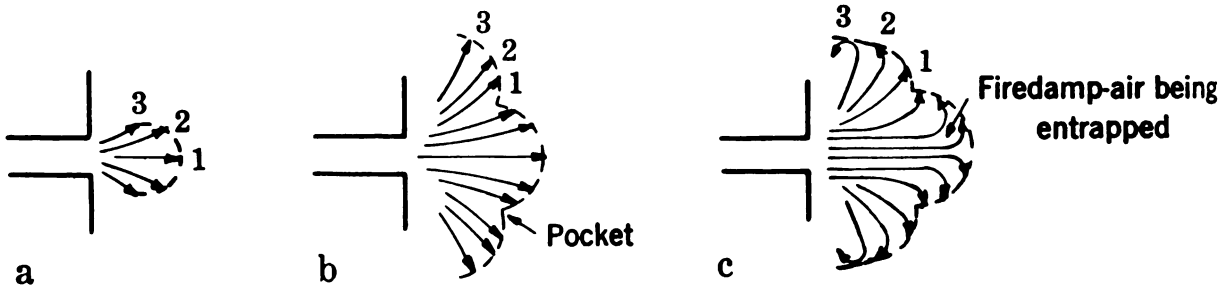

Figure 16. - Schematic diagrams showing flow of streamlines and entrapment of natural gas-air in pockets within hot gaseous products.

The way in which the detonation products mix with the firedamp atmosphere is of major importance in determining ignition. It involves principles of fluid dynamics, formation of vortex rings, turbulence, and disturbances in the flow pattern of the shock wave, flame, and products cloud occasioned by obstacles in front of the borehole or restrictions simulating crevices or breaks in coal seams.

In addition to developing a hypothesis of firedamp ignition, earlier research had shown that the most informative studies in this field were those that applied photographic techniques, such as the rotating drum camera and schlieren flash photographs. However, these techniques were not well-suited to the large experimental galleries previously used for ignition studies. The first step was to develop a suitable experimental set-up, the problem being to establish adequate controls over the borehole and its charge of explosives and the firedamp-air environment in which the explosive products were discharged.

To this end, the arrangement of an explosive in a borehole was studied, and a test procedure was developed in which the many variables considered to have a bearing on incendivity were eliminated or controlled. Next, the reproducibility and dimensions of the flame and products cloud emitted from the borehole were determined by still and high-speed photography. This provided a basis for constructing a small experimental gallery to study the natural gas-air atmosphere. Simultaneously, a suitable technique of high-speed photography, using the Fastax camera at 7,500 photographs per second, was developed and adapted to this gallery.

Figure 17 is the diagram of a small cannon cross section. These cannon were made of cold-rolled mild steel. They were 3 inches in diameter and 5 inches in length, with a continuous 5/16-inch-diameter borehole (tolerances held to ± 0.002 inch throughout). The small gallery into which the cannon were fired (fig. 18) is a square chamber with a volume of 45 cubic feet (3 by 3 by 5 feet), compared with a volume of 628 cubic feet for the conventional gallery. It is made of an open framework of welded angle iron bolted to a substantial substructure. To protect the glass observation windows, one end of the gallery is covered with a paper diaphragm, which vents the explosion. To eliminate variations due to change in the borehole dimensions after firing, a new cannon was used for each shot.

The explosive charge in all tests was tetryl, rear-initiated by 1 gram of 80-20 mercury fulminate-potassium chlorate, initiated in turn by a small copper acetylide match head ignited electrically. This type of initiation eliminated certain variables associated with the use of conventional detonators. Tests showed that a 1-gram charge of fulminate-chlorate fired alone from the borehole did not ignite an 8-percent natural gas-air atmosphere. Tetryl was chosen because it is a pure compound having a particle size and loading density that are readily controlled. It has an oxygen balance of -47.3 percent and produces quantities of unburned carbon when detonated.

Generated on 2024-09-21 14:31 GMT / https://hdl.handle.net/2027/osu.32435030643506
Public Domain, Google-digitized / http://www.hathitrust.org/access_use#pd-google
Digitized by Google
Original from THE OHIO STATE UNIVERSITY

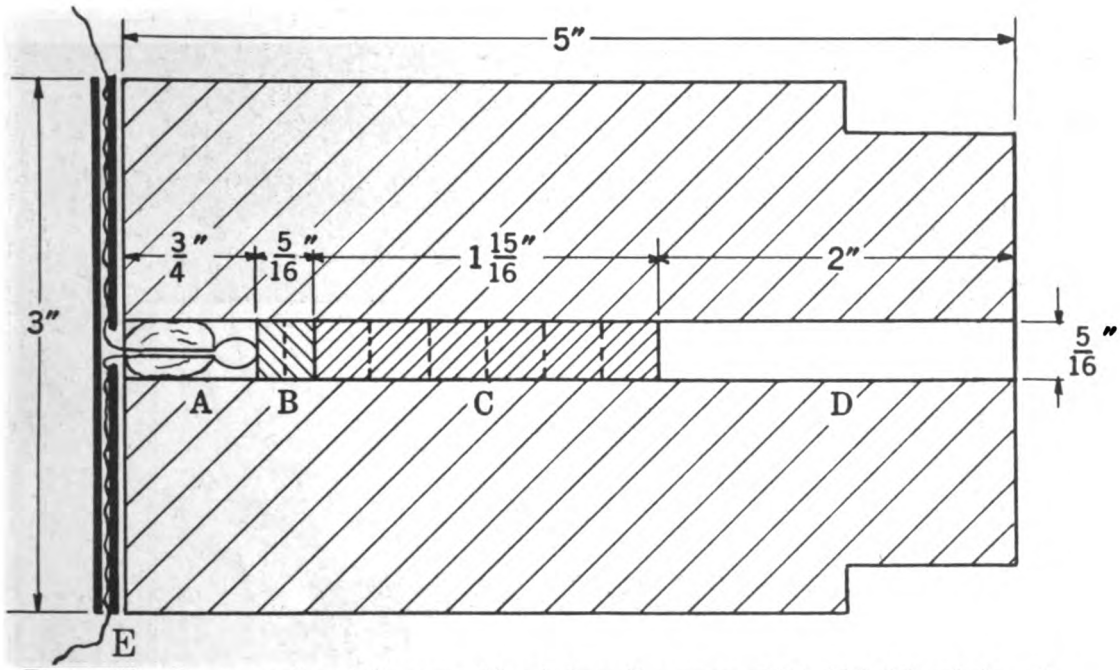

Figure 17. - Cross-sectional diagram of loaded small cannon with half-full borehole: A, Copper acetylide match head wrapped in glass tape; B, 1.0-gram fulminate-chlorate loaded in 0.5-gram increments pressed at 750 p.s.i.; C, 3.0 grams tetryl loaded in 0.5-gram increments pressed at 1,000 p.s.i.; D, 2 inches of free space; E, legwires between 2 asbestos disks.

High-speed photographs were taken with a Wollensak, 8-mm., Fastax camera operated at 7,500 frames per second, with an exposure about 1/30,000 second. In the first photographs taken the flame alone provided illumination, and the photograph lacked detail. Subsequently, incident light from a high-intensity carbon arc (200 amp. at 40 volts) plus several banks of 500- and 750-watt incandescent photospot lamps were directed onto the flame and products cloud. The resulting photographs showed both the luminous and nonluminous portions of the cloud. The camera was equipped with an automatic delay switch for synchronizing the shot and a small light pip that served as a time base on the film.

The experimental work was divided into three phases:

(1) To establish the limiting weight of tetryl, for which ignition occurred consistently, increasing weights of tetryl were fired from small (5-inch) cannon into the large (628-cubic-foot) gallery filled with an 8-percent natural gas-air mixture.[18/] The resulting data were used to plot ignition probability (I.P.) against various weights of tetryl (fig. 19). The most striking feature of this curve is the rapid rise to a maximum for the half-full borehole, followed by an almost equally rapid drop as the borehole is filled with tetryl.

(2) A photographic study was made of the size, nature, flow pattern, and reproducibility of the flame and the cloud issuing from the borehole. The resulting data were used to determine the dimensions required for the small gallery.

(3) Small cannon were fired into the small gallery filled with various atmospheres. Two types of experiments were conducted:

18/ Natural gas: 90 percent methane and 9 percent ethane.

Generated on 2024-09-21 14:35 GMT / https://hdl.handle.net/2027/osu.32435030643506
Public Domain, Google-digitized / http://www.hathitrust.org/access_use#pd-google
Digitized by Google
Original from THE OHIO STATE UNIVERSITY

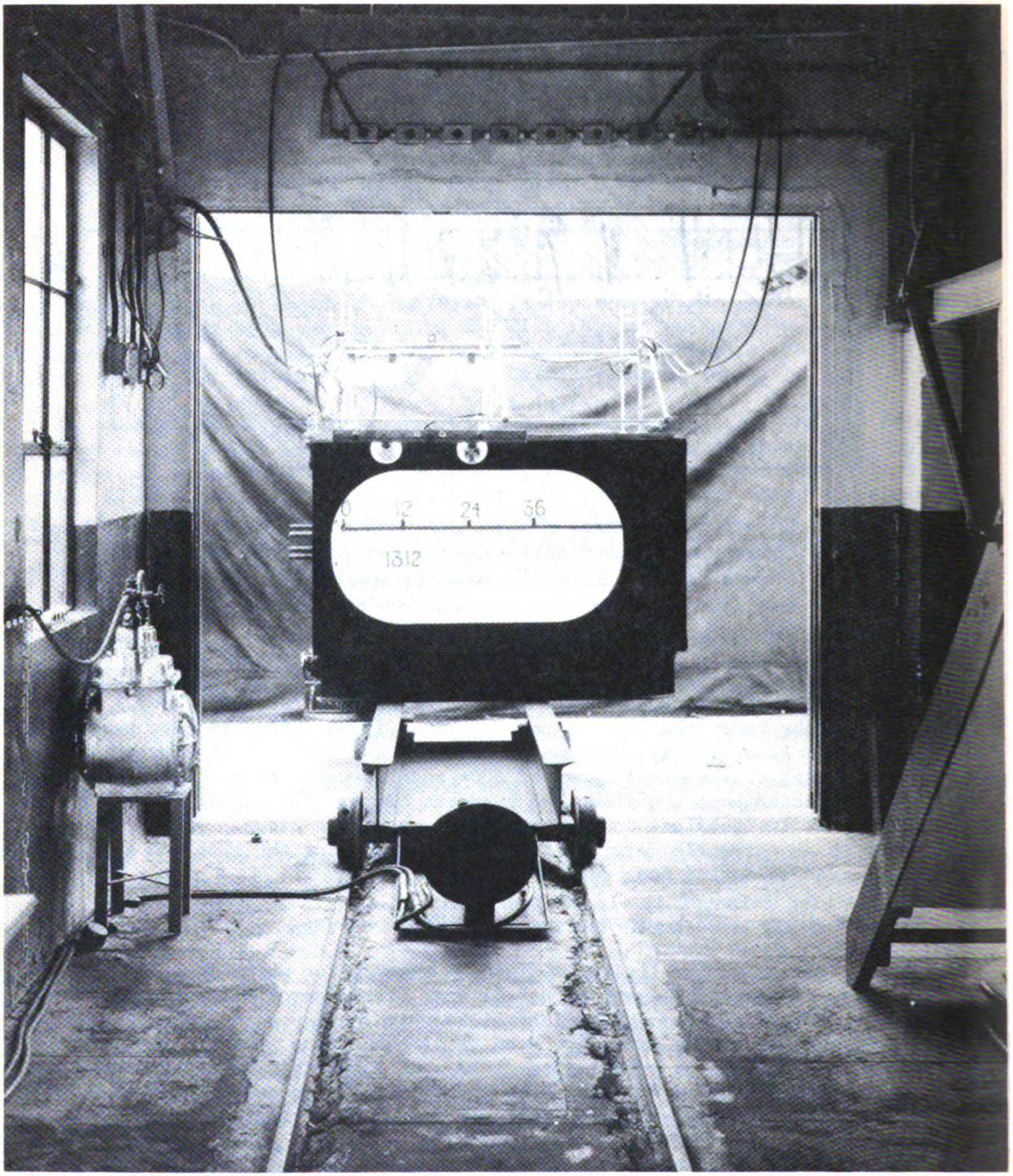

Figure 18. - Small experimental gallery, taken from position of Fastax camera.

Generated on 2024-09-21 14:36 GMT / https://hdl.handle.net/2027/osu.32435030643506
Public Domain, Google-digitized / http://www.hathitrust.org/access_use#pd-google
Digitized by Google
Original from THE OHIO STATE UNIVERSITY

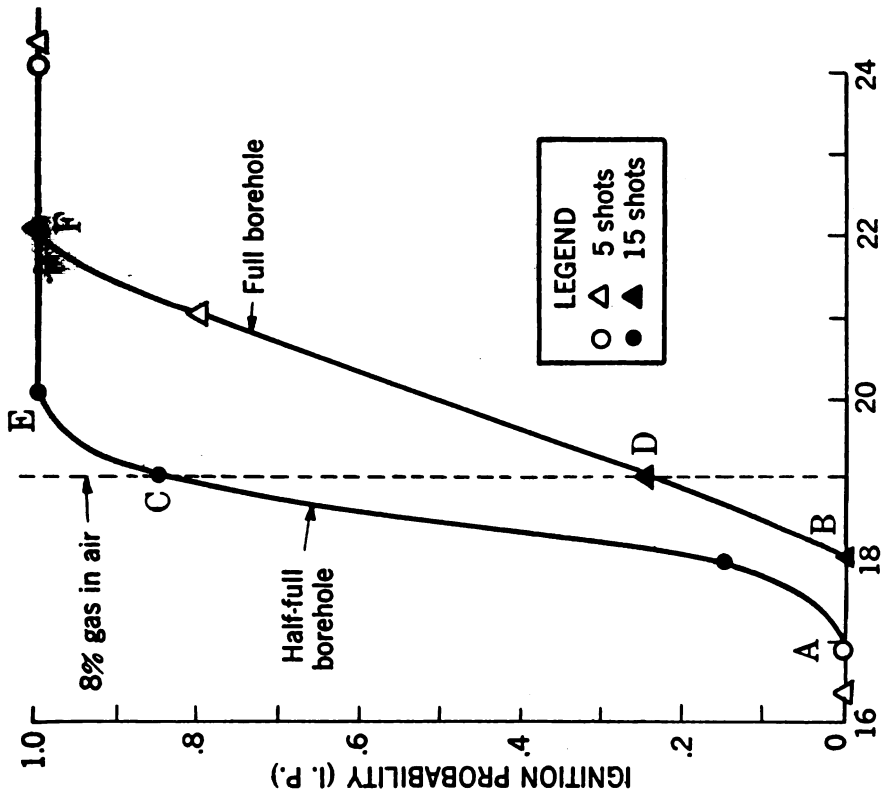

Figure 20. - Effect of oxygen content of gallery atmosphere on ignition probability.

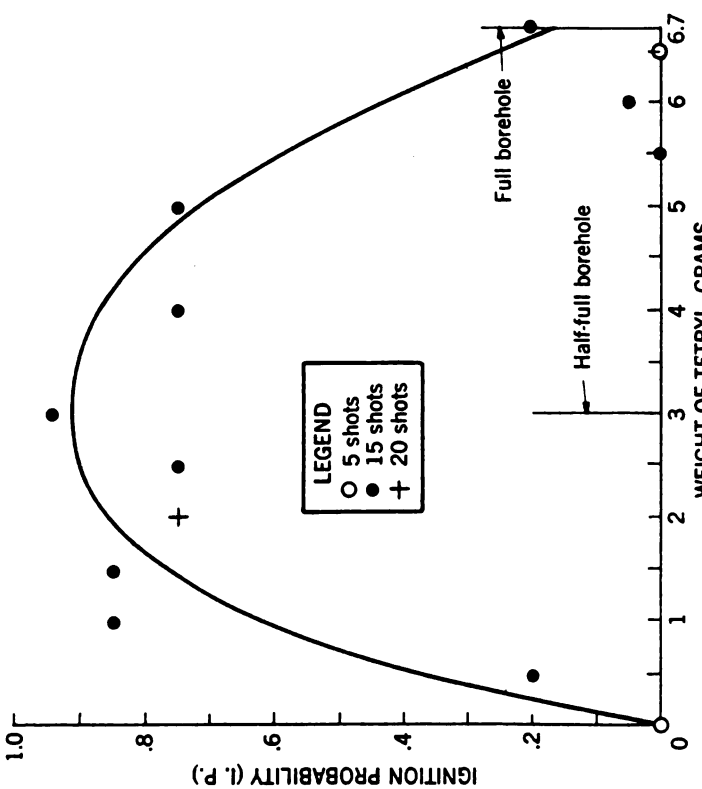

Figure 19. - Results of experiments with 5-inch small cannons fired into 8-percent natural gas-air mixture in large gallery.

Generated on 2024-09-21 14:35 GMT / https://hdl.handle.net/2027/osu.32435030643506
Public Domain, Google-digitized / http://www.hathitrust.org/access_use#pd-google
Digitized by Google
Original from THE OHIO STATE UNIVERSITY

(a) Experiments to determine the influence of various factors (oxygen content of the gallery atmosphere, charge weight) on the I.P., which was found to change from 0 to 1 over a narrow range of oxygen concentrations (fig. 20). The position of this range is determined by the loading condition (full and half-full borehole);

(b) High-speed photography of shots fired under conditions for which the I.P. has been determined. If, as postulated, the primary flame corresponds to the discharge of high-temperature gas from the borehole and the secondary flame corresponds to the reaction of combustible constituents of the products cloud with the oxygen of the atmosphere, the primary flame should be unaffected by the oxygen concentration whereas the secondary flame should be greatly influenced by it. This is borne out by figures 21 and 22, in which the oxygen concentrations are 6 and 32 percent, respectively. Use was made of oxygen-deficient atmospheres to isolate and observe the primary flame (fig. 23), which is very brilliant and extremely short lived (~1/30,000 sec.).

Calculated adiabatic detonation temperatures of explosives such as tetryl lie between 3,500° and 4,000° C. In this range both the suspended particles and the gases are highly luminous. The primary flame[19/] probably owes its brilliant luminosity to the fact that the first gas to issue from the borehole has expended little of its energy in work. In photographs of shots where the oxygen content of the gallery atmosphere was very low, the primary flame is rapidly enveloped by the dark cloud of detonation products. The darkness of this cloud indicates that its temperature is well below 1,000° C. and that a very large fraction of its internal energy is spent in deforming the cannon borehole (fig. 24). The assumption that the work done in deforming the borehole is largely responsible for the low temperature of the products issuing from the borehole is consistent with the observation that the ignition probability is higher for the half-loaded cannon where deformation is restricted to the loaded part of the borehole (fig. 24). In the full borehole the entire space undergoes a funnellike deformation. As a consequence, the flow of products from an incompletely loaded borehole is much less rapid than from a completely loaded borehole. The primary flame from the latter is enveloped and cooled more effectively by the dark detonation products. In the case of an underoxidized explosive, such as tetryl, the product cloud is dark and opaque due to free carbon and can burn in the oxygen of the ambient atmosphere. In an oxygen-deficient atmosphere the primary flame rapidly vanishes, whereas it develops when enough oxygen is present. At this stage the combustion reaction is probably supported by methane in the gallery atmosphere, as well as by the combustible contents of the cloud. If permitted to survive, the flame eventually propagates through the explosive mixture in the gallery. However, the region of combustion is subject to eddying disturbances that tend to entrain the burning gas into the oxygen-deficient interior of the cloud, thus quenching the chemical reaction. This breaks the burning gas into patches, which drift with the eddy currents and grow or vanish randomly. Often a patch of flame is observed to grow in the recess between two vortex rings of the products cloud, in accordance with the "pocket" theory of ignition developed by Lewis and von Elbe.[20/] However, in any

19/ More recent studies with the image-converter camera have shown that the primary flame is the smear produced by the luminosity of the shock wave, which the Fastax camera is too slow to resolve.

20/ Lewis, B., and von Elbe, G., Ignition of Firedamp by Explosives: Bureau of Mines Rept. of Investigations 4382, 1948, 11 pp.; see also Lewis, B., and von Elbe, G., Ignition of Firedamp by Explosives: Bureau of Mines Rept. of Investigations 3463, 1939, 11 pp.

Generated on 2024-09-21 14:33 GMT / https://hdl.handle.net/2027/osu.32435030643506
Public Domain, Google-digitized / http://www.hathitrust.org/access_use#pd-google
Digitized by Google
Original from THE OHIO STATE UNIVERSITY

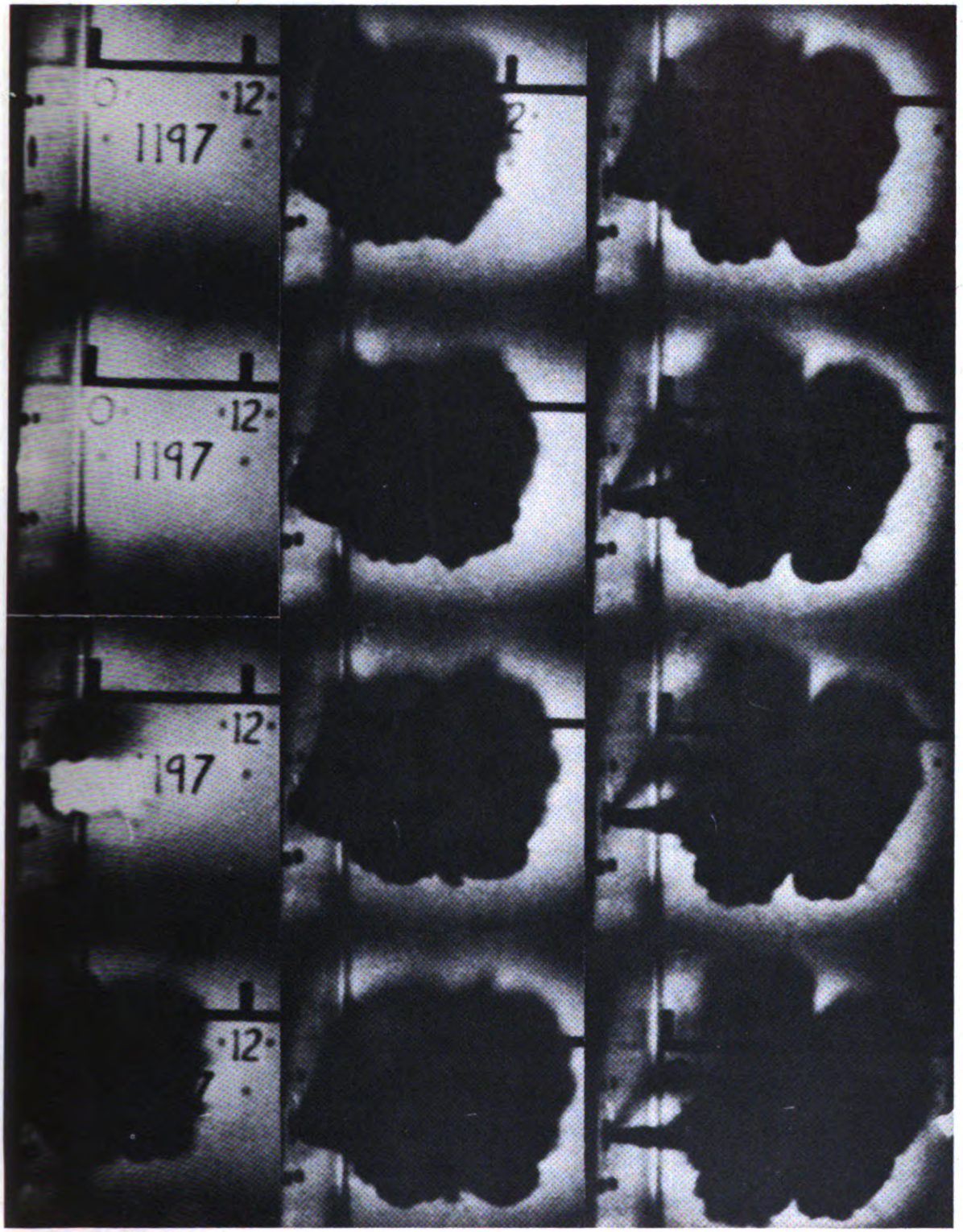

Figure 21. - Shot 1197; half-full borehole side-view small-cannon shot in oxygen-deficient air (6 percent O_2), taken at 7,500 frames per second. Primary flame is shown; secondary flame is absent.

Generated on 2024-09-21 14:33 GMT / https://hdl.handle.net/2027/osu.32435030643506
Public Domain, Google-digitized / http://www.hathitrust.org/access_use#pd-google
Digitized by Google
Original from THE OHIO STATE UNIVERSITY

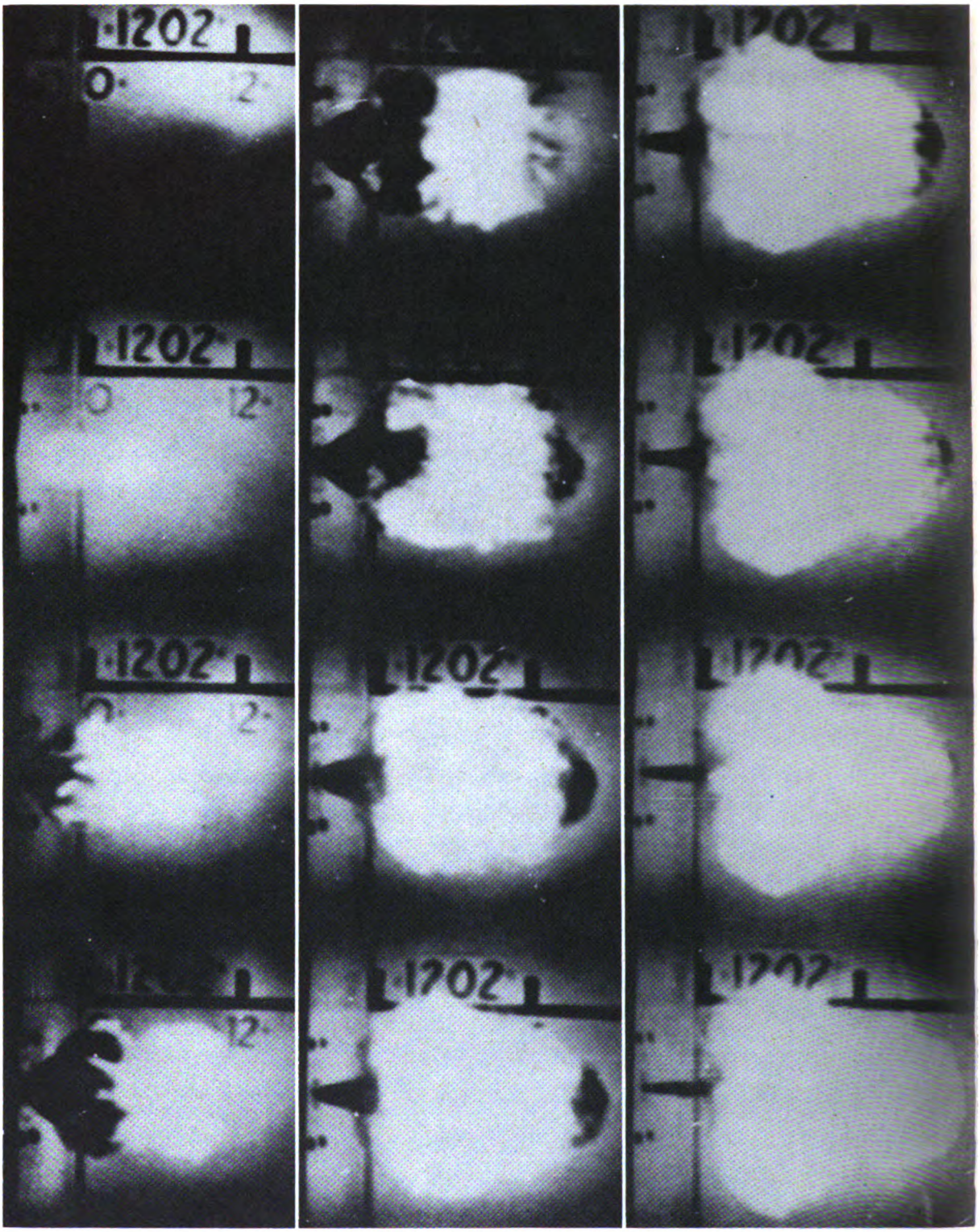

Figure 22. - Shot 1202; half-full borehole side-view small-cannon shot in oxygen-enriched air (32 percent O_2) taken at 7,500 frames per second. Shows rapid development of brilliant secondary flame.

Generated on 2024-09-21 14:33 GMT / https://hdl.handle.net/2027/osu.32435030643506
Public Domain, Google-digitized / http://www.hathitrust.org/access_use#pd-google
Digitized by Google
Original from THE OHIO STATE UNIVERSITY

one experiment, only a few patches of burning gas are formed; under conditions where the chance of survival of an individual patch is about even, the outcome of the experiment - ignition or no ignition - is not predictable. This means that a number of experiments are needed to establish an ignition-probability characteristic of the test conditions.

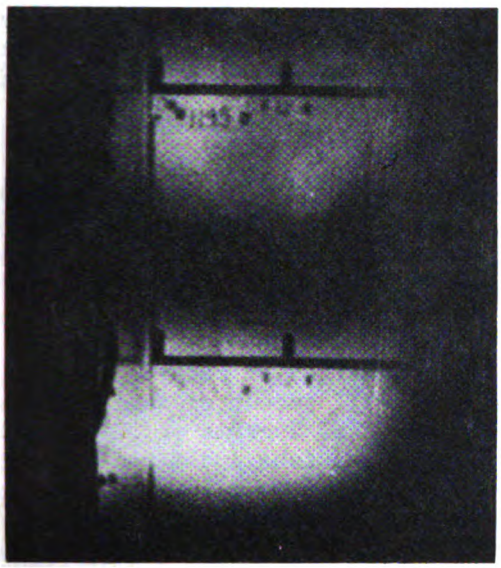

Figure 23. - Brilliant primary flame, as obtained with photograph of shot 1195. Time between first and second frame, 0.125 millisecond.

Systematic variation of the oxygen content of the gallery atmosphere offers a convenient method of studying the ignition probability associated with a given loading condition of the cannon. For any loading condition there should exist an upper limit of oxygen concentration above which ignition is certain and a lower limit below which nonignition is certain. Between these limits ignition is a random occurrence (see fig. 20). The region of oxygen concentration for random ignition is quite

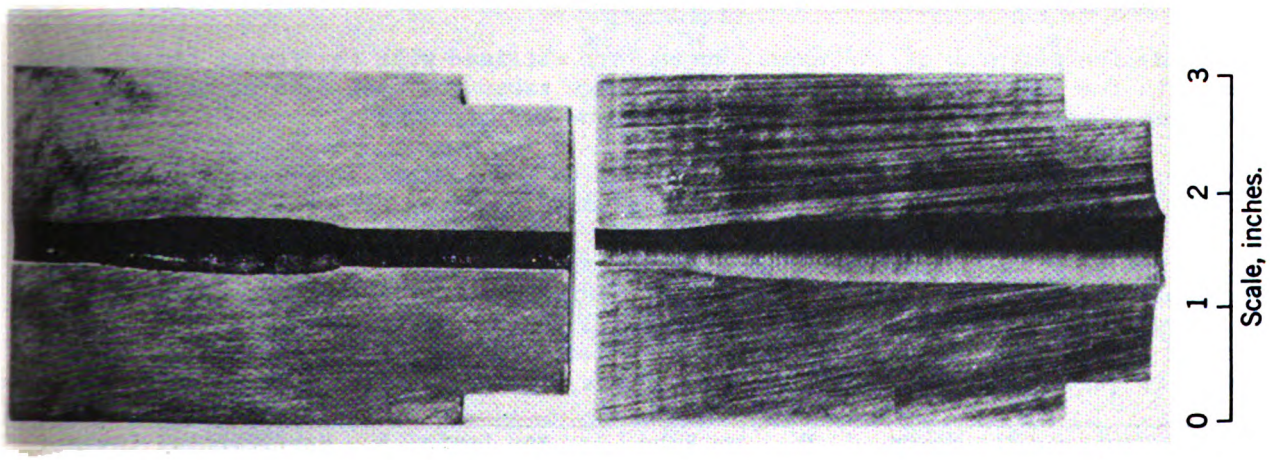

Figure 24. - Cutaway sections of boreholes after firing. Left, half-full; right, full borehole.

Generated on 2024-09-21 14:37 GMT / https://hdl.handle.net/2027/osu.32435030643506
Public Domain, Google-digitized / http://www.hathitrust.org/access_use#pd-google
Digitized by Google
Original from THE OHIO STATE UNIVERSITY

narrow. It is in a higher range of concentration for full borehole shots than for half-full borehole shots, indicating again that a half-full borehole shot is more dangerous than a full borehole shot.

In summary, research indicated that ignition occurs in the initial phase of every shot (formation of primary flame) but that the turbulent cloud of detonation products can quench the incipient flame. Whether or not quenching occurs depends upon the experimental conditions, such as the oxygen concentration of the gallery atmosphere and upon factors influencing the turbulence of the products cloud.

Studies With Suspended Shots

To extend the information of the mechanism of firedamp ignition by explosives a new series of experiments was undertaken, using freely suspended charges.21/ As in the previous investigations (see fig. 20), the incendivities of various shot conditions were compared by plotting the ignition probability (I.P.) against the oxygen content of the gallery atmosphere.

All experiments were performed with 10-gram charges of tetryl prepared by cementing two 5-gram pellets of pure tetyl with a small amount of sodium silicate. The primer was cemented to the charge; it consisted of 2 grams of 80-20 mercury fulminate-potassium chlorate pressed into an asbestos tube and fired with an electric match head. Pure sodium bicarbonate was used as sheathing material for sheathed charges. The primer and the sheathing material were wrapped in double layers of asbestos sheeting (figs. 25 and 26). The gallery was the same small gallery as in the earlier experiments (see fig. 25).

To study the effect of various sheathing conditions, tests were made for each type of sheathing, using gallery atmospheres in which the oxygen-nitrogen ratio was varied systematically for a constant 8-percent methane content. It was found that for each sheathing condition there is one oxygen-nitrogen ratio above which the atmosphere is ignited in every shot and another ratio below which no ignition is obtained in any shot (fig. 27). Within this critical range the I.P. goes from unity to zero. When this range shifts to a higher oxygen content with a change in sheathing type, the incendivity is considered to decrease and vice versa.

Motion pictures of individual shots were obtained with the Fastax camera setup used in the small cannon tests. Pictures were taken for each type of cartridge at the two conditions corresponding to I.P.=0 and I.P.=1.

Figures 28, 29, and 30 show the first five frames for all types of cartridges. As is to be expected, dispersal of an inert dust, such as the sodium bicarbonate used for sheathing, considerably raises the oxygen limit for ignition. By sheathing selected portions of the cartridge it is possible to block off given areas of the explosive surface and thus compare the incendivity of various areas. Inspection of figures 28-31, shows that the jet and central portion of the front face of the main cloud are the most incendive part of the cloud. The rear face of the main cloud also is quite incendive, although it receives some protection from the products cloud

21/ Grant, R. L., Mason, C. M., von Elbe, G., and Lewis, B., Experimental Investigation of the Mechanism of Ignition of Firedamp by Explosives; Studies With Suspended Shots: Pres. at 7th Internat. Conf. of Directors of Mine-Safety Research, Buxton, England, July 7-12, 1952, pub. as Paper 31 by the Safety in Mines Research Establishment, British Ministry of Fuel and Power.

Generated on 2024-09-21 14:32 GMT / https://hdl.handle.net/2027/osu.32435030643506
Public Domain, Google-digitized / http://www.hathitrust.org/access_use#pd-google
Digitized by Google
Original from THE OHIO STATE UNIVERSITY

Generated on 2024-09-21 14:36 GMT / https://hdl.handle.net/2027/osu.32435030643506
Public Domain, Google-digitized / http://www.hathitrust.org/access_use#pd-google

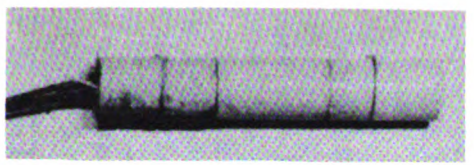

Type 1

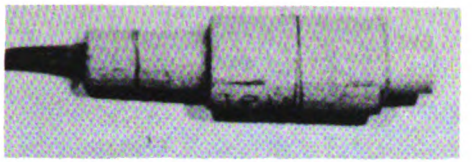

Type 2

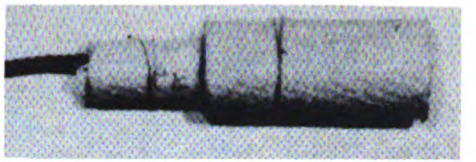

Type 3

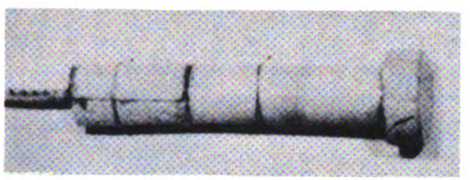

Type 4

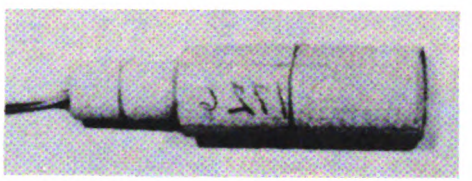

Type 5

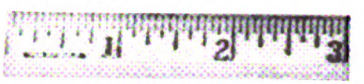

Scale, inches

Figure 25. - Types of suspended tetryl charges, unsheathed and sheathed. For all sheaths shown above, thickness of sodium bicarbonate layer is 1/8 inch. Sodium bicarbonate is contained in asbestos paper.

Digitized by Google
Original from THE OHIO STATE UNIVERSITY

Generated on 2024-09-21 14:30 GMT / https://hdl.handle.net/2027/osu.32435030643506
Public Domain, Google-digitized / http://www.hathitrust.org/access_use#pd-google

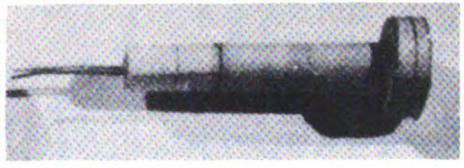

Type 8

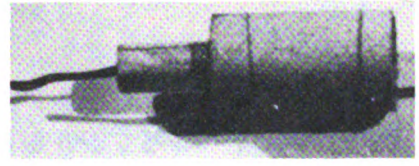

Type 9

Type 10

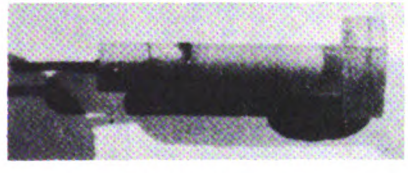

Type 11

Type 12

Type 13

Type 14

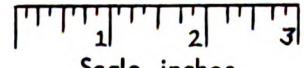

Scale, inches

Figure 26. - Types of sheathed tetryl charges. For all above sheaths thickness of sodium bicarbonate layer is ¼ inch. In type 1, not shown here, tetryl is completely unsheathed.

Digitized by Google
Original from THE OHIO STATE UNIVERSITY

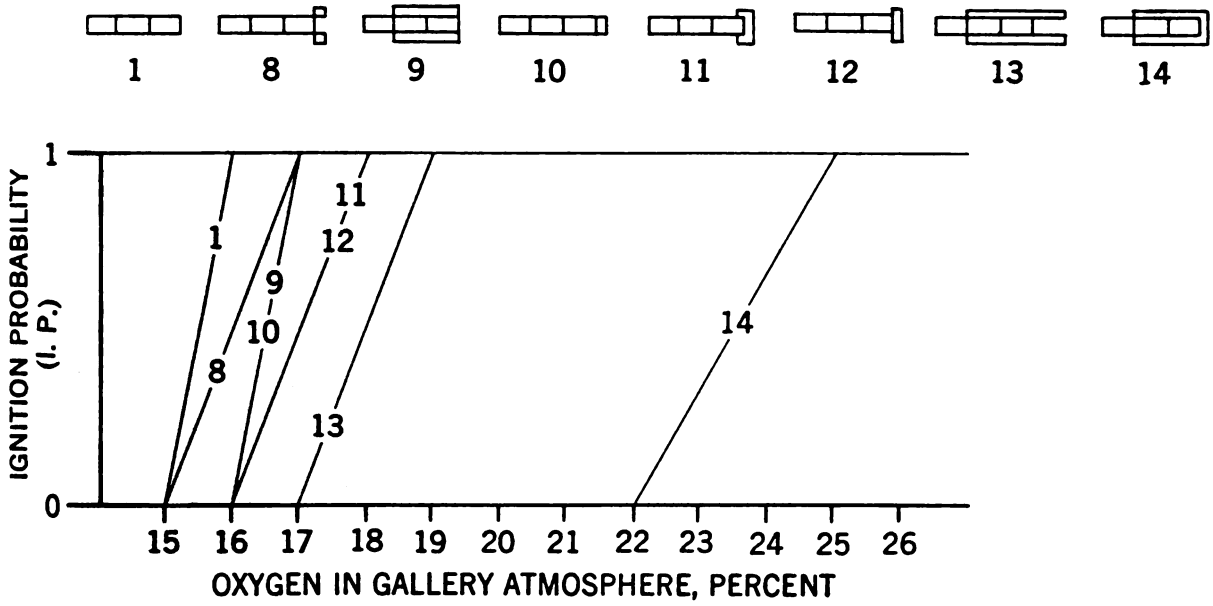

Figure 27. - Plot of ignition probabilities vs. oxygen percentage for ¼-inch sheaths. Numbers on curves refer to type of cartridge.

emitted by the mercury fulminate primer, which has little incendivity. This is consistent with the theoretical picture developed on the basis of earlier research, which indicated that the part of the cartridge that detonates last is the most incendive.22/

When an explosive detonates, a shock wave advances into the ambient atmosphere, and a rarefaction wave recedes into the detonation products. In freely suspended cartridges rarefaction behind the detonation wave begins at the circumference of the cartridge, where the freshly formed gaseous products of high pressure and high density border on the ambient low-pressure atmosphere. From there the rarefaction wave propagates into the interior cartridge volume. At the detonator end the products expand axially as well as laterally, but farther along the cartridge only lateral expansion is possible. To the lateral velocity of the products is added the axial velocity imparted by the detonation process and directed along the path of the detonation wave. This means that the path traveled by the products is inclined toward the cartridge axis. When the detonation wave reaches the end of the cartridge, the products continue to flow along inclined paths. However, at the instant when the detonation wave breaks through the end of the cartridge, the small mass of products behind the wave that has not yet been overrun by the lateral rarefaction wave is projected forward with a momentum corresponding to the original particle velocity in the detonation wave plus the velocity gained by rarefaction in the axial direction (fig. 31). Thus a high-velocity jet emerges from the end of the cartridge. Lewis and von Elbe have suggested that the resulting deep pocket formed by the main cloud and the jet is particularly conducive to heat transfer to the ambient atmosphere and hence to ignition. Whether ignition continues to propagate as a combustion wave through the atmosphere or is quenched depends - as in the case of small cannon shots - on turbulent mixing of the ignited gas with expansion-cooled detonation products.

22/ Payman, W., and Wheeler, R. V., The Ignition of Firedamp by Coal-Mining Explosives: Trans. Inst. Min. Eng., vol. 95, pt. 1, 1938, pp. 13-47. See also work cited in footnote 20 (p. 32).

Generated on 2024-09-21 14:32 GMT / https://hdl.handle.net/2027/osu.32435030643506
Public Domain, Google-digitized / http://www.hathitrust.org/access_use#pd-google
Digitized by Google
Original from THE OHIO STATE UNIVERSITY

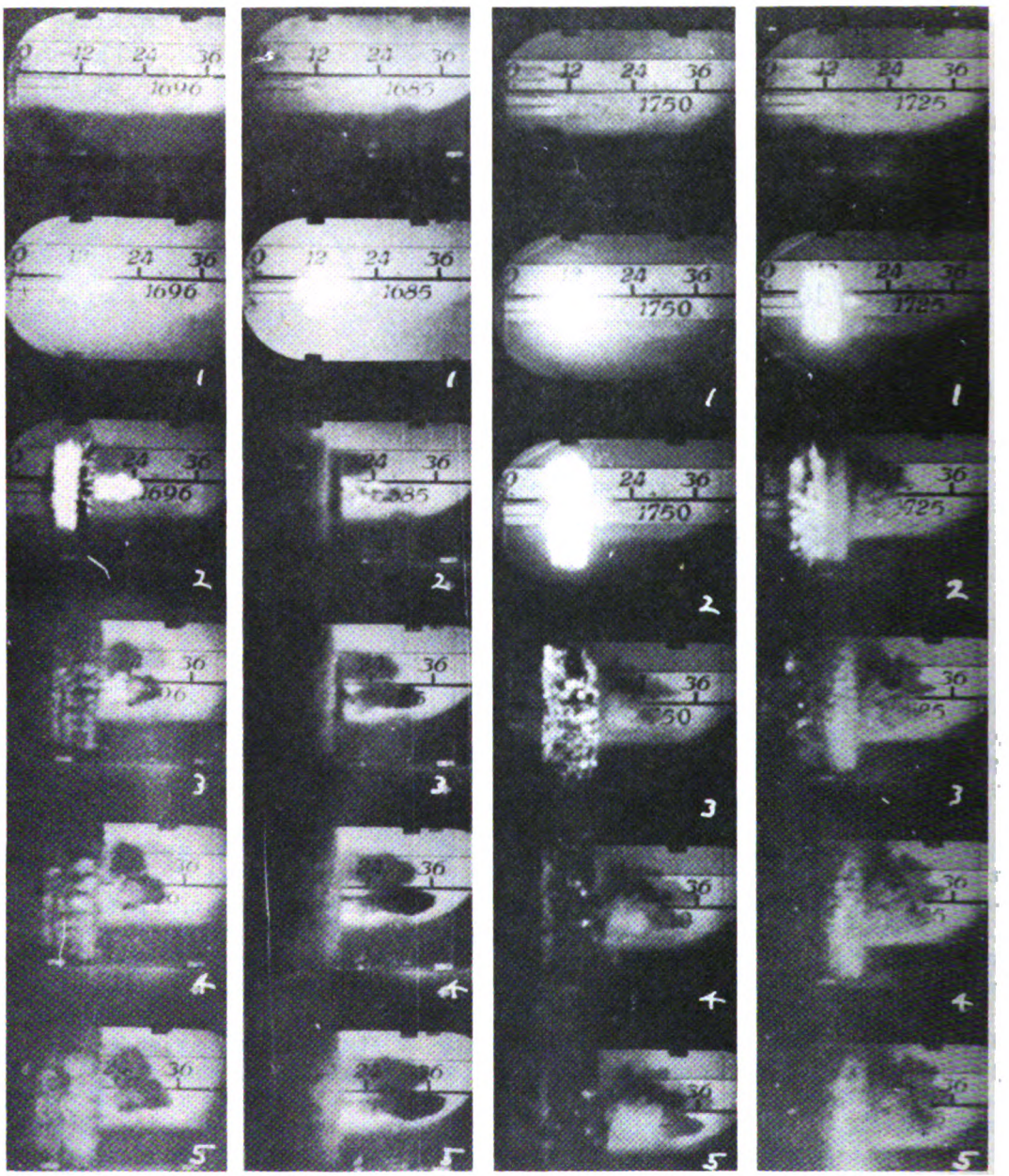

Figure 28. - High-speed photographs of 4 types of sheathed cartridges having 1/8-inch thick sodium bicarbonate sheaths and showing comparative flame patterns.

Generated on 2024-09-21 14:34 GMT / https://hdl.handle.net/2027/osu.32435030643506
Public Domain, Google-digitized / http://www.hathitrust.org/access_use#pd-google
Digitized by Google
Original from THE OHIO STATE UNIVERSITY

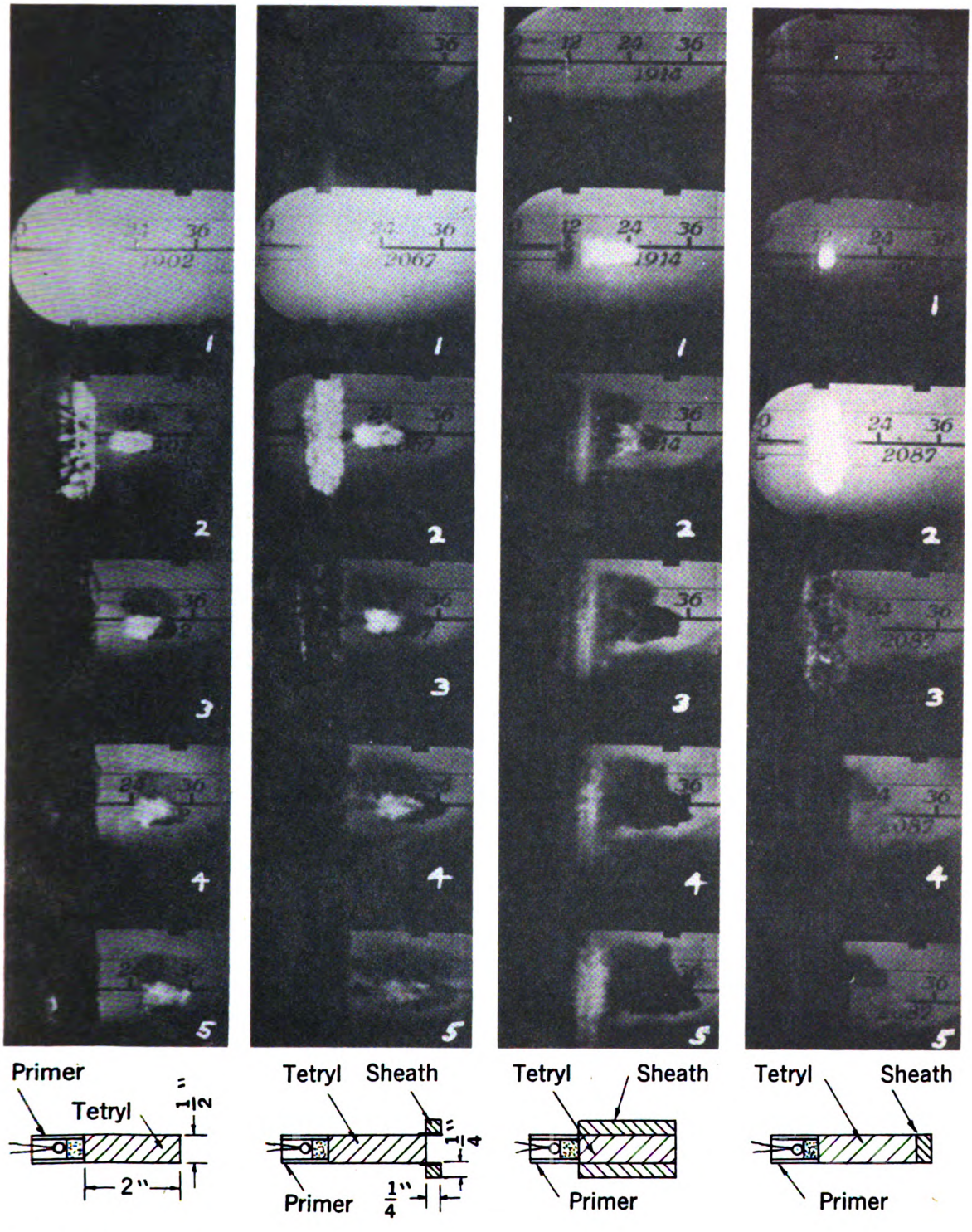

Figure 29. - High-speed photographs of unsheathed tetryl charge and 7 types of sheathed cartridges having ¼-inch-thick sodium bicarbonate sheaths and showing comparative flame patterns (sheet 1).

Generated on 2024-09-21 14:31 GMT / https://hdl.handle.net/2027/osu.32435030643506
Public Domain, Google-digitized / http://www.hathitrust.org/access_use#pd-google
Digitized by Google
Original from THE OHIO STATE UNIVERSITY

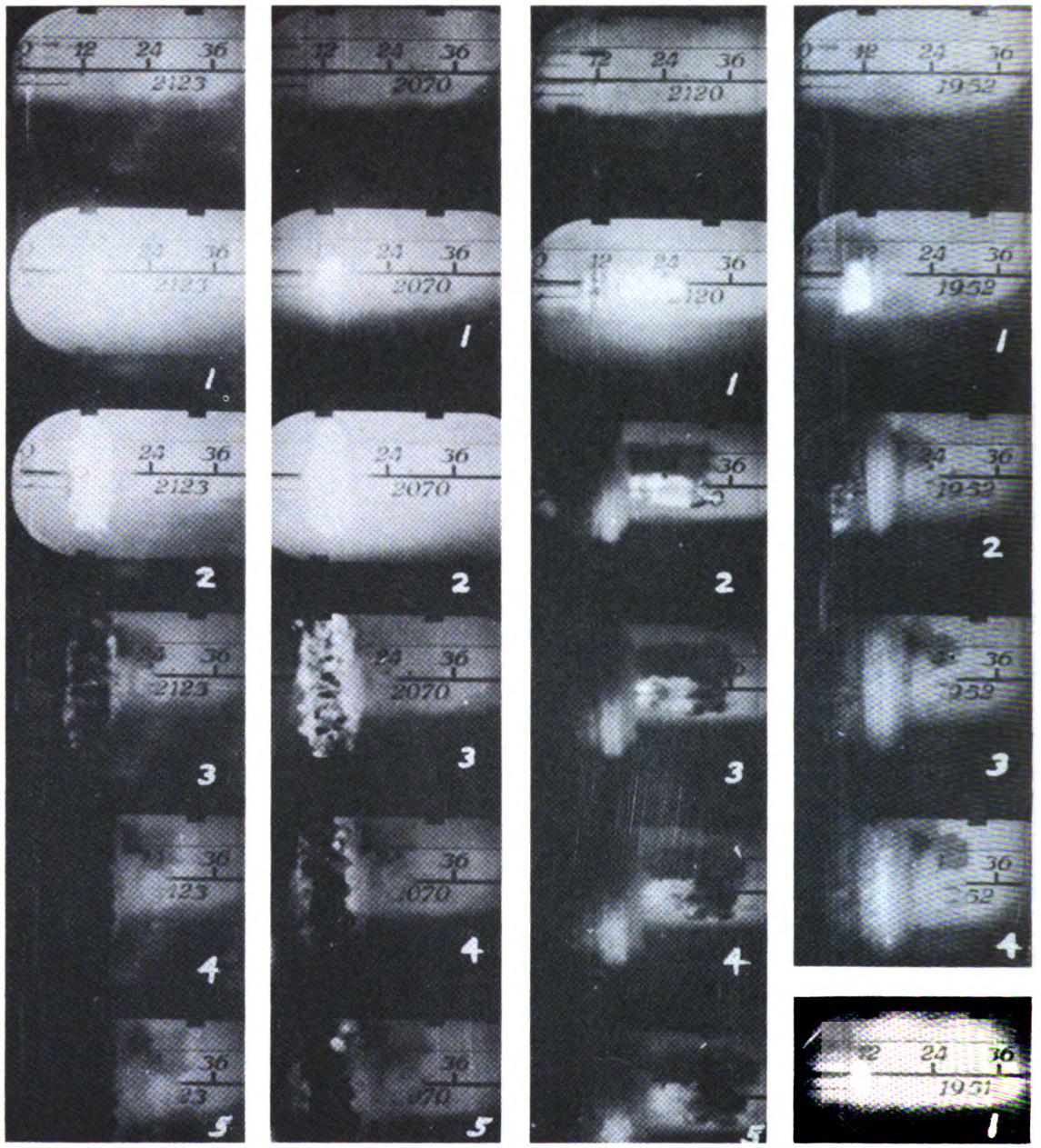

Figure 30. - Same as figure 29, (sheet 2).

Generated on 2024-09-21 14:31 GMT / https://hdl.handle.net/2027/osu.32435030643506
Public Domain, Google-digitized / http://www.hathitrust.org/access_use#pd-google
Digitized by Google
Original from THE OHIO STATE UNIVERSITY

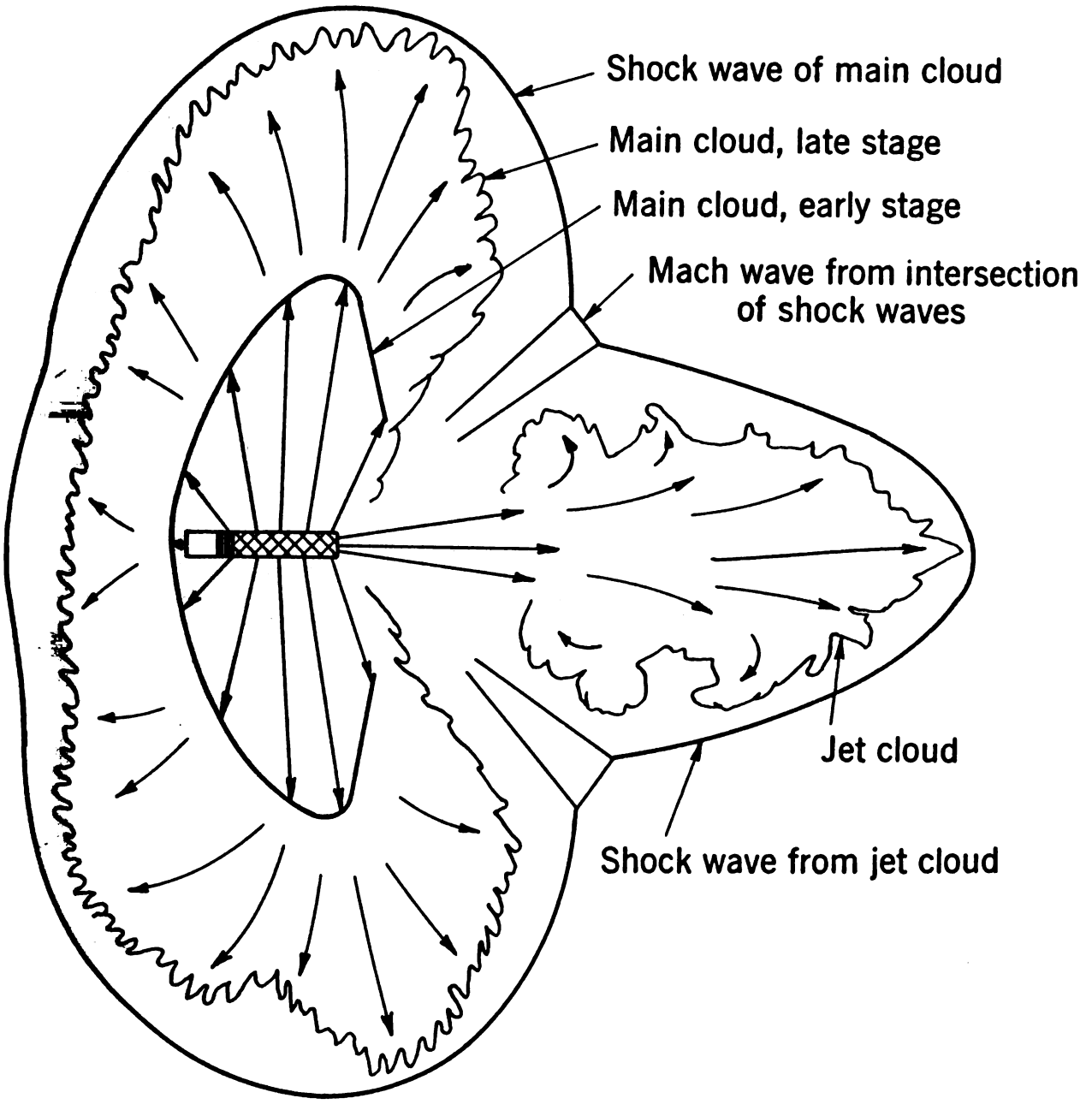
Shock wave of main cloud
Main cloud, late stage
Main cloud, early stage
Mach wave from intersection of shock waves
Jet cloud
Shock wave from jet cloud

Figure 31. - Development of cloud of detonation products and shock wave.

Generated on 2024-09-21 14:34 GMT / https://hdl.handle.net/2027/osu.32435030643506
Public Domain, Google-digitized / http://www.hathitrust.org/access_use#pd-google
Digitized by Google
Original from THE OHIO STATE UNIVERSITY

Experiments With Stemmed Shots

To expand the concept of the mechanism of ignition to unstemmed and stemmed cannon shots, it may be assumed that the detonation front of the explosive has a curved shape (fig. 32, A). When this front breaks through the end of the charge (fig. 32, B) the center leads the wave at the rim. If a finite relaxation time is assumed for the solid particles forming the rim at the breakthrough, it is conceivable that an orifice or nozzle may form through which a portion of the unexpanded gaseous products rushes to form a hot jet (fig. 32, C). This jet could penetrate the air-methane atmosphere of the gallery, where it would provide a boundary containing a fertile source for ignition of the gallery atmosphere. Meanwhile, the gaseous products from the earlier phase of the detonation located farther back in the charge, near the initiator, have lost energy in expanding the borehole and have cooled considerably. Subsequent ejection of these gases surrounds the jet with a relatively cold medium which tends to quench any incipient ignition started by heat transfer from the jet to the ambient atmosphere (fig. 32, D).

To obtain additional information on the orifice effect at the instant of breakthrough, a study was made of stemmed shots, using the small cannon and small gallery.[23] Three-gram charges of tetryl pressed at 1,500 p.s.i. were fired unstemmed and with weights of fireclay stemming up to 3.00 grams (fig. 33, A). The results, plotted as an incendivity curve, are shown in figure 33, B. High-speed pictures of the shots and schlieren shock-wave pictures were obtained.

Analysis of the data for 150 shots showed that, as the weight of stemming increased from 0 to 0.25 gram (corresponding to a disk of stemming 3/32 inch thick), there was a slight but consistent increase in incendivity. As the weight of stemming increased from 0.25 to 0.75 gram, the incendivity decreased rapidly, leveling off between 1 and 3 grams. Figure 34 illustrates the accentuated jet obtained with a small amount of stemming which increases the orifice effect at the instant of breakthrough. Concomitantly, the presence of stemming tends to increase the mass cooling effect, thus reinforcing the quenching action of the products cloud. However, in the case of a thin layer of stemming, the accentuation of the jet more than compensates for the additional work performed by the jet. It is only as the weight of stemming increases that the temperature drop in the jet is sufficient to overcome the amplified orifice effect and make the shot safer. Thus, a slightly stemmed shot must be considered more incendive than an unstemmed one. Similar conclusions were derived from experiments in which microscope coverglasses were substituted for small amounts of stemming. As the jet pierces the glass, the residual glass rim acts as an orifice to increase the velocity of the jet.

Relative Incendivity of Black Blasting Powder

Black blasting powder is known to be hazardous in firedamp. This was confirmed in tests where its relative incendivity was compared with that of tetryl and dynamite.[24] Black powder, whose much slower burning is reflected in a slower pressure buildup in the borehole, does no substantial work in expanding the borehole. As a result, the quenching capabilities of the expanding detonation gases are subordinate to the action of the oxygen-containing particles ejected into the gallery where they deflagrate and become multiple sources of ignition.

23/ Grant, R. L., and Mason, C. M., The Mechanism of Ignition of Firedamp by Explosives: Bureau of Mines Rept. of Investigations 5049, 1954, 8 pp.

24/ Work cited in footnote 23.

Generated on 2024-09-21 14:35 GMT / https://hdl.handle.net/2027/osu.32435030643506
Public Domain, Google-digitized / http://www.hathitrust.org/access_use#pd-google
Digitized by Google
Original from THE OHIO STATE UNIVERSITY

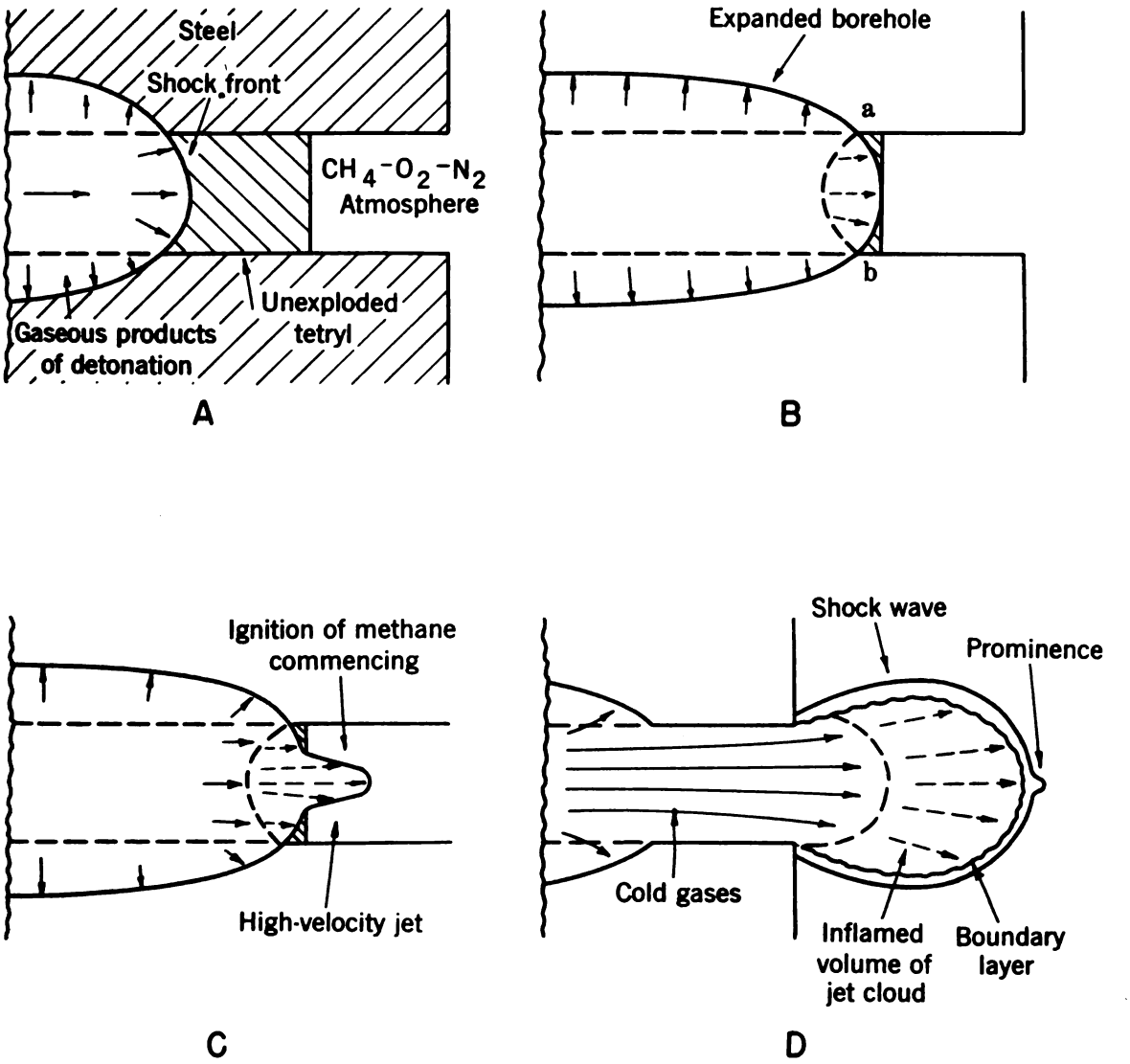

Figure 32. - Development of shock wave and gaseous products of detonation when an unstemmed charge of high explosive is fired from a steel borehole into a flammable atmosphere of firedamp and air.

Generated on 2024-09-21 14:31 GMT / https://hdl.handle.net/2027/osu.32435030643506
Public Domain, Google-digitized / http://www.hathitrust.org/access_use#pd-google
Digitized by Google
Original from THE OHIO STATE UNIVERSITY

Generated on 2024-09-21 14:35 GMT / https://hdl.handle.net/2027/osu.32435030643506
Public Domain, Google-digitized / http://www.hathitrust.org/access_use#pd-google

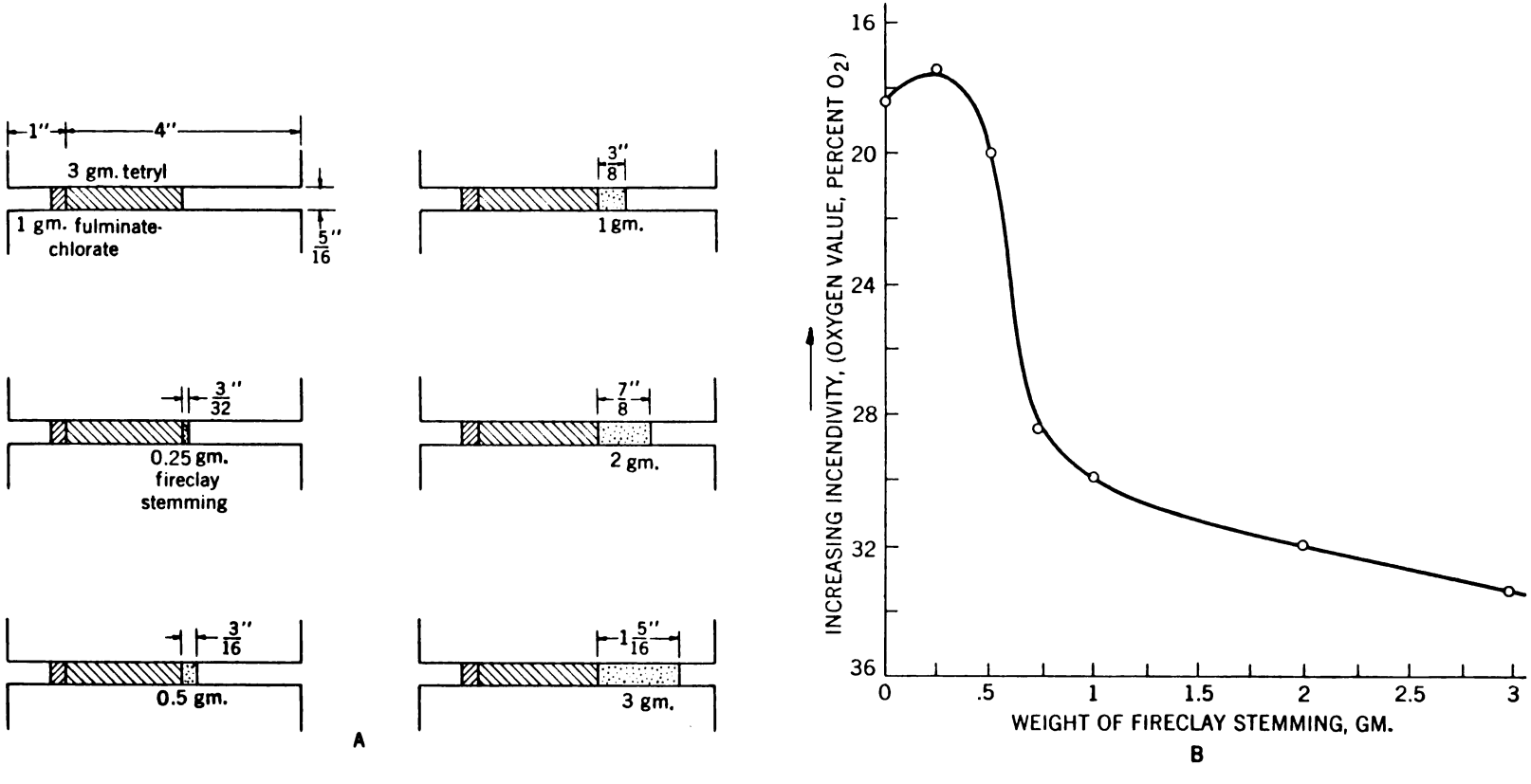

Figure 33. - A, Cross-sectional sketches of boreholes of small cannons, showing dimensions with variable weights of fire-clay stemming; B, effect of stemming on incendivity to firedamp.

Digitized by Google
Original from THE OHIO STATE UNIVERSITY

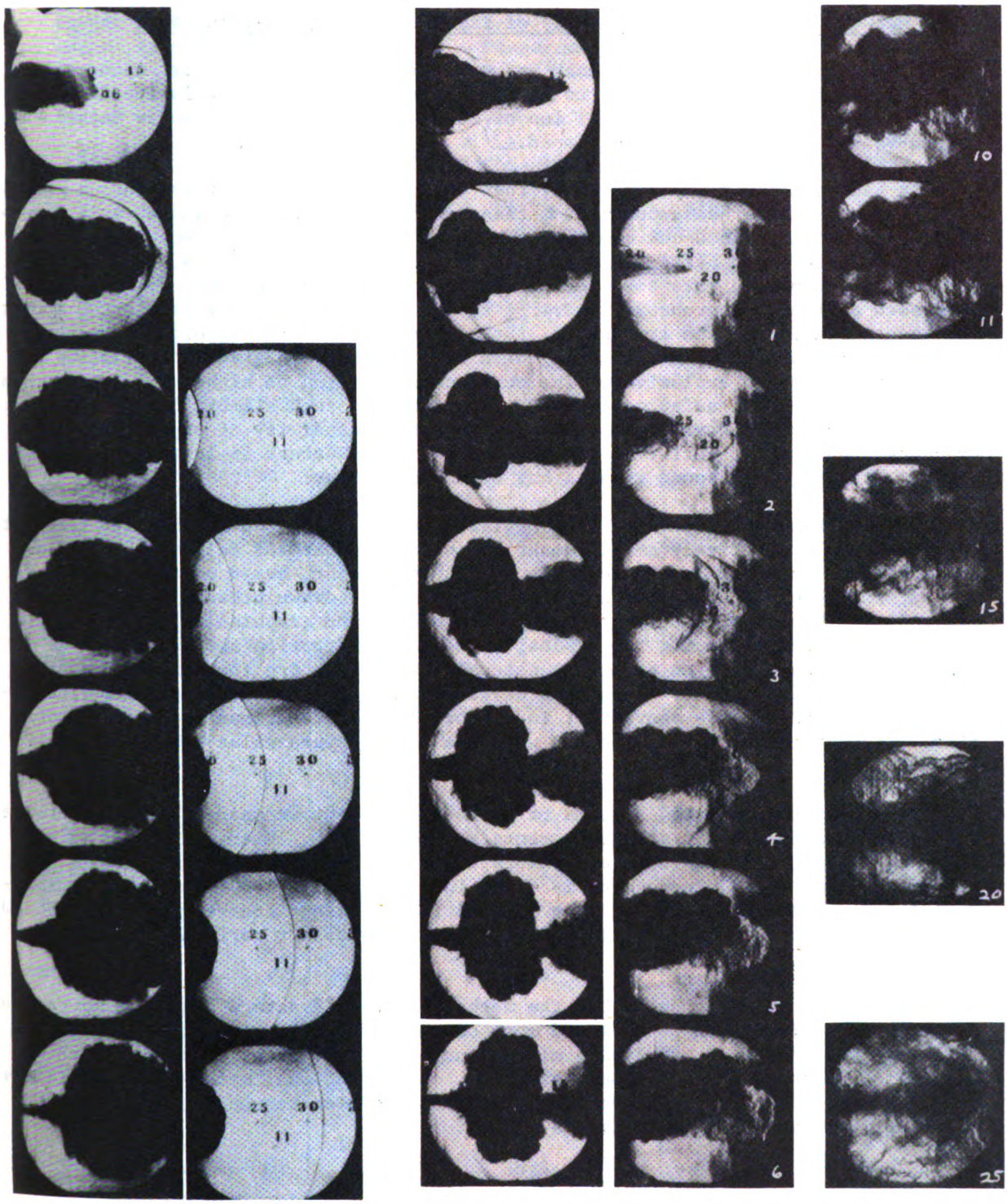

Figure 34. - Shock-wave photographs of stemmed shots.

Generated on 2024-09-21 14:36 GMT / https://hdl.handle.net/2027/osu.32435030643506
Public Domain, Google-digitized / http://www.hathitrust.org/access_use#pd-google
Digitized by Google
Original from
THE OHIO STATE UNIVERSITY

A New Method of Measuring Incendivity of Explosives: Oxygen-Value Test

It has been recognized for many years that a more definitive test is needed to measure the relative incendivity to firedamp of explosives and explosive devices. As a result of studies on the ignition of firedamp by explosives, a new method - the oxygen-value test - has been developed.25/

It had been found experimentally that when an explosive is fired into a gallery where the atmosphere has a constant methane content of 8 percent and a variable oxygen content, ignitions occur consistently for a certain upper percentage of oxygen while a certain lower percentage consistently produces no-ignitions. Intermediate percentages of oxygen give both no-ignitions and ignitions, and the results may be expressed as ignition probabilities. If the ignition probability is plotted against the oxygen content of the atmosphere, the resulting curve is sigmoid. Comparison with the corresponding sigmoid curve for a second explosive gives the relative incendivity of the two explosives. The curve corresponding to higher values of oxygen content indicates the safer explosive. In principle, such sigmoid curves appear to be the most satisfactory method of expressing the incendivity of explosives. In practice, the cost of performing enough shots of this nature in large galleries to provide statistically sound results has been prohibitive.

To obviate this difficulty, the Division has developed an abbreviated test that requires only a relatively small number of shots. Instead of determining the complete sigmoid curve, only the no-point and the yes-point, based on five shots each, are determined experimentally, and a straight line is drawn between the two points (fig. 34). The 50-percent ignition point thus obtained graphically is arbitrarily called the oxygen value for the explosive under consideration and is defined as the percentage of oxygen in an 8-percent natural gas-air mixture for which the ignition probability is 50 percent. Thus, the oxygen value represents a single numerical expression that provides a convenient index for the relative comparison of incendivities. Given two explosives, the one with the lower oxygen value will be the more incendive.

In making these tests, 3 grams of explosive without wrapper is pressed into the small steel cannon in 0.5-gram increments at 1,000 p.s.i. Rear initiation is provided by 1 gram of 80-20 fulminate-chlorate loaded in two 0.5-gram increments and pressed at 750 p.s.i. The charge is fired into the small (3 by 3 by 5-foot) experimental gallery where the natural-gas content is maintained constant at 8 percent and the oxygen content is varied. Incendivity measurements for various explosives are given in table 6.

Results to date indicate that the method has the advantage that a wider range of firedamp incendivity can be measured more conveniently than with other methods. In addition, the procedure involves a minimum number of variables, because the charge weight is constant and no wrapper, stemming, or conventional metal-encased detonator need be considered. A tentative classification has been set up for evaluating the firedamp incendivity of explosives:

25/ Grant, R. L., Mason, C. M., and Damon, G. H., A New Method of Measurement of the Incendivity of Explosives to Firedamp: Bureau of Mines Rept. of Investigations 5050, 1954, 8 pp.

Generated on 2024-09-21 14:32 GMT / https://hdl.handle.net/2027/osu.32435030643506
Public Domain, Google-digitized / http://www.hathitrust.org/access_use#pd-google
Digitized by Google
Original from THE OHIO STATE UNIVERSITY

Oxygen value less than 18 percent - Very dangerous
Oxygen value 18.5 to 21 percent - Dangerous
Oxygen value 21.5 to 23 percent - Borderline
Oxygen value 23.5 to 30 percent - Safe
Oxygen value 30.5 and greater - Very safe

TABLE 6. - Incendivity of various explosives to firedamp-air mixtures
(Explosives tested by firing a 3-gm. charge initiated by 1-gm. of fulminate chlorate into an atmosphere of 8 percent natural gas with variable oxygen content)

Explosive	Composition, percent	Oxygen value, percent O_2	Order of incendivity	Classification
Dynamite No. 5	50 NG 49 kieselguhr 1 $CaCO_3$	15.5	1	Very dangerous.
Black powder	75 $NaNO_3$ 10 S 15 charcoal	16	2	Do.
PETN		16	2	Do.
Tetryl-KNO_3(50-50)		17	3	Do.
RDX		17.5	4	Do.
Dynamite No. 6	50 NG 40 kieselguhr 9 wood pulp 1 $CaCO_3$	17.5	4	Do.
Tetryl, pure		18.5	5	Dangerous.
Tetryl-graphite (90-100)..		19	6	Do.
Dynamite No. 8	50 NG 26 kieselguhr 23 wood pulp 1 $CaCO_3$	20	7	Do.
Dynamite No. 7	50 NG 31 kieselguhr 18 $NaNO_3$ 1 $CaCO_3$	20	7	Do.
Dynamite No. 1	30 NG 23 wood pulp 46 $NaNO_3$ 1 $CaCO_3$	21.5	8	Borderline.
Dynamite No. 3	30 NG 18 wood pulp 51 $NaNO_3$ 1 $CaCO_3$	23.5	9	Safe.
Dynamite No. 10	50 NG 21 kieselguhr 28 $NaNO_3$ 1 $CaCO_3$	37.5	10	Very safe.
Fulminate chlorate(80-20).		38.5	11	Do.
Dynamite No. 2	30 NG 13 wood pulp 56 $NaNO_3$ 1 $CaCO_3$	70 (approx.)	12	Do.

Generated on 2024-09-21 14:37 GMT / https://hdl.handle.net/2027/osu.32435030643506
Public Domain, Google-digitized / http://www.hathitrust.org/access_use#pd-google
Digitized by Google
Original from THE OHIO STATE UNIVERSITY

Tests of Explosives

In the fiscal years 1953 and 1954, 3,556 chemical and physical tests were made at the Bruceton Station on various permissibles, other explosives, and hazardous chemicals.26/ Four new permissible explosives were tested during this period. Three passed all tests and were added to the active permissible list. The fourth failed gallery test 1. Four blasting devices were tested and approved under the provisions of Schedule 26. Fifty-one field samples were tested. One device, designed to replace fireclay or other stemming material, was tested and found acceptable under the provisions of Schedule 27. As of December 31, 1954, the active list included 177 permissible explosives and 10 blasting devices.

Factors Influencing Permissibility of Explosives

Since the Bureau of Mines was organized in 1910, its important activities have included the establishment and maintenance of standards by which explosives are judged to be suitable for use in underground coal mining when they are used in prescribed ways established to further the factors of safety. A continuing program of testing is conducted with the aim of assuring that approved brands of explosives are constantly maintained up to those standards. The importance of this activity is attested by the notable reduction in frequency of coal-mine disasters as permissible explosives have come very largely to supplant other types of explosives for underground coal mining.

In considering permissible explosives a distinction is made between nongelatinous and gelatinous types. Nongelatinous explosives generally are used for shooting coal and are well adapted for blasting in relatively dry mines. Gelatinous explosives are designed especially for blasting rock in coal mines, although under certain conditions they have been found suitable for shooting coal; they are eminently adapted for use in wet work. In April 1954, the "active" list of permissible explosives included 174 different brands, of which 23 were gelatinous and the remainder belonged to the more common granular ammonium nitrate type.

To maintain the necessary standards of safety and quality, the Bureau of Mines conducts two kinds of tests - tests of the basic sample submitted by the manufacturer to establish its essential permissibility and tests of samples collected in the field to check conformance with the basic data. A field sample that does not correspond to the sample as originally approved is immediately declared nonpermissible, and the manufacturer is requested to withdraw the particular lot from the market. Results of field sampling for the fiscal years 1953 and 1954 are given below:

	1953	1954
No. of field samples collected	22	29
Met all tolerances	7	12
Failed gallery test 1	1	4
Failed to propagate	0	0

26/ Bureau of Mines, U. S. Department of the Interior, Schedule 1F, Explosives (including Sheathed Explosives) and Blasting Devices: Federal Register, Feb. 6, 1945, vol. 10, No. 26, and amendments, Federal Register, Mar. 24, 1945, vol. 10, No. 60; Sept. 7, 1945, vol. 10, No. 176; July 20, 1946, vol. 11, No. 141; Mar. 13, 1948, vol. 13, No. 51: and Sept. 17, 1948, vol. 13, No. 182.

Generated on 2024-09-21 14:34 GMT / https://hdl.handle.net/2027/osu.32435030643506
Public Domain, Google-digitized / http://www.hathitrust.org/access_use#pd-google
Digitized by Google
Original from THE OHIO STATE UNIVERSITY

Factors Affecting Incendivity of Permissible Explosives

To satisfy permissibility requirements the explosive must undergo a number of tests, the most important being the two different gallery tests to evaluate the incendivity of the explosive in flammable atmospheres. These gallery tests are designed to simulate the most dangerous circumstances that are likely to occur in a coal mine. In the first test (test 1) the explosive, stemmed with 1 pound of dry fireclay, is fired from a steel cannon directly into a gallery (gallery 1, fig. 35) containing an 8-percent natural gas-air mixture (fig. 36). The weight of explosive charge used in this test is equivalent in strength to 1/2 pound of a standard 40-percent straight nitroglycerin dynamite. To meet the requirements for permissibility, there must be no ignitions in 10 consecutive shots. In the second test (test 4), 1-1/2 pounds of explosive is fired unstemmed, using direct initiation, into a 4-percent natural gas-air mixture containing coal dust in suspension. For permissibility there must be no ignition in five consecutive shots.

In the belief that better understanding of the factors that affect the incendivity of explosives will help to develop safer explosives, a critical survey was made of data from tests of 700 explosives.[27/] The resulting information was supplemented by research on specific incendivity factors in collaboration with another section of the Division (see pp. 36-49).

As data available for gelatinous explosives are limited, the investigation was conducted chiefly on nongelatinous explosives, which are, typically, mixtures of an explosive oil, ammonium nitrate, sodium nitrate, and carbonaceous combustible material and may contain sodium chloride. The explosive oil is usually a 75-25 mixture of nitroglycerin and nitroglycol, added in sufficient quantity to insure complete detonation with a No. 6 detonator.

The relative amounts of the different ingredients vary widely in different permissible explosives:

	Percent
Ammonium nitrate	5-81
Sodium nitrate	0-40
Sodium chloride	0-25
Ammonium chloride	0-15
Carbonaceous combustible material	3-21
Explosive oil	0-33

Factors considered include:

Particle size. - The particle size of the constituents of the explosive is known to affect many of its characteristics. Comparison of photomicrographs of field samples and basic samples suggests that larger particle sizes tend to increase the incendivity of a given explosive. Unfortunately, no definite information as to the particle size of the ingredients is available ordinarily.

Chemical Composition and Physical Characteristics. - Although the chemical composition of an explosive is one of its most important incendivity factors, the compositions of United States permissibles differ so widely that it is difficult to

27/ Hanna, N. E., Tiffany, J. E., and Damon, G. H., Factors Affecting the Incendivity of Permissible Explosives: Bureau of Mines Rept. of Investigations 5051, 1954, 11 pp.

Generated on 2024-09-21 14:36 GMT / https://hdl.handle.net/2027/osu.32435030643506
Public Domain, Google-digitized / http://www.hathitrust.org/access_use#pd-google
Digitized by Google
Original from THE OHIO STATE UNIVERSITY

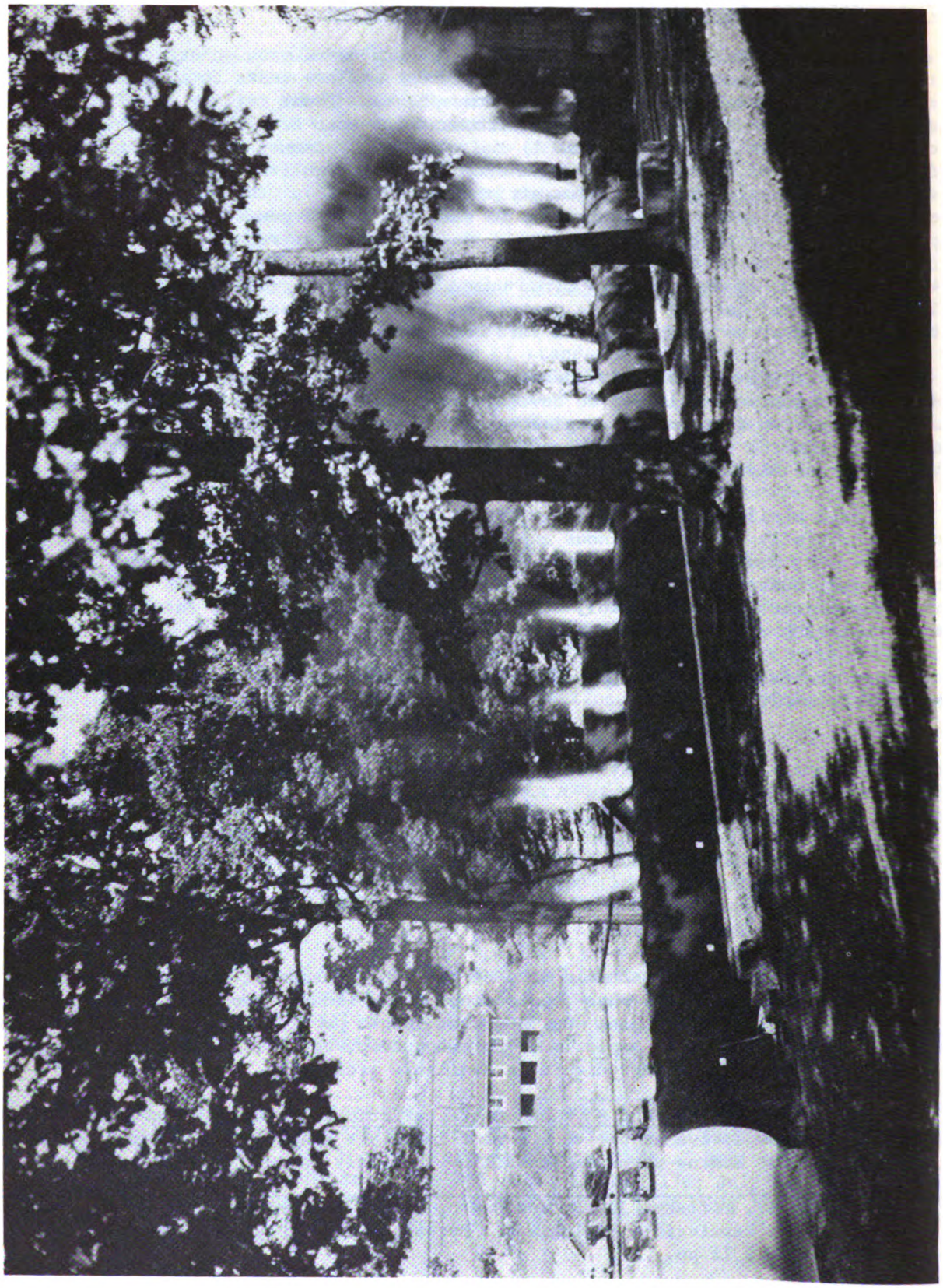

Figure 35. - Gallery explosion to test explosives for permissibility.

Generated on 2024-09-21 14:35 GMT / https://hdl.handle.net/2027/osu.32435030643506
Public Domain, Google-digitized / http://www.hathitrust.org/access_use#pd-google

Digitized by Google

Original from
THE OHIO STATE UNIVERSITY

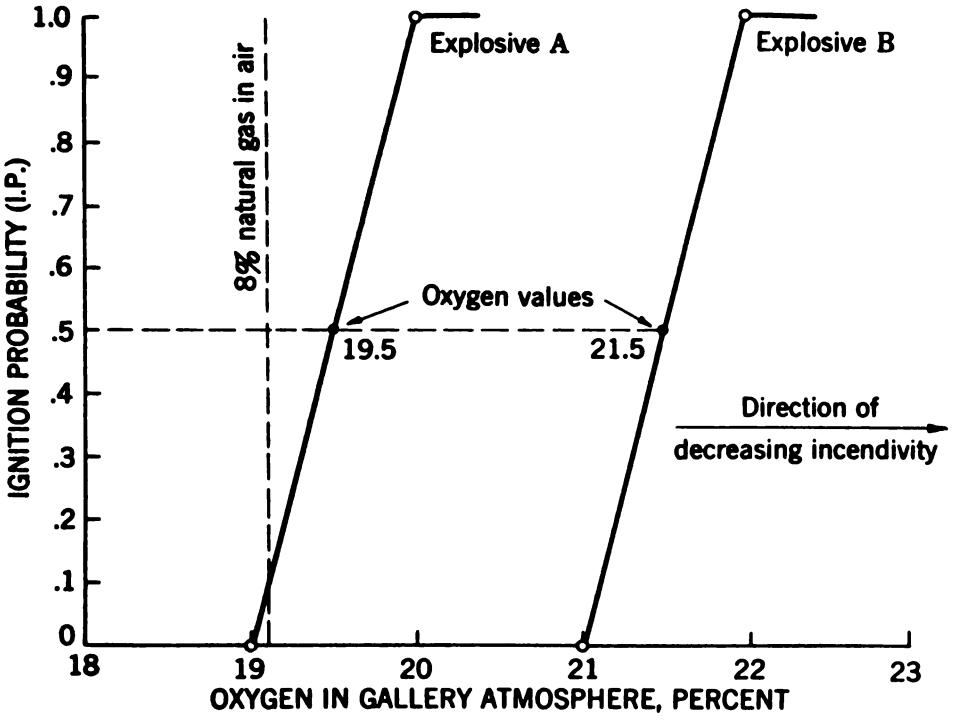

Figure 36. - Abbreviated sigmoid curves for two hypothetical explosives, illustrating graphical plot of relative incendivity according to oxygen values.

evaluate the effect of individual variables. Nevertheless certain definite trends can be detected. The density of nongelatinous permissible explosives depends primarily upon the relative amount and type of carbonaceous material. There is no apparent correlation between the overall density of an explosive and its incendivity. Comparison of permissible explosives indicates that incendivity increases with detonation velocity. This is explained by the fact that, for higher detonation velocities, the temperature of the detonation gases usually is higher. However, a low rate of detonation may lead to incomplete detonation and ejection of hot particles that can be a source of ignition.

Oxygen Balance. - Gallery tests are affected considerably by changes in the oxygen balance of an explosive. Any change in the amount of oxygen available for combustion of the carbonaceous ingredients of the explosive changes the composition of the detonation gases. Variations in oxygen balance were determined for three explosives. The oxygen balances are given in table 7, with the results of tests made in the gallery.

The results indicate that a change in oxygen balance has a definite effect on the limit charge of the explosive. A decrease in oxygen balance of an underoxidized explosive tends to increase the limit charge; the most hazardous condition appears to correspond to an oxygen balance at or near zero.

Carbonaceous Combustible Ingredients. - The carbonaceous combustible ingredients used for permissible explosives vary widely. The most common - wood pulp, sawdust, vegetable ivory, oat hulls, starch, and bagasse - often are used interchangeably,

Generated on 2024-09-21 14:33 GMT / https://hdl.handle.net/2027/osu.32435030643506
Public Domain, Google-digitized / http://www.hathitrust.org/access_use#pd-google
Digitized by Google
Original from THE OHIO STATE UNIVERSITY

which may account for gallery failures on retesting. However, as the nature of these materials is never determined, no conclusions can be drawn.

TABLE 7. - Effect of oxygen balance on incendivity

Sample	Oxygen balance				UDC[1/]	Limit charge[2/]
	Maximum	Minimum	Variation	Average		
	gm./100 gm.	gm./100 gm.	gm./100 gm.	gm./100 gm.	gm.	gm.
A Ingregients only	- 8.9	- 6.6	2.3	- 7.8	-	175
A Ingredients + wrapper ...	-33.1	-26.1	7.0	-29.6	234	275
B Ingredients only	+ 3.7	+ 4.8	1.1	+ 4.2	-	200
B Ingredients + wrapper ...	-25.9	-16.2	9.7	-21.1	213	250
C Ingredients only	+ 5.7	+11.0	5.3	+ 8.4	-	375
C Ingredients + wrapper ...	- 8.7	- .5	8.2	- 4.7	228	350

1/ Unit deflective charge. The weight of explosive that gives the same deflection of the ballistic pendulum as a 1/2-pound charge of the Bureau of Mines standard 40-percent straight dynamite.

2/ Limit charge with test-1 conditions. It is the maximum weight of explosive (± 25 grams) that can be fired into a flammable atmosphere confined in the gallery without causing ignition in 5 consecutive trials.

Sodium Nitrate, Sodium Chloride, and Potassium Chloride. - Limit charges were determined at the gallery under test 1 and test 4 conditions to show the effect of substituting various amounts of sodium nitrate, sodium chloride, or potassium chloride for equivalent amounts of ammonium nitrate in a permissible explosive (table 8). In every instance the limit charge was lower for samples containing sodium nitrate than for samples containing sodium or potassium chloride. Both chlorides behaved almost identically over the range of concentrations tested. In no instance did samples containing sodium or potassium chloride cause failures in gallery test 4. On the other hand, sample G, which contained 13 percent sodium nitrate, failed this test with a charge of only 450 grams. This behavior supports the other evidence indicating that sodium nitrate concentrations in excess of 10 percent have an adverse effect.

TABLE 8. - Effect of sodium nitrate, sodium chloride, and potassium chloride in gallery tests, in percent

Ingredients	Sample designation								
	A	B	C	D	E	F	G	H	I
Moisture	0.5	0.5	0.5	0.5	0.5	0.4	0.4	0.5	0.5
Explosive oil	9.3	9.5	8.9	8.9	9.4	8.7	9.1	9.0	9.9
Ammonium nitrate	80.0	80.0	80.9	75.7	75.2	76.2	70.5	70.8	69.8
Sodium nitrate	3.5	-	-	8.5	-	-	13.2	-	-
Sodium chloride	-	3.0	-	-	7.9	-	-	13.0	-
Potassium chloride	-	-	3.3	-	-	8.1	-	-	13.3
Carbonaceous combustible material	6.7	7.0	6.4	6.4	7.0	6.6	6.8	6.7	6.5
Test-1 conditions Limit charge (grams)	250	300	300	250	325	325	300	375	400
Test-4 conditions Limit charge (grams)	>680	>680	>680	-	>680	>680	450	>680	>680

Generated on 2024-09-21 14:33 GMT / https://hdl.handle.net/2027/osu.32435030643506
Public Domain, Google-digitized / http://www.hathitrust.org/access_use#pd-google
Digitized by Google
Original from THE OHIO STATE UNIVERSITY

Effect of Small Differences in Formulation and Manufacturing Procedure. - The failure of several field samples of permissible explosives to pass gallery test 1 suggested an investigation of the effect of small differences in the formulation of an explosive. It was observed that failures occurred, even when the explosives met the chemical tolerances allowed by the Bureau of Mines. The investigation showed that manufacturing procedures varied from time to time. Sometimes the explosive oil was pregelled before mixing with other ingredients; in other instances, nitrocotton was added to the solid ingredients before the explosive oil. For this purpose, six special explosives were prepared by the Hercules Powder Co. and tested at the gallery. The chemical analyses of the samples are shown in table 9.

TABLE 9. - Chemical analyses of samples tested for incendivity to methane-air mixtures, in percent

Ingredients	Sample designation					
	A	B	C	D	E	F
Moisture	0.2	0.3	0.2	0.3	0.2	0.2
Explosive oil	9.9	9.9	9.4	10.0	9.6	9.8
Ammonium nitrate	73.9	73.4	71.2	70.2	74.4	74.0
Sodium nitrate	6.7	6.9	6.4	6.4	7.1	6.8
Antacid	.6	.6	.5	.6	.6	.6
Carbonaceous combustible material	8.7	8.8	8.9	9.0	7.8	8.3
Nitrocellulose	-	.1	-	.1	.3	.3
Sodium chloride	-	-	3.4	3.4	-	-

All samples were tested at the small experimental gallery[28/] designed for studying the mechanism of ignition of firedamp and at gallery 1, used routinely for determining the permissibility of explosives. In the small-gallery tests, 10-gram charges were fired from a small cannon into a carefully controlled flammable atmosphere. The oxygen content of the atmosphere was varied until zero and unit probability, respectively, had been determined on the basis of five trials. The average of the upper and lower limits represents the oxygen value, which is inversely proportional to the incendivity of the explosive. The results of both series of tests are presented in table 10. Samples C and D are measurably safer than the other samples, suggesting that the presence of approximately 3.0 percent sodium chloride tends to reduce the incendivity of explosives. Pregelling nitroglycerin before the other ingredients are added does not appear to have any appreciable effect (samples E and F). In all tests samples E and F, with 0.3 percent nitrocotton, appear slightly safer than samples A and B, suggesting that small amounts of nitrocotton may make the explosive safer. However, further tests are required on this point.

Conclusions

1. Careful examination of the results of tests of American explosives over a period of 45 years shows no apparent correlation between the density of explosives and incendivity.

2. Both sodium and potassium chlorides show similar favorable effects on incendivity.

28/ Grant, R. L., and Mason, C. M., The Mechanism of Ignition of Firedamp by Explosives: Bureau of Mines Rept. of Investigations 5049, 1954, 8 pp.
Grant, R. L., Mason, C. M., and Damon, G. H., A New Method of Measurement of the Incendivity of Explosives to Firedamp: Bureau of Mines Rept. of Investigations 5050, 1954, 8 pp.

Generated on 2024-09-21 14:35 GMT / https://hdl.handle.net/2027/osu.32435030643506
Public Domain, Google-digitized / http://www.hathitrust.org/access_use#pd-google
Digitized by Google
Original from THE OHIO STATE UNIVERSITY

3. Explosives containing sodium nitrate in excess of 10 percent show a greater probability of failing test 4 (gas and dust), while those containing less than 10 percent have a greater probability of failing test 1 (gas).

4. A decrease in the oxygen balance of an underoxidized explosive tends to increase the limit charge.

5. Pregelling the explosive oil had virtually no effect on incendivity.

6. Addition of nitrocotton up to 0.3 percent appears to have little effect on incendivity, but the available data are inconclusive.

7. Available information on gelatinous explosives is insufficient to justify any reasonable conclusions as to their incendivity.

8. The relation between the particle size of the ingredients of the explosive and its incendivity cannot be determined from the data available. Thorough examination of these factors should prove very valuable.

9. The source and state of division of the carbonaceous combustible material in the explosive may have a definite effect on its incendivity. More data are needed before definite conclusions can be reached on this point.

TABLE 10. - Results of incendivity tests in methane-air mixtures showing effect of nitrocellulose, sodium chloride, and pregelling of explosive oil in the experimental gallery and gallery 1

Sample	Percent		Experimental gallery[1]			Gallery 1			
			O_2, percent				Grams		
	Nitrocotton	Sodium chloride	Zero probability	Unit probability	Average oxygen value[2]	Zero probability	Unit probability	50% ignition probability[2]	Ignition probability, using 350-gm. charge[3]
A	0.0	0.0	19	22	20.5	275	375	325	0.60
B	.1	.0	19	22	20.5	250	375	312	.60
C	.0	3.0	19	24	21.5	300	450	375	.13
D	.1	3.0	19	26	22.5	325	400	363	.27
E[4]	.3	.0	18	24	21.0	275	400	337	.53
F[5]	.3	.0	19	23	21.0	225	425	325	.54

1/ Data collected by R. L. Grant.
2/ Average of unit and zero probabilities.
3/ Based on 15 trials.
4/ Pregelled.
5/ Not pregelled.

Current Trends in Usage of Explosives and Coal-Breakage Devices

Directly or indirectly, explosives and blasting devices are used in producing almost all the coal currently mined in the United States. Recent developments, such as the continuous miner which digs coal out of the solid face, may some day alter this situation, but at present their contribution to the total production is small.

Generated on 2024-09-21 14:39 GMT / https://hdl.handle.net/2027/osu.32435030643506
Public Domain, Google-digitized / http://www.hathitrust.org/access_use#pd-google
Digitized by Google
Original from THE OHIO STATE UNIVERSITY

As a result, the yearly consumption of explosives by the United States coal-mining industry is enormous.29/

Explosives used in the United States for coal mining include: Permissibles, explosives other than permissibles, black blasting powder, and liquid-oxygen explosives. Consumption of high explosives other than permissibles has been increasing, corresponding to the increase in surface mining, with heavy overburden blasting. In underground mining considerations of safety have been responsible for a continuous trend from black powder toward permissible explosives and blasting devices, such as Cardox and Airdox. Although there has been a considerable increase in the proportion of coal produced by these latter systems, permissible powders remain the most important breakage agent.

Permissible Explosives

The first list of permissible explosives published in 1909 by the Federal Geological Survey gave 17 powders designed to reduce the hazards attendant upon the use of black blasting powder. By 1944 permissibles accounted for 85 percent of the coal produced in underground bituminous mines; the percentage is even higher today, and in 1954 the list of permissibles approved by the Federal Bureau of Mines included 178 different brands, offering the coal-mining industry an ample range of physical characteristics to meet its diversified needs.30/ Table 11 gives the chemical analyses and physical constants for 2 types of very different permissible explosives and compares them with 2 dynamites.

The term "permissible explosive," as applied to explosives tested and approved by the Bureau of Mines for use in blasting coal, implies not only that the explosive is similar in all respects to the sample originally tested but is used according to certain prescribed regulations. All permissibles now listed are detonating explosives, in contrast to black powder, which is a deflagrating explosive. Permissible explosives must be fired by electric detonators of not less than No. 6 size.

29/ Industrial consumption of permissible and other high explosives other than liquid-oxygen explosives for fiscal years 1953 and 1954, in million pounds:

	In coal mining		Total	
	1953	1954	1953	1954
Permissible explosives	86.4	76.9	87.3	78.0
Other high explosives	134.2	117.2	640.3	640.2
Black powder	6.2	4.3	9.7	10.5
Total	226.8	198.4	737.3	728.7
Permissible: Black-powder ratio	14.1	19.1	-	-

(Information obtained from monthly reports of the Institute of Makers of Explosives, New York, N. Y.)

The reduction in the consumption of permissibles as compared with the previous years (107 million pounds in fiscal year 1951 and 102 million pounds in fiscal year 1952) doubtless can be attributed to the increased use of compressed air for coal breakage, especially in large-scale exploitation, as well as to the decrease in the overall coal output. The substantial decrease in the relative usage of black powder over the years is very encouraging.

30/ Tournay, W. E., Hanna, N. E., and Damon, G. H., (Current Trends in the American Usage of Explosives and Breakage Devices for the Mining of Coal): Rev. ind. min., vol. 33, No. 586, 1952, pp. 863-866

Hanna, N. E., and Damon, G. H., Active List of Permissible Explosives and Blasting Devices Approved Before December 31, 1951: Bureau of Mines Inf. Circ. 7640, 1952, 12 pp.

Generated on 2024-09-21 14:35 GMT / https://hdl.handle.net/2027/osu.32435030643506
Public Domain, Google-digitized / http://www.hathitrust.org/access_use#pd-google
Digitized by Google
Original from THE OHIO STATE UNIVERSITY

TABLE 11. - Comparison of chemical analysis and physical properties of 2 permissible explosives with 40-percent dynamites

	Permissible non-getalinous	Permissible gelatinous	40-percent ammonia gelatin dynamite	40-percent straight dynamite
Chemical analysis, percent:				
Moisture	0.4	0.8	0.8	0.9
Explosive oil	4.9	32.3	24.4	40.0
Nitrocullulose	-	.6	.4	-
Sulfur	-	-	3.3	-
Ammonium chloride	-	11.0	-	-
Ammonium nitrate	81.0	29.4	14.4	-
Sodium nitrate	5.3	20.6	45.8	44.1
Calcium carbonate	.5	.8	1.0	1.1
Carbonaceous combustible material	7.9	4.5	9.9	13.9
Physical properties:				
Density	1.05	1.36	1.59	1.37
Velocity of detonation...m./sec.	1,500	5,100	4,590	4,500
Unit deflective[1/] charge...grams	239	237	261	227
Ballistic mortar.....percent TNT	111.2	102.8	89.1	95.6

1/ See table 7, footnote 1.

Some of the gases given off by permissibles are poisonous. The quantity of poisonous gases given off by a shot is an important factor and has been evaluated in the past from tests in the Bichel gage. These results have been compared with recent data obtained in the Experimental Coal Mine, Bruceton, Pa., under actual mining conditions. It was found that about 20 percent less carbon monoxide was liberated in the mine tests than in the Bichel gage. The concentration of nitrogen oxides was approximately the same in both cases. In general, it was found that the Bichel-gage tests do not predict with certainty the quantity of toxic gases that would be liberated at the working face, but they err on the side of safety and give a relative index of the hazards from poisonous gases.

Blasting Devices

Next to permissible explosives in importance for coal breakage in the United States are two blasting devices - Cardox and Airdox - which utilize high-pressure discharges from a pressurized shell in the shothole. In Cardox, liquid carbon dioxide is gasified by heat from an electrically ignited heating element. The high pressure produced by heating the carbon dioxide is released at high velocity by shearing a replaceable steel disk at the shell discharge head. The Cardox shell must be charged and serviced outside the mine after each discharge. Airdox utilizes highly compressed air. Its discharge involves neither spark nor flame, and its shell is inert until pressure is applied.

Although devices such as Cardox and Airdox eliminate or reduce certain hazards associated with explosives, they introduce others. The most serious hazard with Cardox is the possibility of the shell flying out of the shothole; with Airdox it is a ruptured air line, which would thrash about and raise considerable dust. However, the overall safety record of these blasting devices compares favorably with that of permissible explosives and in recent years there has been a definite increase in their usage, particularly Airdox. This latter is strongly favored in States where the use of explosives or flame-generating systems is prohibited during working shifts.

Generated on 2024-09-21 14:37 GMT / https://hdl.handle.net/2027/osu.32435030643506
Public Domain, Google-digitized / http://www.hathitrust.org/access_use#pd-google
Digitized by Google
Original from THE OHIO STATE UNIVERSITY

Both Airdox and Cardox produce a better prepared coal than explosives, which tend to tear and shatter it. Moreover, they allow a quicker return of workers to the face, as the quantity of toxic fumes released into the atmosphere is negligible with Cardox and zero with Airdox.

Black Powder

In spite of half a century of effort to eliminate black-powder blasting in underground mines, a small proportion of coal is still mined in this way. The underground use of black powder is limited chiefly to small operations where blasting devices are not readily available and where the advantages of permissible blasting are not fully recognized.

High Explosives in Strip Mining

In recent years more than 20 percent of the total coal output has been produced in open pits or strip mines. In strip mining blasting of overburden often constitutes the greatest single operating cost item and may even be a limiting factor. Thanks to technological developments, the ratio of the depth of overburden to the thickness of the coal seams that can be stripped is increasing, and large stripping operations now work in overburdens up to 80 feet or more.

Economic, efficient blasting is essential in this type of mining, and to obtain a valid evaluation of blasting costs both drilling and explosive costs must be integrated in terms of yardage of effectively blasted overburden. Broadly speaking, two important classes of explosives are used in strip mining: High-ammonium nitrate fixed explosives and liquid-oxygen explosives. The latter offer unexcelled high performance but are available only to relatively large consumers because of the costs of field installation, equipment, and the additional personnel they require. Low-density, ammonium nitrate-base, fixed explosives have a lower performance than the gelatins and nitroglycerin grades, but their lower cost has made them the accepted standard for strip-mining coal. They offer a considerable range of performance, depending on the amount and kind of sensitizing agents used and on the degree of boostering employed in their detonation.

Future Developments

The most important new development is a new blasting device known as Chemecol.[31/] Similar to Cardox in that it involves a high-pressure discharge from a steel shell, it permits convenient reloading at the face and offers several other safety features.

In the field of open-pit high-explosive blasting, the Division is studying possible application of nitrogen tetroxide explosives, which appear to offer excellent performance at very low cost; however, their high toxicity and corrosiveness present difficult practical problems.

Short-Delay Blasting in Experimental Coal Mine

The record of safety in the use of permissible explosives in the United States coal mines has been excellent, thanks in great measure to Bureau of Mines research and to the cooperation of mine operators and workers in using permissibles. In recent years the expansion of coal mining, the increased coal production during World

31/ This device has since been approved by the Bureau of Mines but is not available commercially at present.

Generated on 2024-09-21 14:30 GMT / https://hdl.handle.net/2027/osu.32435030643506
Public Domain, Google-digitized / http://www.hathitrust.org/access_use#pd-google
Digitized by Google
Original from THE OHIO STATE UNIVERSITY

War II, the changes in mining conditions and methods, and the development of new mining machinery have all contributed to the introduction of new or modified blasting practices. Among other things, efforts to increase the rate of coal production have promoted various forms of multiple blasting, some of which are potentially dangerous, whereas others offer definite economic and safety advantages. These latter include a new method - known as short-delay blasting - developed a few years ago for use in quarries and now widely employed in construction work, rock mining, and tunneling. In coal mines the procedure has been used experimentally in this country and in England, Japan, Belgium, and other countries; more recently it has been applied in the Pennsylvania anthracite fields. To implement this procedure, a special electric-delay detonator has been developed, variously referred to as the short-delay, fast-delay, rapid-delay, split-second delay, microsecond-delay, and millisecond-delay. In short-delay blasting the detonators may be connected in series to a firing device and the successive charges are fired at intervals, the most common intervals being 25 and 50 milliseconds; or detonation of successive charges may be timed by a mechanically driven sequence switch or timer.

Advocates of short-delay blasting claim that it affords greater speed, less exposure to weakened roof structure and to dust and fumes at the face, less roof vibration, better breakage of coal, reduction in the quantity of explosives used, reduction of float dust, etc. Possible disadvantages of short-delay blasting are thought to be the potential hazards of gas (and perhaps coal-dust) ignition during firing of larger total charges and the difficulty of detecting misfires. For these reasons many States prohibit or discourage all forms of multiple blasting in coal mines.

Although the Bureau of Mines has taken no official stand to date on the practice of short-delay multiple blasting, it recognizes that, under certain conditions (bad mine roof, coal seam with marked pitch), this practice may be safer than single-hole shooting. Several years ago it undertook to determine what hazards, if any, exist in short-delay multiple blasting and to compare its findings with the hazards of single-shot and simultaneous multiple blasting.32/

On the basis of investigations in the Experimental Coal Mine, Bruceton, Pa., a number of recommendations have been made,33/ which recognize both the advantages and drawbacks of short-delay multiple blasting. It is suggested that, if this practice is adopted in coal mines, the following conditions should be met, in addition to the normal safety requirements for blasting with permissible explosives:

1. Only specially trained, certified shot firers should be employed for multiple blasting. One duty of these men is careful inspection of the face after blasting to detect misfires.

2. Shot-firing circuits should be carefully checked and tested before firing. This includes a limit on the maximum resistance of the circuit, a limit on the

32/ Hartman, I., Nagy, J., and Howarth, H. C., Experiments on Multiple Short-Delay Blasting of Coal; Part I: Bureau of Mines Rept. of Investigations 4868, 1952, 16 pp.
Nagy, J., Hartmann, I., Christofel, F. P., and Seiler, E. C., Experiments on Multiple Short-Delay Blasting of Coal; Part II: Bureau of Mines Rept. of Investigations 4875, 1952, 22 pp.

33/ Hartmann, I., and Lewis, B., Experiments on Short-Delay Blasting in the Experimental Coal Mine: Bureau of Mines Rept. of Investigations 5026, 1954, 6 pp.

Generated on 2024-09-21 14:32 GMT / https://hdl.handle.net/2027/osu.32435030643506
Public Domain, Google-digitized / http://www.hathitrust.org/access_use#pd-google
Digitized by Google
Original from THE OHIO STATE UNIVERSITY

number of splices in the circuit, the use of detonator leads long enough to eliminate extra splices between detonator and shot-firing cable, insulation of all splices, and other necessary steps to prevent short circuits and current leakage to ground, especially in damp places and near tracks or other metallic objects.

3. Permissible shot-firing devices of adequate capacity should be employed, with a definite upper limit placed on the number of shots fired in a sequence. Recent experimental work indicates that, to insure complete firing of a 10-shot series circuit, the firing current must be at least 1.1 amperes d.c. or 1.8 amperes a.c. at 25 cycles to 1.2 amperes at 200 cycles. This current must flow through the circuit for at least 12 milliseconds. Within 30 milliseconds after the shot-firing devices go into action the terminal voltage must not exceed 12 volts.

4. All detonators in the face must be connected in series. As an added precaution, no instantaneous or zero-delay detonators should be used in short-delay blasting. This would eliminate misfires from detonator leads broken by the first shot by assuring enough time for current to pass through all detonators to start the explosive-initiating trains before the first blast.

5. The interval between successive shots should not exceed 50 milliseconds, and the delay between the first and last shots of a series should not exceed 500 milliseconds.

6. Explosives should be file-loaded and rear-initiated to avoid separating the primer cartridge from the main charge by break of the front of a hole by an early shot.

7. The explosive should be examined before charging; wet or deteriorated cartridges should be discarded.

8. A record should be kept of all misfires and their causes.

Neither the earlier conclusions as to the relative safety of short-delay multiple blasting nor the above recommendations constitute official approval of this practice by the Bureau of Mines.

Revised Schedule for Testing Blasting Devices

New developments in the science of explosives and in the explosives industry necessitate periodic revisions of test procedures and specifications. In consultation with the manufacturers, the Division prepared a revised schedule,[34/] regulating the testing of blasting devices and the conditions under which such devices may be used in mines.

The two principal potential hazards associated with the operation of blasting devices in underground workings are:

1. The ignition of firedamp and/or coal dust.

2. The emission of toxic gases as products of the explosion of the device.

Blasting devices are approved on the basis of chemical and physical tests similar to those used for permissible explosives. Conditions under which a blasting device must be used to be permissible are the following:

34/ Bureau of Mines Permissibility Schedule 26, amendments as published in Federal Register, Feb. 20, 1953, vol. 18, No. 35; and Jan. 14, 1954, vol. 19, No. 9 (refer to predecessor Schedule 1F and its five amendments).

Generated on 2024-09-21 14:34 GMT / https://hdl.handle.net/2027/osu.32435030643506
Public Domain, Google-digitized / http://www.hathitrust.org/access_use#pd-google
Digitized by Google
Original from THE OHIO STATE UNIVERSITY

1. The device must conform to the specifications for the model as originally approved.

2. The device must not be discharged in the presence of firedamp that can be detected with a permissible flame safety lamp.

3. The unit used to fire the blasting device must be suitable for the purpose and meet the Bureau of Mines requirements applicable to that particular type of unit. The unit also must be used in a manner prescribed by the Bureau.

4. The device must not be fired until everyone is 100 feet or more from the shot and protected by adequate cover, having 1 and if possible 2 right angles between them and the blast.

5. The coal to be blasted must be undercut or equivalently relieved; the length of the shothole must be at least 6 inches less than the depth of the undercut or equivalent relief; and the shothole shall be at least 6 inches away from the side of the undercut or equivalent relief.

6. No blasting device shall be assembled or disassembled in a mine unless such permission is specifically stated in the original approval.

7. A misfired device may not be opened in the mine unless an exception to this section is included as part of the approval for each specific device. The conditions that constitute a misfire will be specified in the original approval.

8. A waiting period of 15 minutes shall be required before any personnel are allowed to return to the face after a misfire has occurred.

9. Other conditions that will be set down by the Bureau as appropriate to the particular device tested.

As in the case of permissible explosives, field samples of permissible blasting devices are collected periodically and reexamined. A device that fails to pass retests must be withdrawn by the manufacturer until it meets the basic specifications.

FLAMMABILITY OF GASES AND VAPORS

Investigation of Surge-Ignition Sparks

Of the various possible sources of ignition considered in the study of explosive gas mixtures the electric spark offers especial interest in that it can easily be measured and has proved - under certain conditions - to be the most effective of all. Two of its most important characteristics are spark energy and spark duration.

Most workers have measured spark energies by calculating the energy stored in a capacitor and assuming that virtually all of this stored energy is dissipated in the spark during discharge. This dissipated energy has been evaluated by calorimetric methods[35/] and by analysis of current-voltage oscillograms.[36/] The latter method

35/ von Elbe, G., The Problem of Ignition: 4th Symposium (Internat.) on Combustion, Williams & Wilkins Co., Baltimore, Md., 1953, pp. 13-17.
Roth, W., Guest, P., von Elbe, G., and Lewis, B., Heat Generation by Electric Sparks and Rate of Heat Loss to the Spark Electrodes: Jour. Chem. Phys., vol. 19, 1951, p. 1530.

36/ Swett, C. C., Jr., Effect of Gas Stream Parameters on the Energy and Power Dissipated in a Spark and on Ignition: 3d Symposium on Combustion, Flame, and Explosion Phenomena, Williams & Wilkins Co., Baltimore, Md., 1949, p. 38.

Generated on 2024-09-21 14:39 GMT / https://hdl.handle.net/2027/osu.32435030643506
Public Domain, Google-digitized / http://www.hathitrust.org/access_use#pd-google
Digitized by Google
Original from THE OHIO STATE UNIVERSITY

has been applied at these laboratories to the measurement of electric sparks generated in connection with a study of the flammability of hydrocarbon vapors in air.37/

Apparatus and Procedure

The surge generator was chosen for the production of sparks of various characteristics as the simplest and most flexible device available. The block diagram of the system (fig. 37) shows the surge generator, power supply, current- and voltage-measuring units, synchronizing circuit, clipping circuit, and oscillograph. A glass bomb (4 inches i.d. by 50 inches length) containing the spark electrodes made of No. 20 platinum wire was used for the ignition studies. The charging voltage, capacity, and series inductance and resistance of the surge generator were varied to obtain a wide range of spark characteristics. To simplify the measurements, only overdamped (nonoscillatory) discharges were used.

A Dumont 304-H was used as the basic oscillograph. An auxiliary, or "slave" oscillograph having common sweep signal with the 304-H or "master" unit made it possible to record simultaneously oscillograms of voltage and current as a function of time. Two Dumont Type 296 cameras were used to record the oscillograms on Syper XX film. Although the analysis is more time consuming, it was felt that more accurate and more easily interpreted results could be obtained by plotting current and voltage separately against time than by plotting current against voltage.

In making a test the gas mixture in the bomb was adjusted to the desired conditions and a pulse applied to the center electrode of the surge-generator double gap. The pulse was opposite in polarity to the potential of the electrode on the surge-generator side of the double gap, and its voltage was sufficient to break down the first gap, causing the second gap to break down almost immediately. This, in turn, raised the potential on the test gap and its shunt resistance until it, too, sparked over and the surge circuit was completed.

Analysis of Oscillograms

Oscillograms on 35-mm. film were enlarged to about 3 by 4 inches. A typical pair of oscillograms - voltage versus time (fig. 38, A) and current versus time (fig. 38, B) - are shown with their respective time-base calibrations. In figure 39 the numerical values of voltage and current transients are plotted against the same time base for all tests. A curve of instantaneous power versus time is developed by multiplying together, point by point, the ordinates of the other two curves at simultaneous points of time (fig. 39, 5c). A point on the power curve gives the time rate of energy input to the spark gap. The area under the derived power curve is the total energy dissipated by the spark itself. A wide variety of sparks for use in determining the limits of flammability of combustible gas mixtures can be obtained by varying the parameters of the surge generator.

Limits of Flammability of Complex Hydrocarbon Fuels at High Altitudes

The rapid advances of high-altitude aviation in recent years have placed a growing emphasis on the problems encountered in combustion at high altitudes, that is, at low temperatures and pressures. Flammability studies over a wide range of temperatures and pressures have shown that certain factors, unimportant at ordinary temperatures and pressures, become important at low temperatures and subatmospheric

37/ Richmond, J. K., and Furno, A. L., The Production and Measurement of Surge-Ignition Sparks: Rev. Sci. Instr., vol. 24, No. 12, 1953, pp. 1107-1112.

Generated on 2024-09-21 14:36 GMT / https://hdl.handle.net/2027/osu.32435030643506
Public Domain, Google-digitized / http://www.hathitrust.org/access_use#pd-google
Digitized by Google
Original from THE OHIO STATE UNIVERSITY

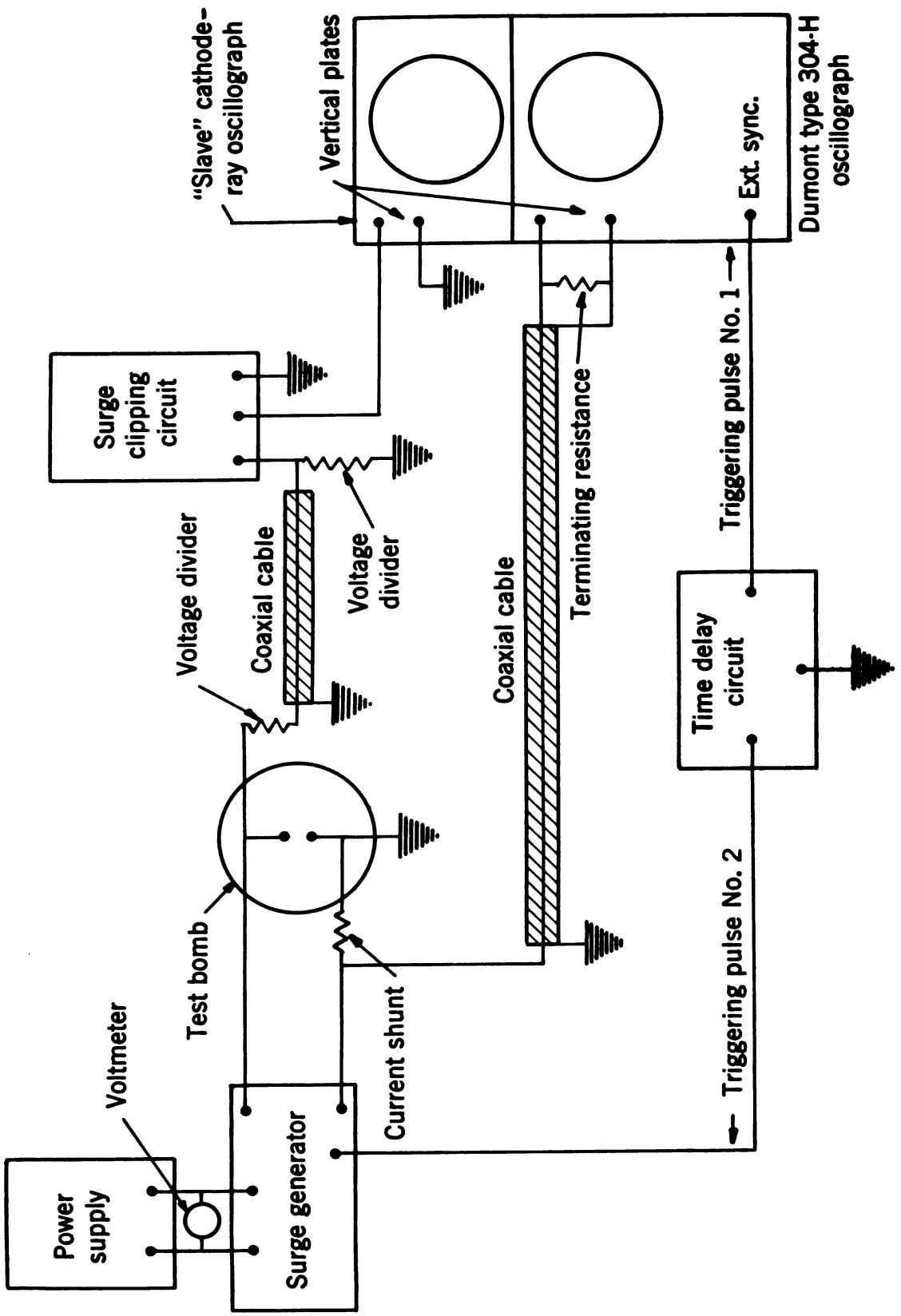

Figure 37. - Block diagram of apparatus for measurement of spark ignition energy.

Generated on 2024-09-21 14:33 GMT / https://hdl.handle.net/2027/osu.32435030643506
Public Domain, Google-digitized / http://www.hathitrust.org/access_use#pd-google
Digitized by Google
Original from THE OHIO STATE UNIVERSITY

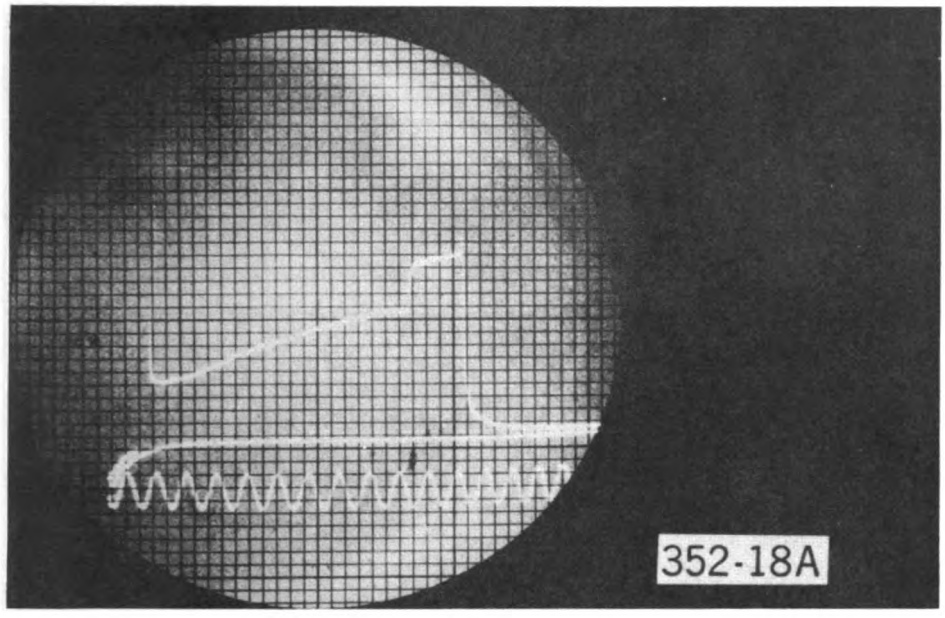

A

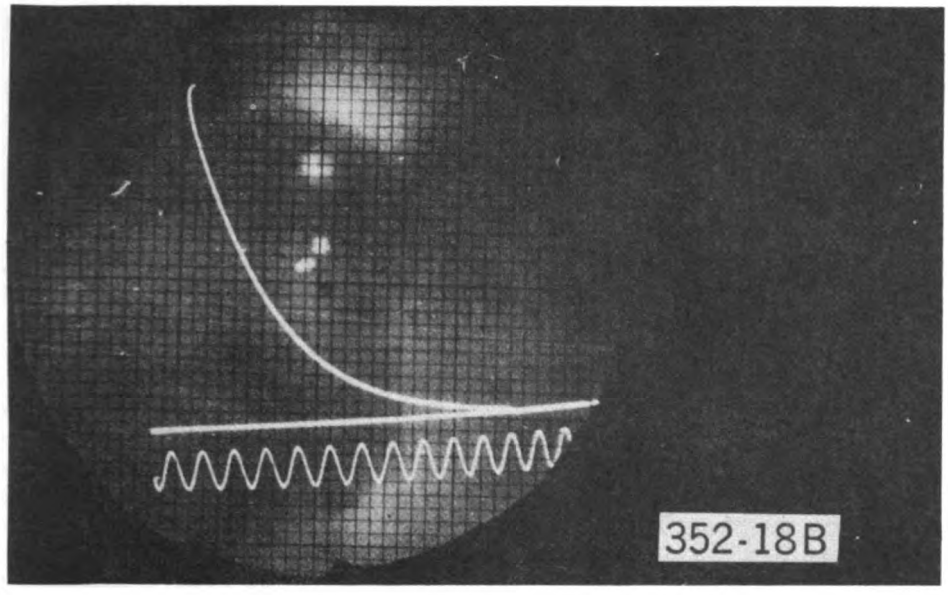

B

Figure 38. - Typical pair of oscillograms. A, Oscillogram of spark voltage vs. time; vertical calibration, 121.5 volts per inch; horizontal calibration, 946 microseconds per inch. B, Oscillogram of spark current vs. time; vertical calibration, 21.2 amperes per inch; horizontal calibration, 909 microseconds per inch.

Generated on 2024-09-21 14:38 GMT / https://hdl.handle.net/2027/osu.32435030643506
Public Domain, Google-digitized / http://www.hathitrust.org/access_use#pd-google
Digitized by Google
Original from THE OHIO STATE UNIVERSITY

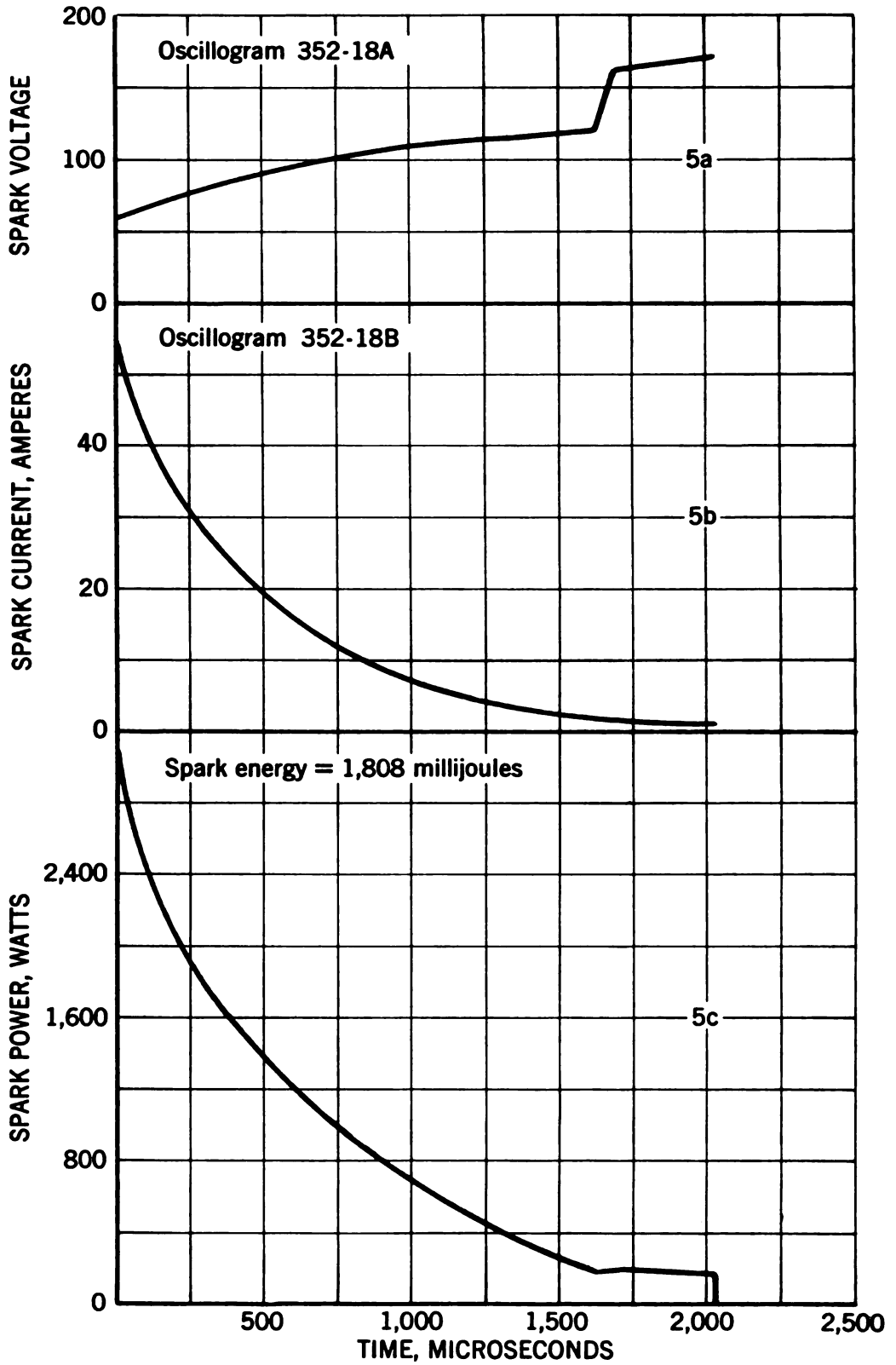

Figure 39. - Analysis of oscillograms of figure 38.

Generated on 2024-09-21 14:41 GMT / https://hdl.handle.net/2027/osu.32435030643506
Public Domain, Google-digitized / http://www.hathitrust.org/access_use#pd-google
Digitized by Google
Original from THE OHIO STATE UNIVERSITY

pressures. In designing limit-of-flammability apparatus for investigations under these conditions, special consideration must be given to the size and shape of the test chambers and to the source of ignition. Combustible liquid mixtures must be handled with care before testing to prevent loss by vaporization of highly volatile constituents that play a negligible part at higher temperatures but may be very important at low temperatures and pressures. Experiments[38/] on typical aviation gasolines and jet fuels have illustrated these points.

Apparatus and Procedure

Limit-of-flammability experiments fall into four categories:

1. Determination of the absolute limits of flammability[39/] of a combustible as a function of pressure for a fixed temperature and diluting atmosphere.

2. Determination of the absolute limits of flammability of a combustible as a function of the diluting atmosphere for a fixed temperature and pressure.

3. Determination of the absolute limits of flammability of a combustible as a function of temperature for a fixed pressure and diluting atmosphere.

4. Determination of the saturated limits of flammability of a combustible liquid or solid as a function of pressure for a fixed diluting atmosphere. When the vapor pressure of the combustible as a function of temperature is known, the saturated limits may be expressed in terms of fuel concentration.

A typical apparatus used for limit-of-flammability experiments in categories 1 and 2 is diagramed in figure 40. The combustible liquid is placed in a sample bottle p. Baseplate b is pressed onto the ground-glass flange of explosion chamber a, using a hydrocarbon-insoluble grease as lubricant. Mercury seal c is placed in position, stopcocks r and d are opened, and the entire system is evacuated through drying columns s and t. Before evacuation the mercury level in mixing bottle f' is raised to the zero mark on steel scale l by placing bottle f on a preadjusted platform. The mercury in mixing bottle g' is lowered to a level slightly below that illustrated in the figure for f', and the hose that couples bottles g and g' is clamped so that the mercury in g' remains at this low level during evacuation and the subsequent period when the combustible gas and the diluting atmosphere are added. The pressure in the system is indicated by the mercury level in manometer k. A McLeod gage indicates when the system has been evacuated to a pressure of approximately 100 microns. Stopcocks r and d then are closed, and a test mixture is prepared by the partial-pressure method as follows: Combustible vapors are admitted to the system through stopcock o until the desired partial pressure is indicated on steel scale l; the diluting atmosphere for example, air, is admitted to the system by opening stopcock q. In some cases, this must be done in several steps because condensation may occur when the diluting atmosphere is added. Combustible and diluent are mixed thoroughly by the mercury mixing pumps f' and g'. The mixture is passed through tube h and glass nozzle z into gas bottle j and then out again through tube i at least six times to insure proper mixing. When a mixture has been prepared, it is tested at a number of

---

38/ Zabetakis, M. G., and Richmond, J. K., The Determination and Graphic Representation of Limits of Flammability of Complex Hydrocarbon Fuels at Low Temperatures and Pressures: 4th Symposium (Internat.) on Combustion, Williams & Wilkins Co., Baltimore, Md., 1953, pp. 121-126.

39/ For a particular combustible, the absolute limits of flammability are, by definition, functions only of the diluting atmosphere, temperature, and pressure.

Generated on 2024-09-21 14:32 GMT / https://hdl.handle.net/2027/osu.32435030643506
Public Domain, Google-digitized / http://www.hathitrust.org/access_use#pd-google
Digitized by Google
Original from THE OHIO STATE UNIVERSITY

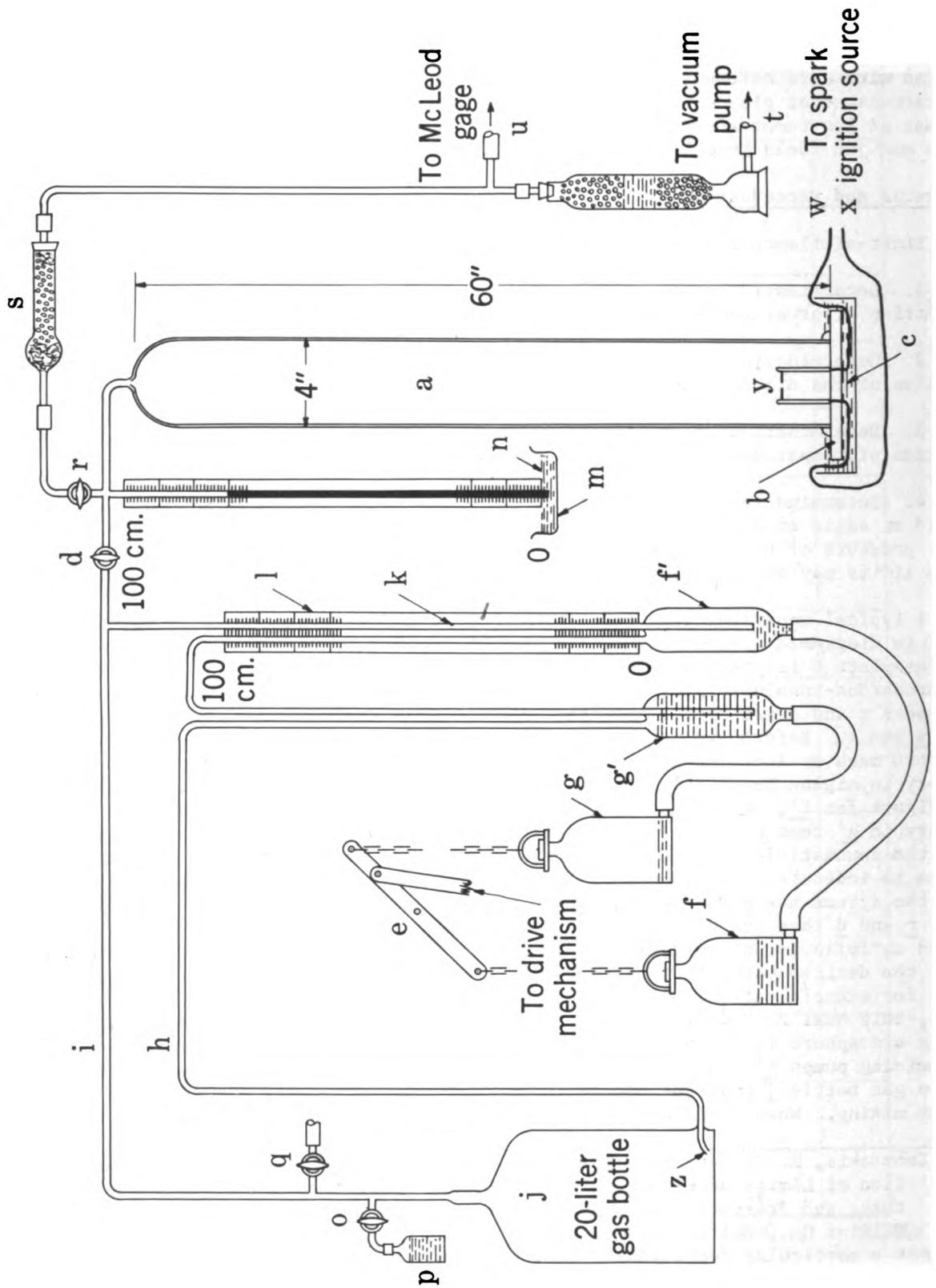

Figure 40. - Schematic diagram of F-24 limit-of-flammability apparatus.

Generated on 2024-09-21 14:40 GMT / https://hdl.handle.net/2027/osu.32435030643506
Public Domain, Google-digitized / http://www.hathitrust.org/access_use#pd-google
Digitized by Google
Original from THE OHIO STATE UNIVERSITY

pressures by introducing a measured quantity into the explosion chamber a and producing a spark between electrodes y. The initial test pressure is read on the steel scale attached to the system below stopcock r. A mercury manometer is used. As the area of the free mercury surface n in dish m is much larger than the cross-sectional area of the manometer, the zero reference level of the manometer does not differ appreciably at various test pressures.

The mixture in tube a is considered flammable if a flame propagates through the entire length of the tube. The source of ignition is considered unsatisfactory if it does not produce a flame that travels a short distance from the source when testing a nonflammable mixture the composition of which lies near an absolute limit of flammability. A number of ignition sources that are quite satisfactory at atmospheric pressure have proved unsatisfactory at low pressures. Both the total energy and duration of the spark are important in determining the efficiency of an ignition source. The source finally selected for ignitions at low pressures is the surge generator described above,[40/] which delivers its energy to the spark gap in a single pulse preadjusted to last 80 to 8,000 microseconds. This source is quite efficient for pressures down to 10 mm. Hg, the spark-gap length being increased as the absolute pressure is decreased to obtain the best conditions for spark ignition. The time rate of the energy delivered to the spark is obtained by a point-by-point multiplication of the voltage across, and the current through, the spark gap at corresponding times. The total energy is determined by calculating the area under the power-time curve in the usual manner.

Only a limited number of experiments were made in category 3 with combustible-liquid mixtures. The apparatus and results are discussed elsewhere.[41/]

Limit-of-flammability experiments in category 4 were conducted with a flow apparatus which has been used successfully over a temperature range of -100° to +200° F. and at pressures from 1.8 to 29.4 inches Hg. Dried air is fed to the apparatus through an adjustment valve and then into a heat exchanger. From the heat exchanger it goes into a saturator maintained at the temperature and pressure at which the test is to be conducted. The saturated vapor-air mixture passes into a cylindrical explosion chamber, where it is tested in the same way as the mixtures in categories 1 and 2. The exhaust gases and/or vapor-air mixtures are passed through absorption towers; the residual gases are exhausted into the atmosphere. A series of valves adjusts the pressure in the explosion chamber and isolates the chamber during a test. All limit-of-flammability tests are made under static conditions.

Experimental Results

Figures 41 to 43 illustrate the types of data obtained. Figure 41 gives the absolute limits of flammability for vapor-air mixtures of a typical complex hydrocarbon fuel (Avgas 100/130) at 78±1° F. (category 1). The dashed curves represent limits of ignitibility due to limitations of the source of ignition. Similar curves have been obtained for other gasolines and for a hydrocarbon-type aviation jet fuel (JP-3). Attempts to obtain similar data at subzero temperatures were unsuccessful due to condensation of the heavy fractions at these temperatures. Figure 42 gives the corresponding limits for vapor-air-inert gas mixtures at 80±1° F. and 16 inches of Hg absolute pressure (category 2). The diluting atmospheres for curve A consist of mixtures of air and carbon dioxide; for curve B they are mixtures of air and added

---

40/ See footnote 37, p. 63.

41/ Zabetakis, M. G., Scott, G. S., and Jones, G. W., Limits of Flammability of Paraffin Hydrocarbons in Air: Ind. Eng. Chem., vol. 43, No. 9, 1951, pp. 2120-2124.

Generated on 2024-09-21 14:40 GMT / https://hdl.handle.net/2027/osu.32435030643506
Public Domain, Google-digitized / http://www.hathitrust.org/access_use#pd-google
Digitized by Google
Original from THE OHIO STATE UNIVERSITY

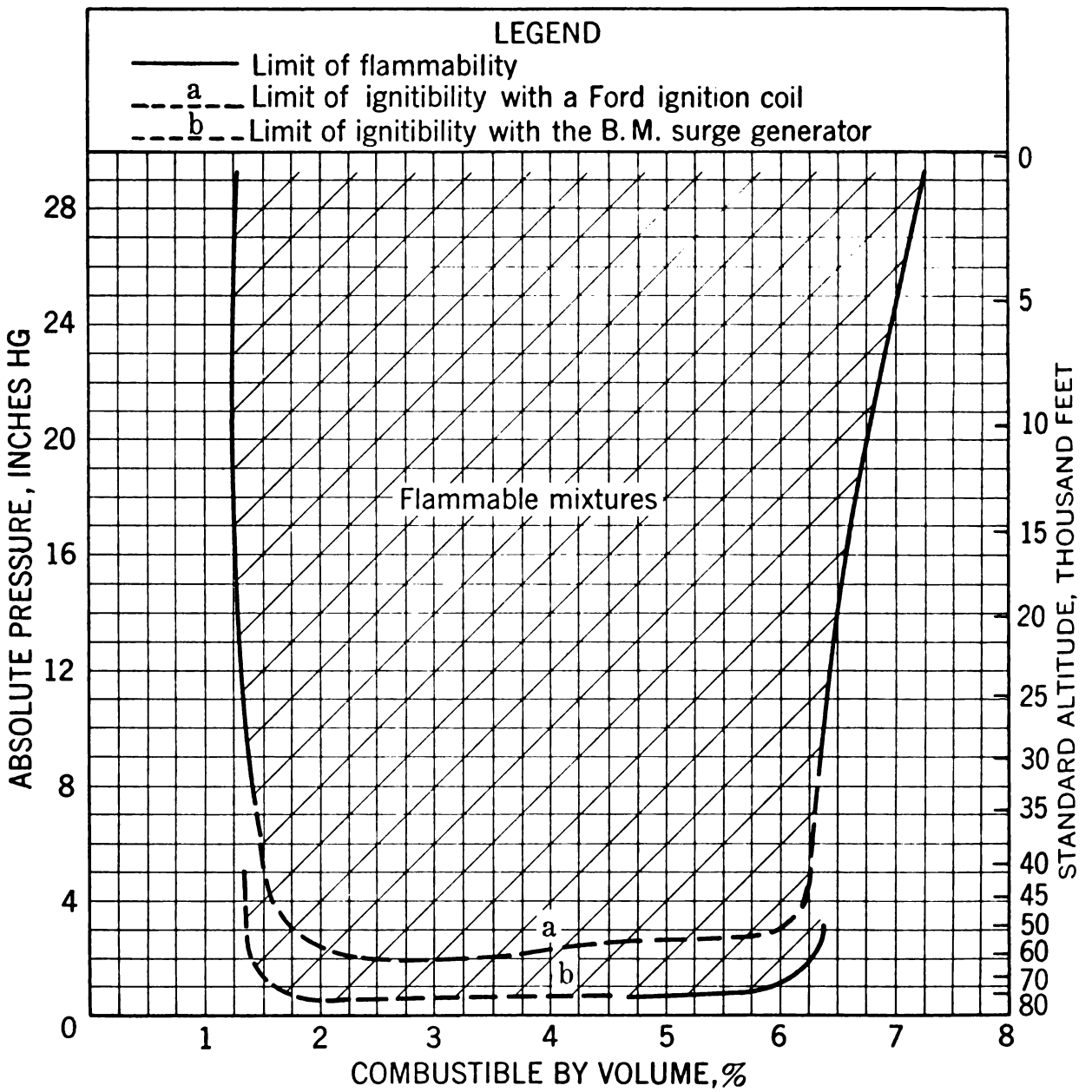

Figure 41. - Absolute limits of flammability for Avgas 100/130 vapor-air mixtures at 78± 1° F.

Generated on 2024-09-21 14:39 GMT / https://hdl.handle.net/2027/osu.32435030643506
Public Domain, Google-digitized / http://www.hathitrust.org/access_use#pd-google
Digitized by Google
Original from THE OHIO STATE UNIVERSITY

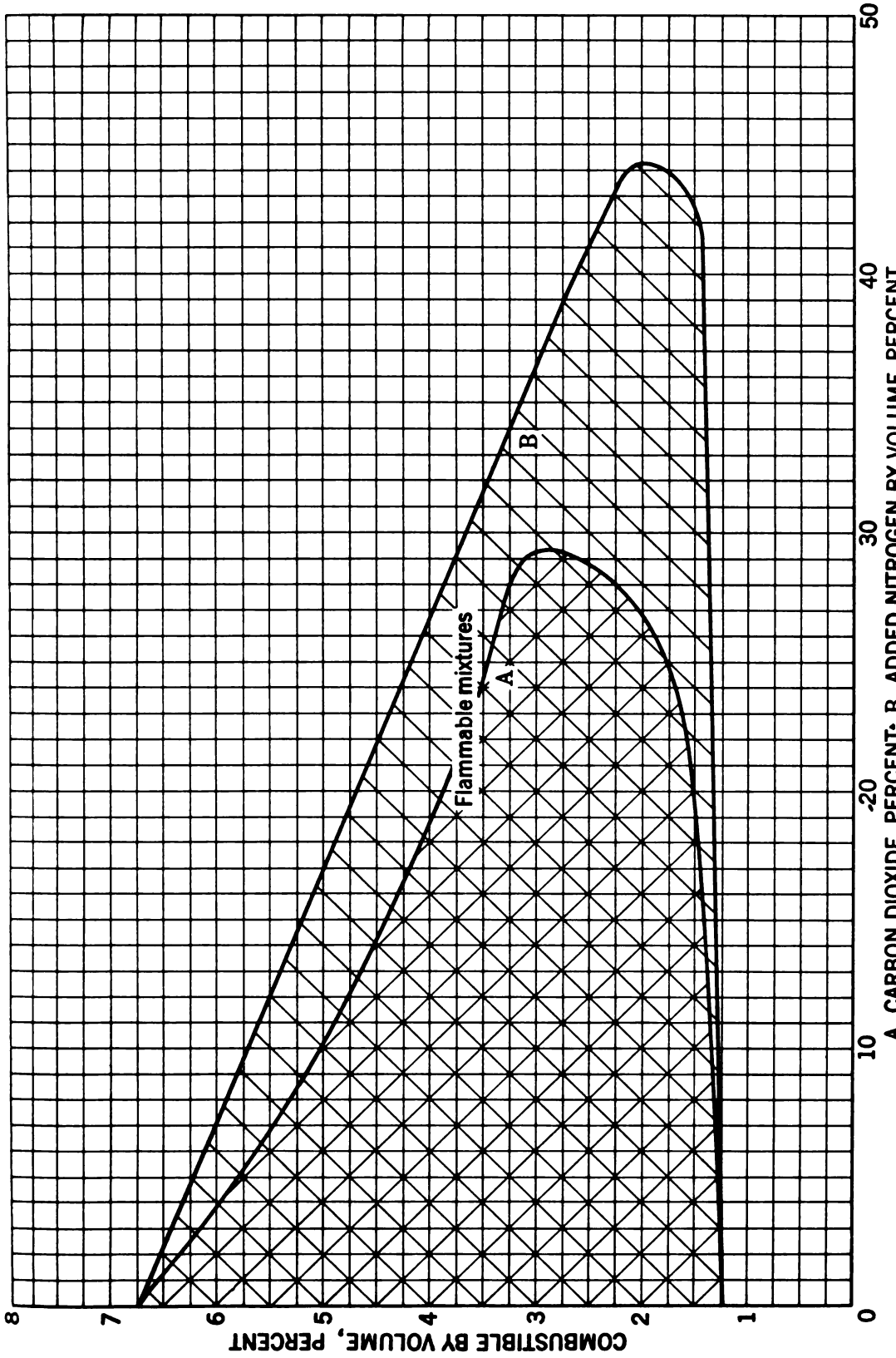

Figure 42. - Absolute limits of flammability for, A, Avgas 100/130 vapor-air-carbon dioxide mixtures at 16 inches Hg absolute pressure and 80±1 °F.; B, Avgas 100/130 vapor-air-nitrogen mixtures at 16 inches Hg absolute pressure and 80±2 °F.

Generated on 2024-09-21 14:30 GMT / https://hdl.handle.net/2027/osu.32435030643506
Public Domain, Google-digitized / http://www.hathitrust.org/access_use#pd-google
Digitized by Google
Original from THE OHIO STATE UNIVERSITY

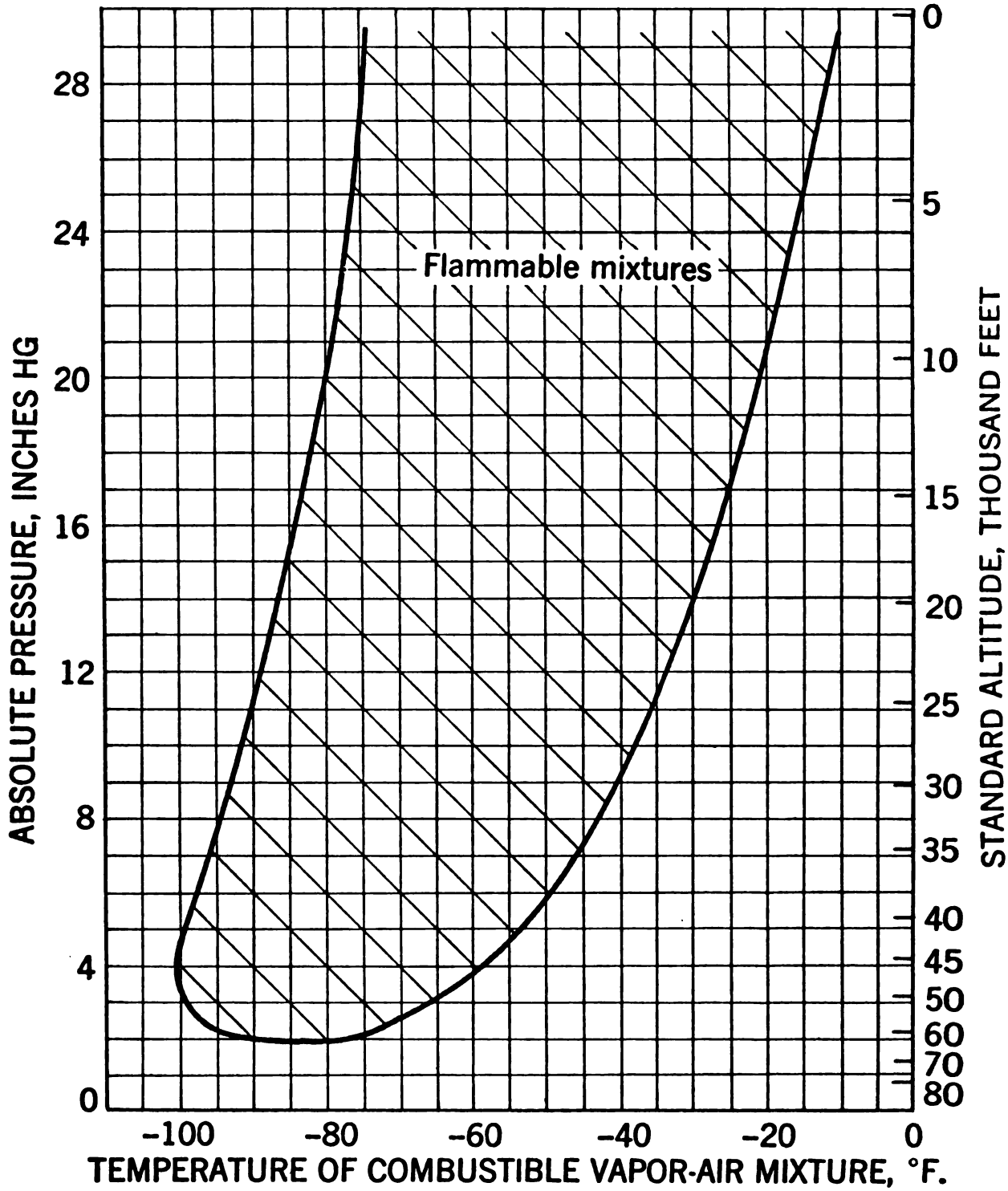

Figure 43. - Saturated limits of flammability of 0- to 5-percent fraction of Avgas 100/130 vapor-air mixtures over temperature range—100° to 0° F. (the 0- to 5-percent fraction of this fuel was distilled under temperature and pressure conditions of each test).

Generated on 2024-09-21 14:39 GMT / https://hdl.handle.net/2027/osu.32435030643506
Public Domain, Google-digitized / http://www.hathitrust.org/access_use#pd-google
Digitized by Google
Original from THE OHIO STATE UNIVERSITY

nitrogen. Similar data have been obtained at other pressures. Figure 43 gives the corresponding saturated limits of flammability as a function of pressure. This curve actually represents the saturated limits of flammability of the 0- to 5-percent fraction of the fuel used to saturate the air fed into the test chamber under the actual temperature and pressure conditions of each test.

The experimental data for categories 1, 3, and 4 usually are represented by appropriate 2-dimensional curves that outline the flammable mixtures; however, they may be combined to give a 3-dimensional figure that outlines the flammable mixtures for the combustible in a specified diluting atmosphere as a function of temperature and pressure. A general three-dimensional flammable volume of a combustible vapor-air mixture has been constructed in this way in figure 44. The pressure P, temperature T, and concentration of combustible are expressed as the ratio of the vapor pressure of the combustible to the total pressure. The three types of data ordinarily obtained for the limits of flammability of a combustible in air are represented by (1) curves such as $L_1P_{L1}P_{U1}U_1$, $L_2P_{L2}P_{U2}U_2$, etc., that outline the absolute limits of flammability of a combustible in air as functions of pressure for fixed temperatures (category 1); (2) curves such as $L_4L_3L_2L_1$ and U_2U_1 that outline the absolute limits of flammability of a combustible in air as a function of temperature for a fixed pressure (category 3); and (3) a trace such as $T_4T'_LP'_LT_2$ that outlines the saturated limits of flammability of saturated combustible vapor-air mixtures as a function of pressure on the temperature-pressure plane (category 4). This trace can be converted to the actual curve $L_4L'_5P_1U'_4U'_3U_2$ if the vapor pressure-temperature curve of the combustible is known. It should be noted that points such as U''_3 along the curve $L_4U''_3U_2$ are not limit-of-flammability points but represent flammable mixtures saturated with the combustible vapor. The absolute limit-of-flammability curve in the T_3 constant-temperature plane is represented by $L_3P_{L3}P_{U3}U'_3$.

Limit-of-flammability curve $L_4P_{L4}P_{U4}U'_4$ in the T_4 constant-temperature plane is interesting, in that it contains point L_4, which is a lower limit concentration and also represents a saturated combustible vapor-air mixture at one atmosphere pressure. This unique point is known as the "flash point." Curves such as those in figure 42 (category 2) may be considered as traces of the actual absolute limit-of-flammability curves in a three-dimensional representation at a fixed temperature and pressure where the three variables are the concentrations, respectively, of the combustible vapor, the initial diluting atmosphere and the added inert atmosphere. Figure 45 is a sketch of a general absolute limit-of-flammability curve illustrating the principles involved. As the sum of the concentrations of combustible, air, and inert on a percentage basis totals 100, absolute limit-of-flammability curve LNMU lies on plane XYZ. The trace of this curve on the XOY (percent inert-percent combustible) plane yields curve L'N'M'U', which corresponds to the trace given in figure 41 for the aviation gasoline vapor-air-inert curves at 80±1° F. and 16 inches Hg absolute pressure. Traces such as LM"U in figure 45 have been widely used in the past to determine the minimum air or oxygen required for flame propagation when a particular inert is used at a specified temperature and pressure. This minimum value is represented by point C and the OZ-axis. The construction lines ABC and A'B'O can be used to obtain the value represented by point C from the point M' on the XOY plant at which the line A'B' (slope = -1) is tangent to the curve L'N'M'U'.

Generated on 2024-09-21 14:33 GMT / https://hdl.handle.net/2027/osu.32435030643506
Public Domain, Google-digitized / http://www.hathitrust.org/access_use#pd-google
Digitized by Google
Original from THE OHIO STATE UNIVERSITY

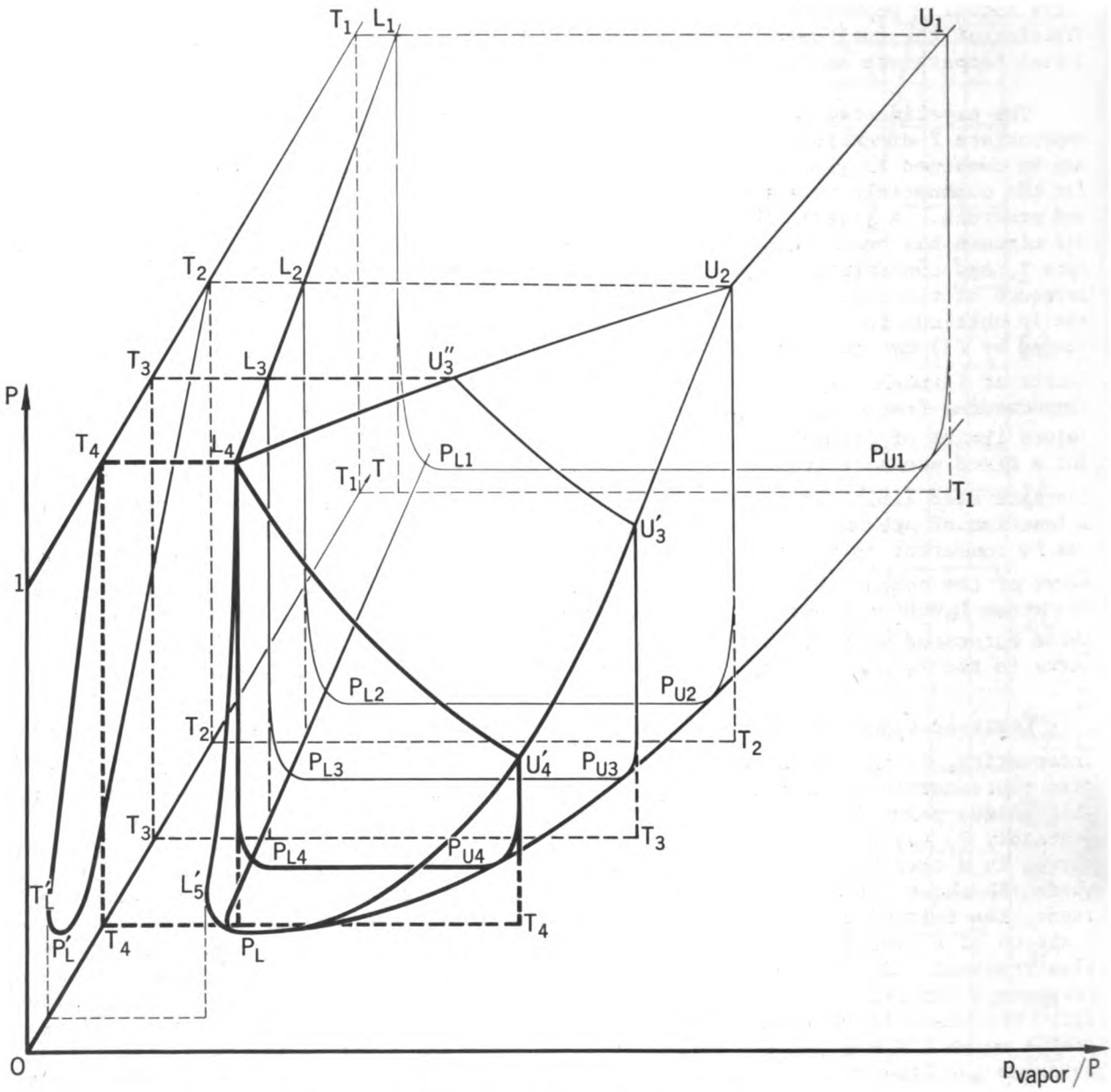

Figure 44. - General flammable volume of a combustible vapor-air mixture.

Generated on 2024-09-21 14:34 GMT / https://hdl.handle.net/2027/osu.32435030643506
Public Domain, Google-digitized / http://www.hathitrust.org/access_use#pd-google
Digitized by Google
Original from
THE OHIO STATE UNIVERSITY

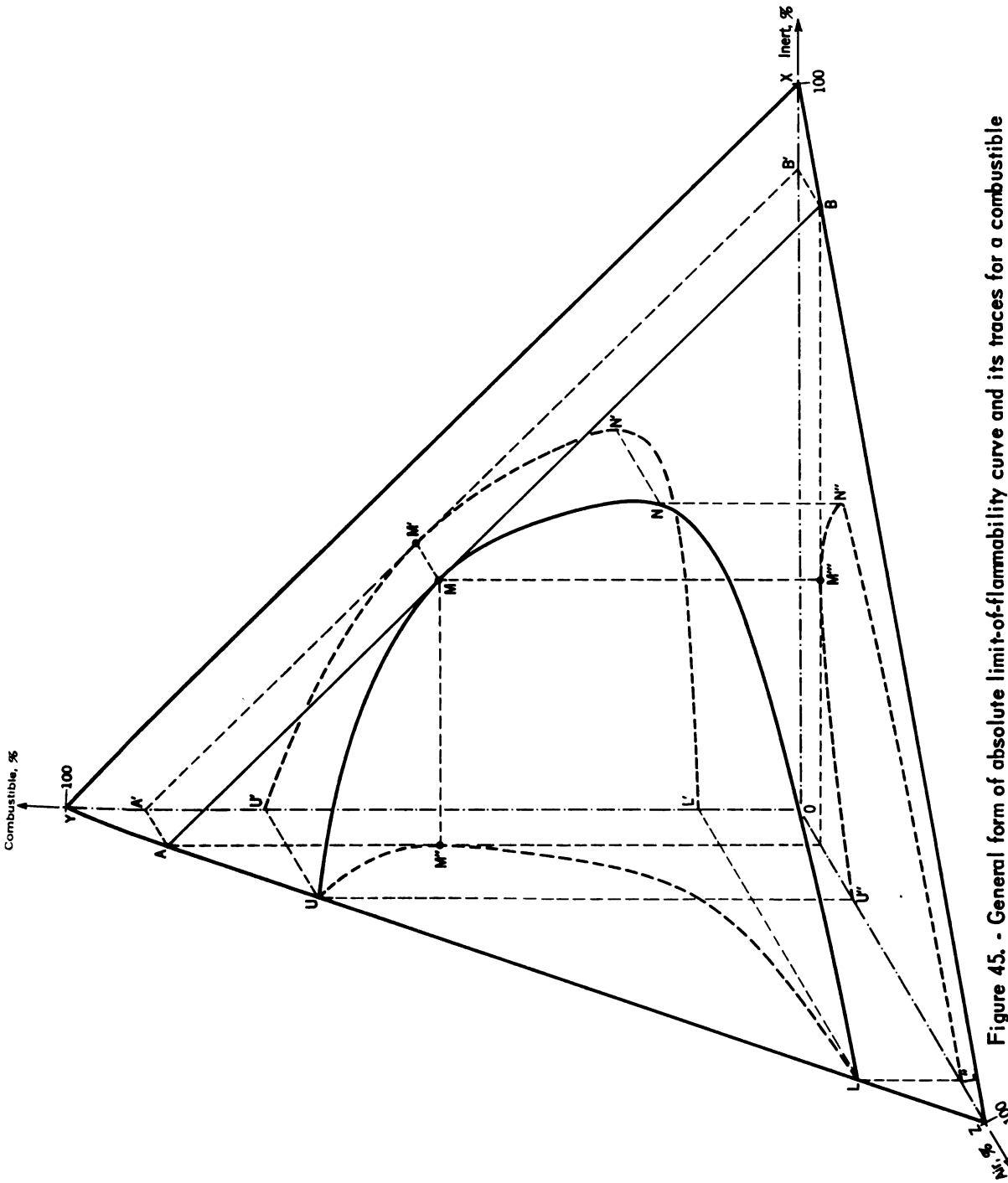

Figure 45. - General form of absolute limit-of-flammability curve and its traces for a combustible vapor-air-inert mixture at constant pressure and temperature.

Generated on 2024-09-21 14:41 GMT / https://hdl.handle.net/2027/osu.32435030643506
Public Domain, Google-digitized / http://www.hathitrust.org/access_use#pd-google
Digitized by Google
Original from THE OHIO STATE UNIVERSITY

Flammability of Carbon Disulfide in Mixtures of Air and Water Vapor

Water vapor has been used as a flame-quenching agent in many processes at elevated temperatures; however, few laboratory tests have been conducted to determine its effectiveness as an inert agent in combustible gas or vapor mixtures. A study of this type was undertaken using carbon disulfide-air-water vapor mixtures at 100° C. and 1 atmosphere pressure.42/

For this purpose, limits of flammability of carbon disulfide-air and carbon disulfide-air-water vapor mixtures were measured in a modified version of the Bureau of Mines high-temperature apparatus.43/ It was found that the lowest concentration for which carbon disulfide-air mixtures are flammable at 100° C. and atmospheric pressure is 1.20 percent CS_2 by volume. The minimum concentration of oxygen for flame propagation through a mixture of carbon disulfide, air, and water vapor at 100° C. and 1 atmosphere pressure is 7.6 percent by volume. A carbon disulfide vapor-air flame with constituents initially at 100° C. can be extinguished by 4.3 pounds of water per pound of carbon disulfide or 3.4 gallons of water per gallon of carbon disulfide on a volume basis.

The procedure applied in this investigation represents a new and rapid technique for determining accurately the effectiveness of water or other vapor in quenching flames of combustible vapor-air mixtures at high temperatures.

DUST-EXPLOSION INVESTIGATIONS

Incombustible Requirements on Floors and Overhead Surfaces in Coal Mines

The fire and explosion hazard created by excessive coal-dust deposits in mines has been recognized for many years, and important measures have been developed for reducing dust formation and allaying loose dust near its source. Nevertheless, it has been estimated that, in the course of normal operations, 1 to 10 percent of the total coal mined is reduced to dust of through-20-mesh fineness. In highly mechanized, continuous mining operations the production of fines is even greater. Although most dust is trapped near its point of origin and removed from the mine, important quantities are transported by the air current and by haulage into entries, where the greatest proportion settles on the floor and the balance on the rib and roof surfaces. The fact that rib and roof dusts are generally finer than floor dusts, coupled with their more advantageous position for dispersion, makes them a greater potential explosion hazard. Currently, the most important safeguard against widespread explosions in American coal mines is generalized rock dusting. Experiments have shown that more rock dust is needed to prevent explosions in fine overhead dust than in floor dust; however, the requirements for generalized rock dusting are that the incombustible content of the dust be 65 percent or more for the entire perimeter of the mine entry.

After rock dust is applied in mine workings, the dust on the floor often is rapidly contaminated by coal spilled during haulage, coal abraded from the ribs, and coal dust settling from the air current. As a result, the incombustible content of the floor dust often falls below 65 percent, whereas that of the less contaminated overhead dust remains above the required limit. The question often has been raised

---

42/ Zabetakis, M. G., and Jones, G. W., Flammability of Carbon Disulfide in Mixtures of Air and Water Vapor: Ind. Eng. Chem., vol. 45, No. 9, 1953, pp. 2079-2080.

43/ Work cited in footnote 41 (p. 69).

Generated on 2024-09-21 14:39 GMT / https://hdl.handle.net/2027/osu.32435030643506
Public Domain, Google-digitized / http://www.hathitrust.org/access_use#pd-google
Digitized by Google
Original from THE OHIO STATE UNIVERSITY

as to whether a deficiency of rock dust on the floor may be tolerated with safety and whether such deficiency can be compensated by excess rock dust on the rib and roof surfaces. A limited number of tests conducted by the Bureau of Mines several years ago[44] indicated that the incombustible content of floor dust could be lower than on the ribs and timbers, but the differences that can be tolerated were not determined with any degree of accuracy.

With the passage of the Federal Coal-Mine Safety Act,[45] the problem of the relative incombustible requirements over the perimeter of mine entries assumed new importance. In some quarters it was suggested that these requirements would be met if the arithmetic mean of the average incombustible content of floor and overhead dusts was 65 percent or more; however, the very much greater proportion of floor dust makes this solution unsatisfactory. To study the problem an investigation was made at the Experimental Coal Mine at Bruceton, Pa.[46]

Experimental Arrangements

About 70 single-entry explosion tests were made in the 1,308-foot-long main entry (9 feet wide by 7 feet high) of the Experimental Coal Mine. The explosions were initiated at the face (E-1308) of the entry, and the test zone extended 558 feet outby to a point designated as E-750. Bituminous Pittsburgh coal dust was used in all tests. It was prepared so that all particles passed through a 20-mesh Tyler sieve, and 20 percent by weight passed through a 200-mesh (74 microns square) sieve; in a few tests with electric-arc ignition, 28 to 30 percent of the dust was finer than 200-mesh. The rock dust used in the tests was limestone of a type common in western Pennsylvania mines. It contained 0.1 percent moisture and 99.9 percent total incombustible; 75 to 80 percent passed through a 200-mesh sieve.

Coal dust and limestone were mixed intimately on the surface. Usually, separate mixtures were prepared for loading on the floor and for the side and overhead shelves in the test zone. The dust was distributed manually with hand scoops (fig. 46). To study the effect on the rock-dust requirements of different dust conditions in mines, the rate of dust loading was varied in different groups of experiments as follows:[47]

1. 2/3 pound on rib-roof (one-half is always placed on longitudinal side shelves and one-half on cross shelves), 1/3 pound on floor.

2. 2/3 pound on rib-roof, 2/3 pound on floor.

3. 2/3 pound on rib-roof, 1-1/3 pounds on floor.

4. 1/3 pound on rib-roof, 1-1/3 pounds on floor.

5. 1/6 pound on rib-roof, 1-1/2 pounds on floor.

The incombustible content of the dust mixtures on the floor ranged from 36 to 68 percent and in the rib-roof dust from 36 to 86 percent.

44/ Rice, G. S., Greenwald, H. P., and Howarth, H. C., Explosion Tests of Pittsburgh Coal Dust in the Experimental Mine, 1925 to 1932, Inclusive: Bureau of Mines Bull. 369, 1933, pp. 38-41.

45/ Public Law 552, 82d Cong., 2 session.

46/ Hartmenn, I., Nagy, J., and Christofel, F. P., Incombustible Required on Floor and on Rib-Roof Surfaces of Coal Mines to Prevent Propagation of Explosions: Bureau of Mines Rept. of Investigations 5053, 1954, 7 pp.

47/ The values indicate the weight of coal dust in the dust mixtures per linear foot of entry, uniformly applied from the ignition zone to E-750.

Generated on 2024-09-21 14:35 GMT / https://hdl.handle.net/2027/osu.32435030643506
Public Domain, Google-digitized / http://www.hathitrust.org/access_use#pd-google
Digitized by Google
Original from THE OHIO STATE UNIVERSITY

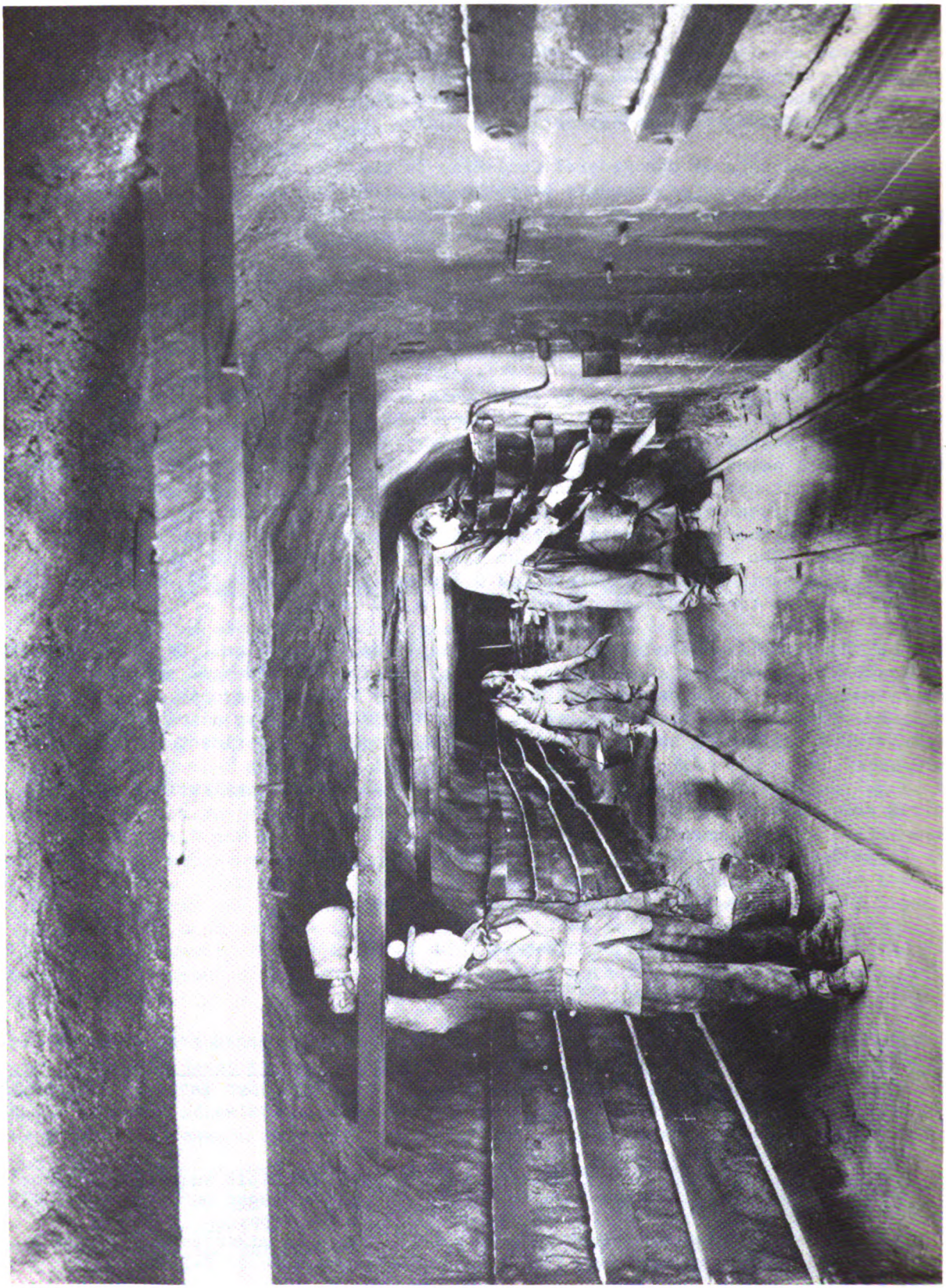

Figure 46. - Distribution of coal dust-limestone mixture in test zone of main entry.

Generated on 2024-09-21 14:30 GMT / https://hdl.handle.net/2027/osu.32435030643506
Public Domain, Google-digitized / http://www.hathitrust.org/access_use#pd-google
Digitized by Google
Original from
THE OHIO STATE UNIVERSITY

In every test measurements were made of the pressures developed, the flame velocities and direction of air movement at several points in the entry, and the total length of flame. An explosion was considered stopped and propagation arrested if the flame did not extent more than 558 feet from the face, that is, beyond the end of the coal dust-rock dust mixture at E-750.

As explosions initiated by a strong source of ignition that disperses considerable coal dust require a higher proportion of incombustible for quenching than explosions started by a weak source, four different sources of ignition were used. They are shown schematically in figure 47, which also indicates flame lengths, pressures, and velocities produced by the ignitions. The ignition sources are arranged in order of strength, going from the weakest (5-ampere electric arc) to the strongest (Special B source).

Experimental Results

The effect or reducing the incombustible content of the floor dust is shown in figures 48 and 49. For clarity, the data are plotted in three separate blocks on each figure, corresponding to three sources of ignition; no curves are given for the few tests with Standard B source. In figure 48 the incombustible in the rib-roof dust is plotted against the incombustible in the floor dust; figure 49 shows the incombustible in the total dust, with relation to incombustible in floor dust. The curves on both figures are smoothed, average limiting curves, generally drawn between the test data for propagation and nonpropagation. Areas above the curves (for given dust distributions) represent regions of nonexplosibility; areas below the curves represent regions of explosibility.

Comparative data with all 3 sources of ignition are available only for the coal distribution of 0.67 pound on the rib-roof and 0.33 pound on the floor. These show that the incombustible requirements are highest for explosions started by Special B source and lowest for those initiated by an electric arc. The curves in figure 48 show that, for this dust distribution, when the incombustible in the floor dust was reduced 10 percent, the incombustible in the overhead dust had to be raised about 3 percent with all 3 sources of ignition. Figure 49 shows that, with the same dust distribution, the incombustible in the total dust remains constant when the incombustible on the floor is reduced. In other words, deficiency of rock dust on the floor was exactly compensated by the increase on the rib-roof surfaces in all three series of explosion tests.

The data from explosion tests initiated by gas ignition (C-25) with 0.67 pound of coal dust overhead and 0.67 and 1.33 pounds on the floor gave identical curves in figures 48 and 49. The latter curve shows that as the incombustible in the floor dust is reduced, the weighted incombustible in the total dust (floor plus rib-roof) decreases slightly. This apparent anomaly is explained if one remembers that in these explosions all or nearly all the overhead dust of high incombustible content is dispersed off the shelves, whereas only a fraction of the dust is dispersed from the floor. Thus the average incombustible content of all the dust actually is suspension (in these tests about 64 percent) is sufficient to prevent propagation.

This trend is evident also in the curves with coal dust distributions of 0.33 pound overhead, 1.33 pounds on floor (C-25 and Special B ignitions), and with 0.17 pound overhead, 1.50 pounds on the floor. Although Special B source can raise considerable dust from the floor, it is evident from the slope of the curves in figure 4 that in these explosions the floor dust was not dispersed completely.

Generated on 2024-09-21 14:30 GMT / https://hdl.handle.net/2027/osu.32435030643506
Public Domain, Google-digitized / http://www.hathitrust.org/access_use#pd-google
Digitized by Google
Original from THE OHIO STATE UNIVERSITY

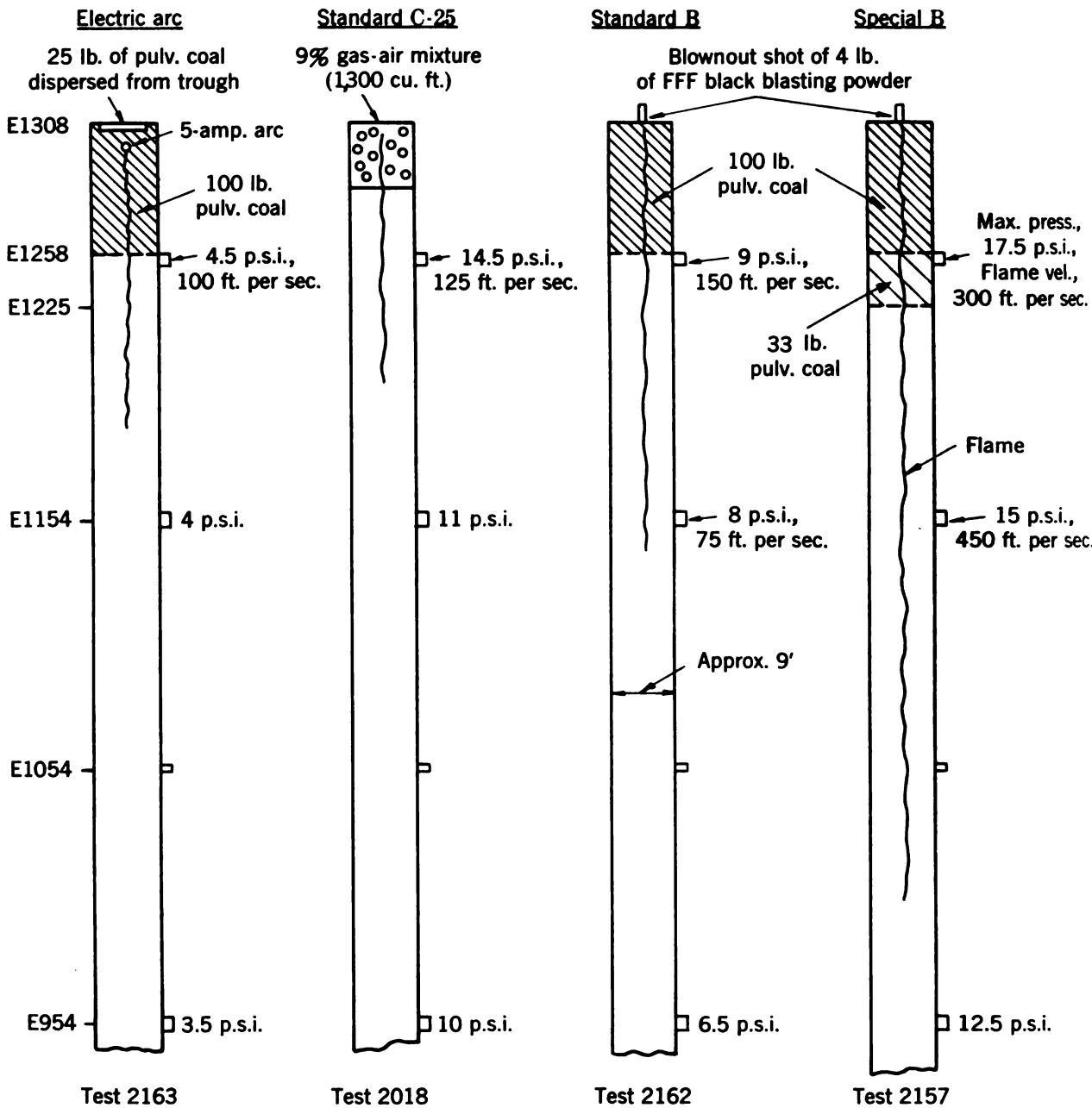

Figure 47. - Sources of ignition used in Experimental Coal-Mine explosion tests.

Generated on 2024-09-21 14:38 GMT / https://hdl.handle.net/2027/osu.32435030643506
Public Domain, Google-digitized / http://www.hathitrust.org/access_use#pd-google
Digitized by Google
Original from THE OHIO STATE UNIVERSITY

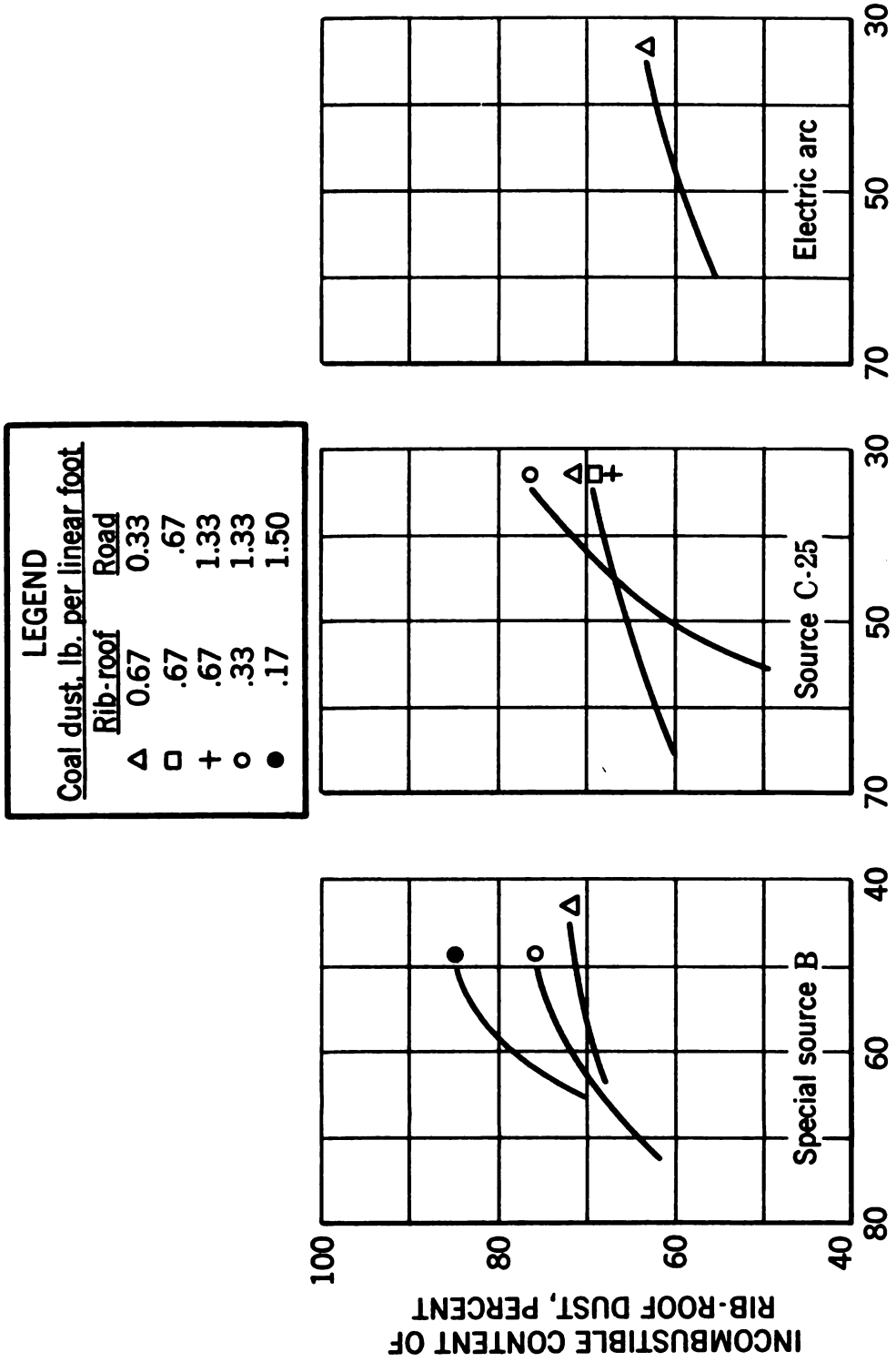

Figure 48. - Incombustible content of floor and rib-roof dusts in explosion-limiting mixtures.

Generated on 2024-09-21 14:30 GMT / https://hdl.handle.net/2027/osu.32435030643506
Public Domain, Google-digitized / http://www.hathitrust.org/access_use#pd-google
Digitized by Google
Original from THE OHIO STATE UNIVERSITY

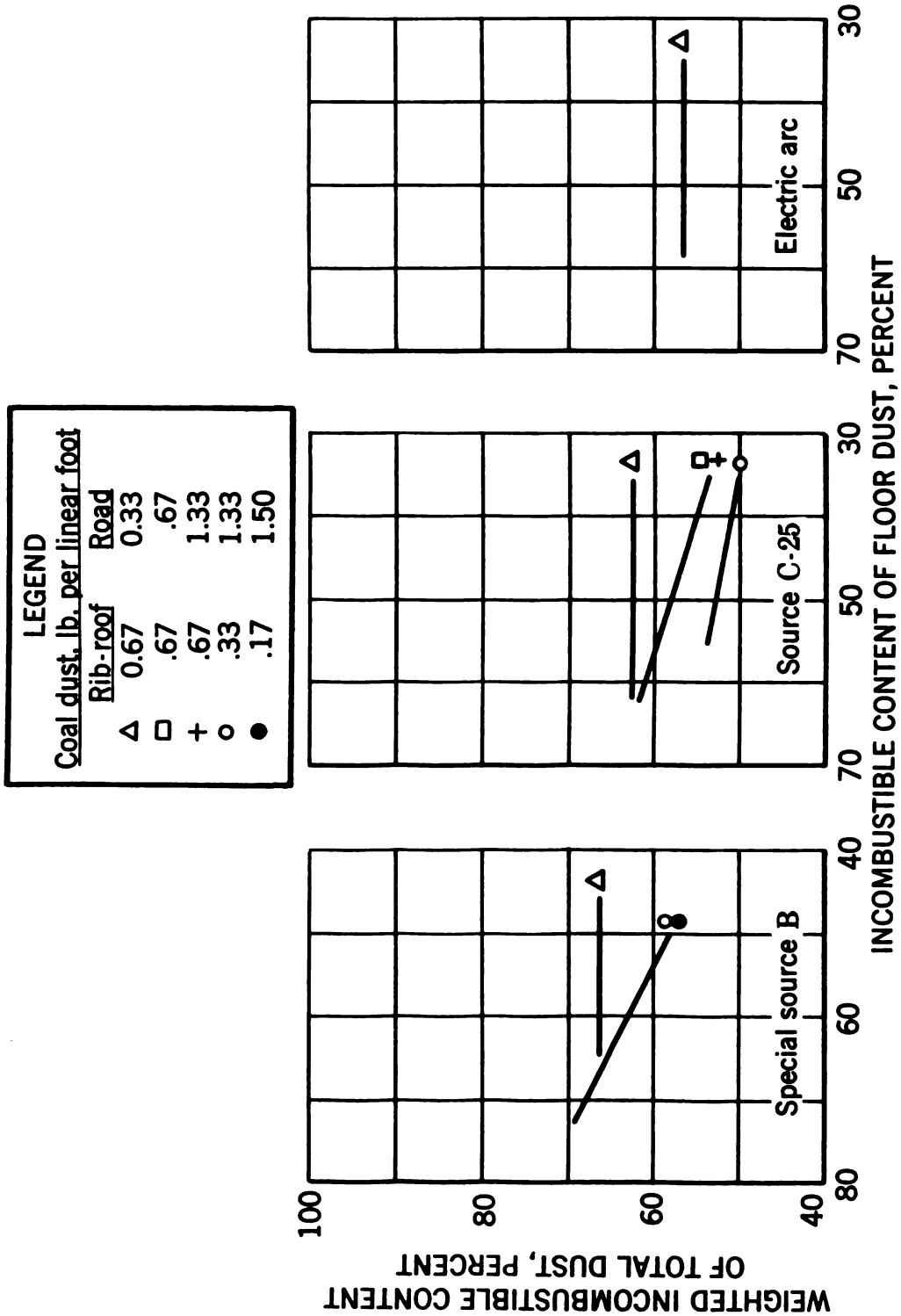

Figure 49. - Relation of incombustible contents in total dust to floor dust in explosion-limiting mixtures.

Generated on 2024-09-21 14:39 GMT / https://hdl.handle.net/2027/osu.32435030643506
Public Domain, Google-digitized / http://www.hathitrust.org/access_use#pd-google
Digitized by Google
Original from THE OHIO STATE UNIVERSITY

Two tests were made with Special B ignition to determine whether deficiency of rock dust on rib-roof surfaces can be compensated by an equivalent weight of excess rock dust on the floor. It was found that this cannot be done and that the incombustible content of the total dust must be increased to prevent flame propagation (see fig. 49). This finding emphasizes the greater importance of rib-roof dust in explosions.

Conclusions

The experimental results indicate that deficiency of rock dust on the floor of mine workings can, within certain limits, be compensated by enough excess rock dust on the rib-roof surfaces to maintain the weighted incombustible content of the total dust around the perimeter of an entry at 85 percent. The limits depend on the strength of the potential explosion and on the distribution of dust on the floor and overhead. In most mines the amount of floor dust is many times greater (10 to 50 or more) than the overhead dust. For protection against an explosion initiated by a strong source that might disperse 3 times as much floor dust as rib-roof dust, if the incombustible in the floor dust is reduced to 55 percent, the incombustible in the overhead dust must be 95 percent to bring the value in the total dispersed dust to the necessary minimum of 65 percent. Under such conditions virtually no rock-dust deficiency can be tolerated.

Intensive Sampling of Coal-Mine Dusts

The Bureau of Mines has been charged by the Congress with administering the provisions of the Federal Coal-Mine Safety Act, and one of the important duties of Bureau inspectors under this act is to determine whether the necessary measures are taken to prevent mine explosions. In most mines this includes adequate rock dusting. If a mine proves deficient in rock dust, the operator can be cited for violating the law. In severe cases men may be summarily withdrawn from a section of the mine, or the entire mine may be ordered closed until corrective measures have been taken. This places great responsibility on the mine inspectors, and it is important that their decisions be well founded.

Rock dust is commonly applied by machine or by hand; occasionally, it is applied by special methods, such as dispersal from bags placed on sticks of permissible explosives on the mine floor. At the time when the act went into effect, data were lacking for establishing just how uniformly and efficiently this distribution was accomplished. The quantity of rock dust used varied greatly from mine to mine and from State to State.

To insure compliance with rock-dusting requirements, dust is sampled by Federal and State inspectors, rather than by mine operators. Sampling is only one of the tasks that make up a complete mine inspection. During the fiscal year 1952 Bureau inspectors collected 6,193 dust samples in 1,083 mines and shipped them to the Analytical Laboratory at Pittsburgh, Pa. This represents an average of 5.7 samples per mine. Although this number of dust samples does not permit even a semiquantitative check of compliance with rock-dusting requirements, the tremendous task represented by the collection and analysis in a single laboratory makes the need for a rapid on-the-spot method of dust sampling evident.

This need, coupled with the explosion in the Orient No. 2 mine, Franklin, Ill., on December 21, 1951, which showed that much information was lacking on rock-dusting and dust-sampling practices in the United States, led to an intensive sampling survey

Generated on 2024-09-21 14:36 GMT / https://hdl.handle.net/2027/osu.32435030643506
Public Domain, Google-digitized / http://www.hathitrust.org/access_use#pd-google
Digitized by Google
Original from THE OHIO STATE UNIVERSITY

by the Bureau in an Indiana coal mine.[48/] In this study (conducted cooperatively by several technical groups of the Bureau of Mines coordinated by a Supervisory Committee on Revision of Methods of Sampling Mine Dusts) samples were collected at the Indiana mine by mine inspectors from the Vincennes Area Office. Less intensive sampling at several Pennsylvania mines was performed by inspectors from the Pittsburgh Area Office. Chemical analyses of the samples were made by the Coal Analysis Section at Pittsburgh. Most of the planning the particle-size determination, and the data evaluation were the work of the Dust-Explosions and Coal-Mine-Experiments Branch, Pittsburgh.

Plan of Investigation

About 1,050 dust samples were collected from the Indiana mine in 3 parallel entries in each of 2 sets of panels; in 2 main haulageways; in 7 adjoining, parallel active and worked-out rooms; and at 27 random locations in the mine. The original plan called for sampling entries adjacent and parallel to the main haulageways, but owing to considerable spalling of the roof and rib surfaces no samples were collected in those areas. The lengths of sampled areas included approximately 3,600 feet of panel entries, 22,000 feet of main haulageways, and 1,100 feet of rooms. The distance between sampling points was 15 feet in several 300-foot-long sections; in other areas, samples were taken 100,300, 900, and 1,800 feet apart. In general, the road samples were taken to a depth of 1 inch; but, at selected places, the dust was sampled to a depth of 1/4 to 1 inch, 1 to 2 inches, 2 to 3 inches, 3 to 4 inches, and down to the full depth of the dust deposit. A rib-roof sample also was taken at every sampling point.

Peripheral or band samples were taken initially at several locations. As band sampling would reduce the time required for collecting, quartering, packing, and handling, as well as for chemical analysis, the question was whether it could be adopted without sacrificing safety in coal mines. To this end, road and corresponding band samples from 417 locations at the Indiana mine were studied, with smaller numbers of samples from 14 Pennsylvania mines. The average analyses from all mines are summarized in the following table:

	Average incombustible, percent			
	Number	Road dust	Band dust	Difference
Indiana mine	417	60.4	63.2	2.8
Pennsylvania mine No. 1	31	75.8	79.1	3.3
Pennsylvania mine No. 2	28	77.3	79.0	1.7
Pennsylvania mine No. 3	24	68.3	72.9	4.6
11 Pennsylvania mines	24	81.5	85.9	4.4

These data show that the average incombustible contents of band samples are slightly higher than values for corresponding road samples. This is to be expected, as rib-roof dusts nearly always contain more incombustible than road dusts, and the quantity of dust on the road is many times greater than overhead. On the basis of these data the Bureau of Mines recently adopted band sampling in place of separate road and rib-roof sampling. To reduce the time and labor required for collecting and analyzing mine-dust samples, thereby enabling the inspectors to examine more locations in mines and gain a better overall picture of rock-dust conditions, various estimating techniques were studied. These included: Reexamination of standard

48/ Hartmann, I., Nagy, J., and Rauschenberger, J. K., Lessons From Intensive Dust Sampling of a Coal Mine: Bureau of Mines Rept. of Investigations 5054, 1954, 12 pp.

Generated on 2024-09-21 14:30 GMT / https://hdl.handle.net/2027/osu.32435030643506
Public Domain, Google-digitized / http://www.hathitrust.org/access_use#pd-google
Digitized by Google
Original from THE OHIO STATE UNIVERSITY

and modified volumetric procedures; relation of incombustible to apparent and actual density of dust mixtures; separation of rock dust by centrifuging; color measurements by reflectometers; and visual color examination by comparison with standard dust mixtures. The specific objective of the work was to eliminate underground all or most dust samples that contain 75 percent or more incombustible. As 50 percent or more of all dust samples received during a month by the analytical laboratory frequently contain over 80 percent incombustible, underground elimination of samples with high incombustible content would mean an important saving of effort.

Following preliminary laboratory studies, it was concluded that visual color comparison with standard dust mixtures prepared from mine-dust samples might provide a rapid practical method. In undertaking studies of this method, account was taken of earlier experience in several European countries, including the visual and instrument sorting used currently in British laboratories. Although the method is subject to uncertainties and difficulties (effect on color of various contaminants, particle size of coal dust, particle size of rock dust, moisture content, degree of mixing, segregation and stratification of constituents, etc.), the laboratory work seemed promising, and underground sorting was undertaken in four coal mines in Pennsylvania. In spite of many unforeseen problems, the results were encouraging, and no dust samples deficient in incombustible (less than 65 percent incombustible) were judged safe.

No decision has been reached yet concerning possible adoption of the color-sorting method by Federal inspectors. Should the procedure be adopted, it is planned to ship all samples of the same or darker color than the standard mixture to the laboratory for analysis. Occasionally, a lighter color sample would be submitted as a check.

Results of Investigation

Sampling studies at several bituminous-coal mines have shown that:

1. Band or perimeter sampling of dust can be substituted, with no sacrifice in safety, for the more tedious road and rib-roof sampling.

2. The incombustible in the top 1-inch layer of dust on roadways gives a good estimate of the incombustible in the full-depth dust deposit.

3. The quantity of dust on haulageways and other roads may be excessively high, thus requiring very large tonnages of rock dust. Every effort should be made to persuade mine operators to reduce dust formation during mining and to allay and clean up all dust that is formed.

4. The weight of dust deposited on the floor exceeds the dust on rib and roof surfaces many times.

5. The incombustible content is higher in overhead dust than in road dust.

6. The theoretical minimum number of dust samples required to give adequate information on the average incombustible content in mine workings is greater than could be collected with desired frequency by Federal inspectors using present sampling procedures. As a partial remedy of the situation, coal-mine operating personnel might, following proper instruction, be asked to collect supplementary samples. Bureau inspectors could examine more locations than hitherto by taking spot increments in some areas between strip samples and sorting out underground samples of high incombustible content by the visual color-sorting techniques.

Generated on 2024-09-21 14:43 GMT / https://hdl.handle.net/2027/osu.32435030643506
Public Domain, Google-digitized / http://www.hathitrust.org/access_use#pd-google
Digitized by Google
Original from THE OHIO STATE UNIVERSITY

7. The incombustible in many mine dusts contains large proportions of sand, shale, or other coarse material much less effective in stopping explosions than finely divided limestone. To ascertain the proportion of this type of inert, the calcium carbonate contents of at least 1 or 2 dust samples from each mine might be determined and a sieve analysis made of the same dusts.

Laboratory Studies of Dust Explosibility

The explosion hazards of 170 dust samples submitted by various companies and agencies were determined during the fiscal years 1953 and 1954. The dusts or powders examined included: Coal-mine dusts; factory and foundry dusts; herbicides and fungicides; alfalfa, tanin, gluten, cocoa, sugar, furfural residues, tea, and coffee; boron, ferrosilicon, aluminum-nickel, aluminum-cobalt, titanium, metal sulfides, and other metal compounds; military pyrotechnic mixtures; detergents, nylon polymer, polyethylene, polystyrene resin, synthetic rubber, and other new plastics and related compounds; vitamin B and other drugs; and miscellaneous other industrial dusts and powders.

Explosibility of American Coals

The explosibility of coal dusts has been the subject of many investigations in laboratories and coal mines on the origin, development and prevention of mine explosions. Prompted by the expanding use of pulverized coal for industrial applications, such as pulverized-coal boilers, fluidized fuels, turbines for railroad locomotives, coal gasification, chars of low-rank coals, activated carbons, foundry facings, synthetic liquid fuels, plastics, chemicals, etc., the Bureau of Mines undertook a laboratory study[49/] of the explosive characteristics of several ranks of American coals ranging from lignite to meta-anthracite (table 12).

Experimental Procedure and Results

Most of the studies were made on coal dusts of through-200-mesh (74-micron-square) fineness. Some experiments were conducted with so-called mine-size dusts in which all particles were finer than 20-mesh (Tyler-sieve scale), and 20 percent by weight passed through a 200-mesh sieve. In tests on the effects of particle size, samples composed of definite sieve fractions were used (48- to 65-, 65- to 100-, 100- to 150-, 150- to 200-, 200- to 270-, 270- to 325-, and through 325-mesh). In another set of experiments the effect of varying proportions of through-200-mesh particles in the samples was studied by adding the fine dust to coarse aggregates consisting of particles between 20- and 200-mesh.

To evaluate the effect of moisture on the explosibility of coal dust, experiments were made with bituminous Pittsburgh coal to which various percentages of water had been added and with an initially moist subbituminous coal that was dried gradually so as to retain various amounts of moisture. The amount of dust used in most tests was 1 gram or less; in the explosion-quenching and pressure-release experiments in the galleries, samples of 10 to a few hundred grams were dispersed and exploded.

49/ Hartmann, I., Jacobson, M., and Williams, R. P., Laboratory Explosibility Study of American Coals: Bureau of Mines Rept. of Investigations 5052, 1954, 8 pp.

Generated on 2024-09-21 14:32 GMT / https://hdl.handle.net/2027/osu.32435030643506
Public Domain, Google-digitized / http://www.hathitrust.org/access_use#pd-google
Digitized by Google
Original from THE OHIO STATE UNIVERSITY

Generated on 2024-09-21 14:34 GMT / https://hdl.handle.net/2027/osu.32435030643506
Public Domain, Google-digitized / http://www.hathitrust.org/access_use#pd-google

Digitized by Google

TABLE 12. - Classification and analysis of coal samples

Sample No.	State	County	Coal bed	Classification of coal	Proximate analysis, percent				Heat value, B.t.u./lb.	Volatile ratio, percent $\left(\frac{V}{V + F.C.}\right)$	Volatile matter (DMM-free), percent
					Moisture	Volatile matter	Fixed carbon	Ash			
1759	R. I.	Providence	Cranston mine	Meta-anthracite	0.2	3.0	64.1	32.7	8,720	4.5	2.0
1760	Pa.	Luzerne	Buck Mt.	Anthracite	4.1	4.0	82.5	9.4	12,830	4.6	3.6
1761	do.	Northumberland	Shamokin	Semianthracite	2.1	8.2	80.4	9.3	13,600	9.3	8.4
1762	Va.	Montgomery	Brushy Mt.	do.	1.2	12.1	64.7	22.0	11,650	15.8	13.2
1736	W. Va.	McDowell	Pocahontas No. 3	Low-volatile	3.6	16.5	72.8	7.1	13,960	18.5	17.8
1737	Pa.	Cambria	Lower Kittanning	do.	1.1	15.7	75.7	7.5	14,340	17.1	16.5
1738	Ala.	Jefferson	Pratt	Medium-volatile	2.7	24.7	65.9	6.7	14,050	27.2	26.7
1739	Pa.	Indiana	Lower Kittanning	do.	.7	24.8	65.6	8.9	14,140	27.4	26.7
1741	do.	Washington	Pittsburgh	High-volatile A	1.2	34.8	56.0	8.0	13,770	38.3	37.8
1740	do.	Allegheny	Pittsburgh ECM	do.	1/ 2.0	1/ 37.0	1/ 54.0	1/ 7.0	14,300	40.7	40.4
1743	W. Va.	Kanawha	No. 2 Gas	do.	1.5	37.1	56.8	4.6	14,330	39.5	39.2
1744	Pa.	Allegheny	Thick Freeport	do.	1.7	35.6	53.9	8.8	13,600	39.7	39.2
1742	Ky.	Knott	Whitesburg	do.	3.0	40.5	53.7	2.8	14,060	43.0	42.8
1745	Ill.	Williamson	Illinois No. 5	High-volatile B	4.9	34.7	51.3	9.1	12,630	40.4	39.7
1746	do.	Vermillion	Illinois No. 7	High-volatile C	9.7	43.9	41.0	5.4	12,340	51.7	51.4
1747	Wyo.	Sweetwater	No. 3	do.	8.7	39.5	49.7	2.1	12,460	44.3	44.2
1764	Colo.	Fremont	Brookside	Subbituminous A	10.7	34.6	46.3	8.4	11,020	42.8	42.2
1765	do.	El Paso	Fox Hill	Subbituminous C	24.8	32.4	37.7	5.1	8,570	46.2	45.8
1763	N. Dak.	Ward	Coteau	Lignite	39.9	27.0	30.0	3.1	6,800	47.3	47.0

1/ Average analysis of several samples.

Original from THE OHIO STATE UNIVERSITY

The test data represent relative rather than absolute values, as results depend to some degree on the size, shape, and other characteristics of the explosion vessels, the uniformity of the dust clouds, the exact particle-size distribution, the intensity, size, and duration of the ignition source, etc. However, graphic representations of these first results indicate important trends of the principal variables. They show the relative amounts of incombustible dust required to prevent flame propagation in dust clouds of various coals (fig. 50); the effect of volatile content on the lower explosive limit, minimum ignition energy, and ignition temperatures of coal dusts (fig. 51); the effect of volatile content on the maximum pressures and rates of pressure rise developed by explosions of dust clouds in a closed bomb (fig. 52); and the effect of dust concentrations on the pressures and rates developed by explosions (fig. 53). The effects of particle size of segregated fractions of Pittsburgh coal on various explosive characteristics and on volatile content are shown in figures 54 and 55. Increase in particle size reduced the ease of ignition and the pressure developed by explosions. Figure 56 shows the effect of various proportions of fine (through-200-mesh) dust particles on the explosibility of Pittsburgh coal in air. The effect of moisture on explosibility of coal dust is important in some industrial processes and with relation to rock dusting under special mining conditions (fig. 57).

In industrial construction much reliance is placed on pressure-release vents as a means of reducing damage from accidental explosions. One of the important requisites of effective vents is that they open rapidly to permit efflux of the combustion products during the initial stage of an explosion. Normally the vents open directly to the outside or are connected with the outside by short ducts. In such instances the maximum pressure is directly related to the area of the vent opening. Occasionally the explosion products cannot be released to an unlimited outside volume, but must be led to an adjoining larger volume of limited size. Figure 58 shows the relation of vent size (between a small explosion gallery and the adjoining larger chamber) to the maximum pressures developed by explosions of bituminous coal dust.

Frequently in industrial explosions and occasionally in mine explosions it is not the initial ignition that is the most destructive, but delayed secondary and even tertiary explosions, which generally involve greater quantities of dust and larger areas than the first explosion. Studies with bituminous-coal and various other dusts on the formation and prevention of secondary explosions show that secondary explosions show that secondary explosions can be prevented by venting the duct and by dispersing water, limestone, salt, or other quenching agents in the duct.

Conclusions

Analysis of the data on American coal dusts indicates that:

1. The ignition sensitivity and the explosion hazard of coal dusts generally increases, although not linearly, with increase in volatile ratio.

2. The hazard of coal-dust explosions in an oxygen atmosphere is several times as great as in air.

3. Explosibility increases with reduction in particle size.

4. The effect of moisture on coal-dust explosibility is unimportant below about 10 percent.

5. Increase in initial pressure and surrounding temperature increases the explosion hazard.

Generated on 2024-09-21 14:39 GMT / https://hdl.handle.net/2027/osu.32435030643506
Public Domain, Google-digitized / http://www.hathitrust.org/access_use#pd-google
Digitized by Google
Original from THE OHIO STATE UNIVERSITY

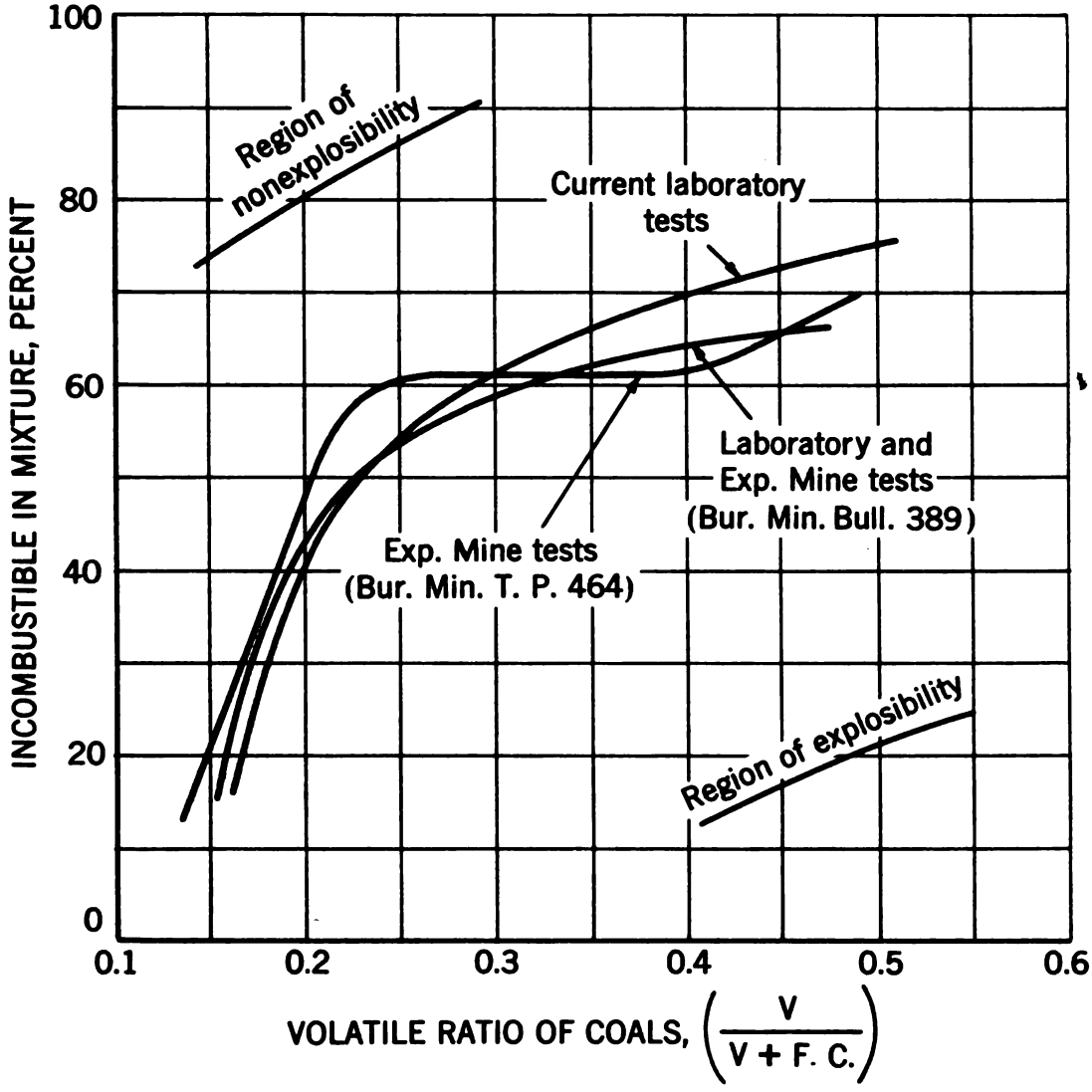

Figure 50. - Explosibility of mine-size coal dusts based on tests in Experimental Coal Mine and in laboratory.

Generated on 2024-09-21 14:39 GMT / https://hdl.handle.net/2027/osu.32435030643506
Public Domain, Google-digitized / http://www.hathitrust.org/access_use#pd-google
Digitized by Google
Original from THE OHIO STATE UNIVERSITY

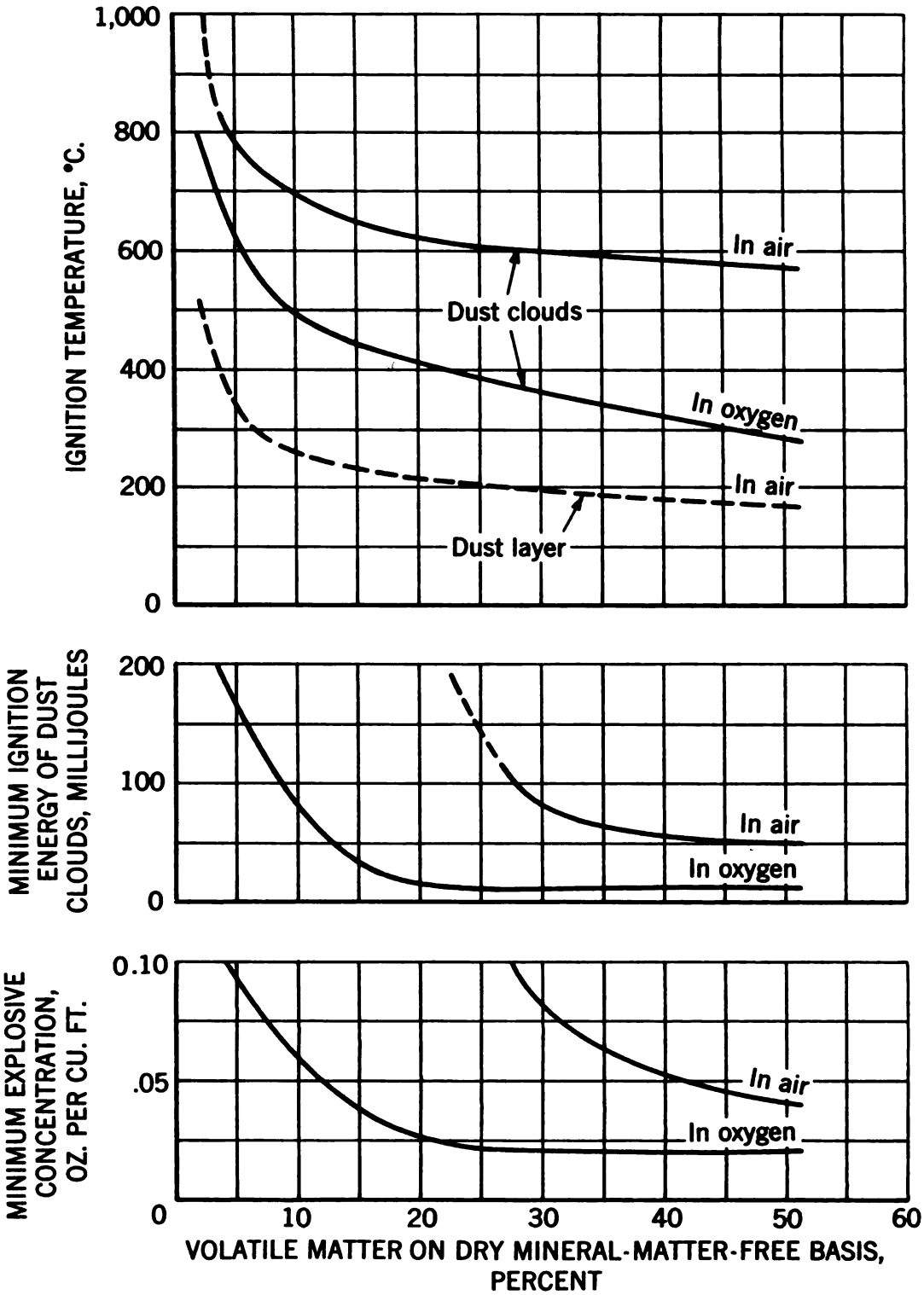

Figure 51. - Minimum explosive concentration, minimum igniting energy, and ignition temperature of through-200-mesh coal dusts in air and in oxygen.

Generated on 2024-09-21 14:43 GMT / https://hdl.handle.net/2027/osu.32435030643506
Public Domain, Google-digitized / http://www.hathitrust.org/access_use#pd-google
Digitized by Google
Original from THE OHIO STATE UNIVERSITY

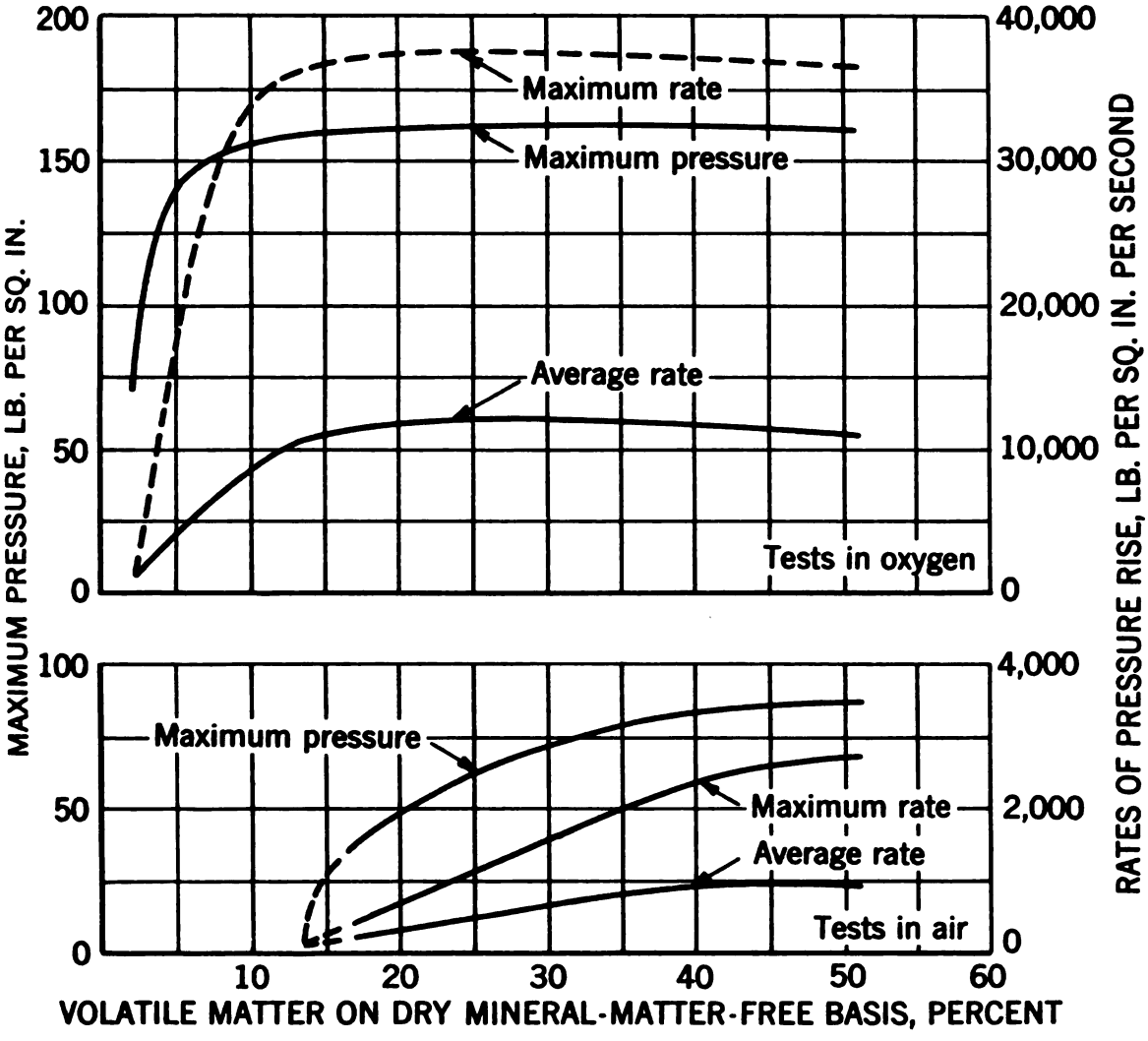

Figure 52. - Maximum pressures and rates of pressure rise developed by explosions of through-200-mesh coal dusts in air and in oxygen (dust concentration = 0.50 oz./cu. ft.).

Generated on 2024-09-21 14:41 GMT / https://hdl.handle.net/2027/osu.32435030643506
Public Domain, Google-digitized / http://www.hathitrust.org/access_use#pd-google
Digitized by Google
Original from THE OHIO STATE UNIVERSITY

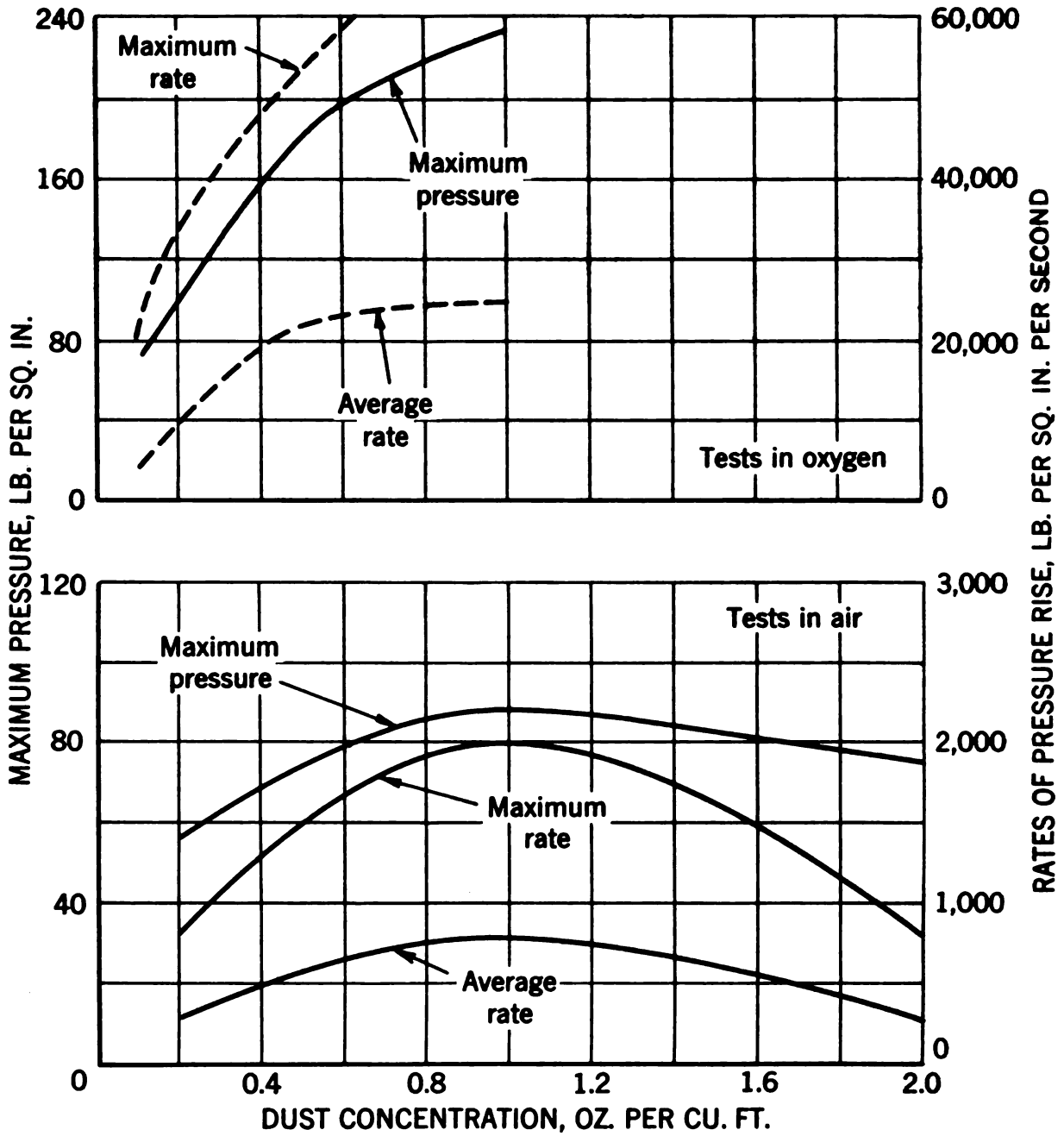

Figure 53. - Effect of concentration on maximum pressure and rates of pressure rise developed by explosions of through-200-mesh bituminous-coal dust in air and in oxygen.

Generated on 2024-09-21 14:38 GMT / https://hdl.handle.net/2027/osu.32435030643506
Public Domain, Google-digitized / http://www.hathitrust.org/access_use#pd-google
Digitized by Google
Original from THE OHIO STATE UNIVERSITY

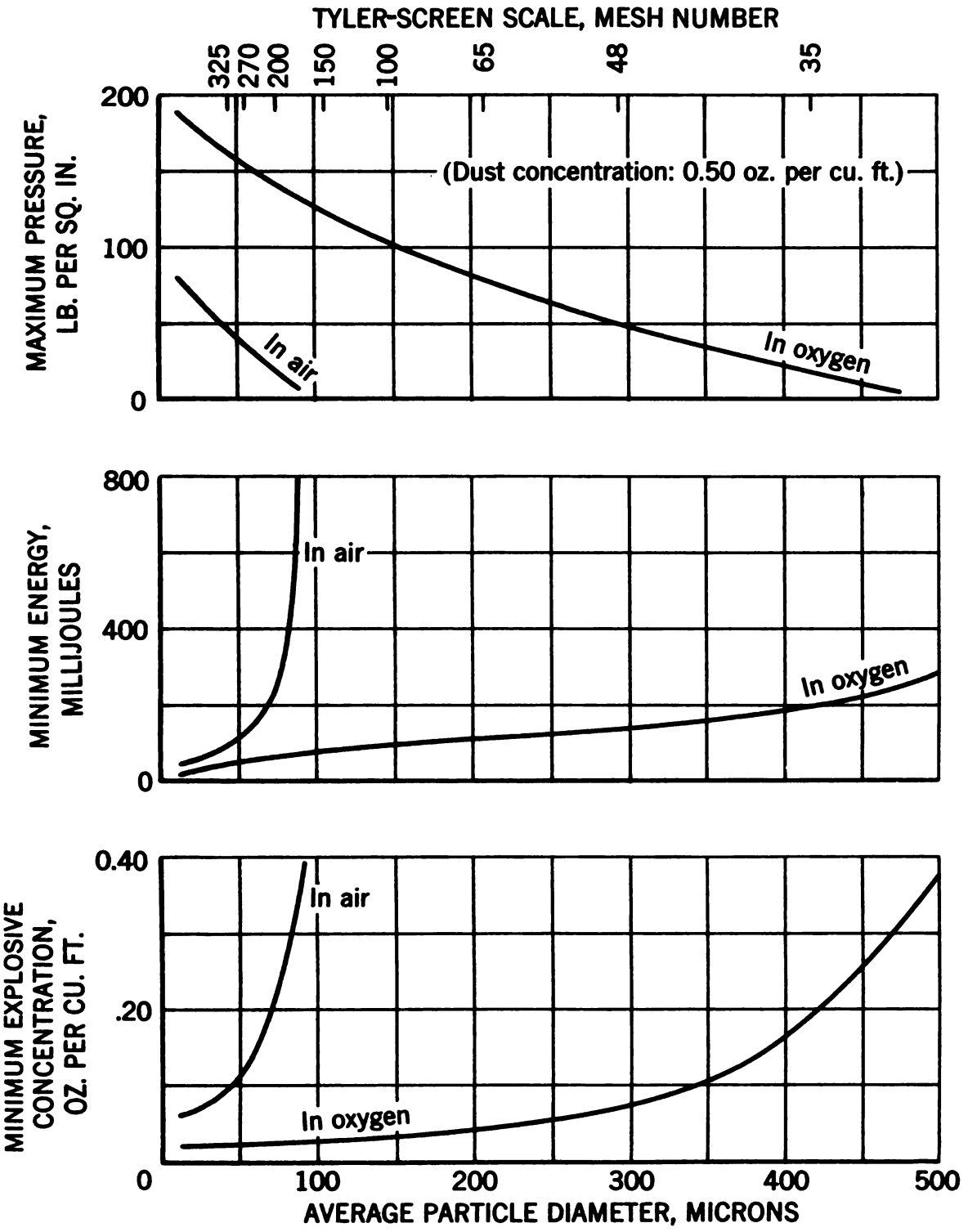

Figure 54. - Effect of particle size on minimum explosive concentration, minimum igniting energy, and pressures developed by explosions of dust clouds of bituminous Pittsburgh coal in air and in oxygen.

Generated on 2024-09-21 14:31 GMT / https://hdl.handle.net/2027/osu.32435030643506
Public Domain, Google-digitized / http://www.hathitrust.org/access_use#pd-google
Digitized by Google
Original from THE OHIO STATE UNIVERSITY

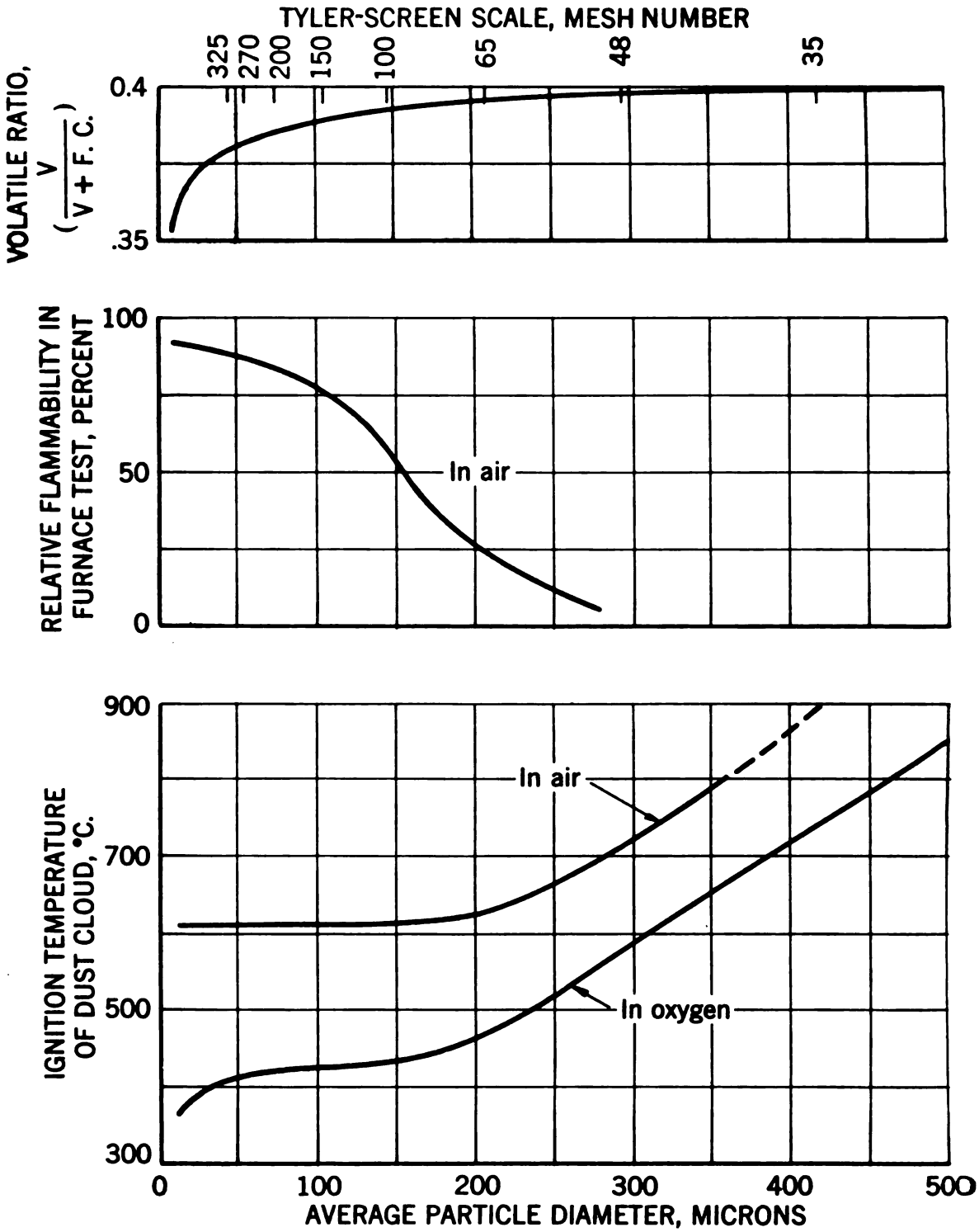

Figure 55. - Relation of particle size to ignition temperature, relative flammability, and volatile ratio of bituminous Pittsburgh coal.

Generated on 2024-09-21 14:34 GMT / https://hdl.handle.net/2027/osu.32435030643506
Public Domain, Google-digitized / http://www.hathitrust.org/access_use#pd-google
Digitized by Google
Original from THE OHIO STATE UNIVERSITY

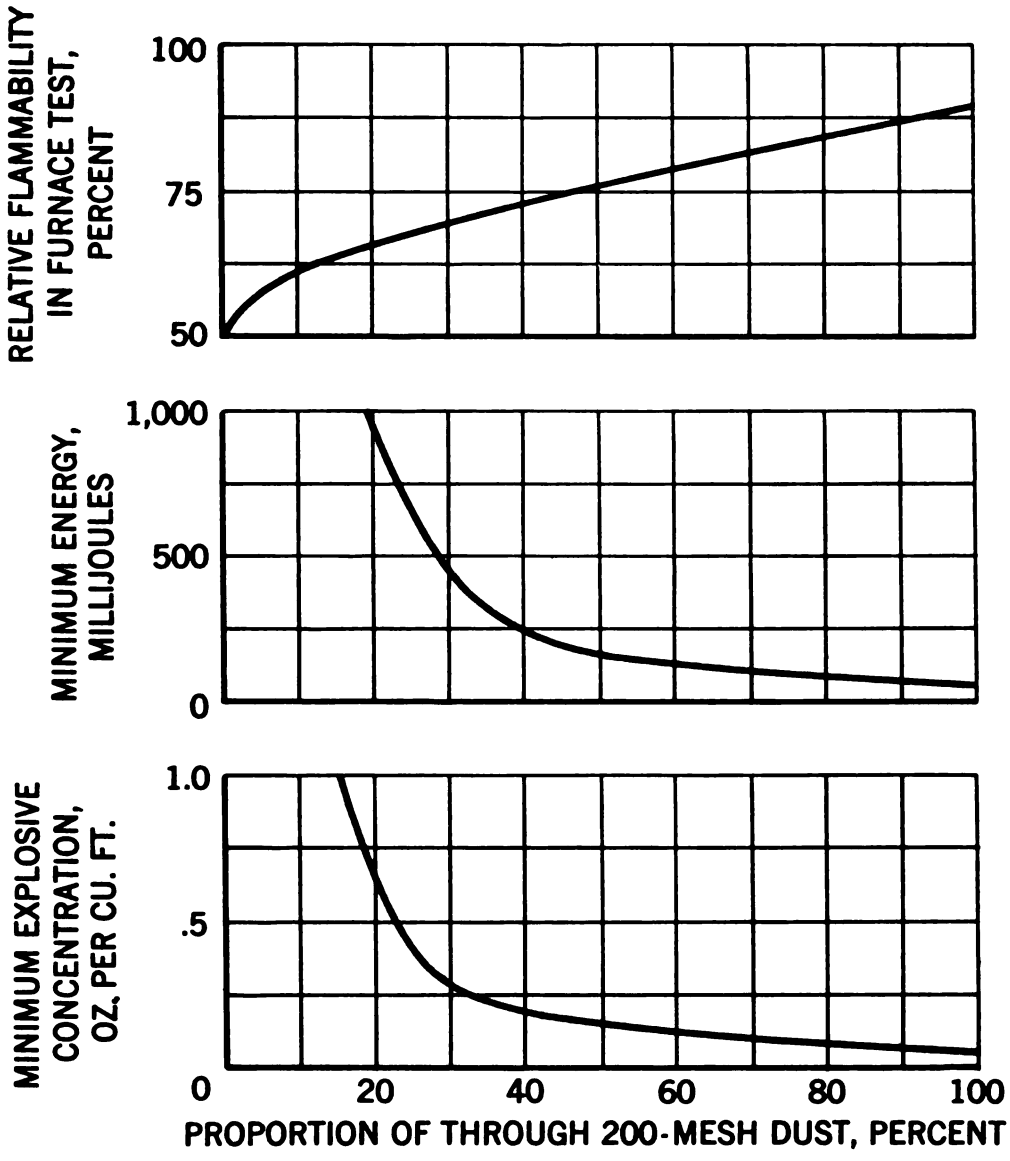

Figure 56. - Effect of various proportions of through-200-mesh particles in through-20-mesh dust on minimum explosive concentration, minimum igniting energy, and relative flammability of bituminous Pittsburgh-coal-dust clouds in air.

Generated on 2024-09-21 14:33 GMT / https://hdl.handle.net/2027/osu.32435030643506
Public Domain, Google-digitized / http://www.hathitrust.org/access_use#pd-google
Digitized by Google
Original from THE OHIO STATE UNIVERSITY

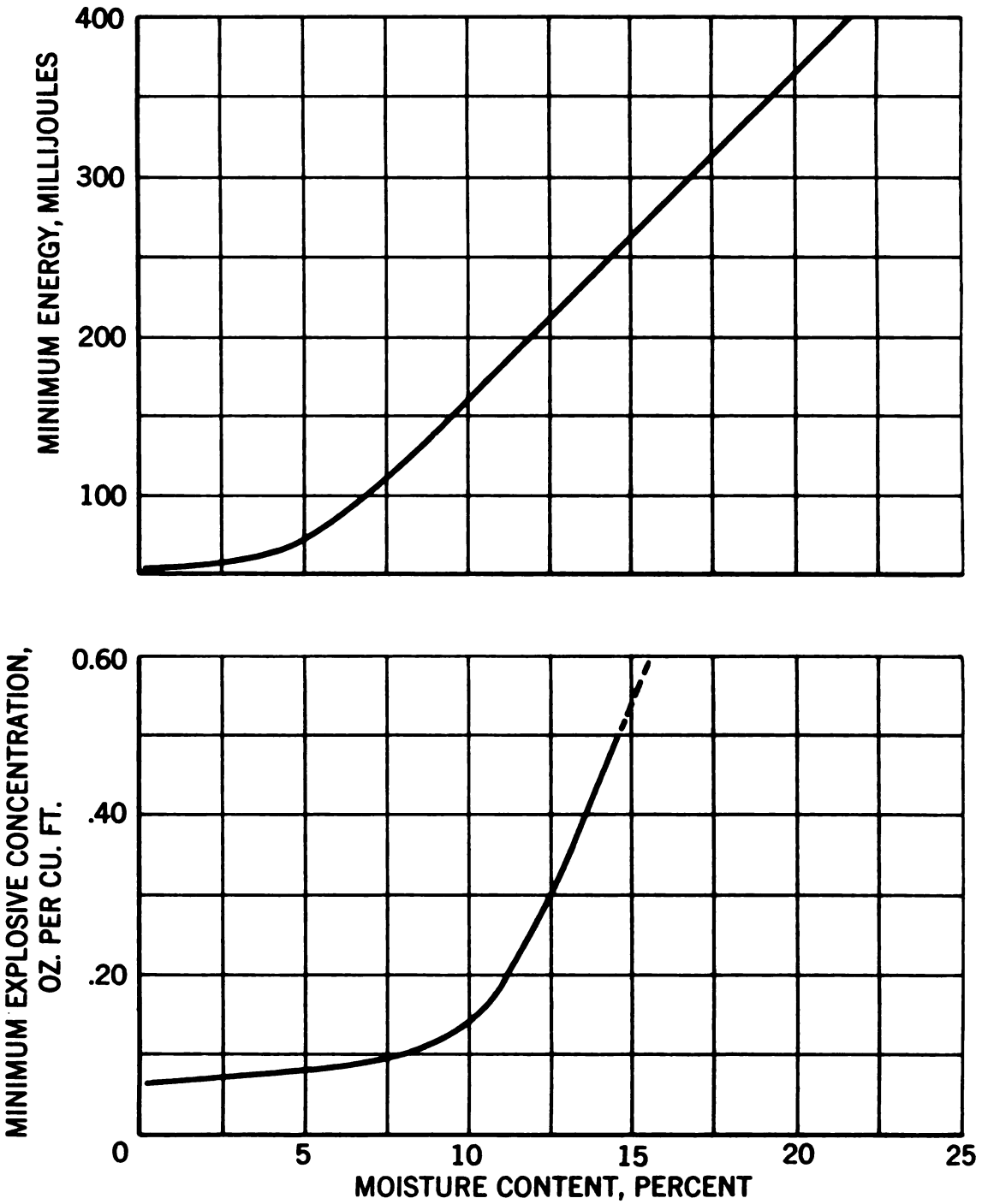

Figure 57. - Effect of moisture on minimum explosive concentration and minimum electrical spark energy required to ignite dust clouds of through-200-mesh bituminous Pittsburgh coal in air.

Generated on 2024-09-21 14:30 GMT / https://hdl.handle.net/2027/osu.32435030643506
Public Domain, Google-digitized / http://www.hathitrust.org/access_use#pd-google
Digitized by Google
Original from THE OHIO STATE UNIVERSITY

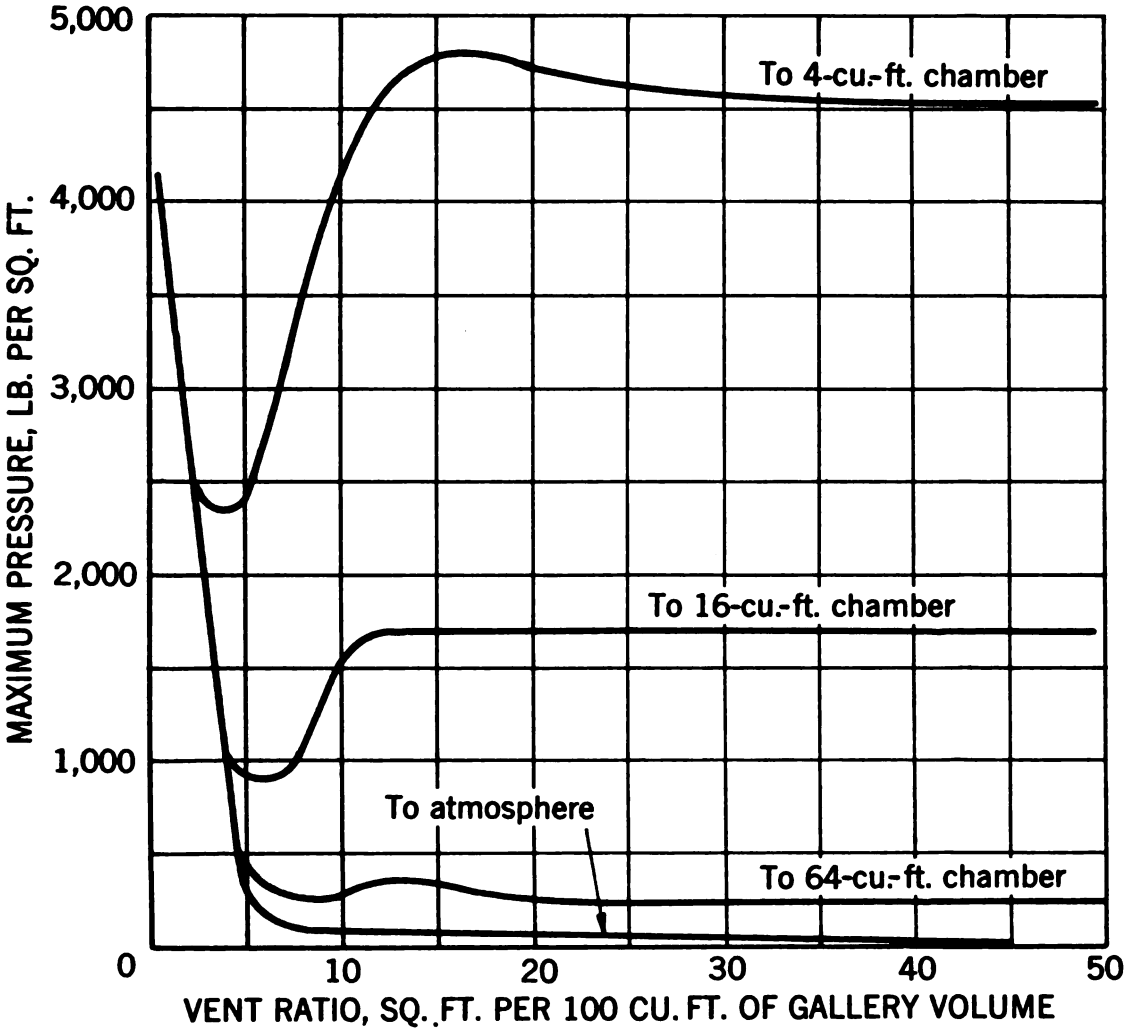

Figure 58. - Venting coal-dust explosions from 1-cu.-ft. gallery to atmosphere and to cubical chambers of various sizes (dust concentration = 0.60 oz./ cu. ft.).

Generated on 2024-09-21 14:37 GMT / https://hdl.handle.net/2027/osu.32435030643506
Public Domain, Google-digitized / http://www.hathitrust.org/access_use#pd-google
Digitized by Google
Original from THE OHIO STATE UNIVERSITY

6. Release of explosions to larger adjoining spaces of limited volume presents special problems and can produce strong explosions in the larger enclosure.

7. Some dust explosions are quenched successfully during their initial stage, and secondary explosions can be prevented by prompt dispersal of quenching agents.

COMBUSTION RESEARCH

Problems of Ignition

The quantitative study of ignition presents theoretical and experimental difficulties that have been the subject of extensive research. The essential problem is the formation of combustion waves from localized ignition sources.

A drastically simplified treatment of heat flow from a point source in a reacting medium, proposed by Jost, resulted in an approximate relationship between minimum ignition energy, burning velocity and thermal diffusivity. Approaching the problem in another way, Lewis and von Elbe developed the concept that a spherically growing flame, such as develops from a point source, acquires its excess enthalpy at the expense of the heat content of the burning gas, except near the origin where this enthalpy must be furnished by the source. This minimum ignition energy H supplied by the source can be expressed as

$$H = \pi d^2 h;$$

where d is the separation of the electrodes necessary to produce ignition with a minimum spark energy, and h is the excess enthalpy calculated approximately from experimental data.

Calculated and experimental values of H have been compared.50/ The agreement is remarkably good for mixtures of hydrocarbon and oxygen and hydrogen and air but poor for mixtures of hydrocarbon and air. It has been suggested that this may be due to the relative rates of the chemical reactions and their effect on the diffusional change of the mixture composition, which would be important for relatively slow reactions, such as those in hydrocarbon-air mixtures.

Where the ignition-source temperature is low, the threshold condition for ignition may change from a minimum ignition energy (applicable to rapid, virtually massless sources) to a quasiconstant minimum ignition temperature. This appears to be generally true for ignition of solid and liquid explosives by hot wires, frictionally heated particles, etc.

Burning Velocities on Slot Burners

For many years the Bureau of Mines has conducted fundamental research on problems of ignition and combustion of flammable liquids and gases. One of the most important characteristics of a flammable gas or gas mixture is its laminar burning velocity, that is, the rate at which the combustion wave moves relative to the oncoming, nonturbulent stream of unburned gas in a direction perpendicular to the flame surface. For a given temperature and pressure of the unburned gas the burning velocity is characteristic of the composition of the gas stream. Thus, it is an essential factor in problems of fuel utilization and combustor design. Numerous

50/ von Elbe, G., The Problem of Ignition: 4th Symposium (Internat.) on Combustion: Williams & Wilkins Co., Baltimore, Md., 1953, pp. 13-20.

Generated on 2024-09-21 14:31 GMT / https://hdl.handle.net/2027/osu.32435030643506
Public Domain, Google-digitized / http://www.hathitrust.org/access_use#pd-google
Digitized by Google
Original from THE OHIO STATE UNIVERSITY

investigators have developed or modified methods for measuring burning velocities, but the divergence of results obtained, not only by different methods but with the same method applied by different workers, shows the need for a standardized procedure capable of reproducible results.

Measurements of Cylindrical Burners

Of the procedures developed, the most widely used has been the Bunsen-burner technique, in which the burning velocity is considered equal to the normal component of flow rate of the unburned gas as measured on a photograph of the luminous flame cone. The relationship is shown by the simple equation:

$$S_u = U_u \sin \alpha; \quad (1)$$

where S_u is the local burning velocity, in cm. per sec., at a specific point on the inner edge of the luminous cone, U_u is the linear gas velocity in cm. per sec. at this point, and α is the angle formed by the cone surface and the flowline on the unburned side. It was found that the values of S_u measured at the base and top of the cone diverged widely but that, by limiting measurements to points along the central cone frustum or "truncated" cone, an average value could be calculated for the burning velocity.[51] [52]

Although the cylindrical burner tubes used in making these measurements were long enough to insure laminar flow, the values obtained in this way were averages at best. Moreover, comparison of data obtained at the Bureau of Mines and in other laboratories showed that in conical flames attached to cylindrical burners, the central frustum does not have a constant burning velocity and that the average value of this nonconstant region depends on the method of calculation and on the dimensions of the burner tube.

Measurements on Slot Burners

To eliminate these difficulties and obtain more accurate burning-velocity values, a new series of measurements was undertaken in which the truncated-cone method was applied to thin, flat flames produced on special slot burners developed for this purpose.[53]

Mixtures of propane-air, methane-air, and ethylene-air were chosen for these experiments because of their frequent occurrence in the literature. All gases, including air, were supplied from compressed-gas cylinders and metered to an accuracy of 0.3 percent. After metering, the gases were mixed successively in four chambers connected in series. The completed mixtures were supplied to jacketed rectangular burner tubes long enough to insure laminar streamline flow. Mass-spectrometer

---

51/ Harris, M. E., Grumer, J., von Elbe, G., and Lewis, B., Burning Velocities, Quenching and Stability Data on Nonturbulent Flames of Methane and Propane With Oxygen and Nitrogen; Application of Theory of Ignition, Quenching and Stabilization to Flames of Propane and Air: 3d Symposium on Combustion and Flame and Explosion Phenomena, Williams & Wilkins Co., Baltimore, Md., 1949, p. 88.

52/ Lewis, B., and von Elbe, G., Combustion, Flames, and Explosions of Gases: Academic Press, New York, N. Y., 1951, p. 471.

53/ Singer, J. M., Burning-Velocity Measurements on Slot Burners; Comparison With Cylindrical Burner Determinations: 4th Symposium (Internat.) on Combustion, Williams & Wilkins Co., Baltimore, Md., 1953, pp. 352-358.

Generated on 2024-09-21 14:30 GMT / https://hdl.handle.net/2027/osu.32435030643506
Public Domain, Google-digitized / http://www.hathitrust.org/access_use#pd-google
Digitized by Google
Original from THE OHIO STATE UNIVERSITY

analyses of the gas mixtures agreed with compositions calculated from flowmeter readings to within 1 percent. The minimum burner width was 1-1/ times the quenching distance. Experimentally it was found that the best ratio of long side of the rectangular tube to the short side was 3:1. The flame cone was analyzed from photographs of luminous and schlieren cone outlines.

The advantage of the slot burner is that the resulting combustion wave assumes the shape of two inclined-plane surfaces. This eliminates cylindrical symmetry and curvature of the combustion surface. It can be shown, both theoretically and experimentally, that such curvature will, in general, increase the burning velocity. The curved surface of a flame attached to a cylindrical burner surface supplies more heat and free radicals to the unburned gas than the plane-surfaced flame. This means that in the case of a conical flame the burning velocity along the flame surface increases proportionately to the amount of curvature, whereas the plane combustion surface produced by a slot burner shows a decreased burning velocity over the entire area, as well as a constant burning-velocity region that does not exist in the conical flame.

In figure 59 burning velocities determined on slot burners of different sizes are compared with the burning velocity measured on a cylindrical burner. As the tube cross section tends toward a square, the effect of curvature is reintroduced into the flame surface, and the resulting values are closer to the cylindrical case. Figure 59 shows that, if the minimum ratio of one side to the other is approximately three and certain limiting values are avoided (quenching and penetrating distances), consistent burning velocities are obtained for slot burners of different dimensions.

Burning velocities on slot burners were calculated by the truncated-cone method adapted to flat flames. The following equation was applied successfully to the two-dimensional case at the central plane of the rectangular tube:

$$S_u = \frac{U_o}{s}\left[(r_b - r_a) - \frac{(r_b^3 - r_a^3)}{3R^2}\right] ; \qquad (2)$$

where U_o is the axial streamline flow in cm. per sec., r_b and r_a are the half-widths of the frustum in the central plane, R is the half-width of the burner, and s is the length of flame outline or slant height of the frustum. U_o may be determined experimentally, or calculated using Cornish's formula for laminar flow through a tube of rectangular cross section.[54/]

Equation (2) offers a number of advantages over equation (1). Not only does it eliminate curvature effects, but the length of the flame outline, s, can be measured exactly, whereas with the cylindrical flame either the area of revolution of the curved frustum must be calculated, or the sides of the frustum must be assumed to be straight. Moreover, with equation (2) it no longer matters whether the reference surface is the innermost luminous, the shadow, or the schlieren outline, provided the outlines are parallel to each other and close together.

Evaluation of Results

Two criteria were applied to the validity of the data obtained by the slot-burner method.

54/ Smith, R. W., Edwards, H. E., and Brinkley, S. R., Jr., Tables of Velocity of Steady Laminar Flow in Channels of Rectangular Cross Section: Bureau of Mines Rept. of Investigations 4885, 1952, 41 pp.

Generated on 2024-09-21 14:38 GMT / https://hdl.handle.net/2027/osu.32435030643506
Public Domain, Google-digitized / http://www.hathitrust.org/access_use#pd-google
Digitized by Google
Original from THE OHIO STATE UNIVERSITY

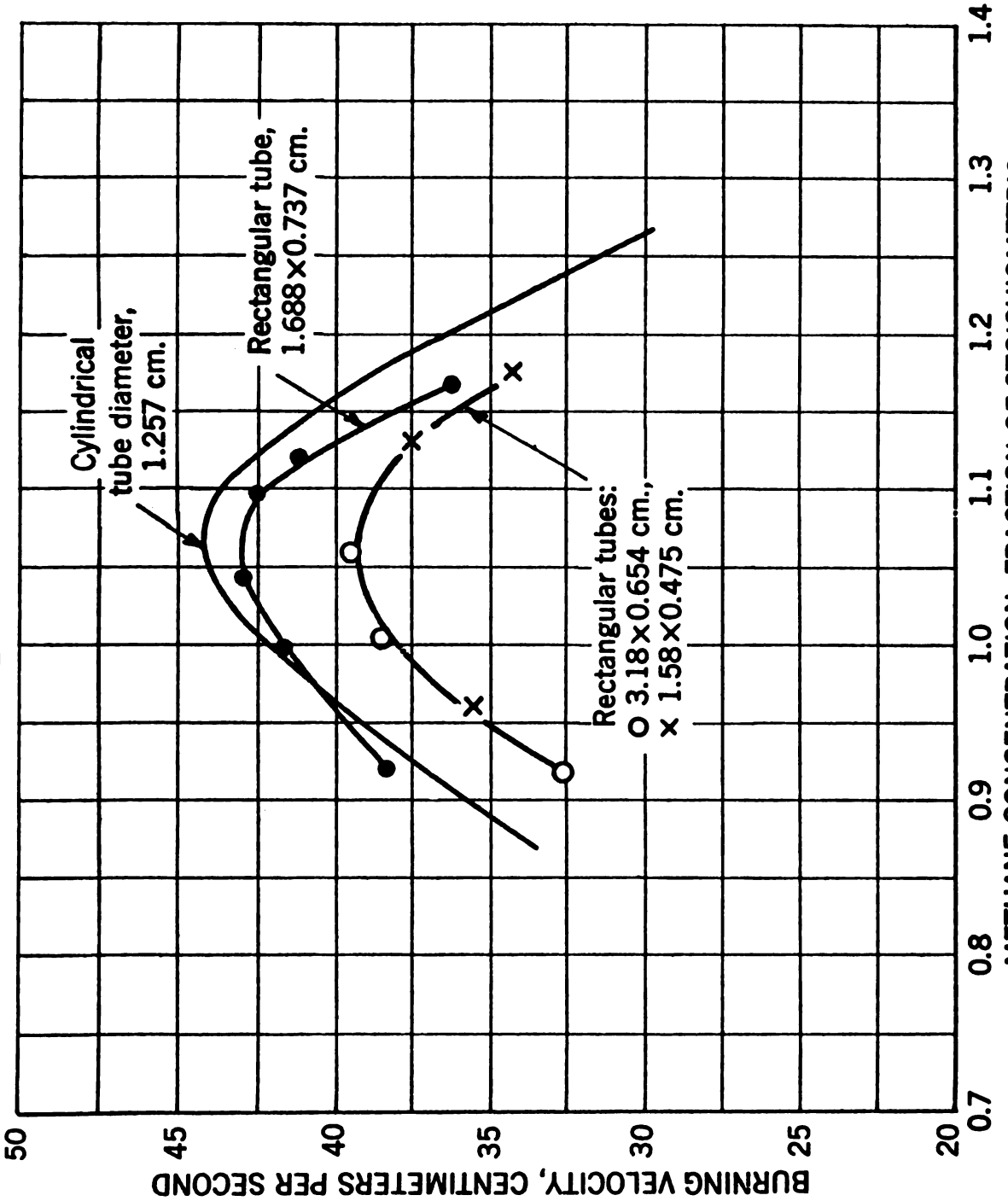

Figure 59. - Burning velocities of methane-air mixtures.

Generated on 2024-09-21 14:34 GMT / https://hdl.handle.net/2027/osu.32435030643506
Public Domain, Google-digitized / http://www.hathitrust.org/access_use#pd-google
Digitized by Google
Original from
THE OHIO STATE UNIVERSITY

First, the shape of the innermost or schlieren cone was reconstructed with the condition that $S_u=U_u \sin\alpha$ at the flame surface.[55] For this purpose a number of frustums were constructed, using reasonable burning velocity values and compared with the experimental frustum of the flame cone. In each case the value of S_u that best fitted the experimental cone agreed exactly with the value determined on slot burners by equation (2).

The second criterion was comparison of values obtained by equation (2) with values measured by the spherical-bomb method (see ref. 57). Values listed below for propane-air, methane-air and ethylene-air mixtures show that the agreement between these two radically different methods is well within the experimental error (2-3 percent).

Comparison of burning velocities by slot-burner method and spherical-bomb method

	Propane-air	Methane-air	Ethylene-air
Composition ..... percent	4.02	9.47	6.51
Burning velocity by slot burner ..... cm./sec.	41.2	37.0	64.0
Burning velocity by spherical bomb ..... do.	40.4	36.5	63.0

Burning-Velocity Measurements in a Spherical Vessel

The spherical-vessel or spherical-bomb method for measuring burning velocities has been described elsewhere in detail.[56] Developed to meet the need for a process that produced an approximately plane combustion wave, undisturbed by heat loss to solid bodies or by interdiffusion with the ambient atmosphere, the spherical bomb to date offers the most effective procedure for observing the flow of unburned gas through the wave and measuring burning velocity. Like the slot-burner method it has been applied to burning velocity measurements of propane-air, methane-air and ethylene-air mixtures,[57] which are the mixtures most frequently cited in the literature.

Theory and Experiment

A spherical vessel is filled with an explosive gas mixture which is ignited at the center. The resulting combustion wave propagates spherically from the center to the wall. As the flame progresses, the hot burned gas expands so that its pressure always is close to the pressure of the unburned gas. This expansion carries the spherical flame forward, its diameter increasing faster than it would by flame propagation alone. Photographs of the growing flame and records of the pressure rise are obtained simultaneously.

Two methods are available for calculating the normal burning velocity from these data. In the first method the volume occupied by the initial unburned gas is calculated for any instantaneous flame diameter, with the aid of the pressure record. The normal burning velocity is obtained from the time variations of this volume. In the second method, only the pressure record of the experiment is used, but the final temperature of the combustion must be calculated thermodynamically. This final

55/ Work cited in footnote 52 (p. 99) p. 248.
56/ Work cited in footnote 52 (p. 99) p. 456.
57/ Manton, J., von Elbe, G., and Lewis, B., Burning Velocity Measurements in a Spherical Vessel with Central Ignition: 4th Symposium (Internat.) on Combustion, Williams & Wilkins Co., Baltimre, Md., 1953, pp. 358-363.

Generated on 2024-09-21 14:33 GMT / https://hdl.handle.net/2027/osu.32435030643506
Public Domain, Google-digitized / http://www.hathitrust.org/access_use#pd-google
Digitized by Google
Original from THE OHIO STATE UNIVERSITY

temperature and the instantaneous pressure are used to calculate the fraction of gas burned. The burning velocity is calculated as follows:

$$S_u = \frac{dr_i}{dt}\left(\frac{r_i}{r_b}\right)^2 \left(\frac{P_i}{P}\right)^{1/\gamma_u} ;$$

where r_i is the instantaneous radius of the sphere before the burned gas has expanded, r_b is the instantaneous radius of the sphere of burned gas, after adiabatic expansion, P_i is the initial pressure, P is the instantaneous pressure of the burned gas, and γ_u is the ratio of specific heats of the unburned gas at constant pressure and constant volume.

This second method is less sensitive than the first to inner distortions of the flame surface. Moreover, the instantaneous pressure can be determined more accurately than the flame diameter. Thus, the second method gives the more exact values.

The average radius of the bomb is 15.295 cm. The spark gap, formed by stainless steel needles of 0.035-inch largest diameter, is located at the exact center. Two vertical slots of plane glass about 6 inches long and 1 inch wide are situated diametrically opposite each other. A single pressure indicator of the diaphragm type is mounted flush with the inside wall of the vessel. The deflection of the diaphragm actuates a small, concave, stainless-steel mirror, which focuses a sharp image of a brightly illuminated pinhole in front of a carbon arc onto a drum camera mounted vertically, so that any buoyancy of the flame sphere can be observed from displacement of the centerline of the flame record. The optical system magnifies the movement of the diaphragm 2,000 times and gives a pressure record of 13.1 cm. for a 20.0-cm.-Hg pressure rise. Calibration of the diaphragm gives a straight line against pressure which is accurately reproducible and has not changed with use. To obtain the record of the flame diameter, a vertical midsection of the flame image (approximately 1/16 inch wide) is screened out by a slot diaphragm close to the film surface, and the flame is photographed with a schlieren optical system. Pressure and flame records are obtained on the same film. The timing marks are 1,000-per-second flashes from a glow modulator lamp. The spark is programed properly with the camera shutters. Each film is measured on a Gaertner comparator. A traverse is made of the flame radius and pressure rise at successive intervals with an accuracy of 0.01 mm. All gases, including air, used in the experiments were obtained from compressed-gas cylinders. The fuels were propane, methane, and ethylene. Mass-spectrometer analysis of the fuels gave a purity of 99.6 percent for methane, 97.0 percent for propane and 99.7 percent for ethylene.

Experimental Results

Stoichiometric mixtures were studied, as this composition generally insures diffusion stability of flame front.[58] The value for the relationship between pressure and flame radius for a given mixture and initial pressure was reproducible in all cases.

58/ Manton, J., von Elbe, G., and Lewis, B., Nonisotropic Propagation of Combustion tion Waves in Explosive Gas Mixtures and the Development of Cellular Flames: Jour. Chem. Phys., vol. 20, 1952, p. 153.

Generated on 2024-09-21 14:32 GMT / https://hdl.handle.net/2027/osu.32435030643506
Public Domain, Google-digitized / http://www.hathitrust.org/access_use#pd-google
Digitized by Google
Original from THE OHIO STATE UNIVERSITY

Before burning velocities could be determined, it was necessary to investigate the effect of the ignition spark on the flame shape. Using 0.012-inch platinum wires and 0.035-inch stainless-steel needles as electrodes, the spark energy was varied from 0.4 to 5 millijoules, for both capacitance and inductance sparks. It was found that, for a given energy of the capacitance or inductance spark, there are two critical gap widths at which the flame becomes truly spherical. This observation was made directly by high-speed motion-picture photography and confirmed in the present experiments by agreement between calculated and observed values of the flame radius r_b. When the gap width was varied, a succession of flame shapes resulted. Near the smallest gap that would permit ignition, the flame was an ellipsoid, with its longer axis along the electrodes. As the gap was increased, the flame became spherical and then assumed a toroid form, indented at the electrodes. These results were observed for gap widths within the quenching distance of the electrodes. As the gap width increased beyond the quenching distance, the sequence reversed itself, with the flame becoming in turn spherical and ellipsoidal. Remarkably, when the gap width was increased so that the flame changed from a sphere to a toroid, the observed flame speed $\frac{dr_b}{dt}$ and the rate of pressure rise $\frac{dP}{dt}$ both became somewhat smaller, indicating a decreased overall burning rate.

It also has been noted that, with overextended spark gaps and large spark energies, the flame assumes cell structure, even in stoichiometric mixtures that do not generally show this phenomenon. The appearance of cell structure suggests that the mixture composition is diffusionally changed at the flame surface. In stoichiometric mixtures some regions become overrich in fuel, others overrich in oxygen. As the stoichiometric composition nearly coincides with the composition of maximum burning velocity, it is to be expected that any shift of composition will lead to a decrease in the overall burning rate, as is the case.

Data for spherical flames of stoichiometric ethylene-air, methane-air, and propane-air mixtures at 1 atmosphere pressure showed that remarkably good agreement exists between the 2 methods of calculation, proving that the results are self-consistent and credible.

Flame Stabilization on Burners With Short or Noncircular Ports

The problem of interchanging or supplementing gas supplies is becoming increasingly important to the gas industry. In particular, the industry must be able to predict the performance of burners on company lines when the composition of the fuel varies. The groundwork in the solution of this problem was laid in studies by the Bureau of Mines, which established the fundamental principles of flame stabilization[59 60/] and air entrainment in gas burners.[61/] These findings formed the starting point of a research program, sponsored jointly by the Bureau and the American Gas Association, which led to a new theory for predicting the interchangeability of fuels.[62/] The theory has the advantage that it requires only data that are readily

59/ Lewis, B., and von Elbe, G., Stability and Structure of Burner Flames: Jour. Chem. Phys., vol. 11, 1943, pp. 75-97.

60/ Lewis, B., and von Elbe, G., Ignition and Flame Stabilization in Gases: Trans. ASME, 1948, pp. 307-316.

61/ von Elbe, G., and Grumer, J., Air Entrainment in Gas Burners: Ind. Eng. Chem. vol. 40, 1948, pp. 1123-1129.

62/ Grumer, J., Predicting Burner Performance With Interchanged Fuel Gases: Ind. Eng. Chem. vol. 41, 1949, pp. 2756-2761.

Generated on 2024-09-21 14:40 GMT / https://hdl.handle.net/2027/osu.32435030643506
Public Domain, Google-digitized / http://www.hathitrust.org/access_use#pd-google
Digitized by Google
Original from THE OHIO STATE UNIVERSITY

obtainable - the density, the gasline pressure, and the flame-stability diagrams for both fuels. A flame-stability diagram for methane-air mixtures is shown in figure 60. It contains 2 curves that define 3 regions of flame behavior on burners - 1 region where flames flash back, 1 of stable flames, and 1 of blowoff. Such diagrams are characteristic of the fuel gas and correlate the flashback and blowoff limits of the fuel for all burners, except in certain definable instances.

The coordinates of a flame-stability diagram involve new concepts and as such bear definition.[63] The boundary velocity gradient is the slope, near the port wall, of the curve of local stream velocity versus distance from the port wall. It can be calculated readily when the total flow and flow profile near the port wall are known. Any flow through a burner port can be characterized by a value for the boundary velocity gradient g. The word "critical" designates a particular boundary velocity gradient, corresponding to a flow at the flashback or blowoff limit, g_F being the critical boundary velocity gradient at flashback and g_B the critical boundary velocity gradient for blowoff. The abscissa of a flame-stability diagram is used to plot the relative amounts of fuel and primary air in the burner stream. The particular unit used is F, the fuel-gas concentration expressed as fraction of stoichiometric. Thus, F is the actual fuel-gas percentage of fuel, S, in a stoichiometric mixture in air. For rich flames, F is greater than 1; for lean flames, it is less than 1.

The earlier investigations of flame stabilization were made on cylindrical burners that were long enough to allow parabolic (Poiseuille) flow; however, most gas appliances do not have circular ports with Poiseuille flow. As it is of practical significance to correlate the performance of a wide variety of burners, the Bureau of Mines has extended its investigation to burners with short, cylindrical ports with nonparabolic flow and noncircular ports with parabolic flow.[64]

The stability of a burner flame depends on the flashback and blowoff characteristics of the fuel gases, which, in turn, depend both on the composition of the fuel-gas mixture and the burner design. On a circular burner with parabolic flow, these characteristics can be described for each fuel by its flame-stability diagram, consisting of a curve of critical boundary velocity gradients for flashback versus gas-air mixture composition and a similar curve for blowoff (see fig. 60). For parabolic flow on circular ports the boundary velocity gradient is defined as

$$g = 4V\pi R^3, \qquad (1)$$

V being the volumetric flow through a port of radius R.

In the case of short, sharp-edged ports with nonparabolic flow such as are found on the usual gas appliances, Wilson[65] and Grumer[66] successfully correlated the flashback and blowoff limits of fuel relating the boundary velocity gradient of the fuel stream to the average flow velocity in the port by means of friction coefficients. In this case, the boundary velocity gradient for both flashback and blowoff is defined as:

63/ Grumer, J., New Theories of Burner Performance: Gas, vol. 30, No. 3, 1954, pp. 47-51.

64/ Grumer, J., Harris, M. E., and Schultz, H., Flame Stabilization on Burners With Short Ports or Noncircular Ports: 4th Symposium (Internat.) on Combustion, Williams & Wilkins Co., Baltimore, Md., 1953, pp. 695-701.

65/ Wilson, C. W., Lifting and Blowoff of Ethylene-Air Flames on Short Cylindrical Burner Ports: 120th Meeting, Am. Chem. Soc., September 1951.

66/ Work cited in footnote 64.

Generated on 2024-09-21 14:32 GMT / https://hdl.handle.net/2027/osu.32435030643506
Public Domain, Google-digitized / http://www.hathitrust.org/access_use#pd-google
Digitized by Google
Original from THE OHIO STATE UNIVERSITY

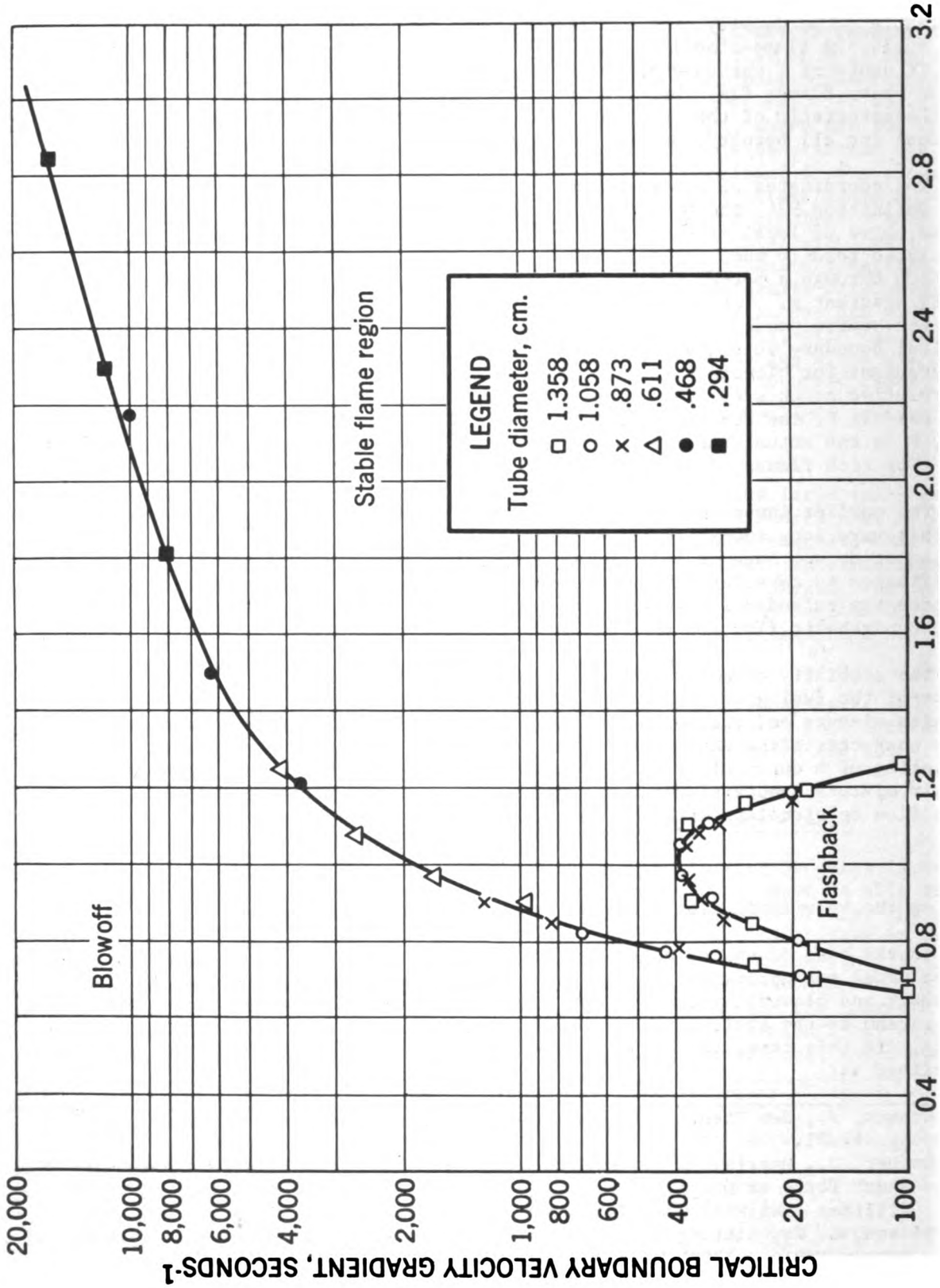

Figure 60. - Flame-stability diagram for 100-percent methane.

Generated on 2024-09-21 14:33 GMT / https://hdl.handle.net/2027/osu.32435030643506
Public Domain, Google-digitized / http://www.hathitrust.org/access_use#pd-google
Digitized by Google
Original from
THE OHIO STATE UNIVERSITY

$$g = \frac{\lambda \quad V^2}{8\pi \quad R^4 \nu} \qquad (2)$$

where λ is a frictional coefficient determined from pressure drop measurement, and ν is the kinetic viscosity. Knowing the boundary velocity gradients, the requisite flame-stability diagrams can be established, just as in the case of circular ports long enough for parabolic flow.

Stabilization on Noncircular Ports

The next problem was to investigate the effect of the shape of the burner cross-section. This was done on channels of square and rectangular cross-section long enough to allow parabolic flow. The velocity and velocity-gradient profiles for laminar flow through such channels were calculated.[67/] It was found that, unlike cylindrical ports, in noncylindrical ports, the boundary velocity gradient and local burning velocity contours do not follow the channel wall.

In a long, cylindrical channel, where flow velocity and burning velocity are uniform at all points equidistant from the wall, the probability of flashback or blowoff is the same for all points on the tube boundary. This is not the case for noncircular channels, where the velocity and velocity gradients are higher near the midpoint of the sides than at the corners. Due to increased quenching at the corners, the flame recedes farther into the stream near the corners than near the midpoint of the sides, and thus there is a specific location for ports of noncircular cross-section where the flame is stabilized. This means that, in addition to defining the velocity profile, it is necessary to locate the point where the local flow velocity equals the local burning velocity at the instant of blowoff or flashback. However, experimental measurements show that, irrespective of the location of this point, the flame-stability limits of noncircular burners again can be correlated through the concept of critical boundary velocity gradients. For this purpose, the boundary velocity is:

$$g = 8\lambda V \, Re/16\pi R^3, \qquad (3) \qquad (Re= \text{Reynolds number})$$

λ being redefined for each individual port shape.

Figure 61 for methane flames shows that, when equation 3 is used with appropriate values of λ, there are satisfactory data for cylindrical and noncircular channels.

Conclusions

Studies of flame stabilization for round ports, with and without Poiseuille flow, and noncircular ports show that the concept of critical boundary velocity gradients for flashback and blowoff is more generally applicable to burners than was previously reported. Long, cylindrical tubes with Poiseuille flow are the simplest for measuring the flame-stability diagram of a fuel.

In treating problems of flame stabilization fuel factors can be dissociated from burner factors. Flame-stability diagrams are characteristic of the fuel gas. The friction coefficient λ depends on burner conditions. Ambient conditions, such

67/ Smith, R. W., Jr., Edwards, H. E., and Brinkley, S. R., Jr., Tables of Velocity of Steady Laminar Flow in Channels of Rectangular Cross Section: Bureau of Mines Rept. of Investigations 4885, 1952, 51 pp.

Generated on 2024-09-21 14:37 GMT / https://hdl.handle.net/2027/osu.32435030643506
Public Domain, Google-digitized / http://www.hathitrust.org/access_use#pd-google
Digitized by Google
Original from THE OHIO STATE UNIVERSITY

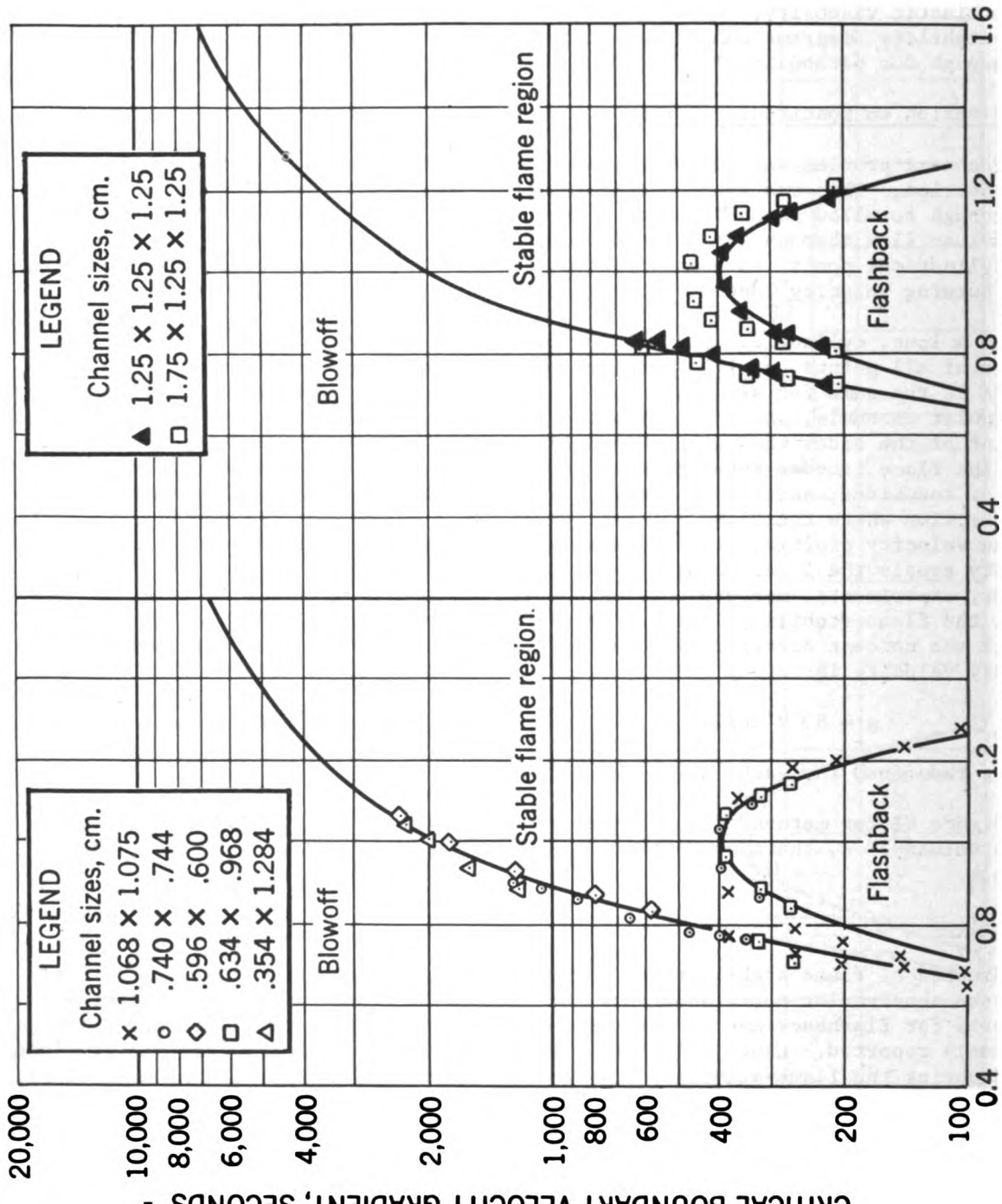

Figure 61. - Flame-stability diagram for 100-percent methane; comparison of points for square, rectangular, and triangular channels and curves for long, cylindrical tubes.

Generated on 2024-09-21 14:33 GMT / https://hdl.handle.net/2027/osu.32435030643506
Public Domain, Google-digitized / http://www.hathitrust.org/access_use#pd-google
Digitized by Google
Original from THE OHIO STATE UNIVERSITY

as pressure, temperature, and secondary air, also may be accessible to independent treatment.

Gas-Burner Flashback on Turndown

Flashback on turndown can occur on a burner with a high flame and low flame setting when the gas valve is rapidly turned from the high to the low position, while stable flames are obtained if the burner is ignited at either setting. As this condition may arise with some supplemental gases on natural-gas burners and may be the limiting factor in distribution of such gases to the public, the Bureau of Mines, in cooperation with the American Gas Association, was led to examine the nature of flashback on turndown.[68/]

Normally flashback occurs on a burner when the total flow through the flame port falls momentarily below the critical flow. In the case of flashback on turndown abrupt throttling of the fuel jet probably causes partial decay of the jet into eddies, producing an excessive drop in the entrainment of primary air. This momentary anaeration makes the mixture at the upstream end of the burner overrich, whereas the mixture composition at the port still corresponds to the high setting. The flame flashes back because the boundary velocity gradient at the port has dropped below the critical boundary velocity gradient for flashback of the mixture corresponding to the high setting.

If the above theory is correct, the flame size should shrink during turndown because the total flow of the initial high-setting mixture drops, and this slug of the initial mixture should be followed through the ports by a slug that is richer than the final low-setting mixture. The flames appearing during turndown can be made to reveal the passage of an overrich slug through the ports if the mixture composition at the high and low settings is just on the lean side of the yellow-tip limit. In this case, any overrich mixture will momentarily produce a yellow-tipped flame. These two events can be observed on a burner where flashback on turndown is prevented by small-diameter ports.

A burner was built to meet these experimental conditions for propane. Motion pictures were taken of the flames preceding, during, immediately following, and after turndown. The first strip in figure 62 shows the stable flame at the high setting. The top frame shows a photograph of the burner (laboratory Meker burner). The second strip shows the transient flame formed on turndown. This flame clearly diminishes in size as the total flow drops, until it becomes smaller than the stable flame formed at the low setting (fourth strip, fig. 62). The transient flame formed immediately following turndown (third strip, fig. 62) is the flame of the overrich slug resulting from the momentary breakdown of air entrainment. It is yellow-tipped, proving that it is richer than either of the two stable flames.

A commercial two-position gas valve was used in these experiments. The flow characteristics of the valve are shown in figure 63. Flames from figure 62 are superimposed on the curve in figure 63 to show the correspondence between flame characteristics and the degree of turndown of the gas valve.

It is felt that the very sharp drop in gas flow from the high to the low setting causes the short-lived decay of air entrainment and that a basic remedy for flashback on turndown would be a gas valve that would lower the gas flow gradually from a high to a low setting.

68/ Grumer, J., Nature of Gas-Burner Flashback on Turndown: Ind. Eng. Chem., vol. 45, 1953, pp. 1775-1776.

Generated on 2024-09-21 14:36 GMT / https://hdl.handle.net/2027/osu.32435030643506
Public Domain, Google-digitized / http://www.hathitrust.org/access_use#pd-google
Digitized by Google
Original from THE OHIO STATE UNIVERSITY

Generated on 2024-09-21 14:31 GMT / https://hdl.handle.net/2027/osu.32435030643506
Public Domain, Google-digitized / http://www.hathitrust.org/access_use#pd-google

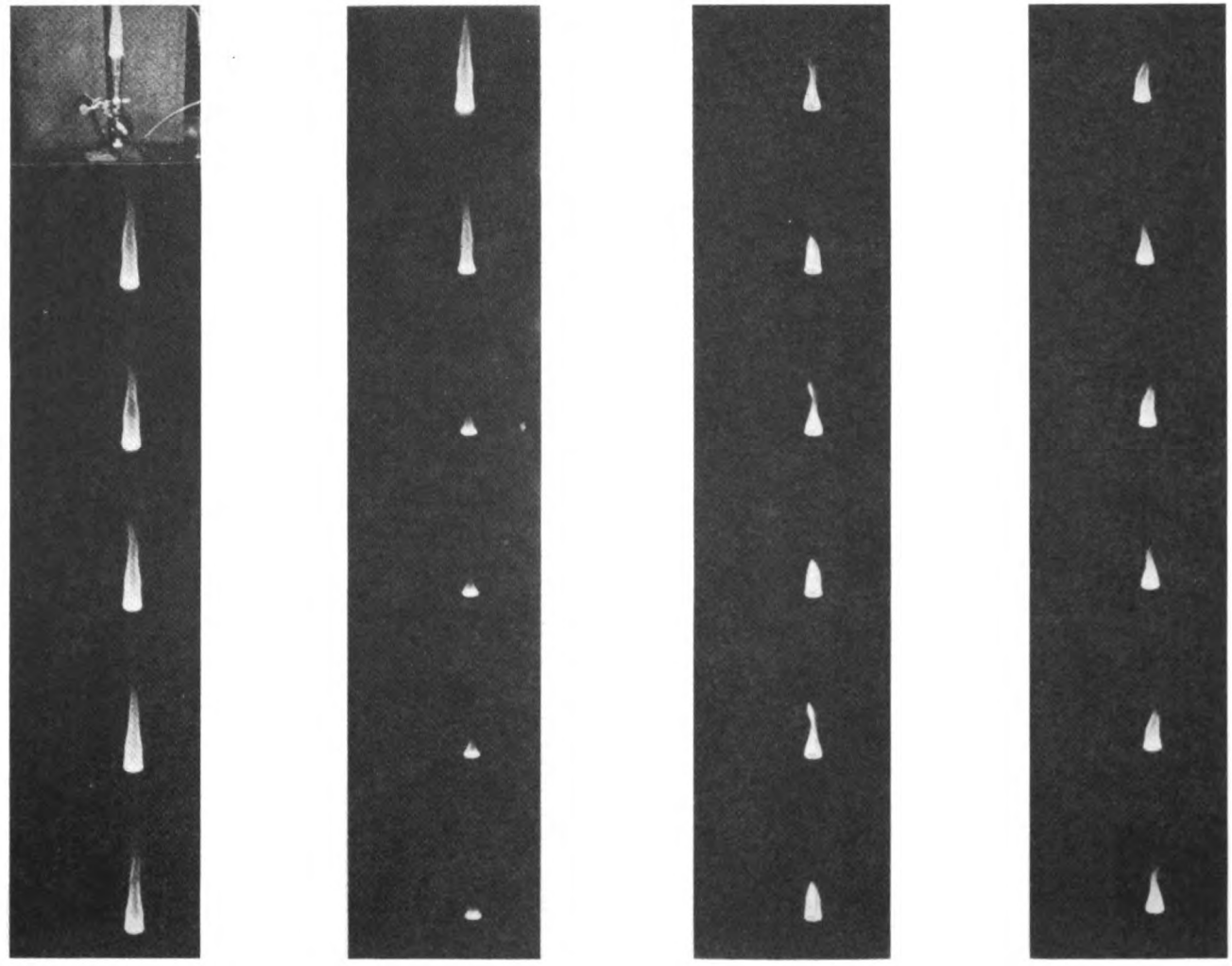

Figure 62. - Burner flames during turndown of two-position gas valve.

Digitized by Google
Original from THE OHIO STATE UNIVERSITY

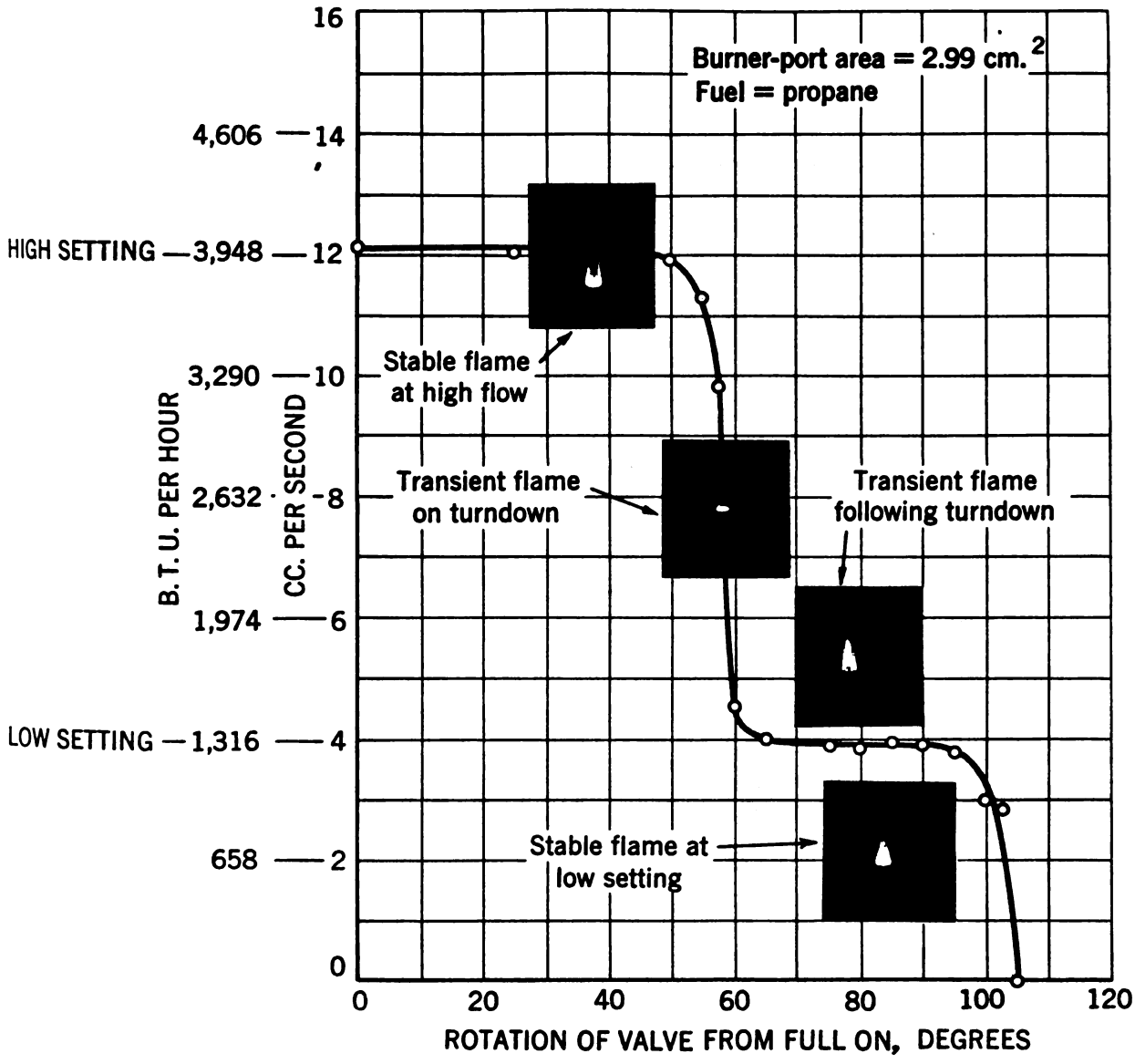

Figure 63. - Air entrainment and flow of fuel in burner during turndown of two-position gas valve.

Generated on 2024-09-21 14:32 GMT / https://hdl.handle.net/2027/osu.32435030643506
Public Domain, Google-digitized / http://www.hathitrust.org/access_use#pd-google
Digitized by Google
Original from THE OHIO STATE UNIVERSITY

Calibration of Glass-Wool Flowmeters

During the war the National Bureau of Standards developed a linear-resistance flowmeter with a glass-wool porous plug as the resistance element. Subsequent research by the Bureau of Mines[69] has shown that a single calibration of such a flowmeter can be extended to other gases on the basis of the following equation:

$$V_a \mu_a P_b / V_b \mu_b P_a = 1 ;$$

where V is volumetric flow, cc. per second; μ is viscosity of gas, poise; and P is pressure drop between ends of plug, cm. Subscript a refers to a base stream and subscript b to a substitute stream. This means that a flowmeter calibrated on one gas can be used for all gases of known viscosity when the calibration is virtually linear. This applies also to mixtures of gases, as it is known that the viscosities of mixtures can be conveniently calculated from the viscosities of their components.

Research on Turbulent Flames

During the past 15 years turbulent flame phenomena have been the subject of intensive study. The work of Mallard and Le Chatelier and of Damköhler, Shelkin, Bollinger, and Williams and others led to a clear distinction between large- and small-scale turbulence, to the theory that the main effect of large-scale turbulence is to enlarge the surface area of the combustion wave, and to an anticipation of turbulence production by the flame. However, theories of turbulent burning velocity were at variance with one another and with the experimental results.

More recently, a theory of flame propagation in turbulent explosive mixtures has been developed in the laboratories of the Division, based on the assumption that additional turbulence is generated by the turbulent flame. The postulated mechanism and theory of flame-generated turbulence have been described[70] and compared with experimental data for support.

The stability of turbulent flames is also an important question. It has been shown that the stability considerations of Lewis and von Elbe can be extended to the turbulent region and that the critical boundary velocity gradient for blowoff is the same for turbulent and laminar flames.[71] At higher flow velocities, the boundary velocity gradients become too high, and the flames must be stabilized by holders or pilot flames. At even greater flow velocities the combustion wave can no longer propagate across the steep velocity gradient.

The next step, in the light of this theory, is to extend the studies to turbulent flames burning at reduced pressures and at very high flow velocities and turbulence intensities and to study the distribution of flame-generated turbulence and flame propagation in nonuniform mixtures.

69/ Grumer, J., Schultz, H., and Harris, M. E., Calibration of Glass-Wool Flowmeters: Anal. Chem., vol. 25, 1953, p. 840.

70/ Karlovitz, B., Open Turbulent Flames: 4th Symposium (Internat.) on Combustion: Williams & Wilkins Co., Baltimore, Md., 1953, pp. 60-67.
Karlovitz, B., Effect of Flame-Generated Turbulence on Heat Transfer From Combustion Gases: Bureau of Standards Circ. 523, 1954, pp. 119-121.

71/ Karlovitz, B., Denniston, D. W., Jr., Knapschaefer, D. H., and Wells, F. E., Studies on Turbulent Flames: 4th Symposium (Internat.) on Combustion: Williams & Wilkins Co., Baltimore, Md., 1953, pp. 613-620.

Generated on 2024-09-21 14:33 GMT / https://hdl.handle.net/2027/osu.32435030643506
Public Domain, Google-digitized / http://www.hathitrust.org/access_use#pd-google
Digitized by Google
Original from THE OHIO STATE UNIVERSITY

Relation Between Sampling-Tube Measurements and Concentration Fluctuations in a Turbulent Gas Jet

The degree of mixing attained with industrial types of burners is a problem of considerable practical importance. Ordinarily this degree is determined from the chemical analysis of samples of gas taken with a sampling tube from various locations of the furnace. Hawthorne, Weddell, and Hottel[72] have presented a method for calculating the concentration fluctuation in a gas jet from the composition of gas removed through a chilled sampling tube. It has been objected that, in this method of analysis, the Gaussian distribution function employed to describe the fluctuating composition at a given point does not correspond to a physical reality. The method has now been refined conceptually and quantitatively by a more exact statistical treatment and by substituting a function that is physically more realistic for the Gaussian distribution function.[73] In connection with this work, values of the beta function $\beta(p,q)$ and the incomplete beta function $\beta(1/2, p,q)$ were computed and tabulated.[74]

Combustion of Carbon in High-Temperature, High-Velocity Air Streams

The combustion of carbon at high temperatures and high air velocities is of interest because of the increasing use of solid fuels in processes based on rapid combustion. Much of the work in this field has been limited to relatively low temperatures and velocities; considerable data also have been obtained at high temperatures, but at rather low velocities. To observe the effect of temperature and air velocity in the region of rapid combustion, where the transport of oxygen molecules to the carbon surface appears to be the determining factor, a study was made of the kinetics of combustion of spectroscopic-grade electrode-carbon cylinders.[75]

The overall reaction of oxygen and carbon can be divided into three steps:

1. The transport of the gaseous reactants to the surface.

2. The reaction at the surface.

3. The transport of the gaseous products from the surface.

Thus, the controlling factor of the reaction will be diffusion or chemical reactivity, depending on which is the slower process. At relatively low temperatures, the reaction tends to follow an equation of the Arrhenius type, where it is assumed that the primary reaction is the formation of carbon dioxide. At high temperatures (above 800° C.), for an electrode-type carbon, the temperature dependence diminishes,

---

72/ Hawthorne, W. R., Weddell, D. S., and Hottel, H. C., Mixing and Combustion in Turbulent Gas Jets: 3d Symposium on Combustion, Flame, and Explosion Phenomena, Williams & Wilkins Co., Baltimore, Md., 1949, pp. 266-288.

73/ Richardson, J. M., Howard, H. C., Jr., and Smith, R. W., Jr., Relation Between Sampling-Tube Measurements and Concentration Fluctuations in a Turbulent Gas Jet: 4th Symposium (Internat.) on Combustion, Williams & Wilkins Co., Baltimore, Md., 1953, pp. 814-817.

74/ Smith, R. W., and Edwards, H. E., Table of the Beta Function $\beta(p,q)$: Bureau of Mines Rept. of Investigations 4960, 1953, 75 pp.
Smith, R. W., and Edwards, H. E., Table of the Incomplete Beta Function $\beta(1/2, p,q)$: Bureau of Mines Rept. of Investigations 4961, 1953, 138 pp.

75/ Kuchta, J. M., Kant, A., and Damon, G. H., Combustion of Carbon in High-Temperature High-Velocity Air Streams: Ind. Eng. Chem., vol. 44, 1952, pp. 1559-1563.

Generated on 2024-09-21 14:34 GMT / https://hdl.handle.net/2027/osu.32435030643506
Public Domain, Google-digitized / http://www.hathitrust.org/access_use#pd-google
Digitized by Google
Original from THE OHIO STATE UNIVERSITY

and the effect of velocity increases. This suggests that the rate is no longer controlled by the chemical reactivity of the carbon but by the transport of oxygen molecules to the carbon surface, considered to be surrounded by a stagnant film of thickness B. Under these conditions, diffusion is the slow step, and the rate should be proportional to approximately the square root of the temperature. However, as both the diffusion rate and the viscosity of the gas increase with temperature the net effect is to make the reaction virtually independent of temperature.

Apparatus and Experimental Procedure

In the case of a carbon cylinder, geometric considerations show that the specific rate of combustion may be expressed in terms of the change in cylinder size with respect to time,

$$12N = \rho dr/dt; \qquad (1)$$

where the specific reaction rate N represents the moles of carbon burned per unit surface area per unit time (moles carbon/square cm./sec.), ρ is the density (gm./cc.), and r is the radius (cm.). The rates calculated by this method were in good agreement with those obtained by a gas-sampling method used in preliminary experiments. The assumption that the combustion rate is proportional to the geometric surface area should be valid if the rate is controlled by the diffusion of oxygen through a gaseous film.

In the present experimental study, combustion rates were determined by passing heated air at definite flow rates over thin carbon cylinders (diameter, 0.307 cm.) and observing the combustion photographically. The apparatus used for this purpose (fig. 64) consists essentially of 2 nichrome ribbons and 2 platinum-wire heaters, an insulated, clear-quartz combustion tube (i.d., 1.0 cm.), temperature-measuring equipment, and a camera to observe events in the tube. Air, dried by an activated alumina system, is passed through the all-quartz apparatus and heated to a desired temperature. The carbon cylinder then is lowered into the hot combustion tube, and the diameter of the burning carbon is recorded photographically at given intervals. In the present experiments the reference point on the carbon cylinder at which all the rates were measured was located 2 cm. from the upstream end of the cylinder. This point was chosen because it was believed to be in a region of most constant burning.

Ambient air temperatures were observed by platinum-platinum rhodium thermocouples; surface temperatures were observed with an optical pyrometer. Except for the runs at the lower air velocities, gas-sampling methods could not be used in these experiments, because the relative quantities of combustion products were too small to be analyzed with any degree of accuracy. The reaction rates represent definite point values in the region of most constant burning - a fact that must be kept in mind when correlating the experimental data with theory.

Experimental Results

The experimental data are shown in table 13. As the primary object was to study the velocity effect, air velocities are reported at ambient air temperatures. The surface temperatures are considered fairly reliable for the 900° C. air-temperature isotherm, but above this isotherm observations are less reliable because the walls of the combustion tube tend to become opaque owing to devitrification of the quartz and to a fine metallic deposit believed to result from interaction of the quartz tube and platinum wire.

Generated on 2024-09-21 14:33 GMT / https://hdl.handle.net/2027/osu.32435030643506
Public Domain, Google-digitized / http://www.hathitrust.org/access_use#pd-google
Digitized by Google
Original from THE OHIO STATE UNIVERSITY

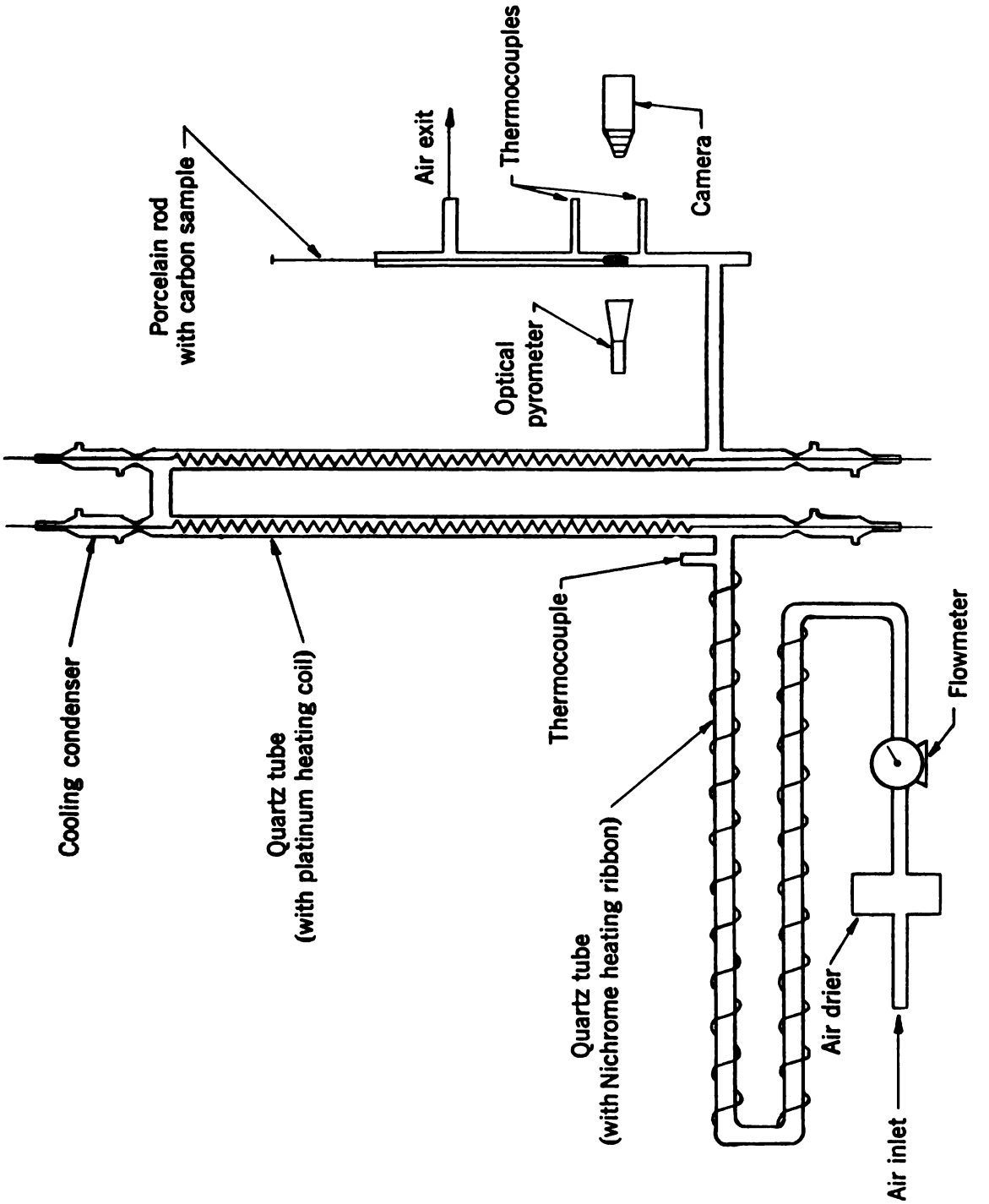

Figure 64. - Combustion apparatus.

Generated on 2024-09-21 14:36 GMT / https://hdl.handle.net/2027/osu.32435030643506
Public Domain, Google-digitized / http://www.hathitrust.org/access_use#pd-google
Digitized by Google
Original from
THE OHIO STATE UNIVERSITY

TABLE 13. - Observed specific reaction rates of spectroscopic carbon cylinders

Air temperature, °C.	Air velocity,1/ ft./sec.	Surface temperature,1/ °C.	Specific reaction rates,1/ mg./sq.cm./sec.
900	29	1,065	1.10
	55	1,085	1.55
	107	1,130	2.00
	213	1,190	2.95
	313	1,230	3.35
	420	1,255	3.85
	525	1,310	4.20
1,000	28	1,145	1.10
	55	1,135	1.70
	108	1,195	2.10
	216	1,245	3.05
	324	1,250	3.45
	432	1,280	4.05
	542	1,320	4.50
1,100	107	1,230	2.20
	215	1,260	3.10
	322	1,270	3.50
	428	1,315	4.15
1,200	321	1,255	3.55

1/ Air velocities (at ambient air temperatures), surface temperatures, and specific reaction rates represent average values of all data collected.

The reaction rates were calculated from the slopes of the radisu-time curves, a series of which is shown in figure 65. If the reaction is in the diffusion-controlled region, the slope of such a series of curves would be greatest for the greatest velocity. The slopes of the curves were taken at a point corresponding to a time when the radius of the burning specimen was 0.105 cm. This reference radius was chosen because it lies in a region of most constant burning for all the experiments made.

The region of constant burning can be analyzed in more detail by dividing the combustion of the carbon cylinders into three stages. The first stage represents the induction period required for the carbon to reach a relatively uniform combustion temperature. The second stage is characterized by the most constant surface temperatures and is the region of most constant burning. In the third stage the combustion rate increases appreciably as the size of the specimen decreases. This pattern of burning is illustrated in figure 66, where each curve represents the change in the burning rate as the sample size decreases for that particular run. The rates, measured at the reference radius of 0.105 cm., fall within the region of most constant burning. This constant burning region coincides approximately with the time when the radius of the specimen is 0.08 to 0.13 cm. The measured rates that fall outside this region change rapidly with time and sample size and therefore are less reliable. Furthermore, the rates that fall outside this region of most constant burning should not be used in attempting to correlate experimental data with theoretical predictions.

According to the results obtained, the specific combustion rate is virtually independent of the air temperature at 900° to 1,200° C. and at air velocities of 28

Generated on 2024-09-21 14:35 GMT / https://hdl.handle.net/2027/osu.32435030643506
Public Domain, Google-digitized / http://www.hathitrust.org/access_use#pd-google
Digitized by Google
Original from THE OHIO STATE UNIVERSITY

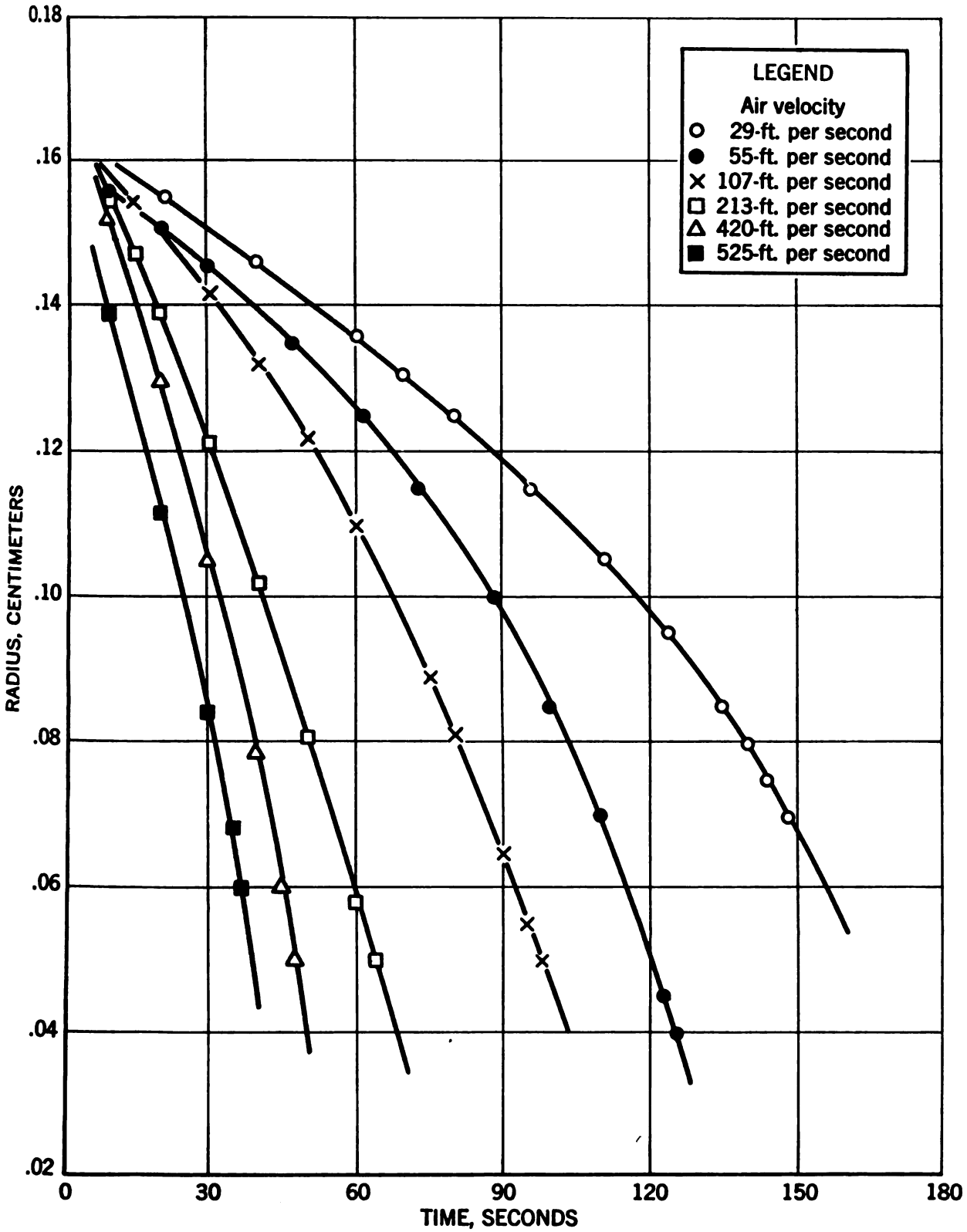

Figure 65. - Variation of radius of carbon cylinder with time (900° C.).

Generated on 2024-09-21 14:33 GMT / https://hdl.handle.net/2027/osu.32435030643506
Public Domain, Google-digitized / http://www.hathitrust.org/access_use#pd-google
Digitized by Google
Original from THE OHIO STATE UNIVERSITY

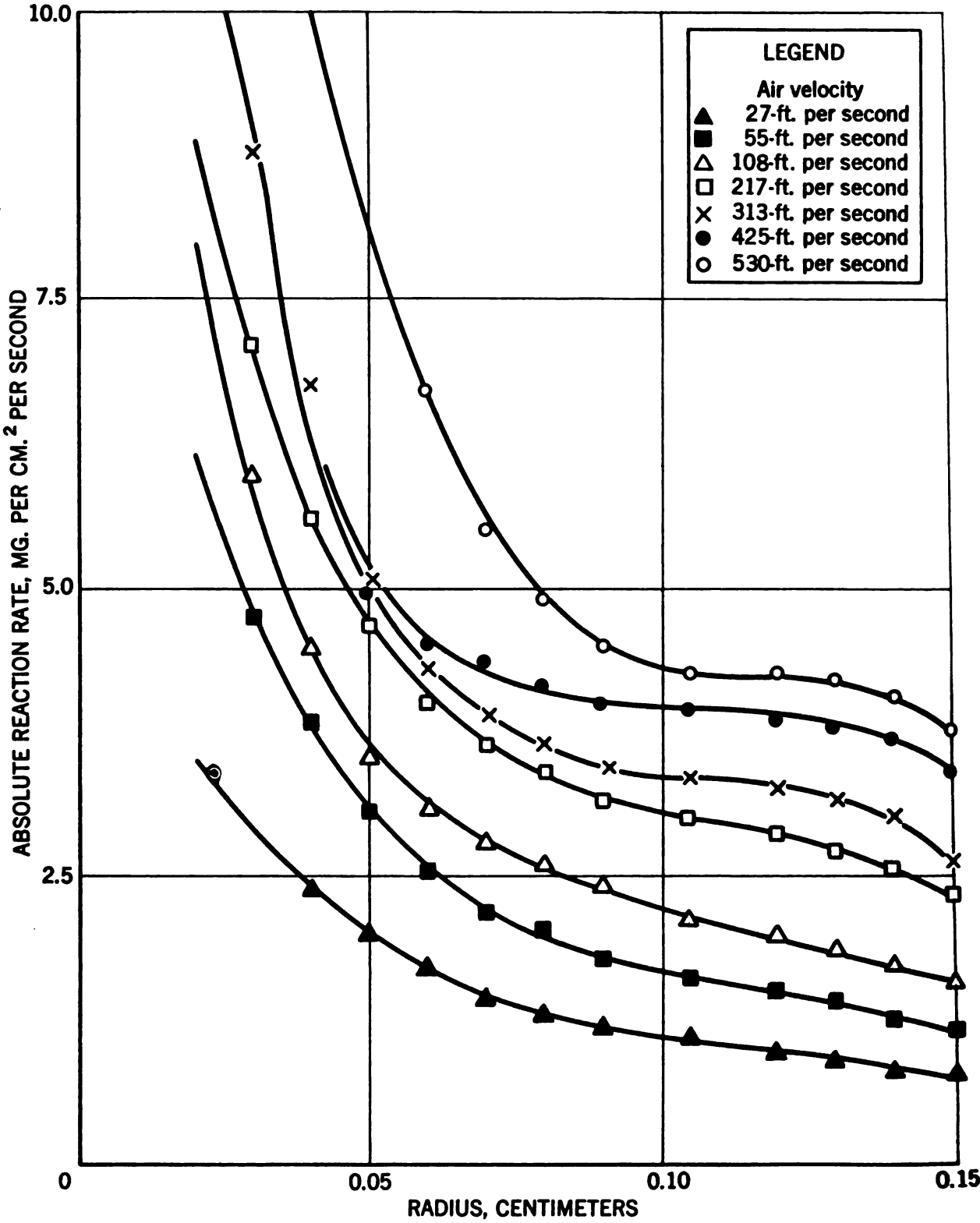

Figure 66. - Effect of sample size on reaction rate.

Generated on 2024-09-21 14:32 GMT / https://hdl.handle.net/2027/osu.32435030643506
Public Domain, Google-digitized / http://www.hathitrust.org/access_use#pd-google
Digitized by Google
Original from THE OHIO STATE UNIVERSITY

to 542 feet per second. The temperature coefficient for the runs made at approximately 320 feet per second is between 0.20 and 0.25. The effect of surface temperature for a given velocity is greater than the air-temperature effect, but its coefficient cannot be evaluated accurately because the data are too meager. The order of magnitude of the air-temperature coefficient is approximately that predicted by theory.

From a practical point of view, the effect of high air velocities on combustion is of prime interest in the field of propulsion. If a stagnant film is assumed to surround the carbon surface, the film resistance B should approach zero at some high high velocity, and any further increase in air velocity should have no effect on the reaction rate. This would result in a plateau that could be considered the region where chemical reactivity is the rate-determining step. At present we have only one one positive limit, $B \rightleftharpoons \infty$, at very low velocities, making it difficult to determine reliable values for B at other velocities. Given a second positive limit ($B = 0$), film thicknesses could be correlated mathematically with reaction rates. This would lead to more definite information on the validity of the film concept in interpreting reaction rates. In practical application, a region where the diffusional resistance is negligible, $B \cong 0$, would be most desirable. Within its limits the combustion rate would be very rapid, which, in conjunction with very high air velocities, would be most favorable for propulsion purposes.

Conclusions

Under the experimental conditions given the reaction of spectroscopic carbon and oxygen may be described by a diffusion-type equation when the specific reaction rate is directly proportional to the square root of the air velocity, or inversely proportional to a film-resistance parameter, and relatively independent of the ambient temperature. Experimental data support this view. However, the experimental data are also shown to be in general agreement with the Arrhenius-type equation, in which the specific reaction rate depends primarily on the surface temperature of the reacting carbon. These differences suggest that the reaction of carbon and oxygen, under the experimental conditions given, lies in an intermediate or transition region where both diffusion and chemical reactivity are rate-controlling factors. To establish a rate expression for these conditions, the interdependence of air velocity, surface temperature, and oxygen partial pressure at the surface must be determined.

Mathematical Model of a Combustion Wave

In the study of one-dimensional combustion waves, the existence of a steady-state solution in the mathematical formulation is a necessary, but not sufficient, condition for a physical steady state. The wave also must be stable. If the stability limit lies within the steady-state limit, the limit of flammability may be taken as the stability limit. If this is not the case, the limit of flammability is simply the limit of existence of the steady-state solution.

To obtain an insight into the nature of flame instability, a mathematical investigation was made, employing a simplified model of the flame that is amenable to exact treatment.[76/] The study was limited to the one-dimensional (that is, plane-combustion) wave, and it was assumed that this wave could be completely characterized

76/ Richardson, J. M., The Existence and Stability of Simple, One-Dimensional Steady-State Combustion Waves: 4th Symposium (Internat.) on Combustion, Williams & Wilkins Co., Baltimore, Md., 1953, pp. 182-189.

Generated on 2024-09-21 14:39 GMT / https://hdl.handle.net/2027/osu.32435030643506
Public Domain, Google-digitized / http://www.hathitrust.org/access_use#pd-google
Digitized by Google
Original from THE OHIO STATE UNIVERSITY

by a single-state variable (for example, temperature). It has been shown that such idealized waves, when they exist in the steady state, are always stable.

Mathematical Representation of Flame Propagation

Formulation of an exact theory of flame propagation presents formidable mathematical difficulties owing to the nonlinear nature of the fundamental equation. In consequence, tractable theories of flame propagation have been based either on assumptions resulting in a simplification of the fundamental equations or on the mathematical description of a simplified physical model. In either instance, it is difficult to ascertain how accurately these approximations describe the actual physical phenomenon.

To obviate this difficulty, a mathematical technique has been developed that permits expansion of the field variables, such as temperature, that appear in, or characterize, the fundamental equation for flame propagation, in terms of the Thiele semi-invariants of these variables.77/

Borrowed from statistical theory, this technique leads to a flame theory consisting of series of successive approximations, which can, in principle, be made as accurate as desired. The lower approximations can be shown to correspond to the various classical theories of flame propagation. The higher approximations not only permit a discussion of the errors implicit in the classical theories but indicate how these theories must be modified.

Thermodynamics of Combustion Gases

The theoretical description of powerplants that derive their energy from combustion of a fuel requires solution of a hydrodynamic problem involving the thermodynamic properties of the combustion products. The thermodynamic properties of fuel gases also are needed for designing appropriate means for their effective utilization. It is usually a good approximation to assume that the properties of the combustion gases are determined by the conditions of thermal equilibrium, and thus to compute them by the methods of classic thermodynamics; however, such computations performed by ordinary numerical methods are extremely tedious and prolonged. It is only with the development of large-scale automatic computational equipment that a systematic program for determining thermodynamic properties of combustion gases became feasible.

In connection with basic research on flames and combustion, the Division has undertaken several series of such calculations for the combustion gases of a variety of hydrocarbons.78/

Properties investigated include:

Constant-pressure temperatures of methane-air and propane-air flames at atmospheric pressure as functions of the mixture ratio and inlet temperature of the fuel-air stream.79/

77/ MacDonald, W. M., III, Richardson, J. M., and Rosenberry, L. P., Representation of Nonlinear Field Functions by Thiele Semi-Invariants: Quart. Appl. Mathematics, vol. 10, No. 3, October 1952, pp. 284-289.

78/ Brinkley, S. R., Jr., and Lewis, B., The Thermodynamics of Combustion Gases; General Considerations: Bureau of Mines Rept. of Investigations 4806, 1952, 61 pp.

79/ Smith, R. W., Jr., Edwards, H. E., and Brinkley, S. R., Jr., The Thermodynamics of Combustion Gases; Temperatures of Methane-Air and Propane-Air Flames at Atmospheric Pressure: Bureau of Mines Rept. of Investigations 4938, 1953, 3 pp.

Generated on 2024-09-21 14:41 GMT / https://hdl.handle.net/2027/osu.32435030643506
Public Domain, Google-digitized / http://www.hathitrust.org/access_use#pd-google
Digitized by Google
Original from THE OHIO STATE UNIVERSITY

Constant-pressure flame temperatures of methane-air, propane-air, ethylene-air, and acetylene-air flames over a range of pressures.[80]

Equilibrium composition of the combustion products and adiabatic flame temperatures of oxyacetylene systems.[81]

Equilibrium composition of combustion products of six leaded octane mixtures with air over a range of pressures and temperatures.[82]

MISCELLANEOUS INVESTIGATIONS

Surface Reaction of Oxygen With Carbon on a Tungsten Crystal

Combustion processes may be considered as oxidation reactions that proceed more or less rapidly. An important step in understanding the physical chemistry of combustion is the study of how oxygen attacks a combustible surface. Such surface reactions are complex, involving adsorption, surface mobility, and geometrical and electronic configuration. Earlier investigators obtained important information on these reactions from observing single crystals. More recently, investigation of surface reactions on single crystals has been refined through the use of a special electronic device - known as the field-emission microscope[83] - developed in Germany. This device, which makes it possible to observe directly reactions on a molecular scale, has been applied at the Bureau of Mines to the study of the oxidation of carbon on a tungsten surface.[84]

Experimental Apparatus and Procedure

The microscope consists of an evacuated tube containing a wire etched to a point of about 1μ radius and directed toward a phosphorescent screen several centimeters from it. Application of potentials of the order of 10^4 volts between the point and the screen produces a high local field ($\simeq 10^8$ V./cm.). Under the action of this field, electrons are emitted approximately radially from the point and impinge on the screen. Here they form a pattern that depends on the state of the crystal surface, emission from a crystal surface depending on the work function of the surface which can be calculated from measured voltages and emission currents.[85]

80/ Smith, R. W., Jr., Manton, J., and Brinkley, S. R., Jr., The Thermodynamics of Combustion Gases; Temperatures of Methane-Air, Propane-Air and Ethylene-Air: Bureau of Mines Rept. of Investigations 4933, 1953, 21 pp.
Smith, R. W., Jr., Manton, J., and Brinkley, S. R., Jr., The Thermodynamics of Combustion Gases; Temperatures of Acetylene-Air Flames: Bureau of Mines Rept. of Investigations 5035, 1954, 14 pp.

81/ Edwards, H. E., Smith, R. W., Jr., and Brinkley, S. R., Jr., The Thermodynamics of Combustion Gases; Temperatures and Composition of the Combustion Products of Oxyacetylene Flames: Bureau of Mines Rept. of Investigations 4958, 1953, 7 pp.

82/ Cook, E. B., Smith, R. W., Jr., and Brinkley, S. R., Jr., Equilibrium Composition of Combustion Products of Leaded Octanes With Air: Bureau of Mines Rept. of Investigations 4947, 1953, 15 pp.

83/ Muller, E. W., Versuche zur Theorie der Electronenemission unter der Einwirkung hoher Feldstärken: Phys. Ztschr., vol. 37, 1936, p. 838.

84/ Klein, R., Investigation of the Surface Reaction of Oxygen with Carbon on Tungsten With the Field-Emission Microscope: Jour. Chem. Phys., vol. 21, 1953, pp. 1177-1180.

85/ Sommerfield, A., and Bethe, H., Elektronentheorie der Metalle: Handbuch der Physik., vol. 24, No. 2, 2d ed., 1933, p. 441.

Generated on 2024-09-21 14:35 GMT / https://hdl.handle.net/2027/osu.32435030643506
Public Domain, Google-digitized / http://www.hathitrust.org/access_use#pd-google
Digitized by Google
Original from THE OHIO STATE UNIVERSITY

In the assembly used to study oxygen-carbon reactions on tungsten (fig. 67) the point was prepared by etching a fine tungsten wire (diameter, 0.01 cm.) with sodium nitrite. Carbon was deposited on the tungsten surface by evaporation from an electrically heated graphite filament, and pure oxygen was supplied by diffusion through a silver thimble. To avoid surface contamination, the setup was equipped with a high-vacuum system capable of producing pressures of the order of 10^{-10} mm. Hg.

When the desired vacuum had been attained, carbon was deposited on the point and oxygen supplied to a pressure of 10^{-5} mm. After regaining a pressure of $\sim 10^{-9}$ mm. Hg, the point was heated to various temperatures for different time intervals, in the absence of a field. After each heating the point was cooled to room temperature and the emission pattern photographed. The voltage required for a 5-microampere emission current was observed.

Experimental Results

Interpretation of the results requires data on the emission patterns and work functions of the individual reactants. Average work functions were calculated from a simplified equation, taking a clean tungsten surface as reference:

$$\varphi_2 = \varphi_1 \left(\frac{V_2}{V_1} \right)^{2/3} ;$$

where φ_2 is average work function of covered tungsten, φ_1 is average work function of clean tungsten, V_1 is applied voltage for 5-microampere emission from clean tungsten, and V_2 is applied voltage for 5-microampere emission from covered tungsten. Several assumptions are inherent in this formula, such as the constancy of the emission area with adsorption, and the use of a single average work function to describe a patchy surface.

To obtain the emission pattern of carbon on tungsten shown in figure 68, A, carbon was condensed on the tip at room temperature and heated to 1,250° K. for 5 minutes before the photograph was taken. The work function of a carbon-on-tungsten surface differed little from that of clean tungsten, regardless of the amount of carbon present.

The reaction between carbon and oxygen on tungsten was studied by preparing the composite surface and observing the pattern changes as the surface temperature increased. Oxygen admitted to the system to a pressure of 10^{-5} mm. and pumped off to a pressure of 10^{-9} mm. was adsorbed by the carbon-on-tungsten point. The emission pattern in figure 68, B, looks like a superposition of the oxygen-on-tungsten pattern on the carbon-on-tungsten pattern. Figure 68, C and D, and figure 69, A, B, and C, represent the course of the surface reaction between adsorbed oxygen and carbon-on-tungsten over a range of temperatures. Figure 69, A, shows no change from 68, D, but figure 69, B, indicates that the reaction is almost complete. Both figures 69, B, and 69, C, are characteristic of an oxygen-on-tungsten surface. Carbon diffusion into the tungsten lattice is not an alternative explanation for the disappearance of the carbon, because the carbon-on-tungsten surface is stable, even at temperatures several hundred degrees higher. The rather large surface coverage of oxygen remaining after the completed reaction suggests that the initial carbon-on-tungsten surface was one of low surface coverage.

Generated on 2024-09-21 14:37 GMT / https://hdl.handle.net/2027/osu.32435030643506
Public Domain, Google-digitized / http://www.hathitrust.org/access_use#pd-google
Digitized by Google
Original from THE OHIO STATE UNIVERSITY

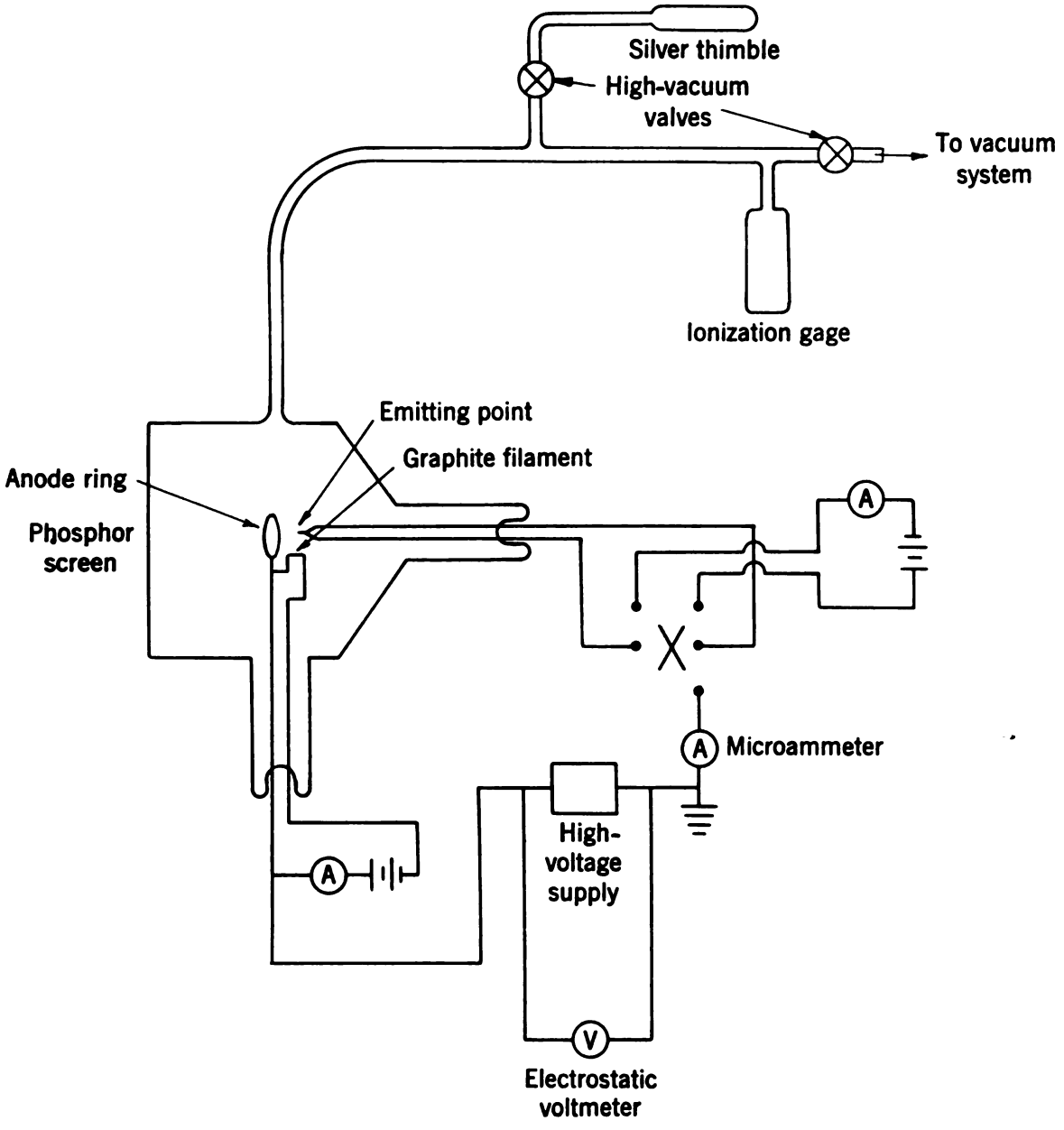

Figure 67. - Field-emission microscope assembly for oxygen-carbon reaction on tungsten.

Generated on 2024-09-21 14:35 GMT / https://hdl.handle.net/2027/osu.32435030643506
Public Domain, Google-digitized / http://www.hathitrust.org/access_use#pd-google
Digitized by Google
Original from THE OHIO STATE UNIVERSITY

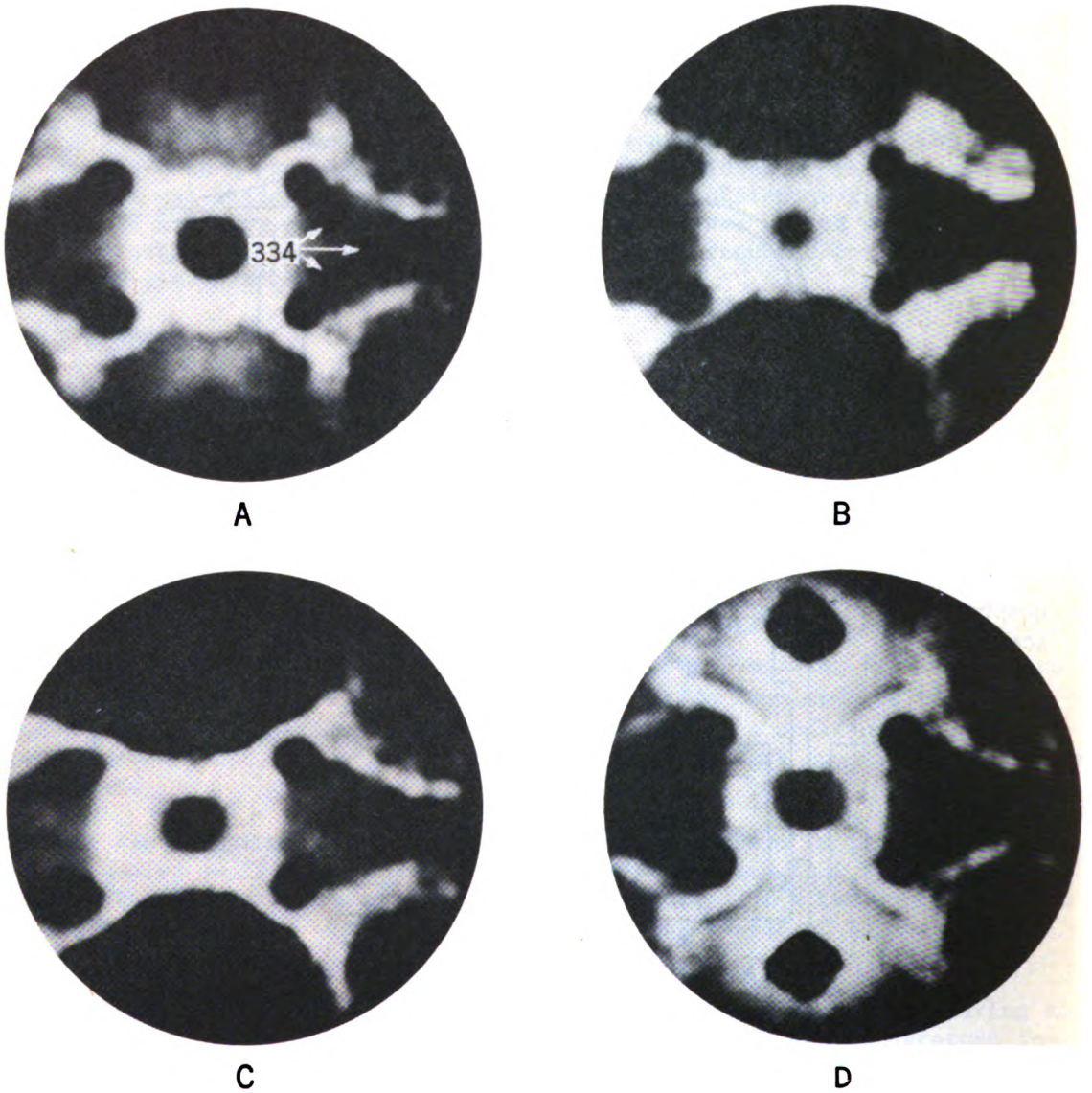

Figure 68. - Surface reaction of carbon with oxygen on tungsten: A, 5,800 volts, 5 microamperes (Carbon alone. For this point when clean, 5,600 volts was required for a 5-microampere emission current); B, 9,800 volts, 5 microamperes room temperature; C, 8,980 volts, 1,000° K., 110 minutes, 5 microamperes; D, 7,800 volts, 1,100° K., 30 seconds, 5 microamperes.

Generated on 2024-09-21 14:30 GMT / https://hdl.handle.net/2027/osu.32435030643506
Public Domain, Google-digitized / http://www.hathitrust.org/access_use#pd-google
Digitized by Google
Original from
THE OHIO STATE UNIVERSITY

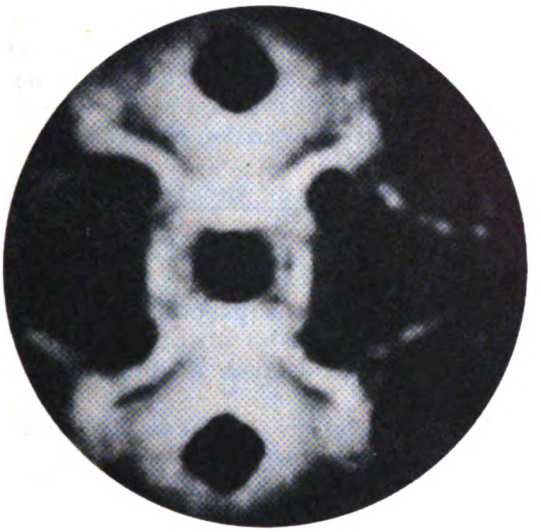

A

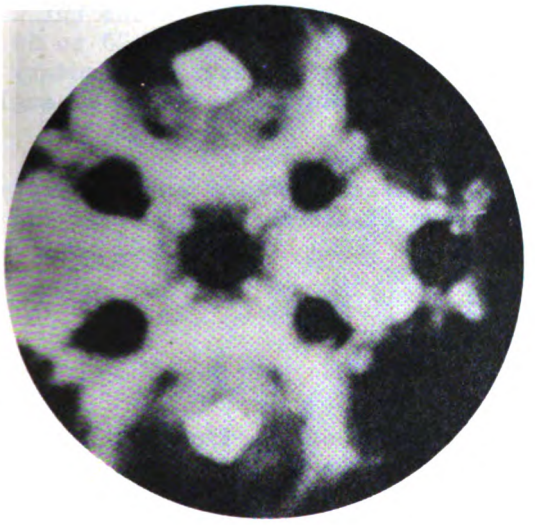

B

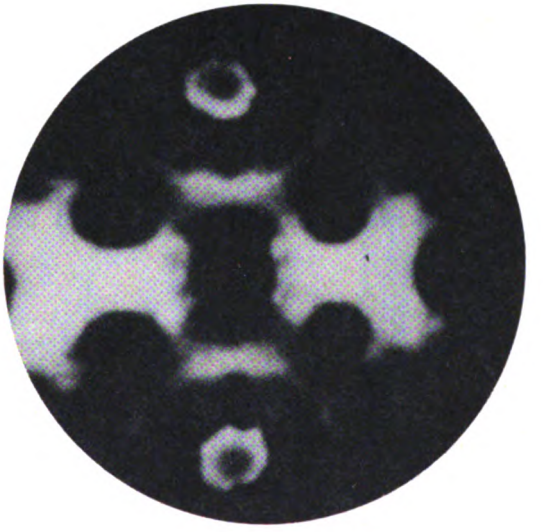

C

Figure 69. - Surface reaction of carbon with oxygen on tungsten (continued): A, 7,700 volts, 1,100° K., 45 seconds, 5 microamperes; B, 8,000 volts, 1,100° K., 11 minutes, 5 microamperes; C, 7,500 volts, 1,150° K., 30 minutes, 5 microamperes.

Generated on 2024-09-21 14:32 GMT / https://hdl.handle.net/2027/osu.32435030643506
Public Domain, Google-digitized / http://www.hathitrust.org/access_use#pd-google
Digitized by Google
Original from THE OHIO STATE UNIVERSITY

The oxidation of graphite occurs at a measurable rate at temperatures several hundred degrees below the 1,100°-1,200° K. region, in which the reaction revealed by the emission pattern changes occurs on tungsten. This suggests that the rate-controlling step in carbon oxidation is the rupture of the tungsten-oxygen bonds of the chemisorbed oxygen. The effects attributable to surface migration of both oxygen and carbon on the tungsten surface remain to be evaluated.

Capillary Jump and Capillary Vortex in Liquid Flow Along Flat Plates

When incompresible liquids expand radially along horizontal plates at very low flow rates, at a certain radial distance the liquid forms a thicker layer over a vortex sheet of dead liquid. This circular discontinuity is called a capillary jump and involves a capillary vortex. It must be distinguished from a hydraulic jump which occurs at higher flow rates and involves a "back roll."

The general features of the capillary jump can be observed by using cigarette ash to trace the streamlines of water flowing from a faucet. Some interesting observations have been made[86/] with finely powdered oxide (ZnO, PbO, Fe_2O_3) dispersed in a water jet. On traversing the boundary, most of the lighter particles are carried along the upper vortex layer until they sink deep enough to be turned back. Some of them reach the jump and start another round trip. Finally, a portion of these particles forms an annular sediment of approximately constant width, the inner rim coinciding closely with the boundary. Figure 70 shows the characteristic pattern of the capillary jump. There is no back roll at the surface; particles of cork dispersed on the surface pass over the hump uninhibited by countercurrents, indicating that the flow direction of the top layer is outward. Below this top layer the motion of small dispersed particles indicates a flat vortex of dead liquid rotating centripetally in the undercurrent below a certain depth. Depending on the thickness of the elevated layer, the vortex may extend along the plate as much as 20 to 30 times its thickness, for example, 5 cm. for a 2-mm. layer of water. At boundary radius r the flat surface of the thin layer and the elevated surface form an angle close to 90°.

Considering the capillary jump as an effect of surface tension and viscosity, the following expression was developed for the radius of discontinuity r_1:

$$r_1 = \frac{\left(\frac{F}{2\pi}\right)^{3/4}}{\left[5 f \sigma \rho \eta\right]^{1/4}};$$

where F is total flow rate, gm./sec., σ is surface tension of the liquid, ρ is density of the liquid, η is viscosity of the liquid, and f is a numerical factor.

Experiments on the behavior of water, ethyl alcohol, and mineral oil were in satisfactory agreement with the derived relation.

86/ Cassel, H. M., Capillary Jump and Capillary Vortex in Liquid Flow Along Flat Plates: Proc., 2d Midwest. Conf. on Fluid Mechanics, Ohio State University, 1952, pp. 99-104.

Generated on 2024-09-21 14:32 GMT / https://hdl.handle.net/2027/osu.32435030643506
Public Domain, Google-digitized / http://www.hathitrust.org/access_use#pd-google
Digitized by Google
Original from THE OHIO STATE UNIVERSITY

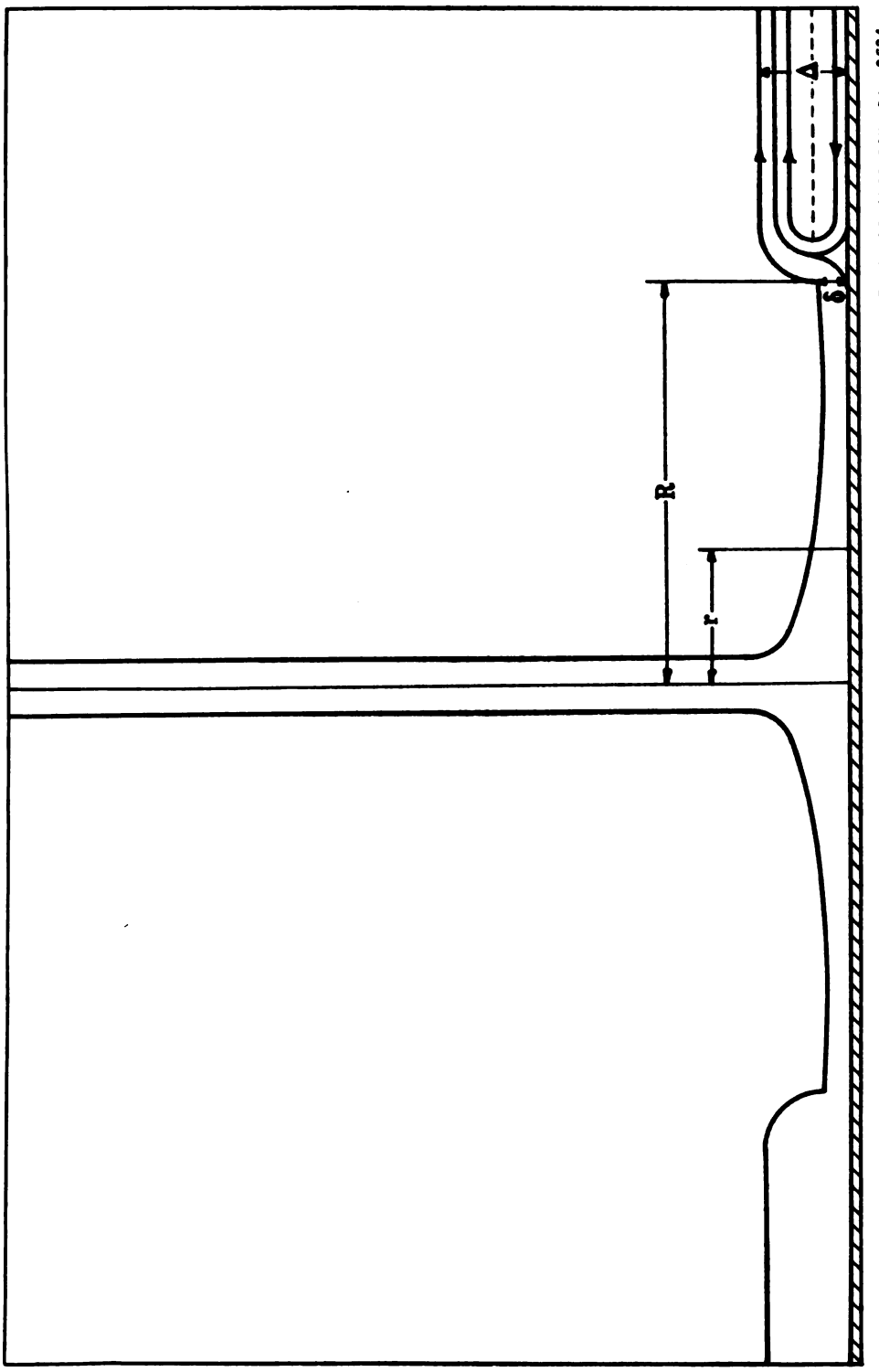

Figure 70. - Vertical cross section of flow pattern.

Generated on 2024-09-21 14:32 GMT / https://hdl.handle.net/2027/osu.32435030643506
Public Domain, Google-digitized / http://www.hathitrust.org/access_use#pd-google
Digitized by Google
Original from
THE OHIO STATE UNIVERSITY